Novel insights into mechanisms partitioning chromatin states

Inauguraldissertation

zur

Erlangung der Würde eines Doktors der Philosophie

vorgelegt der

Philosophisch-Naturwissenschaftlichen Fakultät

der Universität Basel

von

Valentin Benno Flury

aus Deitingen (SO)

Schweiz

Basel, 2017

Genehmigt von der Philosophisch-Naturwissenschaftlichen Fakultät

auf Antrag von

Prof. Dr. Marc Bühler

Dr. Sigurd Braun

Basel, den 23.05.2017

Prof. Dr. Martin Spiess

Dekan

SUMMARY

Eukaryotic chromatin can be divided into two main types: euchromatin with high levels of transcription and heterochromatin, where transcription is repressed. These chromatin types are not static, but show remarkable plasticity during development and adaptation to environmental cues: Heterochromatic genes can get activated, whereas euchromatic genes get repressed. This is orchestrated by a multitude of chromatin-modifying enzymes, which extensively modify the protruding histone tails of the nucleosomes, the fundamental packaging unit of DNA. Such histone modifications serve as binding platforms for a plethora of specific chromatin readers and show distinct characteristics depending on which chromatin state they belong to: Euchromatin is characterized by H3K36me3, H3K4me3 and H2B ubiquitination (H2Bub), whereas heterochromatin is hypoacetylated and carries high levels of H3K9 methylation.

With the development of deep sequencing technologies, the perception of transcriptionally silent heterochromatin changed. It became clear that heterochromatin can also be transcribed, but that these transcripts are quickly recognized and degraded in a chromatin context-dependent manner. This holds true for the fission yeast *Schizosaccharomyces pombe* (*S. pombe*), the model organism that I used in my PhD thesis. It has very similar heterochromatic characteristics compared to other eukaryotes, such as H3K9me2 and heterochromatic transcription. Notably, heterochromatin formation in *S. pombe* involves the RNA interference (RNAi) pathway, which directs *de novo* heterochromatin formation in a sequence-specific manner via small interfering RNAs (siRNAs). Maintenance and spreading of heterochromatin across nucleosomes is achieved by a self-enforcing feedback loop, wherein heterochromatin is stabilized, expanded, and propagated in a sometimes DNA-sequence independent manner.

Although siRNAs are necessary to maintain constitutive heterochromatin, siRNAs targeting a euchromatic locus do not induce heterochromatin formation. This paradox laid the foundation for my PhD thesis by evoking the question how euchromatic genes are protected from *de novo* heterochromatin formation by RNAi.

SUMMARY

In a first study to address this question, I contributed to the discovery that the Polymerase II-associated factor 1 complex (Paf1C) is a main repressor of RNAi-mediated heterochromatin formation. In Paf1C mutant cells, silencing of the siRNA-targeted euchromatic gene occurred in a stochastic manner, but was maintained efficiently with and without the initial source of siRNAs; a truly epigenetic phenomenon. Yet, initiation of silencing was rather limited, suggesting the existence of additional repressive activities that may function specifically at the initiation step.

I identified the histone acetyltransferase Mst2 to be such a repressive factor. The Mst2 complex represses heterochromatin formation specifically at the initiation step, but does not affect maintenance. This is achieved by the exclusion of Mst2C from heterochromatin due to tethering of Mst2C to H3K36me3-marked nucleosomes, a hallmark of actively transcribed genes. This tethering in turn protects euchromatic genes from silencing. Further, to dissect the mechanism of this protection, I aimed at identifying all potential Mst2 substrates. By employing an acetylomics approach, I discovered that Mst2 also acetylates a specific residue of Brl1. This is exciting, because Brl1 is an enzyme responsible for H2B ubiquitination, a second hallmark of active chromatin. Acetylation of Brl1 increases H2Bub and feeds back to increased transcription activity, which is also marked by increased H3K4me3 levels.

In conclusion, my work led to the discovery of a euchromatic feedback loop, which protects euchromatin from *de novo* heterochromatin formation. I am fascinated by this finding, because it implies that euchromatic genes can “remember” their active state and actively counteract heterochromatin formation. Furthermore, the interplay of euchromatic and heterochromatic feedback loops creates epigenetic plasticity, which allows cells to keep genes on or off in an almost digital manner. Since the general characteristics of heterochromatin and all identified factors are conserved, I propose that similar feedback loops likely partition chromatin in active and inactive states also in humans and may help promoting epigenetic robustness against environmental challenges and cancer.

TABLE OF CONTENTS

LIST OF FIGURES

ABBREVIATIONS

A. thaliana	*Arabidopsis thaliana*
ac	acetylated residue
ARC	Argonaute siRNA chaperone
bp	basepair(s)
BruDRB-Seq	BrUTP-5,6-dichlorobenzimidazole 1-β -D ribofuranoside-sequencing
C. elegans	*Caenorhabditis elegans*
ChIP	Chromatin immunoprecipitation
ChIP-Seq	Chromatin immunoprecipitation sequencing
CLRC	Clr4-Rik1-Cul4 complex
cnt	central core (of the centromere)
CPF	Cleavage and polyadenylation factor
CTD	C-terminal domain (of RNA polymerase II)
CTGS	Co-transcriptional gene silencing
D. melanogaster	*Drosophila melanogaster*
DNA	Deoxyribonucleic acid
DSR	Determinant of selective removal
dsRNA	double-stranded RNA
DUB	Deubiquitinase module
E(var)	Enhancer of variegation
EMS	Ethylmethansulfonate
FACT	Facilitates chromatin transcription
FLC	FLOWERING LOCUS C
GTF	General transcription factor
H2BK119	H2B lysine 119
H2BK119R	H2B lysine 119 substitution with arginine
H3K14R	H3 lysine 14 substitution with arginine
H3K4/9/14/27/36	H3 lysine 4/9/14/27/36
H3K36M	H3 lysine 36 substitution with methionine

ABBREVIATIONS

HOX	Homeobox
HP1	Heterochromatin protein 1
HULC	Histone ubiquitin ligase complex
HUSH	Human Silencing Hub
imr	innermost repeats
IRC	Inverted Repeat of Centromere
K242R/Q	Lysine 242 substitution with arginine (R)/glutamine (Q)
KAT	Lysine acetyltransferase (updated for histone acetyltransferase [HAT])
KDAC	Lysine deacetylase (updated for histone deacetylase [HDAC])
KO	knockout
me1/2/3	mono-/di-/tri-methylated residue
mRNA	messenger RNA
MSL	Male-specific lethal complex
Mst2C	Mst2 complex
MTL	Mating type locus
ncRNA	noncoding RNA
NET-Seq	Native elongating transcript-sequencing
nt	nucleotide(s)
ORF	Open reading frame
otr	outermost repeats
qPCR	quantitative Polymerase chain reaction
Paf1C	Polymerase II-associated factor 1 complex
PAS	Polyadenylation signal
Pat1-as2	Pat1-analog-sensitive
PEV	Position effect variegation
PIC	Preinitiation complex
PRC	Polycomb-repressive complex
PRE	Polycomb group response element
priRNAs	primal siRNAs
pTEFb	positive Transcriptional elongation factor b

ABBREVIATIONS

PTGS	Post-transcriptional gene silencing
PTM	Post-translational modification
RNA	Ribonucleic acid
RDC	Rhino-Deadlock-Cutoff complex
RDRC	RNA-directed RNA polymerase complex
REIII	Repressor element III
RITS	RNA-induced transcriptional silencing complex
RNAi	RNA interference
RNAPI-V	RNA polymerase I-V
rRNA	ribosomal RNA
S. cerevisiae	*Saccharomyces cerevisiae*
S. pombe	*Schizosaccharomyces pombe*
SAGA	Spt-Ada-Gcn5-acetyltransferase complex
Serine-2/5/7P	phosphorylated Serine-2/5/7 (of CTD)
SHREC	Snf2/Hdac-containing Repressor Complex
shRNA	small-hairpin-RNA
siRNA	small interfering RNA
SRI	Set2 Rpb1 interaction domain
Su(var)	Suppressor of variegation
TBP	TATA-box binding protein
TGS	Transcriptional gene silencing
TPE	Telomere position effect
tRNA	transfer RNA
TSS	Transcription start site
TTS	Transcription termination site
Tyrosine-1P	phosphorylated Tyrosine-1 (of CTD)
ub	ubiquitinated residue
1-NM-PP1	4-amino-1-tert-butyl-3-(1′-naphthylmethyl)pyrazolo[3,4- d]pyrimidine
4sUDRB-Seq	4sUTP-5,6-dichlorobenzimidazole 1-β -D ribofuranoside-sequencing
3’-/5’-UTR	3’-/5’-untranslated region

INTRODUCTION

This thesis deals with the fascinating mechanisms of how self-enforcing feedback loops partition chromatin into different states such as heterochromatin and euchromatin and how these states are initiated, maintained, and counteracted. To dissect these mechanisms, I used the fission yeast *S. pombe*, which contains well-conserved heterochromatic features compared to humans. Hence, this introduction will mostly focus on *S. pombe*, while highlighting a few mechanistically similar feedback loops in other organisms.

1. Introduction to chromatin and epigenetics

The entire genetic information of every eukaryotic organism is encoded in few simple molecules, the DNA. This information is essential for the organism to survive, develop and reproduce. Importantly, DNA is not present as a naked molecule in the cell, but occurs in a highly complex structure, called chromatin (see Figure 1). Chromatin is composed of DNA, which is wrapped around packaging proteins to form the nucleosome, and further associated proteins and RNAs, which regulate chromatin compaction, stability and accessibility. In order to form the nucleosome, 147 basepairs (bp) of DNA are wrapped around a histone octamer, which consists of two highly positively charged H2A, H2B, H3, and H4 proteins each. In other eukaryotes, histone H1 is an additional histone protein and acts as a clamp stabilizing the nucleosome and protecting the linker DNA, but is absent in *S. pombe* (Godde and Widom, 1992; Whitlock and Simpson, 1976). The nucleosome is the first and basic packaging unit that

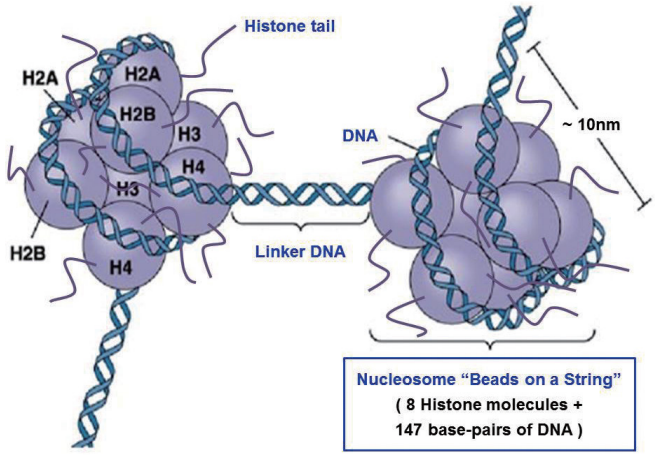

Figure 1: Schematic visualization of the nucleosome in S. pombe. The H1 linker histone is not shown, because it is absent in fission yeast. Picture adapted from Kim, 2014.

compacts DNA 6-7 fold and marks the first step to form higher chromatin structures and ultimately the chromosome. This compaction step can be visualized by electron microscopy, which revealed that oligonucleosomes form a “beads on a string”-like structure (Olins and Olins, 1974).

DNA compaction serves multiple functions in the cell: 1) It allows to package the genetic information into a very dense, but still accessible structure to fit into the nucleus. The magnitude of compaction is vast. For example, the length of the entire human DNA fiber is almost 2 m, but fits into the nucleus with the size of 5 - 10 µm. 2) The assembly of basic histone proteins with the negatively charged DNA gives the structure more stability and thus protects it from mechanical DNA damage. 3) Nucleosomes can be better regulated in terms of accessibility of individual genetic information units (genes) and are thus crucial in orchestrating gene expression.

Regulation of gene expression is achieved on several levels, such as by specific chromatin binding proteins, nucleosome eviction or sliding, direct modification of DNA and histones, or higher ordered chromatin structures (such as heterochromatin, see chapter 3). Whereas the first levels of gene expression rather act on a molecular level regulating individual genes, higher order chromatin structures can extend for kilo- to megabasepairs and can even be visualized by microscopy (see Figure 2). Already in the early 20th century, Emil Heitz and colleagues identified chromatin regions, which are differentially stained in the nucleus during interphase (Heitz, 1928). During this cell cycle stage, many transcriptional processes take place within chromatin, which is decondensed and thus only light stained. This part of chromatin is called euchromatin and is gene-

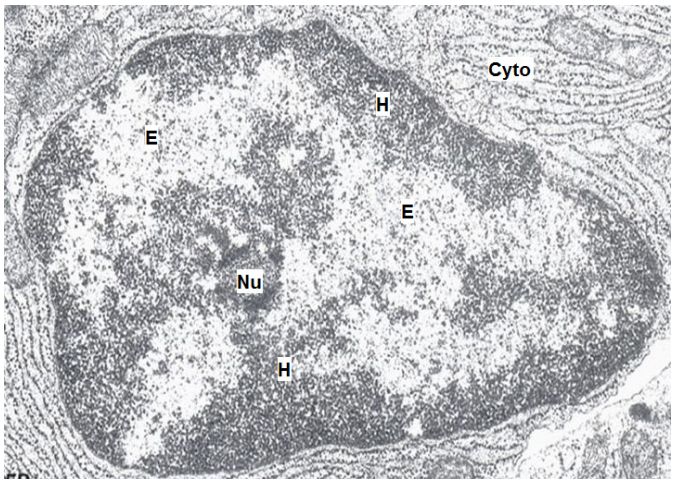

Figure 2: Electron micrograph of a human plasma cell nucleus. Heterochromatin clusters at the nuclear periphery or the nucleolus, whereas euchromatin resides in the middle of the nucleus. Picture adapted from Young and Heath, 2000.

E: euchromatin
H: heterochromatin
Nu: nucleolus
Cyto: cytoplasm

rich, transcriptionally active, and dynamic (see chapter 2). Conversely, the dark stained chromatin area seems to remain condensed also in interphase and is known as heterochromatin, which is gene-poor, rather inaccessible, and transcriptionally repressed (see chapter 3).

Despite this literally black and white picture, the underlying mechanisms that define which parts of the genome are heterochromatic or euchromatic are still not well understood. The most straight forward model is that a sequence-specific protein binds to a gene and induces its activation or repression, including its neighboring regions (reviewed in Bell et al., 2011). Whereas this model is supported by the discovery of many transcription factors that are crucial for the activation of certain genes, only few DNA-binding proteins with repressive functions have been identified, such as Atf1 in the fission yeast *S. pombe* (Jia et al., 2004). Furthermore, recent research implies that repressed chromatin cannot be bound anymore by certain transcription factors, which would lead to an irreversible and potentially harmful repression (Domcke et al., 2015). Hence, these results cannot be explained by the model that the genomic sequence is solely responsible for the expression landscape, but additional mechanisms must exist, which are not dependent on the DNA sequence directly. Such mechanisms are investigated as part of a major research focus, called “epigenetics”, as it deals with effects beyond the genetic information (*Greek*: epi = outside of, around).

1.1. What is epigenetics?

Several definitions exist for epigenetics. A broader, initial definition of epigenetics includes all phenotypes, which cannot be defined only by changes on the DNA level. Hence, changes in gene expression during development, differentiation and in terminally differentiated cells such as neurons could be called “epigenetically” regulated (Nanney, 1958). For example, epigenetics would be responsible for the development of a human being, because the DNA sequence mostly stays identical from the fertilized oocyte to the fully developed adult.

A more recent, and more widely accepted definition defines an epigenetic trait as a “stably heritable phenotype resulting from changes in a chromosome without alterations in the DNA sequence” (Berger et al., 2009). Therefore, all phenotypes during and after development in somatic cells are not truly epigenetic as they will not be inherited to the next generation, but rather are a consequence of differential gene expression. An even more stringent version demands the heritability to even persist in the absence of the initial stimulus (reviewed in Deans and Maggert, 2015). However, this poses an important problem: How can we define a stimulus to be the initial stimulus? How can we be sure that the stimulus is definitely absent? If the stimulus is an environmental signal (such as the control of vernalization by temperature changes in plants (see chapter 3.4.1), Berry and Dean, 2015) this might be still possible. However, stimuli can also arise within the cell and it is usually unclear how many different stimuli contribute how much to the epigenetic phenotype. According to this very stringent definition, as long as we cannot rule out that not a single initial stimulus is still present and induces the heritability, we could not call something “epigenetic”.

Nevertheless, few phenotypes seem epigenetic, because they affect one locus on one chromosome but not a second identical locus on a different chromosome, such as X chromosome inactivation in female cells via the long noncoding RNA Xist (Brown et al., 1991; Lyon, 1961). Another example is the mating type locus in *S. pombe*, where small RNAs and Atf1 induce silencing but either can be deleted afterwards without affecting the repression of the locus (see chapter 3.2.1.1, Jia et al., 2004). This is accomplished by self-enforcing feedback loops, which maintain the current state and provide some kind of memory to that locus. Such feedback loops are often based on directly altering chromatin function via histone and DNA modifications. Although their epigenetic nature (*i.e.* the heritability of the modifications themselves, Ptashne, 2013) is still under debate, it is clear that these modifications have a strong impact on memory and gene expression due to their self-enforcing characteristics and their ability to spread along chromatin.

1.2. Histone code

The role of histone proteins in regulating gene expression and epigenetic phenomena has been underappreciated for a long time, given the fact that they were identified as the core nucleosome particles already in 1884 by Albrecht Kossel (reviewed in Campos & Reinberg 2009). However, it took eighty years to discover that histone proteins are highly modified on their accessible N-terminal tails (and to a smaller extent the C-terminal tail), which protrude from the nucleosome core particle (see Figure 3, Allfrey et al., 1964).

Such post-translational modifications (PTMs) and the amino acid sequence of histones are highly conserved between all eukaryotes, underlining their importance. Moreover, various histone variants have been identified and already few different amino acids can lead to altered nucleosome function or stability (reviewed in Talbert & Henikoff 2016). However, for the sake of brevity, only PTMs will be further discussed here. PTMs can directly affect the chromatin accessibility, especially PTMs on lysines because these amino acids contribute substantially to the overall positive charge of histones. Acetylation of these lysines neutralizes their charge and leads to a looser interaction of the histone with DNA, which renders chromatin more accessible (Allfrey et al., 1964). On the other hand, methylation of lysines slightly concentrates the positive charge on the lysine residue and therefore rather enhances interaction between DNA and histones leading to chromatin repression.

Besides this simple electrostatic interaction, PTMs of histones serve as binding platforms for histone “reader” proteins, which recruit adaptor proteins to induce chromatin changes. Especially the histone methylation marks attract a plethora of specific methylation reader proteins (reviewed in Greer and Shi, 2012), whose effects exceed the minor electrostatic contributions of lysine methylation. Hence, methylated histone residues are nowadays known to mediate not only repression of chromatin, but also have activating functions depending on their position on the histone tails. In more detail, trimethylation of lysine 4 or 36 on histone H3 (H3K4me3 and H3K36me3) are hallmarks of euchromatin whereas H3K9me2/3 or H3K27me3 are specific

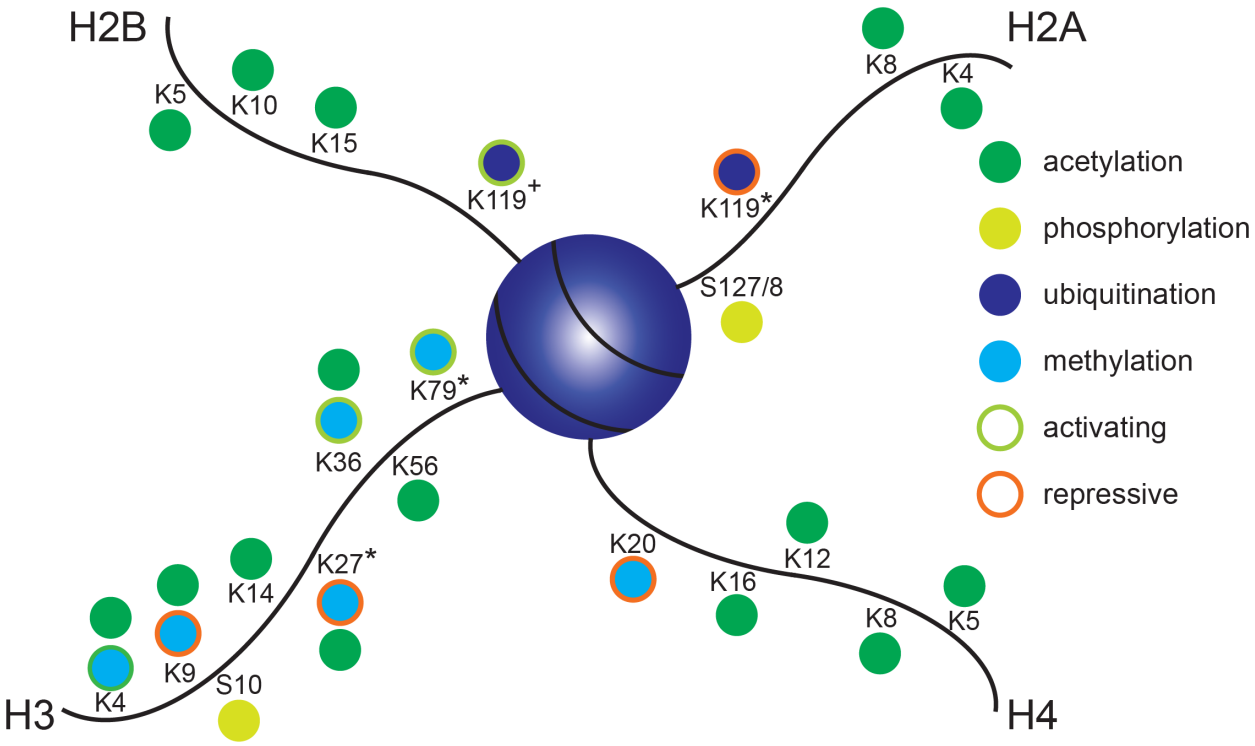

Figure 3: Post-translational histone modifications in S. pombe and metazoans. N- and C-terminal tails of all four histones are merged, harbor multiple modifications and are not in scale. Labelled are the individual modified amino acids and their position in the tail. Methylation sites are indicated as repressive and activating by a red and green ring, respectively. Only consistently identified and characterized PTMs are shown. Multiple PTMs that have well-known roles in other eukaryotes, but have not been identified in *S. pombe* are labelled with an asterisk (H3K27me3, H3K79me3 and ubiquitinated H2AK119). +: H2BK119 ubiquitination in *S. pombe* is the equivalent to K120 in mammals and K123 in *S. cerevisiae*.

features of heterochromatin (see Figure 3). In addition, the degree of methylation can have different effects, *i.e.* mono-, di- and trimethylation of the same lysine can have very diverse functions. For acetylation, hypoacetylated regions are found in heterochromatin and gene bodies, whereas hyperacetylation usually coincides with promoters and transcription start sites.

Besides acetylation and methylation also phosphorylation, ubiquitination and ADP-ribosylation of histones have been reported and were shown to have important biological functions (Carlberg and Molnár, 2014). More recently, many more PTMs were identified with the further development of highly sensitive mass spectrometers, which were able to identify also low abundant modifications (Huang et al., 2015). A recent literature survey identified over 500 different modifications on more than 200 sites on histones (Zhao and Garcia, 2015).

Attributing a biological function for each individual modified residue might be problematic, because PTMs do not always have a biological function alone, but often in combination with other modified histone residues. This is illustrated by H3K27me3 and H3K4me3 marks, which usually repress and activate chromatin, respectively (see above). However, together they mark poised promoters of developmental genes in embryonic stem cells (Bernstein et al., 2006). In the style of the genetic code, this led to the term “histone code”, where a combination of PTMs defines the chromatin state rather than individual PTMs alone (Strahl and Allis, 2000).

The histone code adds another layer of complexity and thereby allows the cells to fine-tune their gene expression programs. This code is subject to many regulatory protein complexes, which either set the mark (histone “writers”) or remove it (histone “erasers”). Such protein complexes often contain histone “reader” domains that recognize certain PTMs and thereby give specificity to the whole complex. A common feature of these multiprotein complexes is that they can read their own mark, which sometimes enhances their own activity: Histone methyltransferase complexes often contain a chromodomain and acetyltransferase complexes usually contain a bromodomain, which specifically recognize a methylated or acetylated residue, respectively (Zhang et al., 2015). Hence, this writing/reading cycle leads to an enforcement and increased activity of enzyme complexes and constitutes a simple, but powerful feedback loop. Since these feedback loops can often connect to the neighboring nucleosome in close distance, they can spread along the chromatin fiber by writing and reading their own mark (see Figures 12, 14 - 17 in the following chapters).

Despite this astonishing complexity, the biological changes in histone tail mutants are often weak, which evoked also a critical perception of the functional importance of the histone code (discussed in Rando, 2012). However, with the use of laboratory-adapted model organisms only limited knowledge of the functionality in the natural context is available and it could well be that this histone code is crucial in buffering and preparing cellular systems against environmental or internal cues, such as damaging agents, stress, and cancer (see Discussion).

2. Euchromatin

Euchromatin displays many different transcriptional activities and hence has very diverse characteristics. A simple classification separates euchromatin into three classes, wherein each class is transcribed by a different RNA polymerase: In general, RNA polymerase I, II and III each transcribe a specific set of genes, which are tRNA, mRNA and rRNA genes, respectively. With the development of deep sequencing technologies, two major findings changed the perception of transcription. Whole human genome sequencing revealed that coding genes make up only 1 % of the genome, but up to 75 - 90 % can be transcribed at sometimes low levels, suggesting that noncoding transcription is far more pervasive than assumed (Birney et al., 2007; Djebali et al., 2012; Venter et al., 2001). This is conserved in *S. pombe*, wherein spurious transcripts have been detected covering 99 % of the genome, but genes make up only 50 % (Dutrow et al., 2008; Wilhelm et al., 2008; Wood et al., 2002). Also heterochromatic regions are transcribed, albeit the resulting transcripts are low abundant, suggesting either impaired transcription or quick degradation of the transcripts (see chapter 3, Bühler et al., 2007). In *S. pombe*, RNA polymerase II (RNAPII) is responsible for heterochromatic and widespread noncoding transcription (Kato et al., 2005), hence I will only focus on RNAPII-mediated transcription.

2.1. Transcription by RNA polymerase II

Transcription by RNA polymerase II is universally conserved and is a very complicated process within a cell. To understand how this machinery is regulated has kept research busy for decades and is still somewhat incomplete. For brevity, I will mostly focus on the mechanism of transcription in our model system *S. pombe* and its distantly relative budding yeast *Saccharomyces cerevisiae* (*S. cerevisiae*). Both model organisms have been widely used to investigate transcriptional processes that are mostly conserved to multicellular eukaryotes and sometimes even in bacteria (Allison et al., 1985).

Transcription can be divided into three major steps, which are all highly regulated by a multitude of factors: Transcription initiation, which includes the correct recruitment of RNAPII and associated factors; elongation, the efficient and correct transcription; and termination, resulting in the release of RNAPII and its finished transcript. During transcription, many additional processes take place co-transcriptionally, whilst the transcript is still attached to RNAPII. They mutually influence and regulate each other and the correct interplay is crucial in determining the fate of the transcript (reviewed in Bentley, 2014). These processes include capping of the RNA, (alternative) splicing of introns, export from the nucleus, RNA-modifications, and co-transcriptional gene silencing (CTGS), but only the last phenomenon will be discussed in more detail (see chapter 3.2.2).

2.1.1. Transcription initiation

Transcription is initiated by the recognition of the core promoter, a 50 - 100 bp DNA stretch upstream of a gene. Various promoter regions and promoter-associated proteins have been identified and characterized, however the detailed mechanistic understanding is still very limited (Roy and Singer, 2015). The best understood example is the TATA box, a promoter element located 20 - 30 bp upstream of the transcription start site (TSS), which serves as binding platform for the general transcription factors (GTFs) (Mathis and Chambon, 1981). Specific “pioneering” transcription factors promote this assembly by opening up the chromatin structure and can bind on very distal DNA elements, such as enhancers and distal promoter elements (for a review see García-González et al., 2016).

With an accessible chromatin structure, TBP (TATA-box binding protein) can bind to the TATA box (see Figure 4). TBP is part of the GTF TFIID, which also aids in promoter recognition (reviewed in Kadonaga, 2012). Subsequently, TFIIA and B bind to TFIID, stabilize it, and recruit RNAPII in complex with TFIIF (Imbalzano et al., 1994; Sawadogo and Roeder, 1985). All GTFs then assist RNAPII in TSS selection and together form the Preinitiation complex (PIC). Next, TFIIE

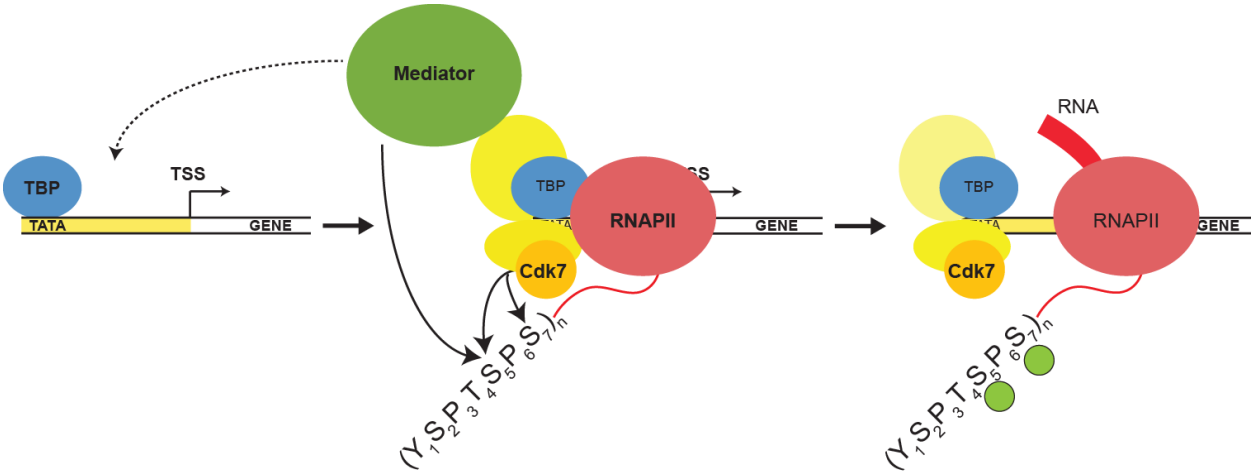

Figure 4: Simplified model of transcription initiation. Transcription initiation starts with the binding of TBP to the TATA box and subsequent assembly of the supercomplex with GTFs (yellow), RNAPII and Mediator, which is known as the PIC. Conversion of the PIC from the closed to the open complex state leads to initial transcription. Cdk7p and/or Mediator subunit Cdk8p phosphorylate Serine-5 and Serine-7 of the Rpb1 CTD, which leads to the release of RNAPII from the GTFs and represents an early state of actively transcribing RNAPII. See text for more information.

and H bind to the PIC and convert it from closed to an open formation, resulting in DNA strand melting and synthesis of the first few nucleotides by RNAPII (Holstege et al., 1996). Not only GTFs play an essential role in transcription initiation, but also Mediator, a multisubunit co-activator complex with crucial functions in transmitting regulatory signals to RNAPII, transcription initiation, pausing and elongation, chromatin remodeling and opening (reviewed in Allen and Taatjes, 2015).

The catalytic subunit of this complex is the RNAPII subunit Rpb1, which has a long, unstructured C-terminal domain (CTD) consisting of heptapeptide repeats (reviewed in Zaborowska et al., 2016). The number of repeats vary from 26 to 52 repeat units from budding yeast to mammals and harbor the canonical amino acid sequence $Y_1S_2P_3T_4S_5P_6S_7$ (see Figure 4). Similar to PTMs on histones, phosphorylation of the different residues in the CTD attracts a multitude of different reader and effector proteins and is essential for efficient transcription and processing of every RNA (Nonet et al., 1987). Important for the release of RNAPII from the GTFs is the phosphorylation of Serine-5 (Serine-5P) and partially Serine-7 (Serine-7P) on the CTD (Glover-Cutter et al., 2009; Hengartner et al., 1998). This is catalyzed mainly by the TFIIH subunit Cdk7p (Mcs6 in *S. pombe*) and partially by the Mediator complex subunit Cdk8p (Srb10)

(Akoulitchev et al., 2000). CTD phosphorylation activates the polymerase activity of Rpb1 and weakens the interactions of the RNAPII complex with the GTFs. This is crucial, because TFIIB hinders Rpb1 from transcribing more than four nucleotides (nt) long transcripts by sterical interference (Kostrewa et al., 2009). Loss of TFII subunits then leads to a switch from a promoter-bound state to a promoter-proximal state at the TSS, wherein RNAPII starts transcribing longer transcripts of 25-50 nt (Rasmussen and Lis, 1993). This in turn stabilizes the RNAPII-DNA interactions and thereby represents a state of early elongation (Liu et al., 2011).

2.1.2. Transcription elongation

The mechanism of transcriptional elongation is not completely conserved between *S. cerevisiae, S. pombe*, and metazoans. Whereas *S. cerevisiae* shows a rather uniform RNAPII occupancy over genes, metazoan and *S. pombe* show a characteristic promoter-proximal pause site approximately 25 - 50 bp downstream of the TSS, which divides elongation into early elongation upstream and productive (late) elongation downstream of this site, respectively (Booth et al., 2016; Nechaev and Adelman, 2011; Steinmetz et al., 2006). An important role in transcriptional elongation has the Spt4/5 heterodimer, an essential complex conserved back to bacteria (Harris et al., 2003). Functional conservation may not be complete, because Spt4/5p in *S. cerevisiae* has so far only been characterized for acting as a stimulant for transcriptional elongation (Hartzog and Fu, 2013). In metazoans, Spt4/5 has both inhibitory and activating roles

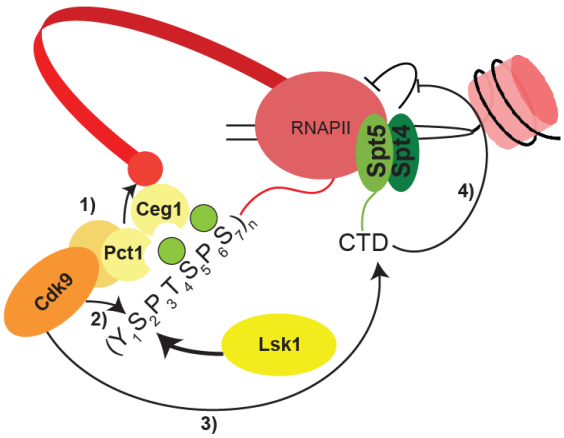

Figure 5: Model of the transition from early to productive elongation step. 1) Serine-5P recruits the capping enzyme complex, which adds the essential cap structure to the nascent transcript. 2 & 3) The cap complex interacts with Cdk9, which phosphorylates Serine-2/5 on Rpb1 and Spt5. In concert with Cdk9, Lsk1 is responsible for bulk Serine-2 phosphorylation. 4) Phosphorylation of Spt4/5 converts it from a negative into a positive elongation factor and RNAPII is released from the pause state and starts transcribing productively. See text for more information.

depending on the phosphorylation status of Spt5 (see Figure 5, Yamada et al., 2006). Loss of the TFII complexes allows Spt4/5 binding to the now accessible surface of RNAPII and initially leads to a block of productive elongation, perhaps through direct interaction with nascent RNA (Martinez-Rucobo et al., 2011). This roadblock has the function to act as a quality control checkpoint ensuring proper capping of the mRNA by capping enzymes, which are recruited directly via interaction of the capping enzymes Pct1 and Ceg1 with Serine-5P (Martinez-Rucobo et al., 2015; Pei et al., 2001). The capping enzymes themselves have important roles in promoting Cdk9, a crucial CTD kinase for the next step in transcription, the transition of RNAPII from early to productive elongation (Pei et al., 2003).

Also Serine-5P has important roles in this transition by helping to recruit Cdk9, the catalytic enzyme of the positive transcriptional elongation factor b (pTEFb) complex. Cdk9 is essential for Spt5 phosphorylation and therewith changes Spt4/5 from a negative to a positive elongation factor and controls the switch from early to late (productive) elongation (Yamada et al., 2006). This is likely due to a reduced interaction of phosphorylated Spt4/5 with capping enzymes and an increased interaction with the RNA polymerase II-associated factor 1 complex (Paf1C), a critical factor for productive elongation (Wier et al. 2013, see also chapter 2.2.1). Although Cdk9 was proposed to be the responsible kinase for Serine-2, the hallmark of elongating RNAPII, it rather phosphorylates Serine-5 *in vitro* (Czudnochowski et al., 2012). The current model suggests that the low activity of Cdk9 towards Serine-2 at the 5'-end of the gene recruits the actual Serine-2 kinase Lsk1 (CDK12 in metazoans), which is responsible for the bulk of Serine-2P within the gene body *in vivo* during productive elongation (Viladevall et al., 2009).

In productive elongation, Serine-2P levels constantly increase over the gene body, whereas Serine-5P levels start declining and the ratio of these two marks is believed to dictate binding and loss of elongation factors (reviewed in Kwak & Lis 2013). Many of them are histone-modifying complexes, ranging from general chromatin modification platforms, such as Paf1C, to specific histone methyl- or acetyltransferases, demethylases and deacetylases, which may provide some

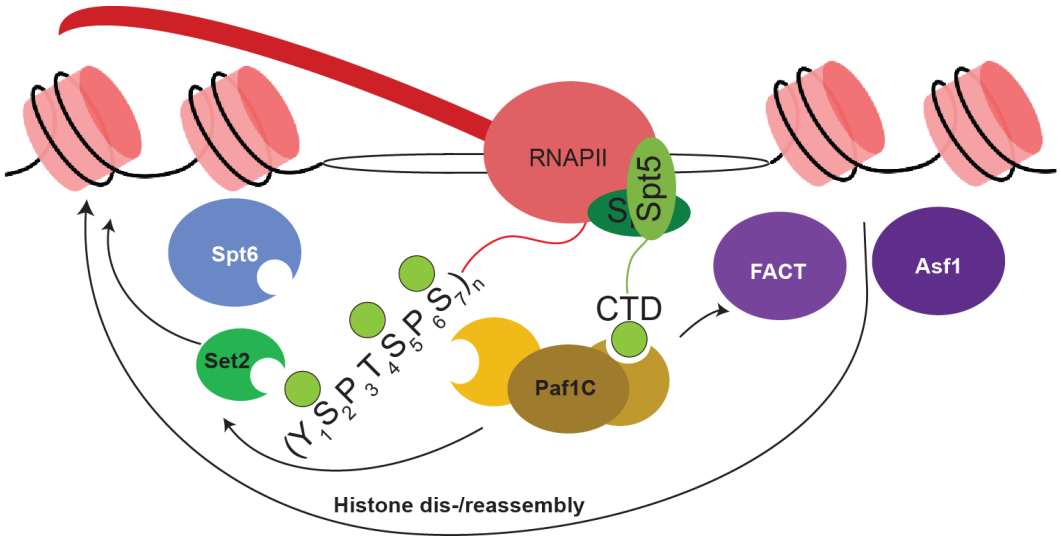

Figure 6: Simplified model of productive elongation during transcription. Concomitant phosphorylation of Serine-2 and Serine-5 on Rpb1 or Spt5-P recruits Paf1C, which is the main platform in orchestrating transcription elongation. Amongst the recruited proteins are FACT and Asf1, which are histone chaperones important for histone reassembly. Chromatin remodeler Spt6 recognizes Serine-2P and recruits Set2, which also can recognize Serin-2/5p. See also text and chapter 2.2 for more information.

feedback stimulus for transcribed genes (see Figure 6 and chapter 2.2). Specifically, concomitant phosphorylation of Serine-2 and -5 seems to specifically recruit Paf1C and Set2 (Kizer et al., 2005; Qiu et al., 2012), but also important RNA processing factors, such as splicing or export factors (David et al., 2011; Harlen et al., 2016; MacKellar and Greenleaf, 2011). A different CTD residue, Threonine-4 is phosphorylated during elongation and proposed to regulate splicing together with Serine-5P (Harlen et al., 2016).

During transcription, nucleosomes are reoccurring obstacles, which have to be correctly removed and reinserted. This is achieved by the actions of the FACT (Facilitates chromatin transcription) complex, a histone chaperone that removes and reinserts a H2A/B dimer from the nucleosome, thus allowing the polymerase to transcribe the DNA without displacing the remaining hexamer (Belotserkovskaya et al., 2003). Spt6 is a different histone chaperone and a nucleosome reorganizer with additional roles in gene activation and important for the recruitment of H3K36 methyltransferase Set2 (DeGennaro et al., 2013). Spt6 acts in a different mechanism than FACT by directly interacting with Histone H3 (Bortvin and Winston, 1996) and is recruited behind the elongating polymerase by interaction with Serine-2P (Yoh et al., 2007). Other elongation factors

play a role in overcoming various difficulties during transcription, such as backtracking for proofreading of the transcript and resuming of transcription after transcriptional arrests, which is orchestrated by TFIIS (tfs1 in *S. pombe*, Kettenberger et al. 2003).

Although crucial in fine-tuning and terminating transcriptional processes at the right place, phosphatases have not been elucidated in detail. Whereas Fcp1 localizes to both ends of the gene to direct Serine-2P dephosphorylation, Ssu72 dephosphorylates Serine-5/7P in the gene body (Cho et al., 2001; Schwer et al., 2015). However, much information about the regulation and recruitment of phosphatases during transcription is still missing. Yet, with increasing Serine-2P, which peaks at the end of the gene body, and diminishing Serine-5P, transcription enters its last stage, where the transcript and RNAPII are released.

2.1.3. Transcription termination

In late elongation, transcription termination factors bind to the CTD of RNAPII to induce cleavage of the nascent transcript and the eventual release of the transcription machinery (see Figure 7). Serine-2P plays an important role in this mechanism, because it is specifically recognized by two termination factors Pcf11, an important scaffold protein for the cleavage and polyadenylation factor (CPF), and transcription termination factor Rtt103 (Licatalosi et al., 2002; Lunde et al., 2010). CPF is a multisubunit complex responsible for the correct 3'-end processing and subsequent polyadenylation of the transcript (reviewed in Porrua & Libri 2015). Binding of CPF does not only require the interaction of CPF with RNAPII, but also specific sequences on the transcribed RNA: Once the polyadenylation signal (PAS) is transcribed and present on the transcript, it is recognized by other CPF subunits and stimulates the cleavage of the transcript 15 - 30 nt downstream of the PAS by CPF subunit CPSF73 and subsequent release from RNAPII and polyadenylation (Ryan et al., 2004).

Interestingly, premature binding of Pcf11 and Rtt103 to RNAPII is prevented by phosphorylation of Tyrosine-1 of the CTD, a recently identified mark that peaks shortly before the

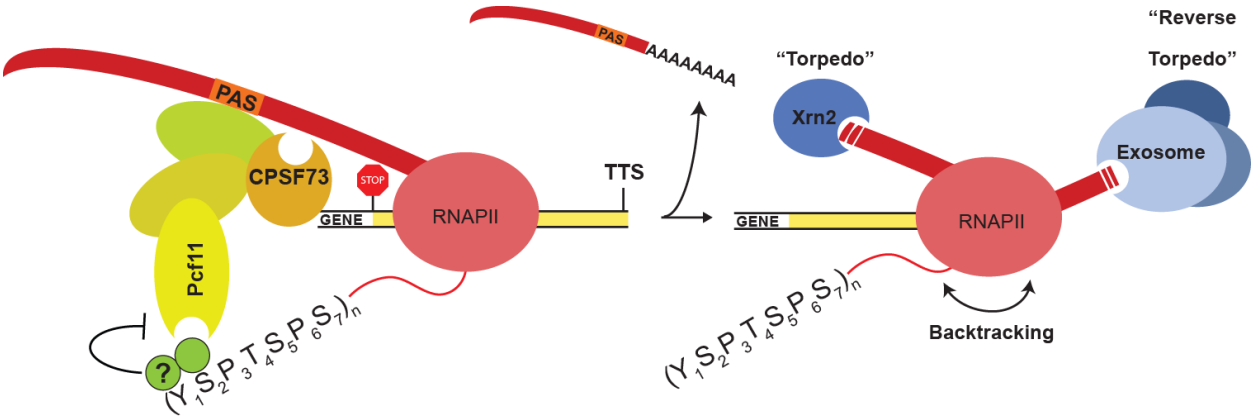

Figure 7: Transcription termination. At the end of the transcription, Serine-2P dominates over Serine-5P and is recognized by Pcf11. Furthermore, other signals of the polyadenylation site (PAS) and potential Tyrosine-1P fine-tune the activity of the CPF complex, which eventually cleaves the nascent transcript and adds the polyA-tail to the released transcript. The still transcribing RNAPII is then terminated by the action of exonucleases and/or other modulatory signals. For the "torpedo" model, 5'-3' exonuclease Xrn2 degrades the cleaved 5'-end of the transcript, whereas the exosome is proposed to degrade the RNA and release RNAPII from the 3'-end of the transcript, made available through backtracking ("reverse torpedo" model). See text for more information.

cleavage occurs. Tyrosine-1P is similarly distributed as Serine-2P but drops shortly before the PAS, thus allowing CPF to bind and cleave (Mayer et al., 2012). However, this mechanism has been only described in *S. cerevisiae* so far and research on metazoans suggested a different function for Tyrosine-1P (reviewed in Jeronimo et al., 2016). Yet, timely recruitment of transcription termination is crucial in determining the length of the 3'-untranslated region (3'-UTR), which has extensive impact on transcript stability, localization, and translation.

RNAPII stays associated with DNA also after the cleavage of the transcript, but the exact mechanism of RNAPII release is still not fully understood. Although different models exist, the so-called "Torpedo model" has been partially elucidated (see Figure 7). In this scenario, Rtt103 recruits the 5' - 3' exonuclease Xrn2 (Dhp1 in *S. pombe*), which then "chases" the transcribing RNAPII by degrading its unprotected 5'-end (Kim et al., 2004b). Other models such as the "reverse torpedo" model include other important complexes such as the 3' - 5' exosome complex, which is proposed to degrade 3'-unprotected transcripts after RNAPII backtracking (Lemay et al., 2014).

2.2. Chromatin modifying enzymes in transcription

A plethora of chromatin modifiers is recruited to the transcribing polymerase by phosphorylation-specific interactions with the CTD of RNAPII or by recruiting platforms, such as Mediator or Paf1C. These complex, but well-coordinated recruiting mechanisms result in relatively distinct CTD and histone PTM patterns across the transcription unit (Figure 8, left panel).

2.2.1. RNA polymerase II-associated factor 1 complex (Paf1C)

As mentioned above, the Paf1 complex is a central platform in recruiting various histone-modifying enzymes and well conserved throughout eukaryotes. Besides its crucial function in transcription, the Paf1 complex has important roles in other cellular processes, such as DNA repair, the cell cycle and even signaling in mammals (reviewed in Tomson & Arndt 2013).

In *S. pombe*, Paf1C consists of the subunits Paf1, Cdc73, Tpr1 (Ctr9p in *S. cerevisiae* and mammals), Leo1, and possibly Prf1 (Rtf1p), which is a known member of Paf1C in *S. cerevisiae*, but not part of the complex in metazoans (reviewed in Jaehning 2010). In *S. pombe*, Prf1 does not stably associate with Paf1C, but rather acts as an individual player in regulating histone

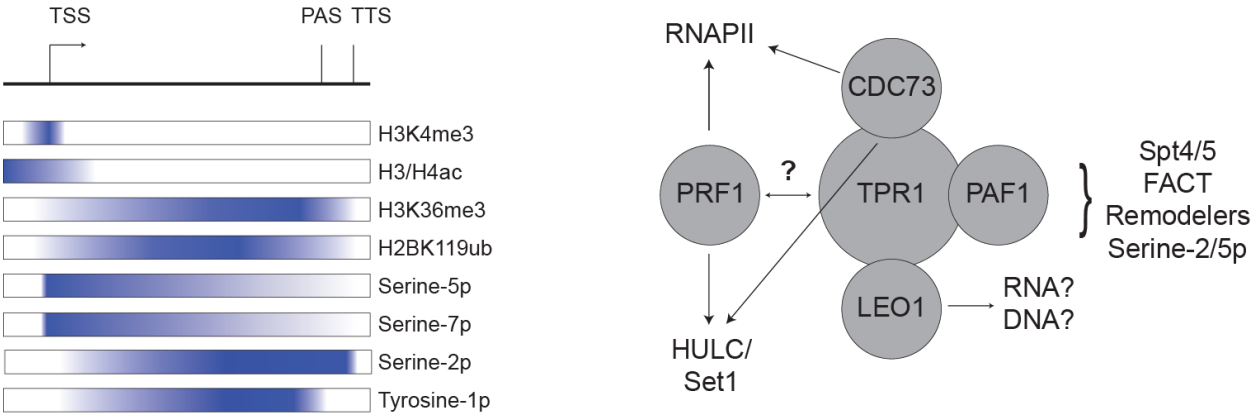

Figure 8: Crosstalk between histone modifications and transcription stages. Left panel: Distribution pattern of multiple PTMs on histones and on the Rpb1 CTD across a transcriptional unit. TSS: transcription start site; PAS: Polyadenylation site; TTS: Transcription termination site; ac: acetylation. Only PTMs discussed in this chapter and present in *S. pombe* are shown. Right panel: Overview of the organization and functions of the Paf1 complex. Since Prf1 may act as an individual player in transcriptional control, it is shown as separate unit. Paf1C regulates multiple steps in transcription and the CTD phosphorylation state; therefore, multiple effects may be indirect. See text for more information.

modifications (Mbogning et al., 2013). Paf1C coordinates proper transcription on multiple levels and hence associates with RNAPII throughout transcription (see Figure 8, right panel). This association is partially mediated by specific interaction of Cdc73 with the phosphorylated form of the CTD of RNAPII, but also with the Spt5-CTD (Qiu et al., 2012). Interaction with RNAPII also feeds back and enhances CTD Serine-5 phosphorylation, as deletion of Paf1C subunits affects Serine-5 phosphorylation levels (Mbogning et al., 2013). Furthermore, Leo1 can bind nucleic acids *in vitro*, which may stabilize Paf1C on the nascent transcript (Dermody and Buratowski, 2010). Despite its unclear affiliation in Paf1C, Prf1/Rtf1p independently associates with RNAPII via its Plus3 domain (Wier et al., 2013).

Once Paf1C is associated with RNAPII, it helps recruit important histone modifiers, amongst them the Set1/COMPASS complex, which trimethylates H3K4, a histone modification associated with the TSS (see chapter 2.2.2, Ng et al., 2003a). Supporting this interaction, deletion of Paf1C subunits leads to a loss of H3K4me3 and another conserved PTM, H2BK119 ubiquitination (H2BK120 in metazoans). Responsible for H2B ubiquitination is the histone ubiquitin ligase complex (HULC, see chapter 2.2.7) and the human Paf1C was shown to directly interact with a HULC subunit, the E3 ubiquitin ligase RNF20/40 (Brl1/2 in *S. pombe*, Hahn et al., 2011). Furthermore, Rtf1p is sufficient to promote H2B ubiquitination *in vitro*, likely due to direct stimulation of HULC subunit Rad6p (Rhp6) (Piro et al. 2012; Van Oss et al. 2016). In *S. cerevisiae*, the Paf1 complex stimulates not only H2B ubiquitination, but also affects the levels of H3K36me3 (Chu et al., 2007). This observation however, could be an indirect effect due to reduced Serine-2P levels in Paf1C mutants and is not conserved to *S. pombe*, wherein Paf1C mutants show unchanged H3K36me3 levels (Mbogning et al., 2013). Besides regulating histone modifications, Paf1C also helps recruiting transcriptional elongator complexes, such as FACT and Spt6 (Adelman et al., 2006) and has been linked to promote 3'-end processing: In addition to the mentioned stimulation of Serine-2P, Paf1C directly interacts with subunits of the CPF complex in *S. cerevisiae* and human cells (Nordick et al., 2008; Rozenblatt-Rosen et al., 2009).

Last but not least, our group could show that Paf1C is an important repressor of *de novo* heterochromatin formation in euchromatin in *S. pombe* (see Results, Kowalik et al., 2015). Intriguingly, all Paf1C members including Prf1 were found to repress ectopic siRNA-mediated heterochromatin formation. Yet, the exact mechanism of this repression remains to be elucidated, although literature suggests that impaired transcription termination or reduced histone turnover may be responsible (see Aim, Kowalik et al., 2015; Sadeghi et al., 2015).

2.2.2. H3K4 methyltransferase Set1/COMPASS

Trimethylated H3K4 is a euchromatic PTM typically residing at the transcription start site of genes (Ng et al., 2003a; Santos-Rosa et al., 2002; Strahl et al., 1999). Whereas multiple enzymes can catalyze H3K4 methylation in mammals, H3K4 in yeast is methylated by the sole methyltransferase Set1/COMPASS complex (Roguev et al., 2001; Santos-Rosa et al., 2002). Serine-5 phosphorylation of RNAPII and Paf1C are both essential for the recruitment of Set1 to the TSS (Ng et al., 2003a). The levels of H3K4me3 are controlled by demethylases, which are Jmj2 and Lid2 in *S. pombe*, whereas in *S. cerevisiae* only Jhd2p has been identified so far (Huarte et al., 2007; Li et al., 2008; Tu et al., 2007).

H3K4me3 is recognized by many different reader proteins, which are part of other multisubunit complexes with very diverse roles (reviewed in Vermeulen & Timmers 2010). Depending on the cell type, developmental state, or stress condition, H3K4me3 readers can induce transcriptional activation, remodel chromatin or lead to transcriptional repression. In order to ensure the specificity and to fine-tune these H3K4me3 readers, multiple ways of regulation evolved, ranging from different H3K4me3 affinities, effects of combinatorial PTMs within the histone code, to sequence-specific interactions with DNA.

A large constituent of H3K4me3 readers are lysine acetyltransferase (KAT) complexes, previously named HAT (histone acetyltransferase). Due to their roles in non-histone protein acetylation, KAT has emerged as a new nomenclature (Allis et al., 2007). Many KATs contain a

H3K4me3 reader domain and are thought to acetylate the nucleosome around the TSS to facilitate transcription (reviewed in Zhang et al. 2015). Nevertheless, KDAC (lysine deacetylase, formerly known as histone deacetylase [HDAC]) complexes also have H3K4me3 recognition domains and a model implies the dynamic histone acetylation and deacetylation cycle in promoting transcription initiation (Aoyagi and Archer, 2007).

2.2.3. Acetyltransferase and Deubiquitinase complex SAGA

Due to recognition of H3K4me3, KATs get recruited to the TSS and therefore acetylated H3 and H4 are usually associated with TSSs (Liang et al., 2004). Furthermore, KATs also interact with GTF subunits and are thought to act simultaneously or even upstream of PIC formation to open up chromatin by acetylation of histones. This is exemplified by a prominent co-activator, the SAGA (Spt-Ada-Gcn5-acetyltransferase) complex, which even contains proteins that were originally identified as TFIID subunits (Grant et al., 1998). SAGA acetylates several histone lysine residues, which then serve as a binding platform for the TFIID subunit Taf1 to stimulate transcription (Jacobson et al., 2000). Furthermore, SAGA can confer transcriptional activity *in vitro* even in the absence of TFIID, emphasizing the impact of SAGA on multiple targets in transcription (Wieczorek et al., 1998).

Besides its function in histone acetylation, SAGA contains a DUB (deubiquitinase) module, which deubiquitinates H2BK119ub on nucleosomes and is proposed to increase Lsk1-mediated Serine-2 phosphorylation (Wyce et al., 2007). SAGA can deubiquitinate H2B also in the context of an evicted H2A/B dimer and thus it is still unknown if deubiquitination occurs in front of or in the wake of transcription (see also chapter 2.2.7, reviewed in Morgan & Wolberger 2017).

Whether acetylation marks have position-specific roles was under debate for a long time, as some views postulated a role as a binding platform for reader proteins and others rather favored a simple position-independent, electrostatic effect (Dion et al., 2005; Kurdistani et al., 2004). However, with the discovery of acetyl-lysine recognizing bromodomains, it became clear

that acetylation marks also serve as binding platforms for many reader proteins, thereby adding another regulatory layer of complexity (Dhalluin et al., 1999). Bromodomain proteins are usually subunits of activating enzymes such as KATs or chromatin remodelers, suggesting that KATs could induce a positive feedback mechanism by reading their own mark, a widespread phenomenon of chromatin readers. Furthermore, bromodomain proteins are of high interest for pharmaceutical research, because they are often misregulated in cancer and may represent good targets for specific inhibitors (Filippakopoulos et al., 2010; Jain, A. K. and Barton, 2016).

2.2.4. H3K36 methyltransferase Set2

Whereas H3K4me3 marks TSSs, H3K36me3 is prevalent across the gene body and correlates with transcription (Morris et al., 2005). Similar to Set1-mediated H3K4 trimethylation, H3K36me3 is deposited by a single enzyme in *S. pombe*, Set2 (Morris et al., 2005). During transcription, Set2 is recruited by recognition of a double phosphorylated CTD at Serine-2P and Serine-5P via its C-terminal SRI (Set2 Rpb1 interaction) domain (Kizer et al., 2005; Xiao et al., 2003). In *S. pombe*, deletion of the SRI domain abolishes H3K36 trimethylation, but retains H3K36 mono- and dimethylation (Suzuki et al., 2016). Furthermore, Paf1C, Cdk9p, and Serine-2P levels influence the stability of Set2p in *S. cerevisiae* and thus promote efficient H3K36 trimethylation (Fuchs et al., 2012b). H3K36 methylation levels are regulated by demethylases, such as Jhd1p and Rph1p in *S. cerevisiae* (Kim and Buratowski, 2007). In *S. pombe,* the homologues of Jhd1p and Rph1p are essential and have not been studied in detail.

Di- or trimethylated H3K36 provides a binding platform for the major KDAC in transcription, the Clr6C-II complex (Rpd3S complex in *S. cerevisiae* and humans, see Figure 9). Importantly, dimethylated H3K36 is sufficient to recruit this KDAC, therefore the exact function of H3K36me3 is still unknown (Li et al., 2009a; Suzuki et al., 2016). H3K36me-mediated recruitment of Clr6C-II/Rpd3S leads to deacetylation of nucleosomes (see below and Figure 9), but H3K36me3 also impedes the recruitment of histone chaperone Asf1, which prevents the incorporation of

newly acetylated histones, thus enforcing the hypoacetylated state of nucleosomes in the gene body (Venkatesh et al., 2012). Additionally, specific chromatin remodelers such as Isw1 and Chd1 get recruited to H3K36 methylated regions in order to ensure proper reassembly of nucleosomes in the wake of transcription (Smolle et al., 2012).

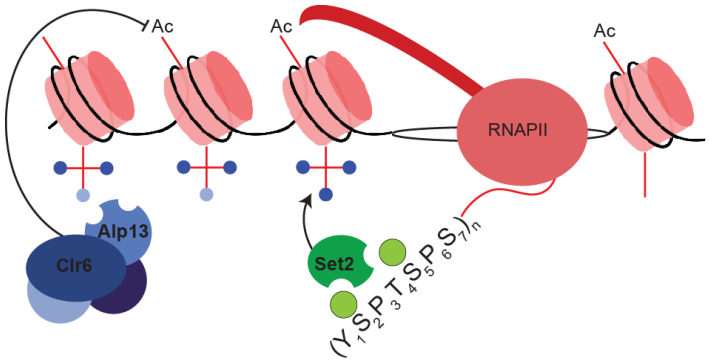

Figure 9: Role of Set2 and H3K36 methylation in transcription. CTD and Paf1C-mediated recruitment of Set2 leads to methylation of K36. This mark in turn is bound by Clr6C-II, which deacetylates acetylated histone and thus protects from aberrant transcription initiation. See text for more details.

2.2.5. Deacetylase complex Clr6C

KDAC Clr6 and its budding yeast homologue Rpd3p exist in multiple complexes and contain a sub form that is responsible for bulk histone deacetylation in gene bodies, namely Clr6C-II and Rpd3S, respectively (Carrozza et al., 2005; Nakayama et al., 2003; Nicolas et al., 2007). Two alternative complexes, called Clr6C-I and Rpd3L, respectively, have not been characterized extensively, but play important roles in gene-specific promoter repression and transcriptional directionality (Kadosh and Struhl, 1997; Nicolas et al., 2007; Zilio et al., 2014).

Clr6C-II and Rpd3S are recruited to chromatin via their subunits Alp13 and Eaf3p, respectively, which specifically recognize di- and trimethylated H3K36 (Carrozza et al., 2005; Nakayama et al., 2003; Nicolas et al., 2007). Both complexes then deacetylate nucleosomes, which is proposed to suppress spurious transcription within the gene body (see Figure 9). Although a clear mechanism is still missing, it seems conceivable that hypoacetylated histones cannot act as binding platform for the transcription initiation machinery and thus impair cryptic transcription initiation. Both deposition and recognition of H3K36 methylation is essential for this suppression, since deletion of Set2 or Alp13/Eaf3p lead to increased antisense transcription within the gene body (Carrozza et al., 2005; Nicolas et al., 2007). In *S. cerevisiae*, Rpd3S is

interacting with the Serine5-p of the transcribing polymerase, thus providing a direct link between deacetylation and transcription (Govind et al., 2010).

2.2.6. Acetyltransferase complex Mst2C

The Mst2 complex (Mst2C) in *S. pombe* was identified ten years ago as a negative regulator of telomere silencing (Gómez et al., 2005). Upon deletion of *mst2*$^{+}$, subtelomeres showed increased silencing which was dependent on the presence of the KDAC Sir2, suggesting that enhanced deacetylation of telomeric regions is responsible for the observed silencing. Research from the Jia group also indicates a role of Mst2C in counteracting heterochromatin at the centromeres, which is dependent on the RNAi pathway (see Figure 10 and chapter 3.2.1.2): Concomitant inactivation of Mst2 and the RNAi pathway reduces this dependence, suggesting that removal of Mst2 bypasses the need of RNAi for heterochromatin maintenance (Reddy et al., 2011). Other results implied a function of Mst2 in counteracting ectopic heterochromatin formation in euchromatin, albeit in combination with the H3K9 demethylase Epe1 and on sites that already harbor low levels of H3K9 methylation (Wang et al., 2015).

Mst2 acetylates H3K14 on nucleosomes and thus acts redundantly with SAGA KAT Gcn5, the other H3K14 KAT in *S. pombe* (Wang et al., 2012). H3K14 acetylation is a hallmark of euchromatin, especially at TSS and concomitant deletion of Mst2 and Gcn5 results in a complete loss of H3K14 acetylation and renders cells more sensitive to DNA damage (Johnsson et al., 2009; Wang et al., 2012). Nevertheless, expression profiling of cells lacking either Mst2, Gcn5, or both proteins do not correlate much, suggesting that Mst2 and Gcn5 have different targets in the cell (Wang et al., 2012). This is supported by the fact that removal of Gcn5 does not bypass the need for RNAi for heterochromatin maintenance (Reddy et al., 2011). Intriguingly, H3K14R mutants which should mimic an unacetylated form of H3K14 (similar to a *gcn5Δmst2Δ*) show multiple additional phenotypes and lose heterochromatin completely (Mellone et al., 2003). This suggests that this lysine residue may be subject to multiple modifications and questions if solely H3K14 acetylation is responsible for the observed phenotypes (see Aim).

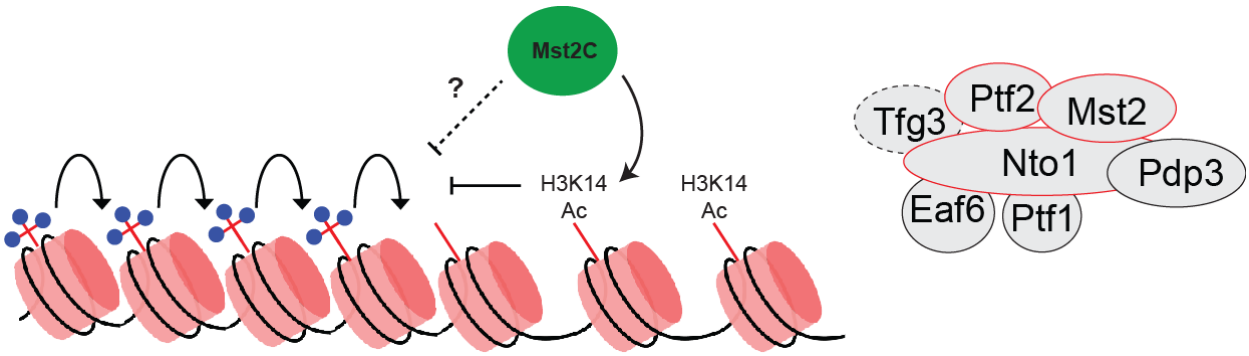

Figure 10: Function and complex composition of Mst2C. The main role of Mst2C is to prevent heterochromatin spreading. This inhibition is proposed to act via acetylation of H3K14, which impairs methylation of H3K9, a residue close by.
The Mst2 complex consists of 6-7 members as depicted in the right panel. Tfg3 is a pleiotropic factor present in multiple complexes and sometimes not considered as integral part of the Mst2C. Subunits essential for the KAT activity of Mst2C are circled in red. Besides the catalytic MYST domain of Mst2, the following subunits contain functional domains: Pdp3: PWWP domain (methylated histone residue recognition); Nto1: PHD finger; Ptf1: Phosphatase domain. See text for more details.

Characterization of the Mst2 complex identified multiple members, which are Mst2, Pdp3, Nto1, Ptf1, Ptf2, Eaf6 and associating factor Tfg3 (see Figure 10, Wang et al. 2012). Nto1 and Ptf2 have essential functions for the acetyltransferase activity of Mst2. Eaf6, Nto1 and Tfg3 are homologues to the *S. cerevisiae* NuA3 complex, suggesting good conservation from budding yeast to fission yeast. Indeed, NuA3 also contains a KAT (Sas3p) responsible for H3K14 acetylation, which acts redundantly with Gcn5p and removal of both KATs is synthetic lethal (Howe et al., 2001). Pdp3, Ptf1, and Ptf2 are unique to Mst2C, although a recent publication identified a Pdp3 homologue in *S. cerevisiae* to be associated as well with NuA3, thus creating a new form of that complex, called NuA3b (Gilbert et al., 2014). The synthetic lethality with Gcn5p is restricted to Sas3p but not Pdp3p, suggesting a distinct function for the NuA3b complex. The same publication also showed that Pdp3p recognizes specifically H3K36me3, which constitutes an alternative recruitment pathway to the canonical NuA3 subunit Yng1p, which binds to H3K4me3 (Gilbert et al., 2014; Taverna et al., 2006). Intriguingly, the Yng1p homologue is missing in Mst2C, suggesting a different way of Mst2C recruitment to chromatin. In addition, the Mst2C does not contain a bromodomain unlike other KATs, which implies that Mst2C may not be part of an acetylation reading/writing-based feedback loop.

2.2.7. H2B ubiquitination ligase complex HULC

HULC is a conserved complex in eukaryotes and ubiquitinates H2B at lysine K119 in *S. pombe* (hereafter referred to H2Bub, conserved as H2BK123 in *S. cerevisiae* and H2BK120 in metazoans, Tanny et al. 2007). It consists of four members, Brl1 and Brl2, which are E3 ligases important for the specificity, Rhp6, the actual ligating E2 enzyme and Shf1 with unknown function, yet essential for the activity (Tanny et al., 2007). HULC is highly conserved to *S. cerevisiae* and metazoans in complex composition and function (reviewed in Fuchs & Oren 2014; Tanny 2015).

Ubiquitination as a PTM is different from all other discussed modifications as it is a big moiety: Ubiquitin is a polypeptide of 76 amino acids and thus weighs almost as much as the actual histone (8.5 kDa vs 13 kDa). Polyubiquitination *per se* promotes degradation of the target proteins via the proteasome pathway, but monoubiquitination of histones has a signaling function (Bonnet et al., 2014). Specific monoubiquitination of H2B induces binding of adaptor proteins, alters the biochemical properties of the ubiquitinated histone, thus modulating higher order chromatin structures, and also affects the stability of ubiquitinated histones (reviewed in Fuchs and Oren, 2014). H2B ubiquitination has been linked to many molecular processes such as DNA damage response, cell cycle control, chromatin segregation, and even RNA splicing and processing, which affect major cellular processes such as apoptosis, tumorigenesis or differentiation. For the sake of brevity, I will discuss only the role of H2Bub in transcription elongation.

HULC is recruited to chromatin via different proposed interactions. In human, the Shf1 homologue WAC interacts preferentially with Serine-2P of the RNAPII CTD, thereby linking H2Bub directly to transcription (Zhang and Yu, 2011). Serine-2 kinase Cdk9 directly phosphorylates the budding yeast Rhp6 homologue Rad6p and stimulates its activity (Wood et al., 2005). Also Paf1C plays important roles in recruiting and stimulating HULC, because different subunits have been shown to interact with HULC in *S. cerevisiae* and human cells (Hahn et al., 2012; Ng et al., 2003b; Van Oss et al., 2016). In *S. pombe*, HULC activity is stimulated by Prf1

(Piro et al., 2012), which is intriguing due to the questioned role of Prf1 as Paf1C subunit. Recent research suggests that Prf1 is stimulatory for H2B ubiquitination, but dispensable for Paf1C functions and that a complex interplay including Cdk9, Spt5, Paf1C and Prf1 regulates transcriptional elongation (Mbogning et al., 2013; Sansó et al., 2012).

The exact function of ubiquitinated H2B is still not completely understood and most research on H2Bub function was done in *S. cerevisiae*, which seems to differ from *S. pombe* and metazoans. Central to its function is the dependence of important PTMs on H2Bub, such as H3K4 methylation, but also H3K79 methylation in *S. cerevisiae* and metazoans, a mark which is absent in *S. pombe* (Kim et al., 2005; Ng et al., 2002; Sun and Allis, 2002). This underlines the importance of H2Bub and puts it in the center in regulating chromatin modifications downstream of Paf1C. Besides that, much is still unclear, such as the stimulating role in H3K4 methylation. *In vitro* data suggests that H2Bub directly stimulates H3K4 methylation by Set1, but more detailed or structural studies are still missing (Racine et al., 2012). Also transcriptional elongation was proposed to be boosted by H2Bub via increased recruitment of Cdk9 (Sansó et al., 2012; Tanny et al., 2007). Since also deubiquitination of H2Bub by SAGA is promoting transcription, a model suggests that creating a dynamic ubiquitination/deubiquitination cycle is the actual boost in transcription elongation (Henry et al., 2003). Additionally, H2Bub also stimulates FACT-mediated histone disassembly and reassembly in the wake of transcription (Pavri et al., 2006). Indeed, H2Bub promotes nucleosome (re-)assembly, but at the same time prevents higher chromatin structures, thus creating an intermediate chromatin state (Batta et al., 2011; Debelouchina et al., 2016; Fierz et al., 2011). Reduced nucleosome reassembly in H2Bub mutants also leads to cryptic transcription, thereby linking H2Bub with H3K36me3 and histone deacetylation (Fleming et al., 2008).

Furthermore, H2Bub has been linked to protecting chromatin from being heterochromatinized, for example at the central core of centromeres, where a H2BK119R mutant has increased H3K9 methylation levels (Sadeghi et al., 2014).

3. Heterochromatin

Since the first characterization of heterochromatin ninety years ago, a vast amount of mechanisms, contributing factors, and pathways has been reported in many different model organisms. In general, one can distinguish between initiation of heterochromatin and its maintenance, which is ensured by the action of self-enforcing feedback loops. However, such feedback loops also preclude a chronological dissection of events in the initiation process (see Aim & Discussion). In this thesis, I will mostly focus on mechanistic insights involving histone modifications and the role of noncoding RNAs (ncRNAs) with special emphasis on my used model system *S. pombe* (see chapter 3.2). Unlike *S. pombe* and metazoans, *S. cerevisiae* uses a quite different system to establish silent chromatin. Yet, the mechanism of establishment is quite well understood and the counteracting functions of euchromatic marks have been partially elucidated. Therefore, I also quickly discuss *S. cerevisiae* as it provides an interesting and conceptually similar resource to understand the interplay between euchromatin and heterochromatin (see chapter 3.3). Finally, I would like to highlight the importance and conservation of heterochromatic feedback loops to higher organisms and therefore included a few examples from metazoans, which also induce heterochromatin by using ncRNAs (see chapter 3.4).

3.1. General characteristics of heterochromatin

In all eukaryotes, repressed regions are usually associated with important structural elements on chromosomes and tend to colocalise in the nucleus either to the nuclear periphery or the nucleolus (reviewed in Buhler & Gasser 2009). Heterochromatin can be divided into two classes:

Constitutive heterochromatin exists in all cell types and occupies telomeres, rDNA repeats and the pericentromeric regions (reviewed in Becker et al., 2016). The pericentromeric regions are insulating the central core of the chromosome, which is important for kinetochore assembly

during cell division (Takahashi et al., 2000). In yeast, heterochromatin also represses the mating-type region, which is important for proper mating-type switching (Egel, 1984).

Fundamental to these regions are repetitive DNA sequences that have to be repressed due to harmful recombination events, which would lead to chromosome fusion/loss or telomere shortening (Allshire et al., 1995; van Steensel et al., 1998). Heterochromatin also represses transposons, virus-based invader elements which have the ability to transpose (or copy) their DNA sequence in the genome. Such transposition events would affect genome organization and thus be detrimental for genomic stability and faithful inheritance of chromatin states (reviewed in Cordaux and Batzer, 2009).

Heterochromatin is characterized by increased chromatin compaction, which reduces the accessibility of transcription factors and of RNAPII (transcriptional gene silencing), but also by multiple co-transcriptional gene silencing mechanisms, which further lower the transcriptional output by degradation of transcripts (CTGS; see 3.2.2). A hallmark of constitutive heterochromatin in *S. pombe* and metazoans is H3K9me2/3, which is recognized by the heterochromatin protein 1 (HP1) (reviewed in Grewal and Jia, 2007). HP1 proteins are conserved across most eukaryotes and play crucial roles in heterochromatin spreading due to their oligomerization capacity (Canzio et al., 2011). Furthermore, HP1 proteins recruit KDACs, which deacetylate histones and thereby lead to increased chromatin compaction. Methylation of DNA cytosine is another repressive mark associated with heterochromatin in mammals, but since DNA methylation is absent in *S. pombe* it will not be discussed in detail here (for review see Li and Zhang, 2014).

Facultative heterochromatin is formed within euchromatin and is dynamic, as it exists only in certain cell types or developmental stages (Trojer and Reinberg, 2007). A major hallmark of facultative heterochromatin in metazoans is trimethylated H3K27. H3K27me3-mediated repression works via the Polycomb-repressive complexes (PRC) and is exemplified by inactivation of the second X chromosome in female cells, homeobox (HOX) gene cluster inactivation during development in mammals or repression of the important FLC locus in plants

(Davidovich and Cech, 2015). Facultative chromatin in metazoans can also carry H3K9 methylation instead of H3K27me3, for example in differentiated cells such as fibroblasts (Hawkins et al., 2010). Similarly, H3K9me2 marks facultative heterochromatin on meiotic genes in *S. pombe*, where H3K27 methylation is absent (Cam et al., 2005).

Much of the current understanding of how heterochromatin is formed, maintained, and controlled originates from an interesting observation in *Drosophila melanogaster* (*D. melanogaster*) by geneticist Hermann Muller in 1930. He was experimenting with X-ray beams, which led to rearrangements of genes in the genome, and observed that a mutagenized fruit fly offspring showed an unusual patterning of white and red eye units in its compound eye (see Figure 11 top; Muller, 1930). The responsible genetic determinant for eye color is the *white*$^+$ gene, which leads to white eyes when mutated (Morgan, 1910). The unusual patterning of red and white eye units suggested that the *white*$^+$ gene was not mutated, which would result in a completely white eye color. Closer examination of the chromosomal context revealed that an inversion translocated the *white*$^+$ gene proximal to a heterochromatic region and led to the definition of position effect variegation (PEV), since the position of the *white*$^+$ gene defines the variegating phenotype (reviewed in Elgin & Reuter 2013). The expression of *white*$^+$ is controlled by its chromatin context, more precisely by the distance heterochromatin spreads, which is a stochastic process. Once the chromatin context is defined, it is stably maintained

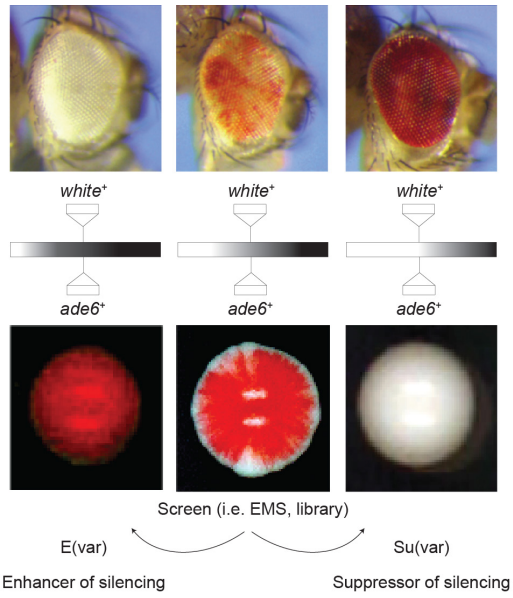

Figure 11: Position effect variegation in D. melanogaster (top) and S. pombe (bottom). Depending on the chromatin context, the reporter gene is silenced (left), expressed (right), or variegating (middle). This phenotype has been exploited to screen for enhancers and suppressors of silencing. See text for more information. Figure adapted from Elgin and Reuter, 2013.

throughout the development of each ommatidium (single eye unit), resulting in either white or red ommatidia (see Figure 11 top). This phenomenon describes the first identified epigenetic mechanism and by now, PEV has also been described for other organisms, such as yeast, plants, and mammals (Allshire et al., 1994; Rakyan et al., 2002; Sandell and Zakian, 1992). In addition, PEV has been exploited to screen for suppressors and enhancers of variegation leading to more red or more white cells and led to the identification of dozens of factors, called Su(var) or E(var), respectively (Reuter and Wolff, 1981; Schultz, 1950). Such screens have been extensively performed in fruit fly, fission yeast, and even mouse and identified many players in heterochromatin formation, spreading, and repression (Blewitt et al., 2005; Ekwall et al., 1999, see Figure 11 bottom). With the recent possibility to screen human haploid cell lines, also unexpected players have been identified, such as the HUSH (Human Silencing Hub) complex, which is not conserved to *D. melanogaster* and therefore could be only identified in mammalian cell lines (Tchasovnikarova et al., 2015).

3.2. Heterochromatin in *S. pombe*

Heterochromatin in *S. pombe* is similar to metazoans with the characteristic H3K9 methylation, histone hypoacetylation, and (co-)transcriptional gene silencing involving multiple RNA degradation machineries. Most parts of chromatin can be transcribed in *S. pombe*, including heterochromatin (Wilhelm et al., 2008), which provides a unique opportunity to investigate distinguishing features of heterochromatic and euchromatic transcription.

3.2.1. Formation of constitutive heterochromatin

Constitutive heterochromatin in *S. pombe* covers the rDNA repeats, the telomeres, the pericentromeric regions and the mating type locus (MTL) with a specialized machinery in each locus (the rDNA repeats are not further discussed here). Characteristic for all other three loci is the partial involvement of the RNAi, although additional pathways contribute to the nucleation of heterochromatin at the telomeres and mating type locus. Fundamental for heterochromatin formation are multiple conserved factors:

In a first step, H3K9 is methylated by the sole H3K9 methyltransferase Clr4, which forms the Clr4-Rik1-Cul4 complex (CLRC) with Rik1, Raf1, Raf2 and Cul4 (Allshire et al., 1995; Horn et al., 2005; Jia et al., 2005). H3K9me2/3 is bound by the HP1 homologues Swi6 and Chp2, but also by two other chromodomain-containing proteins Chp1 and Clr4 itself (Ekwall et al., 1995; Thon and Verhein-Hansen, 2000). Swi6 and Chp2 further contain a chromoshadow domain, which allows oligomerization and is proposed to mediate spreading of heterochromatin in combination with the reading/writing ability of Clr4 (Canzio et al., 2011; Sadaie et al., 2008; Zhang et al., 2008). Multiple KDACs are responsible for deacetylation of histones, such as Clr3, Clr6, and Sir2 to mediate transcriptional gene silencing (TGS) and are partially recruited by Swi6/Chp2 (Grewal et al., 1998; Shankaranarayana et al., 2003). A major effector complex in TGS is SHREC (Snf2/Hdac-containing Repressor Complex), which includes Clr1, Clr2, KDAC Clr3, and chromatin

remodeler Mit1. SHREC reduces access of RNAPII to chromatin and stabilizes nucleosomes (Aygün et al., 2013; Creamer et al., 2014; Job et al., 2016; Sugiyama et al., 2007). Nevertheless, RNAPII transcribes centromeric repeats also in intact heterochromatin, but transcripts are turned over quickly by multiple degradation mechanisms (Bühler et al., 2006, 2007; Keller et al., 2012; Volpe et al., 2002). This suggests that there are different modes of chromatin context-dependent transcription, from which heterochromatic transcription results in CTGS (see chapter 3.2.2).

3.2.1.1. Telomeres and mating type locus

Telomeres in *S. pombe* contain telomeric repeats, which flank the subtelomeric regions on chromosomes. Heterochromatin at the telomeric repeats spreads into subtelomeric regions, where it partially suppresses expression of subtelomeric genes (see Figure 12 left; Kanoh and Ishikawa, 2001). On a mechanistic level, the shelterin complex binds to the telomeric repeats via the subunit Taz1 and recruits SHREC and CLRC via its subunit Ccq1, which promote histone deacetylation and initiates H3K9 methylation (Kanoh et al., 2005; Sugiyama et al., 2007; Wang et al., 2016a). Adjacent to the telomeric repeats, the subtelomeric RecQ helicase genes *tlh1/2*$^{+}$ on

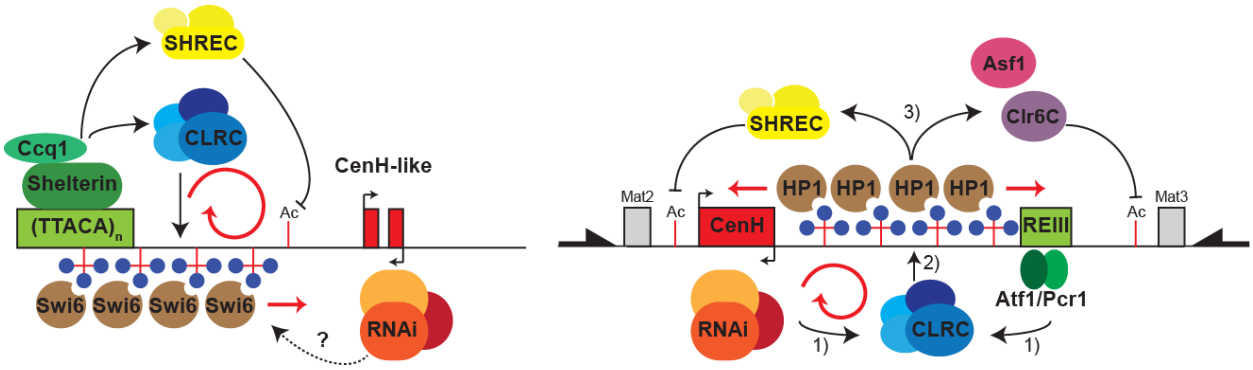

Figure 12: Heterochromatin at (sub)telomeres (left) and MTL (right). Heterochromatin at telomeres involves the Shelterin complex with Taz1 and Ccq1, which recruit CLRC and SHREC for H3K9me2. Swi6 binds to H3K9me2 and spreads across the chromosome, perhaps aided by the RNAi machinery, which is recruited via subtelomeric CenH-like elements. Heterochromatin at the MTL is initiated by two redundant mechanisms involving RNAi and Atf1/Pcr1, respectively (1). Recruited CLRC methylates H3K9 (2), which is bound by HP1 proteins Swi6 and Chp2, which recruit histone chaperones/Clr6C and SHREC, respectively (3). Red arrows indicated positive feedback loops and spreading of heterochromatin. Black arrows depict boundary elements at the MTL that impair further spreading. See text for more details.

subtelomeres IL and IIR harbor DNA sequences that are highly similar to a common repeat motif from the mating type region and centromeres, called CenH (Grewal and Klar, 1997). This DNA motif serves as binding platform for the RITS (RNA-induced transcriptional silencing) complex and leads to the generation of siRNAs (Cam et al., 2005). Hence, RNAi may promote heterochromatin formation at the CenH element and thus enforces subtelomeric silencing by either directly promoting CTGS or indirectly via H3K9me2-mediated recruitment of Swi6 and/or SHREC (Kanoh et al., 2005; Sugiyama et al., 2007).

Nucleation of heterochromatin at the mating type locus involves the RNAi pathway and the ATF/CREB transcription factors Atf1/Pcr1, which both act redundantly (Jia et al., 2004). Atf1 and Pcr1 bind to a specific DNA sequence, called the repressor element (REIII) element, and directly recruit Clr3, Clr4, Clr6 and Swi6 (Ekwall et al., 1991; Jia et al., 2004; Kim et al., 2004a). H3K9me2-dependent binding of Chp2 and Swi6 enhances silencing via the recruitment of Clr3-containing SHREC, whereas Swi6 also interacts with histone chaperone Asf1, which enhances nucleosome stability and recruits more Clr6C (Motamedi et al., 2008; Yamada et al., 2005; Yamane et al., 2011). Whereas these complexes deacetylate histone to enforce transcriptional silencing, RNAi acts *in cis* on the repeat-like CenH element and acts redundantly to Atf1/Pcr1 in maintenance of heterochromatin, but is important in establishment (Jia et al., 2004). Hence, the nucleating actions of RNAi at CenH and of Atf1/Pcr1 at REIII are both needed for establishing a stable heterochromatic domain, potentially through combined CTGS via RNAi and TGS via Atf1/Pcr1/Clr3/Clr6 (Noma et al., 2004).

3.2.1.2. Centromeric heterochromatin formation via RNAi

Centromeric heterochromatin is different to the mating type locus and telomeres by the strict dependence on the RNAi machinery for initiation and maintenance (Volpe et al., 2002). Loss of centromeric heterochromatin disrupts normal chromosome segregation (Allshire et al., 1995). Contrasting to telomeres and mating type region, a defined nucleation element has not been

identified, but it is the particular centromeric sequence and the RNAi pathway, which are fundamental to initiate and maintain the silent state:

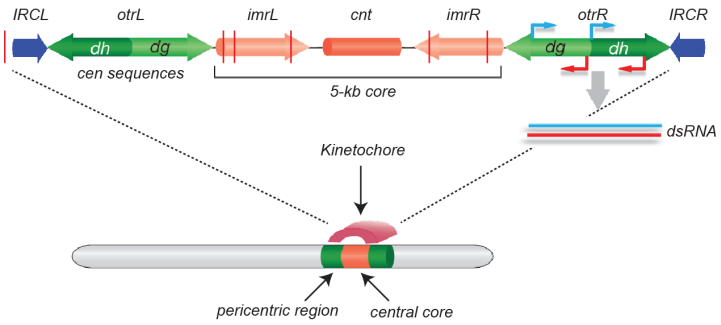

Figure 13: Map of S. pombe centromere I. The *otr*, *imr*, and *IRC* repeats are shown in green, red, and blue, respectively. *otr*s contain a varying number of *dg/dh* repeats amongst the three different chromosomes and are bidirectionally transcribed. Red bars represent tRNA genes, which often flank heterochromatic regions. See text for more details. Figure adapted from Martienssen and Moazed, 2015.

Similar to metazoans, all three centromeres in *S. pombe* consist of repetitive structures, which are divided into the innermost repeats (*imr*) and outermost repeats (*otr*, see Figure 13). These repeats flank on both sites the central core (*cnt*) of the chromosome, which provides the binding platform for kinetochore assembly during mitosis and is marked by the special histone H3 variant Cnp1 (reviewed in Buhler and Gasser, 2009). The *imr* repeats are somewhat less conserved (*i.e.* different on all three chromosomes) and lead to variegating phenotypes of inserted reporter genes, whereas the *otr* repeats are highly similar in sequence, strong silencers of reporter genes and contain the *dg* and *dh* repeat units (Takahashi et al., 1991; Verdel and Moazed, 2005). Outside of the *otr* repeats lie the inverted repeats (*IRC*), which sometimes constitute a boundary by preventing the spreading of heterochromatin outside of the pericentromeric region (Cam et al., 2005). Furthermore, tRNA genes also delimit heterochromatic regions due to their transcriptional activity and recruitment of boundary factors (see chapter 3.2.4, Takahashi et al., 1991).

RNAi as a silencing mechanism was first identified in the nematode *Caenorhabditis elegans* (*C. elegans*), where expression of double-stranded RNA (dsRNA) led to the silencing of a target gene (Fire 1998). Within the last twenty years, it became evident that RNAi is a conserved mechanism inducing gene silencing either post-transcriptionally by targeting the mRNA (post-transcriptional gene silencing; PTGS) or co-transcriptionally (CTGS) by targeting the nascent transcript on chromatin (reviewed in Holoch and Moazed, 2015). RNAi-mediated mechanisms

generally involve the processing of dsRNA by the endonuclease Dcr1 into small RNAs and their loading onto Argonaute protein-containing complexes, which then elicit the silencing by base-pairing to the complementary transcript. In *S. pombe*, the major role of RNAi lies in CTGS and the establishment of heterochromatin. Although PTGS has been reported in *S. pombe*, it will not be covered here (Egan et al., 2014; Sigova et al., 2004).

The current model of RNAi-mediated heterochromatin formation is thought to start by the transcription of the *dg/dh* repeats by RNAPII (see Figure 14, Chen et al., 2008; Kato et al., 2005). These transcripts are then reverse-transcribed by the RDRC (RNA-directed RNA polymerase) complex resulting in dsRNA (Colmenares et al., 2007; Volpe et al., 2002). RDRC and Dcr1 interaction is stabilized by the protein Dsh1, which also localizes the whole process to the nuclear

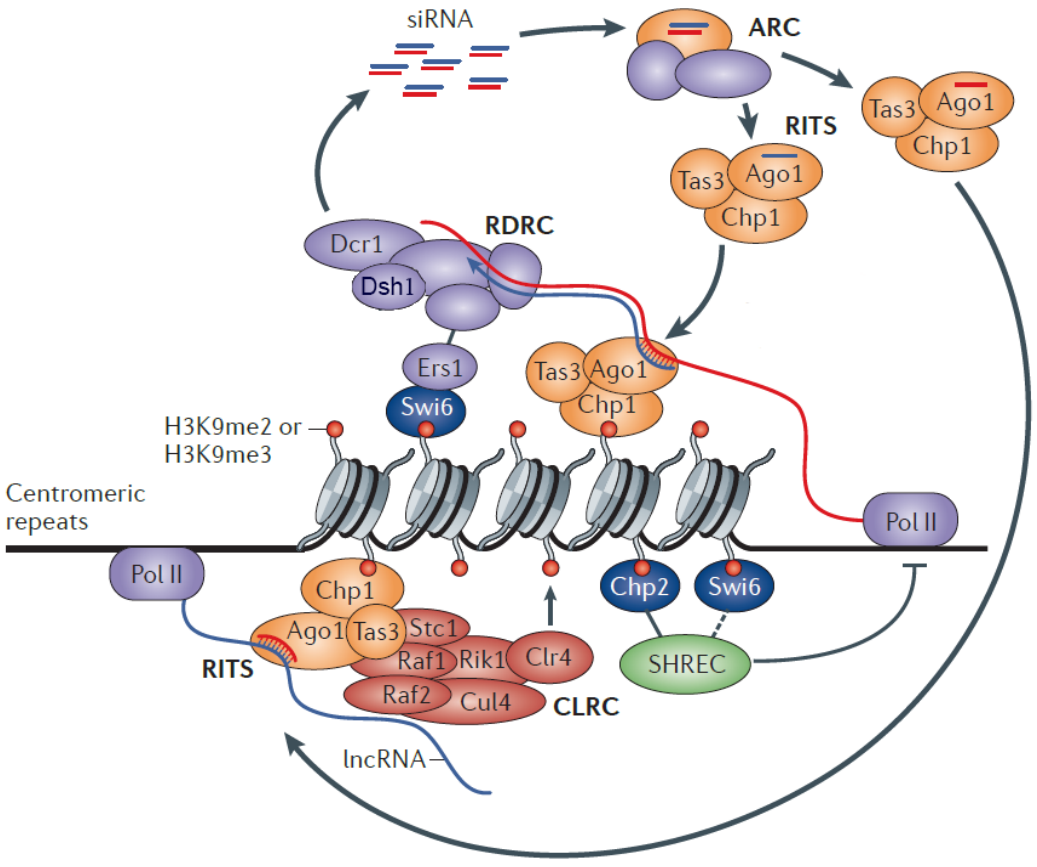

Figure 14: Model of RNAi-mediated heterochromatin formation. Arrows indicate the feedback loops involving RNAi. Additionally, RITS can oligomerize and CLRC and Swi6 can self-propagate due to their writer-reader function and oligomerizing capacity, respectively (not shown). See text for more details. Figure adapted from Holoch and Moazed, 2015a.

envelope (Colmenares et al., 2007; Kawakami et al., 2012). Dcr1 then cleaves these transcripts into 21 - 25 nt long siRNAs, which are loaded onto the Argonaute siRNA chaperone (ARC) complex, containing Ago1, Arb1, and Arb2 (Buker et al., 2007; Holoch and Moazed, 2015b). This complex transforms into the RITS complex by release of Arb1/2 and new association with Tas3 and Chp1, before the passenger strand of the bound dsRNA is released, probably via slicer activity of Ago1 (Jain et al., 2016; Verdel et al., 2004). Artificially tethered RITS is sufficient to induce *de novo* heterochromatin formation and thus acts as an amplifier of heterochromatin assembly by multiple mechanisms (Bühler et al., 2006):

1) The RITS complex binds directly to nascent transcripts in a transcription-rate dependent manner (Shimada et al., 2016), reinforcing their processing into small RNAs.

2) RITS subunit Ago1 directly interacts with RDRC subunit Hrr1 and also recruits the CLRC machinery via interaction with Stc1 (Bayne et al., 2010; Motamedi et al., 2004).

3) Chp1 recognizes H3K9me via its chromodomain and thus stabilizes RITS on heterochromatin (Partridge et al., 2002; Schalch et al., 2009). The chromodomain also has affinity to nucleic acids, which may reinforce RITS targeting to nascent RNA (Ishida et al., 2012).

4) Tas3 can oligomerise and thus spread along nucleosomes, sustaining H3K9 methylation (Li et al., 2009b; Stunnenberg et al., 2015).

Recruited CLRC then methylates H3K9 and allows subsequent binding of Swi6 to H3K9me2, which again recruits RDRC via Ers1 and is crucial in promoting CTGS (Hayashi et al., 2012; Keller et al., 2012; Rougemaille et al., 2012).

3.2.2. Mechanisms of gene silencing

KDACs induce TGS by deacetylating histone residues and thereby reduce the access of RNAPII or general transcription factors (see chapter 2). Important factors therein are Clr3/SHREC, Clr6C and Sir2. Also remodeling of nucleosomes by multiple chromatin remodelers

such as Mit1, Asf1/HIRA, or Spt6 facilitates higher order structures and contributes to TGS (see above; Kiely et al., 2011).

Nevertheless, RNAPII occupancy on heterochromatin genes is still significantly above background, suggesting that TGS contributes to, but is not fully responsible for the silent state of heterochromatin. A model proposes that RNAPII transcribes the heterochromatic regions during S phase, during which heterochromatin is decompacted to allow DNA replication (Chen et al., 2008; Kloc et al., 2008). This model attributes RNAi to function exclusively during S phase to reinitiate heterochromatin after replication. However, RNAPII occupancy only modestly changes during the cell cycle and siRNAs are generated throughout cell cycle, implying that transcription by RNAPII is not restricted to S phase. Furthermore, monitoring Swi6 dynamics as a readout of centromeric RNA production also suggests little differences throughout the cell cycle, implying that RNAi acts throughout the entire cell cycle (Stunnenberg et al., 2015). Hence it seems plausible that beside the contribution of RNAi in the degradation of heterochromatic RNAs (by processing them into siRNAs, (Schalch et al., 2011)), other RNA degradation pathways ensure the proper silencing of heterochromatin in a co-transcriptional manner, which led to the term CTGS (co-transcriptional gene silencing; Bühler et al., 2006). Swi6 plays a central role in CTGS, by recruiting multiple degradation factors by a still unknown mechanism. Amongst them is the Cid14-containing TRAMP complex, which mediates the degradation of nuclear aberrant transcripts and prevents them from being converted into siRNAs (Bühler et al., 2007, 2008). The current model implies that the RNA-binding activity of Swi6 evicts it from chromatin and feeds the bound transcript to TRAMP-mediated degradation (Keller et al., 2012). Furthermore, loss of RNA processing factors including the 3'-5' exonucleases Dhp1 (Xrn2), Triman and the exosome lead to loss of silencing, suggesting that heterochromatic transcripts get marked for degradation (Chalamcharla et al., 2015; Tucker et al., 2016; Zhang et al., 2011). In addition, Triman is important in the generation of primal siRNAs (priRNAs). These likely arise from degradation

products and are loaded onto Ago1, where Triman then trims the ends to the favorable length of 21 - 25 nt, priming them for action (Halic and Moazed, 2010; Marasovic et al., 2013).

3.2.3. Facultative heterochromatin

In general, ectopic heterochromatin formation in euchromatin has been inherently difficult to establish due to multiple euchromatic repression mechanisms (Iida et al., 2008; Simmer et al., 2010). Nevertheless, heterochromatin in fission yeast has been found on meiotic genes, retrotransposons and environmentally regulated genes (Cam et al., 2005; Zofall et al., 2012). Facultative heterochromatin on retrotransposons and environmentally genes is dependent on RNAi or RNA elimination factors, but is highly variable and its physiological role is not clear (Lee et al., 2013; Yamanaka et al., 2013). Facultative heterochromatin on meiotic genes is better understood, but investigation of these loci is hampered by additional post-transcriptional degradation of meiotic transcripts by the NURS complex (Egan et al., 2014). One subunit of this complex is Mmi1, which specifically recognizes a certain DNA element on meiotic genes, called the determinant for selective removal (DSR) (Harigaya et al., 2006). Besides directing meiotic transcripts to the NURS complex and subsequent degradation by the exosome machinery, Mmi1 also recruits RITS and CLRC to induce H3K9 methylation (Hiriart et al., 2012; Zofall et al., 2012). A recent publication linked Dhp1 to the induction of premature transcription termination and interaction with Mmi1 and CLRC for nucleation of heterochromatin (Chalamcharla et al., 2015).

In summary, facultative heterochromatin in *S. pombe* is marked by H3K9me2 and likely depends on the RITS complex. This makes these loci very attractive to study to elucidate the interplay between hetero- and euchromatic factors. However, studying facultative heterochromatin is difficult, as a clear dissection is either convoluted due to the co- and posttranscriptional regulation of such loci or it demands inactivation of important RNA surveillance factors, which could lead to artefacts. Therefore an unperturbed background would be ideal to study heterochromatin assembly in euchromatin (see Aim and Results; Kowalik et al., 2015).

3.2.4. Chromatin state boundaries

Chromatin states have to be propagated faithfully in order to maintain epigenetic robustness, therefore multiple boundary elements have evolved in order to protect spreading of heterochromatin into euchromatin and vice versa.

Stable boundaries

Stable boundaries contain a particular DNA element, which is bound by *trans*-acting factors to insulate this region. In mammals, an important insulator is CTCF, which binds a short DNA motif and was shown to separate active and repressive domains (Cuddapah et al., 2009). In yeast, the presence of tRNA genes restricts the spreading of heterochromatin around the centromere by recruiting TFIIIC/Sfc6, a transcription factor involved in RNAPIII transcription (Donze and Kamakaka, 2001; Noma et al., 2006; Scott et al., 2006). Assembly of the RNAPIII transcription machinery may not even be necessary, because TFIIIC brings the boundary to the nuclear periphery, which also demarcates a boundary element by sterically restricting heterochromatin spreading (Dilworth et al., 2005; Gerasimova et al., 1995).

Dynamic boundaries

Since most eukaryotes harbor multiple loci with facultative heterochromatin, the existence of boundaries for each individual facultative heterochromatic locus is unlikely. Hence, at these dynamic boundaries, a complex interplay between euchromatic and heterochromatic factors determines the extent of heterochromatin spreading (Wang et al., 2014). This spreading is usually dose-dependent, for example, HP1 levels determine the effect of PEV in *D. melanogaster* (Eissenberg et al., 1992). In *S. cerevisiae*, spreading of Sir2/3/4 and heterochromatin is counteracted by acetylation of H4K16 by Sas2 and the extent of heterochromatin depends on the protein ratio of Sir2p and Sas2p (Kimura et al., 2002).

In *S. pombe*, Swi6 plays a central role in guiding boundary formation at tRNA genes-free regions, such as the IRC1R locus, which lacks a clear boundary element. RNA-binding of Swi6 evicts it from chromatin and thus may render the boundary sensitive to transcription (Keller et al., 2012). Indeed, transcription of the ncRNA BORDERLINE (or a sequence-unrelated reporter) leads to a marked decrease of H3K9 methylation at IRC1R, which is dependent on the RNA-binding capacity of Swi6 (Keller et al., 2013). Boundary-forming transcription of ncRNAs has also been recently proposed to play a role in plants, although a clear mechanism is still missing (Böhmdorfer et al., 2016). Furthermore, deletion of *swi6*$^{+}$ leads to RITS-dependent spreading of H3K9 methylation, suggesting that Swi6 also controls RITS-mediated spreading (Stunnenberg et al., 2015). In addition to RNA eviction, Swi6 interacts with Epe1, an important antisilencing factor due to its putative H3K9 demethylase activity and recruitment of additional antisilencing proteins (Wang et al., 2013; Zofall and Grewal, 2006). In order to protect constitutive heterochromatic regions from Epe1 action, Epe1 is targeted for degradation by a heterochromatic E3 ligase complex Cul4-Ddb1^{Ctd2}, which results in the accumulation of Epe1 only at the boundaries of heterochromatin (Braun et al., 2011).

Similar to *S. cerevisiae*, acetylation of histone residues prevents spreading of heterochromatin. This is exemplified by the KAT Mst1, which acetylates H3K4. Acetylation H3K4 counteracts spreading by either restricting RITS or Clr4 from binding to nucleosomes and by recruiting boundary factors (Wang et al., 2013; Xhemalce and Kouzarides, 2010). Recruitment of Mst1 was further proposed to be regulated by Paf1C, suggesting a broader role of Paf1C in recruiting antisilencing factors (Verrier et al., 2015).

3.3. Silent chromatin formation in *S. cerevisiae*

The easy manipulation, fast growth and genetic advantages of yeast favored this model organism in investigating chromatin regulation. Yeast can grow as haploid or diploid cells and thus allows one to easily test mutants in complementation assays to dissect their genetic interactions (reviewed in Forsburg, 2001). Hence, *S. cerevisiae* has been widely used in characterizing important conserved features in eukaryotes such as DNA damage repair, replication, and signaling pathways, but also chromatin regulation. Although *S. cerevisiae* lacks pericentromeric heterochromatin, H3K9 methylation, and the RNAi pathway compared to higher eukaryotes, mechanisms of “silent” chromatin formation at telomeres, rDNA clusters, and mating type regions act conceptually similarly to higher eukaryotes (reviewed Gartenberg and Smith, 2016). This basic silencing system involves only a few proteins and hence offers a great opportunity to dissect general mechanisms of silent chromatin.

Silent chromatin in *S. cerevisiae* is characterized by rather unmodified, hypoacetylated histones especially lacking H4K16 acetylation and low H3K79 methylation, and the presence of the silencing complex, consisting of the heterotrimer Sir2p, Sir3p and Sir4p (Braunstein et al., 1993; Hecht et al., 1996). Establishment of silent chromatin is fairly well understood:

First, short DNA sequences of around 150 bp are bound by the specific DNA binding factors ORC1 (origin recognition complex) or Rap1p and/or Abf1p (Kimmerly et al., 1988). Combined binding of these factors then recruits the Sir2/3/4 complex, sometimes also including Sir1 as a bridging protein (Gardner et al., 1999). Next, the Sir2/3/4 complex spreads across chromatin with active deacetylation of histones by the histone deacetylase Sir2p (Braunstein et al., 1993). The deacetylating activity of Sir2p is coupled with the conversion of the small molecule metabolite NAD to a byproduct, which promotes the oligomerization of Sir3p (Liou et al., 2005; Tanny and Moazed, 2001). Sir3p also plays an important role by binding to nucleosomes in a H4K16Ac- and H3K79me3-sensitive manner (Behrouzi et al., 2016; Onishi et al., 2007), whereas Sir4p acts as a scaffold protein making contacts to all Sir proteins and also interacting with ORC1, Rap1p or

Abf1p (Moazed et al., 1997). Sir2/3/4 recruitment to the unmodified nucleosomes and deacetylation of adjacent nucleosome then facilitates the spreading of the Sir2/3/4 complex, which also aids the compaction of chromatin (Onishi et al., 2007). Spreading of Sir2/3/4 at the telomeres can vary from cell to cell and is interspersed with active chromatin, resulting in variegating expression of reporter genes and referred to as telomere position effect (TPE) following the term of PEV (Sandell and Zakian, 1992).

3.4. Heterochromatin in metazoans

3.4.1. RNAi-mediated repression of chromatin in plants

A positive feedback loop involving siRNAs and gene silencing is also present in the plant model organism *Arabidopsis thaliana* (*A. thaliana)*, resulting in DNA cytosine methylation on repetitive sequences (Zhang et al., 2006). Plant heterochromatin at these repetitive sequences is further characterized by high levels of methylated H3K9 (reviewed in Pikaard and Mittelsten Scheid, 2014). Unlike *S. pombe* and metazoans, *A. thaliana* has five DNA-directed RNA polymerases with RNAPIV and RNAPV being responsible for RNA-directed DNA methylation in heterochromatin (see Figure 15). Briefly, RNAPIV-produced transcripts are reverse transcribed by the plant RNA-dependent RNA polymerase RDR2 and processed by the Dicer-like protein DCL3 into 24 nt siRNAs, which are loaded onto AGO4 (Haag et al., 2012; Havecker et al., 2010).

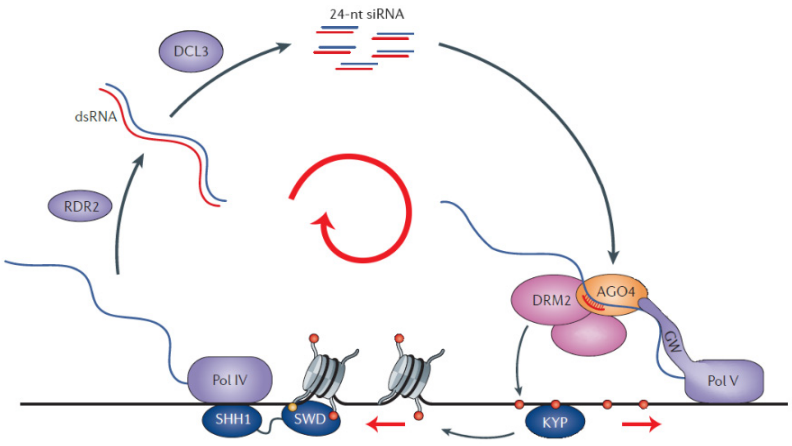

Figure 15: RNAi-directed DNA and H3K9 methylation in A. thaliana. The red arrows indicate the self-enforcing feedback loop via generation of siRNAs and self-enforcing action of DNA and histone methylation, which leads to spreading of these marks. See text for more information. Figure adapted from Holoch and Moazed, 2015a.

Loaded AGO4 then binds to the nascent transcript of RNAPV and recruits the DNA methyltransferase DRM2, which methylates the DNA and also leads to H3K9 methylation (Wierzbicki et al., 2009). The interplay between DNA and histone methylation is still not completely elucidated, but they mutually depend on each other: For example, the H3K9 methyltransferase KYP recognizes methylated DNA and vice versa RNAPIV subunit SHH1 recognizes H3K9me and thus recruits the initial RNAPIV to H3K9 methylated regions, thus promoting DNA methylation (Law et al., 2013). H3K9me2 is also recognized by another DNA methyltransferase CMT3, which is responsible for maintenance of methylated DNA, thus creating a stable self-enforcing loop (Du et al., 2012).

Besides this siRNA-dependent DNA and H3K9 methylation pathway, also H3K27 methylation marks heterochromatin, either constitutive as H3K27me1 or facultative as H3K27me3, and is deposited by different H3K27 methyltransferases (Naumann et al., 2005; Zhang et al., 2007). Unlike in most other eukaryotes, the plant homologue of HP1, LHP1 recognizes rather H3K27me3 than H3K9me3 and thus localizes to facultative heterochromatin (Nakahigashi et al., 2005). The best-studied locus under the control of facultative heterochromatin is the FLOWERING LOCUS C (FLC), which is controlled by the PRC2 complex. FLC is a transcription factor that prevents flowering during warm temperatures unless plants experience a prolonged phase of cold temperatures. This process is called vernalization, in which the FLC locus gets repressed in a quantitative, temperature-dependent manner, and ensures that plants grow vegetatively in winter and only flower in the following spring (reviewed in Berry and Dean, 2015). This interplay between gene expression and environmental signals makes the FLC locus an attractive model locus to study the dynamic epigenetic regulation of chromatin states.

During the experience of cold temperatures, the PRC2 complex binds via VIN3 to the first exon of FLC, where it mediates the nucleation of H3K27me3 across only three nucleosomes (De Lucia et al., 2008). This short stretch of methylated H3K27me3 is crucial in switching the ON state to the OFF state (Angel et al., 2011). Nucleation of the first exon has been linked recently to

specific DNA sequences, which recruit two sequence-specific proteins VAL1/2. These proteins interact with LHP1, but also recognize H3K27me3, thus leading to a stabilization of the H3K27me3 mark and enhanced recruitment of PRC2 (Yuan et al., 2016). Once the switch to the OFF state is completed, PRC2 and H3K27me3 act as part of a positive feedback loop to maintain the OFF state of FLC until embryogenesis is reached, which results in the re-expression of FLC (Choi et al., 2009).

3.4.2. Heterochromatin in the fruit fly D. melanogaster

Heterochromatin in *D. melanogaster* is found at the centromeres and telomeres and covers around 30 % of the genome (Bosco et al., 2007). The spreading nature of heterochromatin and the epigenetic stable inheritance led to the discovery and definition of PEV (see chapter 3.1) and to the identification of many heterochromatin factors (reviewed in Elgin and Reuter, 2013). Heterochromatin is characterized by H3K9me3, which is primarily set by Su(var)3-9, the Clr4 homologue, and bound by HP1 homologue Su(var)2-5 (James and Elgin, 1986; Schotta et al., 2002). Su(var)3-9 and Su(var)2-5 interact directly with each other and mutually affect their localization (Schotta et al., 2002). Not only H3K9me3 is a hallmark of heterochromatin, but also H4K20me3, which is deposited by Su(var)4-20 and also essential for silencing (Schotta et al., 2004). Deacetylation is directly localized to heterochromatin via the interaction of KDAC1 with Su(var)3-9 and also dephosphorylation of H3S10 and demethylation of H3K4 are essential for heterochromatin spreading (Czermin et al., 2001; Ebert et al., 2004; Rudolph et al., 2007).

Facultative heterochromatin in *D. melanogaster* is characterized by H3K27me3 and the involvement of PRC. Indeed, PRC proteins were initially identified in this model organism to maintain the repression of the developmentally regulated HOX genes (Lewis, 1978). Mechanistically, the operating mode of PRC in *D. melanogaster* is highly similar to mammals and will be discussed in the next chapter. Yet, a distinguishing feature of PRC is the mode of recruitment, which relies on Polycomb group response elements (PREs) (Simon et al., 1993).

PRE is a short DNA sequence, which is recognized by multiple DNA-binding proteins such as PHO/PHOL (YY1 in mammals) to just name the most studied ones (Brown et al., 1998, 2003). These sequence-specific proteins then recruit PRC1/2 to mediate facultative heterochromatin assembly.

A major function of heterochromatin in general is to repress transposons, which make up a large fraction of metazoan chromatin. In *D. melanogaster*, this repression is mediated by piRNAs, which are small RNAs ranging from 23 - 30 nt, as well as multiple Argonaute proteins and takes place in germline and somatic cells by similar mechanisms (see Figure 16, Aravin et al., 2003):

In the germline, piRNAs are encoded as piRNA clusters in the genome and transcribed by RNAPII (Brennecke et al., 2007). Transcription takes place in heterochromatin and is regulated by the Rhino-Deadlock-Cutoff (RDC) complex, which promotes transcriptional read-through from neighboring genes to transcribe piRNA clusters (Mohn et al., 2014). The resulting transcripts then get exported to the cytoplasm and processed into piRNAs by multiple factors, involving the nuclease Zucchini (Pane et al., 2007). Zucchini cuts the precursor transcripts with the help of Argonaute proteins with different sequence biases and thus designs piRNAs to be loaded onto

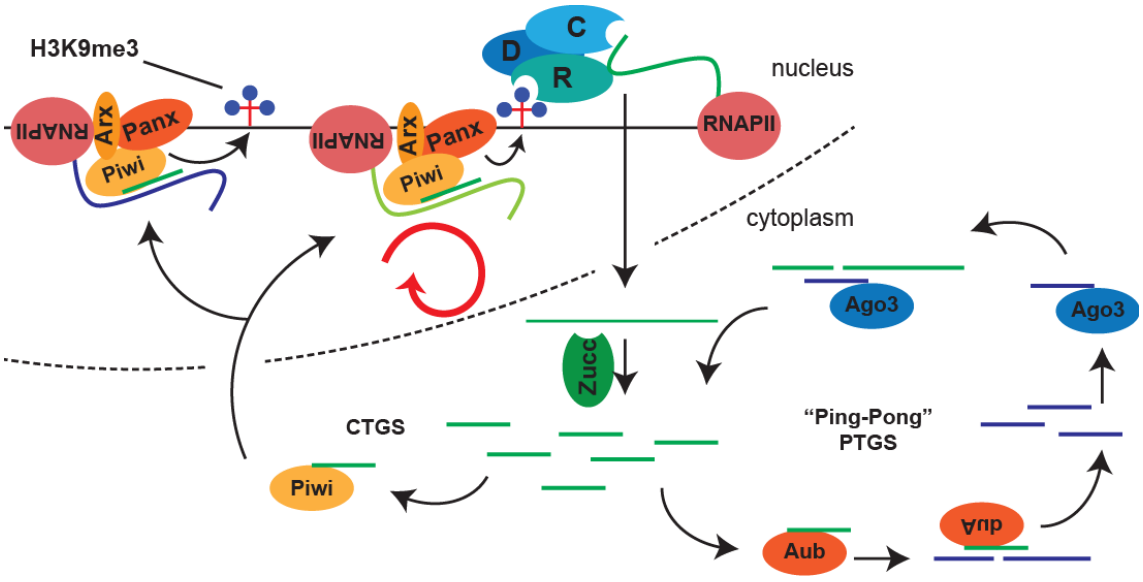

Figure 16: RNAi-mediated transposon silencing in fruit flies. RDC: Rhino-Deadlock-Cutoff complex. Transcripts are color-coded in the following way: dark/bright green: double-stranded piRNA cluster, blue: transposons. The red arrow depicts a feed-forward feedback loop. See text for more detailed information.

different Argonaute proteins, called Piwi, Ago3, and Aub (Mohn et al., 2015). Ago3 and Aub then direct PTGS on transposon transcripts by amplifying their effect with a “Ping-Pong” cycle. This cycle consists of Aub cutting the transposon transcript, which gets recognized by Ago3, which again cuts the piRNA precursor transcript, thus creating again more and more diverse templates for Aub (Brennecke et al., 2007).

Not only PTGS is involved in controlling transposon expression in the germline, but also CTGS (Sienski et al., 2012). In this not fully understood pathway, piRNA-loaded Piwi plays a central role by interacting with the nascent transcript and recruiting the scaffold protein Arx and Panx (Sienski et al., 2015; Yu et al., 2015). Panx then acts as a link between the piRNA machinery and heterochromatin formation and can elicit ectopic heterochromatin formation when tethered to a reporter – similar to RITS in *S. pombe*. This completes the feedback loop, because RDC relies on methylated H3K9 to act on chromatin (Mohn et al., 2014). The exact mechanism of the degradation of heterochromatic transcripts is still unclear (Yang and Xi, 2017). Yet, literature suggests that degradation happens downstream of and dependent on H3K9me and involves the RNA-binding protein Maelstrom (Sienski et al., 2012).

In somatic cells, a similar mechanism takes place, including many of the above-mentioned factors. Differences in the somatic mechanism compared of the gonadal one are the lack of the Ping-Pong amplification loop and thus the PTGS pathway. Likely, since sporadic transposon translocations are not inherited in somatic cells, there was no need for the evolution of such an additional safeguard mechanism. Furthermore, the biogenesis and processing of somatic piRNAs is also different. Precursor loci for piRNA show canonical euchromatic features, such as a TSS, H3K4 methylation and hence do not involve the RDC complex (Goriaux et al., 2014).

3.4.3. Heterochromatin in mammals

Besides general heterochromatin at pericentromeric and telomeric repeats, mammalian genomes also harbor a large fraction of retroviral insertions, which look repeat-like due to their

high copy number (reviewed in Groh and Schotta, 2017). Therefore, mammalian cells evolved multiple mechanisms to silence these retrotransposons by constitutive heterochromatin. Constitutive heterochromatin in mammals is characterized by H3K9me3; but also H4K20me3, special histone variants and DNA methylation contribute to the silencing (reviewed in Saksouk et al., 2015). Perhaps due to the increased complexity of mammals, multiple H3K9 methyltransferases and HP1s are involved in heterochromatin formation in a locus-specific manner:

Pericentromeric heterochromatin and also the inactive X chromosome contain high levels of H3K9me3, which are set by the homologues of Clr4, Suv39h1 and Suv39h2 (Peters et al., 2001). On the other hand, transposon insertions are recognized by DNA sequence-specific KRAB zinc finger proteins, which are subsequently bound by Trim28, a key effector in transposon silencing. Trim28 then recruits Setdb1, a different H3K9 writer enzyme crucial for transposon repression, but with only minor functions on pericentromeric heterochromatin (Schultz et al., 2002). Common to all aforementioned methyltransferases is the H3K9me-recognizing chromodomain, which allows them to spread along the nucleosomes perhaps in conjunction with the three HP1 homologues HP1α, β, and γ (Rebollo et al., 2011; Wang et al., 2016b). Current research on these three HP1 homologues suggests that HP1α and β are the classic heterochromatin proteins, whereas HP1γ rather localizes to euchromatic loci. Nevertheless, all HP1 isoforms have been linked to not only shape constitutive heterochromatin, but also to be involved in transcriptional control, alternative splicing and DNA damage (reviewed in Kwon and Workman, 2011; Ostapcuk et al., *unpublished*).

Facultative heterochromatin in mammals requires the PRC1 and PRC2, which are responsible for H2AK119 ubiquitination and H3K27 methylation, respectively (see Figure 17). These complexes are not present in budding and fission yeast, suggesting that they evolved later. PRC2 acts upstream of PRC1 by trimethylation of H3K27, which then provides a binding platform for PRC1 leading to H2AK119ub (reviewed in Piunti and Shilatifard, 2016). Recruitment of PRC2

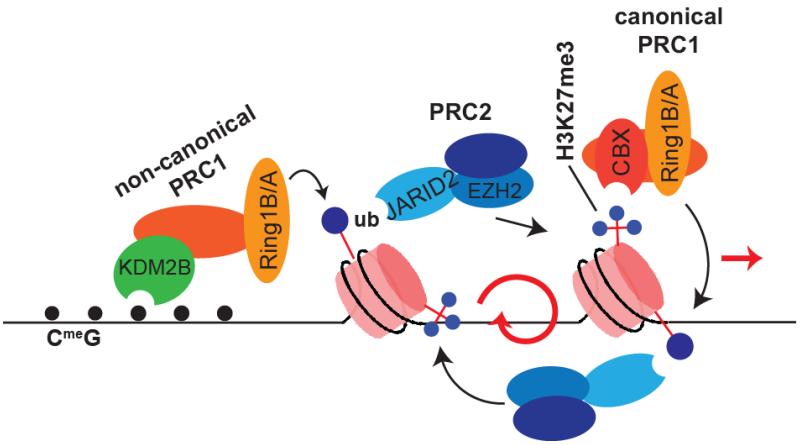

Figure 17: PRC-mediated formation of facultative heterochromatin in mammals. Non-canonical PRC1 gives specificity due to recognition of methylated CpG and provide a nucleation site and low H2Aub levels. These levels are reinforced by combined action of PRC2/canonical PRC1, which form a positive feedback loop, resulting in high levels of H3K27me3 and H2Aub and potential spreading (red arrows).

to specific sites in chromatin is still unclear in mammals, because they lack the Polycomb-responsive element that is present in *D. melanogaster*. Multiple recruiting signals have been suggested, such as GC content, CpG islands, ncRNAs or also a feedback mechanism with PRC1 subunits (Blackledge et al., 2014; Mendenhall et al., 2010; Riising et al., 2014). Upon methylation of H3K27 by PRC2 methyltransferase EZH2, the PRC2 subunit EED can bind H3K27me and enforces the activity of EZH2, thus creating a positive feedback loop (Margueron et al., 2009). H3K27me3 is also recognized by multiple chromobox-containing (CBX) subunits of the PRC1 complex, which then ubiquitinates H2A via its E3 ligase subunit RING1A/B (Wang et al., 2004).

A more recent model suggests that PRC1 complex recognizes CpG islands via its non-canonical subunit KDM2B and recruits PRC2 by H2AK119ub, thereby inverting the order of PRC complex binding (Blackledge et al., 2014; Kalb et al., 2014). This convertibility exemplifies another positive feedback loop of repressive complexes (see Figure 17).

Similar to the piRNA pathway in fruit flies, also mammals have a co-transcriptional, small RNA-mediated pathway, acting in the germline. In male cells, PIWI proteins MILI, MIWI and MIWI2 seem to be crucial for proper spermatogenesis and *de novo* DNA methylation of retrotransposon elements (Aravin et al., 2006, 2008; Kuramochi-Miyagawa et al., 2008). In addition to this TGS, PIWI proteins also direct PTGS with the involvement of the ping-pong amplification cycle (De Fazio et al., 2011).

4. Aim of this thesis

As outlined above, euchromatin and heterochromatin have very different characteristics in terms of function, transcriptional output, and chromatin accessibility. Research showing that most parts of chromatin including heterochromatin can give rise to transcripts evokes the question underlining the general aim of my thesis:

How are heterochromatic and euchromatic loci distinguished?

A possible explanation is that chromatin "remembers" in which state it is through the establishment of positive feedback loops. Several self-enforcing regulatory circuits that maintain heterochromatin have been characterized in the recent years in multiple organisms (see Figures 12, 14 - 17). However, studying these feedback loops has not enabled us to clearly dissect the initiation process. In order to achieve this, I was aiming at using a naïve, non-repetitive chromatin context to study specifically the initiation of heterochromatin assembly. Thanks to the involvement of RNAi in the initiation process of heterochromatin and the possibility to target RNAi to any euchromatic sequence using ectopically expressed siRNAs, the model organism *S. pombe* allowed me to study heterochromatin nucleation, spreading, and its interplay with euchromatic marks and machineries. Prior knowledge made me focus on the Mst2 complex. The following specific questions I set out to address for my PhD project:

- How is heterochromatin formation **initiated** and what is the role of **transcription**?
- What prevents **RNAi-mediated** heterochromatin formation in euchromatin?
- **What** is the function of the **Mst2 complex** in this prevention? **Where** does it localize? **How** does it prevent heterochromatin formation?

RESULTS

1. Paf1C represses ectopic siRNA-mediated heterochromatin formation

The Paf1 complex represses small-RNA-mediated epigenetic gene silencing
Kowalik KM*, Shimada Y*, Flury V, Stadler MB, Batki J & Bühler M
Nature. 2015 Apr; *520*, 248-52. * Equal contribution

The entire article can be found in the appendix section.

Summary

Despite crucial functions of RNAi and siRNAs in establishing heterochromatin at pericentromeric regions in *S. pombe*, attempts to induce *de novo* heterochromatin formation by RNAi have been only partially successful. Although some silencing could be achieved, it was very inefficient, highly unstable, and dependent on the genomic locus (Iida et al., 2008; Simmer et al., 2010), suggesting the existence of repressive mechanisms that counteract ectopic heterochromatin formation. Hence, our goal was to identify repressing activities in an unbiased ethylmethansulfonate (EMS) screen, where synthetic small-hairpin-RNAs (shRNAs) against the *ade6*$^{+}$ reporter were expressed ectopically. Amazingly, all identified mutations, which allowed *ade6*$^{+}$ silencing, mapped to the Paf1 complex subunits. Re-introducing these mutations into *wild type* cells confirmed this effect, resulting in H3K9 methylation on *ade6*$^{+}$, which was dependent on functional RNAi pathway, CLRC and other important silencing factors. Initiation of silencing was stochastic, but maintained very efficiently, suggesting the stable propagation of the silent state once it is established. Importantly, expression of shRNAs was not further needed upon initiation of stable silencing and the silencing propagated stably over multiple generations, but strictly depended on mutated Paf1C, showing that this is a true epigenetic phenomenon. Since Paf1C has several functions in transcription (but also in cell cycle regulation and other important cellar processes), I started to dissect the mechanism of repression and showed that inefficient

transcription termination seems to provide a kinetic window of opportunity for RNAi to act on the nascent transcript.

My contribution

In this study, I specifically looked at the mechanism by which Paf1C prevents RNAi-mediated heterochromatin formation (see Figure 18). Paf1C is a main orchestrator of transcription with various effects on transcription (see chapter 2.2.1). Deletion of histone methyltransferases *set1*$^+$ or *set2*$^+$ did not result in silencing of the *ade6+* reporter, suggesting that H3K4 and H3K36 methylation do not play an essential role in repressing RNAi. However, when I mutated *res2*$^+$ and *ctf1*$^+$ I could observe many cells that silenced the reporter (Figure 18A). Both proteins have a role in RNAPII release after transcription termination, as RNAPII gets stuck on chromatin in their absence, but the transcript is still normally processed (Aranda and Proudfoot, 2001). Quantification of the silencing revealed that most cells do not stably maintain the silent state of the reporter and start to variegate, suggesting that an arrested RNAPII is not solely responsible for allowing RNAi to take effect (Figure 18B and C). This is in agreement with a model proposing that accumulation of nascent transcripts due to impaired transcription termination and stuck polymerases offers an opportunity for RNAi to bind and induce silencing.

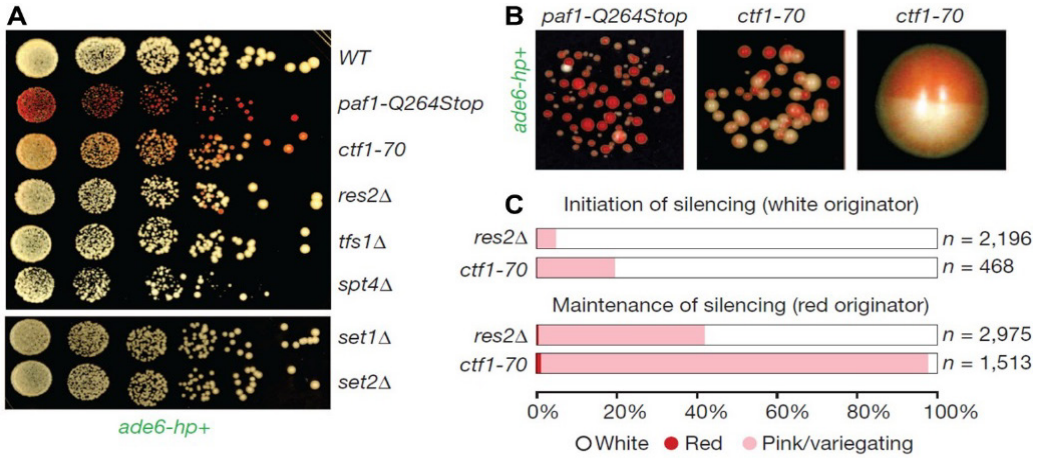

Figure 18: Mechanistic insight into Paf1C-mediated repression of heterochromatin formation. **A**, **B** Silencing assays showing that *ade6*$^+$ siRNAs can initiate repression of *ade6*$^+$ in transcription termination mutants, which renders cells growing red. Note the unstable repression in *ctf1-70* and *res2*Δ cells. WT, wild type. **C**, Percentage of naïve cells (white originator) that establish heterochromatin within 20 – 30 mitotic divisions (initiation) and stability of ectopic heterochromatin in descendants thereof (maintenance). n: number of scored colonies.

2. Mst2 protects euchromatin from epigenetic silencing by acetylating the HULC subunit Brl1

The histone acetyltransferase Mst2 protects active chromatin from epigenetic silencing by acetylating the ubiquitin ligase Brl1
Flury V, Georgescu PR, Iesmantavicius V, Shimada Y, Kuzdere T, Braun S & Bühler M
Molecular Cell, in revision

The entire unpublished manuscript can be found in the appendix section.

Summary

With the identification of Paf1C as a repressor of siRNA-mediated heterochromatin formation, it became possible to characterize *de novo* heterochromatin formation in a non-repetitive, unbiased background. In a first step, I asked why initiation in a *paf1* mutant (*paf1**) background is still hampered. I could show that the histone acetyltransferase Mst2 is important for repressing initiation, but dispensable for maintenance of heterochromatin. Genome-wide Mst2 localization studies revealed that the Mst2C is excluded from heterochromatic regions, thus leaving heterochromatin unperturbed once it is established. Further dissection of the localization determinants showed that Mst2C subunit Pdp3 anchors Mst2 in euchromatin by specific recognition of Set2-mediated H3K36me3. This links Mst2C to RNAPII-transcription and specifically to the gene body. Deletion of *pdp3*$^+$ or *set2*$^+$ led to an increased heterochromatin initiation efficiency and strongly reduced Mst2C binding to chromatin. Besides its crucial role in protecting euchromatic regions from RNAi-mediated heterochromatin formation, we found that anchoring of Mst2C to H3K36me3 also protects pericentromeric heterochromatin from the action of Mst2C. Deletion of *pdp3*$^+$ led to a Mst2-dependent loss of silencing at those regions, suggesting that promiscuous binding of Mst2 to heterochromatin disrupts silencing. I could recapitulate this effect by artificially tethering Mst2 to a heterochromatic reporter. Tethering of active Mst2 led to a complete derepression of the reporter upon deletion of *pdp3*$^+$ or *set2*$^+$, further corroborating the

role of these two factors in anchoring Mst2C to euchromatin, whereas tethering of catalytically dead Mst2 had no effect.

Hence, the activating function of Mst2C depends on its acetyltransferase activity. However, acetylation levels of H3K14, the proposed histone substrate of Mst2C, remained unchanged upon deletion of *mst2*$^{+}$. In order to find other targets of Mst2, I established and performed acetylomics, which for the first time identified thousands of acetylation sites in the proteome of *S. pombe*. Deletion of *mst2*$^{+}$ changed the abundance of one acetylation site, lysine K242 on Brl1, a E3 ligase responsible for H2BK119 ubiquitination. By specifically mutating K242 to R or Q to mimic a constantly deacetylated or acetylated residue, respectively, I found that K242R mutants promoted initiation, whereas K242Q prevented initiation of heterochromatin, hence phenocopying the effects of *mst2*Δ cells. Addressing the underlying mechanism of this protection, I could show that H2BK119ub levels were reduced in K242R and stabilized in K242Q mutants, respectively. These changes also lead to altered H3K4me3 levels, a H2Bub-dependent histone modification, which is a hallmark of active transcription and thereby closes the cycle to Set2 and H3K36me3.

In summary, we discovered a novel positive feedback loop that functions in euchromatin to protect genes from being silenced by siRNAs (see Figure 19). This has important implications in addressing fundamental questions, such as how transcriptional memory is achieved, maintained, and propagated. Furthermore, our results suggest that feedback loops partition euchromatin and heterochromatin and to confer epigenetic robustness. Because all factors are highly conserved, it is likely that similar feedback loops are widespread in eukaryotes.

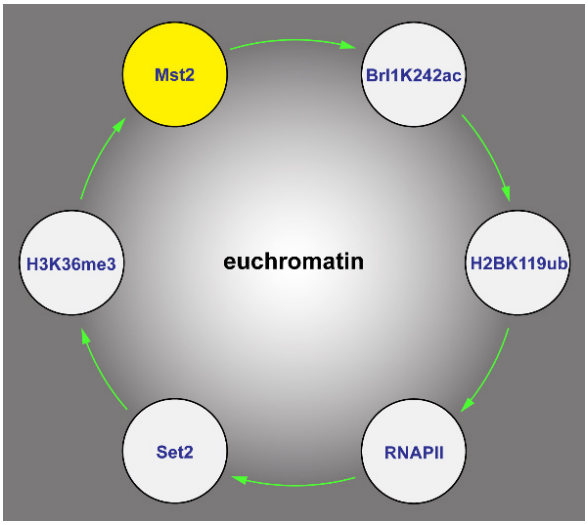

Figure 19: Schematic visualization of the identified euchromatic feedback loop. H3K36me3 by Set2 recruits Mst2C, which acetylates Brl1, leading to higher H2Bub levels. Ubiquitinated H2B in turn is a hallmark for active transcription. Increased transcriptional activity leads to increased Set2 recruitment, which closes the feedback loop.

Contributions

This work comprises my main project during my PhD and hence, I was developing and performing many experiments. Furthermore, this work has been done in an excellent collaboration with Paula Georgescu from the Braun laboratory in Munich. Whereas Paula addressed the important question of the functional role of Pdp3 in preventing promiscuous action of Mst2C in heterochromatin, I looked at the euchromatic role of Mst2C preventing *de novo* heterochromatin formation. Both of us were involved in dissecting the determinants of Mst2C localization by independent, complementary methods, therefore corroborating the results. Furthermore, I established and performed acetylomics experiments including the follow-up experiments concerning the novel Mst2 substrate Brl1.

DISCUSSION

Given that both hetero- and euchromatic regions give rise to transcripts and are transcribed by the same polymerase, how are regions initially distinguished? This question has been inherently difficult to address due to heterochromatic feedback loops (see Introduction), which impede a clear dissection of events in this process. Hence, it is fundamental to dissect the molecular mechanisms that allow *de novo* heterochromatin formation. In *S. pombe*, this has been achieved by tethering heterochromatic factors to euchromatic reporters (Bühler et al., 2006; Buscaino et al., 2013; Gerace et al., 2010; Kagansky et al., 2009). However, testing which euchromatic factors counteract initiation of heterochromatin has been neglected for many years, but is – in my opinion – equally important to understand the interplay between hetero- and euchromatic factors.

During my PhD, I addressed this important issue and contributed to the identification of Paf1C as a repressor of de novo heterochromatin formation (Kowalik et al., 2015). My main achievement was the identification of Mst2C as a specific repressor of initiation of heterochromatin formation, but not maintenance. This provides first insights into mechanisms that protect euchromatin from inactivating signals (Flury *et al.*, in revision). Intriguingly, the mechanism I discovered acts via a self-enforcing feedback loop by recruiting Mst2C to transcribed, H3K36me3-rich genes, where Mst2C-mediated Brl1 acetylation enhances H2B ubiquitination, a hallmark of transcribed genes (see Results).

In this discussion, I will first provide some more data on how *de novo* heterochromatin is initiated in the absence of Mst2 and draw a model of the molecular functions of Mst2C and Brl1 in repressing heterochromatin. In a second part, I speculate on the physiological role of the identified feedback loop in *S. pombe* and if such a phenomenon may be conserved to other eukaryotes. Finally, as part of a broader conclusion of my PhD work, I will bring in my perspective about the relevance of such self-enforcing feedback loops in chromatin organization.

Model of *de novo* heterochromatin formation in *S. pombe*

Ectopic heterochromatin formation in *mst2*Δ cells

My work identifies a unique role of Mst2C as a global repressor of heterochromatin, as it localizes throughout euchromatin, but is excluded from heterochromatin unlike Paf1C (data not shown). Importantly, Mst2C is not enriched at heterochromatin boundaries such as Swi6 or Epe1 (Stunnenberg et al., 2015; Zofall and Grewal, 2006). My work significantly extends previous knowledge about Mst2C counteracting spreading of H3K9me2 at boundaries, subtelomeres or meiotic genes (Gómez et al., 2005; Wang et al., 2015).

Intriguingly, the RNAi machinery seems to be genetically linked to Mst2, because lack of Mst2 allows simultaneous deletion of RNAi factors while maintaining heterochromatin (Reddy et al., 2011). Although the Jia group presented Dcr1-independent ectopic heterochromatin upon *mst2*$^+$ deletion, no one investigated if such heterochromatin is formed also independent from the RITS complex (Wang et al., 2015). Even more, my results suggest that the RITS complex subunit Tas3 has to be present also in the absence of Mst2 to maintain heterochromatin, allocating an essential role of Tas3 in heterochromatin initiation, but also maintenance (see below). With our shRNA-based reporter assay, we cannot investigate if Mst2 also prevents RNAi-independent heterochromatin formation because we rely on the processing of the hairpin RNA to siRNAs.

Paradoxically, deletion of *mst2*$^+$ does not result in stable repression of the *ade6*$^+$ locus despite extensive H3K9 methylation across a large chromatin domain and the generation of secondary small RNAs (see Figure 20A-C). This suggests that H3K9 methylation alone does not lead to stable (co-)transcriptional silencing, but depends on the presence or absence of other factors, which are missing in the *mst2*Δ background. We are currently conducting an EMS screen in a *mst2*Δ background to identify factors that prevent silencing. Another approach would be to overexpress a cDNA library and screen for factors that enforce silencing in *mst2*Δ cells. However, interpretation of these screen results might be difficult, because these factors may not necessarily be actively preventing the silencing or rely on co-factors to be functional when overexpressed.

Therefore, I postulate that studying the mechanism of *de novo* H3K9 methylation and propagation may reveal how downstream events are coordinated to induce gene silencing and ultimately allow a better understanding of how H3K9me2 connects to silencing. On our targeted

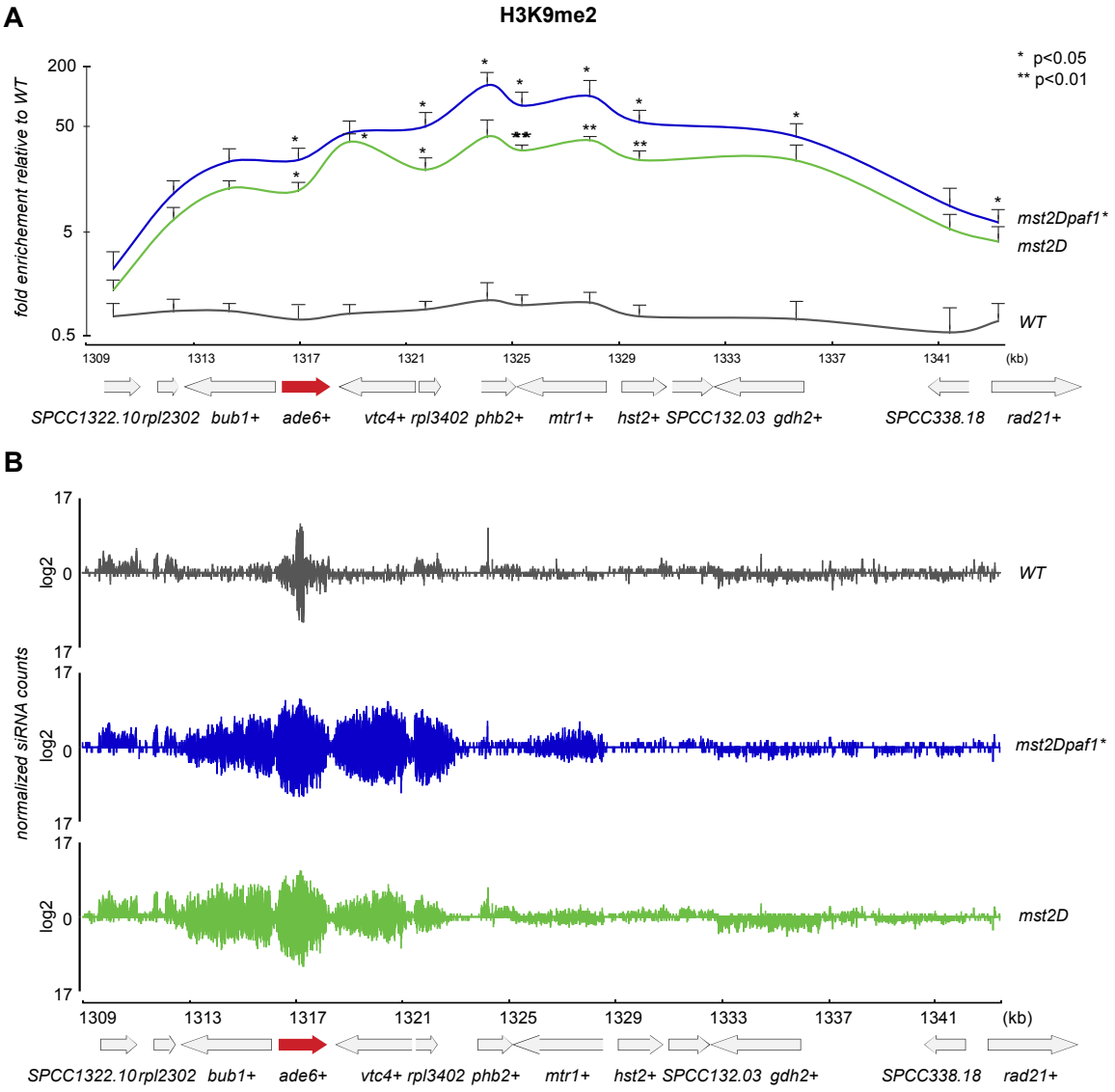

Figure 20: Deletion of mst2+ allows formation of heterochromatin without transcriptional repression. **A**, Chromatin immunoprecipitation (ChIP) showing the high amounts of H3K9me2 in *mst2*Δ, similar to *mst2*Δ*paf1** cells. **B**, siRNA sequencing of *mst2*Δ cells reveals generation of secondary siRNAs **C**, RNA expression analysis shows that in *mst2*Δ, silencing does not occur compared to *mst2*Δ*paf1**, where silencing of H3K9me2 harboring genes is very efficient.

ade6^{+} reporter gene H3K9 methylation spreads far more than secondary siRNAs, raising the question of whether these siRNAs are a cause or consequence of high H3K9 methylation (see Figure 20A and B).

To gain insight into the causal role of siRNAs in heterochromatin propagation, I investigated a different locus, the IRC1R locus. This locus demarcates a heterochromatin boundary without a discernable *cis*-acting DNA element such as a tRNA gene, which makes it ideal to study the interplay between eu- and heterochromatic factors (Keller et al., 2013; Noma et al., 2006). Intriguingly, IRC1R harbors increased H3K9 methylation in *mst2*Δ cells, but shows reduced siRNAs levels, which points towards a more efficient propagation of H3K9me2 without extensive siRNA generation.

In general, formation and propagation of H3K9me2 can be promoted by four factors, which each contain a H3K9me2-recognizing chromodomain: Swi6, Chp2, Clr4, and Chp1. The HP1 protein Swi6 recognizes H3K9me2 and may propagate H3K9me2 via its ability to oligomerize (Canzio et al., 2011). However, Swi6 does barely bind to euchromatin and is evicted from chromatin upon binding to RNA (Keller et al., 2012; Woolcock et al., 2011). Furthermore, deletion of *swi6*$^{+}$ actually increases H3K9 methylation at the IRC1R boundary, pointing towards a rather inhibitory function of Swi6 in spreading of heterochromatin into euchromatin, similarly to Mst2 (Stunnenberg et al., 2015). I tested if spreading in a *mst2*Δ is epistatic to *swi6*Δ, but observed an even higher accumulation of H3K9me2, suggesting that both Swi6 and Mst2 control spreading of H3K9me2 independently at the IRC1R boundary (see Figure 21A). Another factor binding H3K9me2 is the second HP1 homologue Chp2, but deletion of c*hp2*$^{+}$ does not change H3K9me2 at the IRC1R boundary (Stunnenberg et al., 2015). Thus, the HP1 proteins in *S. pombe* likely do not to contribute to spreading of H3K9me2 at heterochromatin boundaries.

Also the H3K9 methyltransferase Clr4 contains a chromodomain, which recognizes H3K9me3 and is required for efficient spreading and propagation of methylated H3K9 (Ragunathan et al., 2015; Zhang et al., 2008). However, the chromodomain of Clr4 recognizes H3K9me2 with rather low affinity and is outcompeted by the far more abundant HP1 protein Swi6,

which allows efficient spreading across nucleosomes (Al-Sady et al., 2013). Nevertheless, Clr4 is an attractive explanation for the observed ectopic H3K9 methylation. For a more detailed mechanistic insight, I propose to test the Clr4 mutant lacking the chromodomain (Clr4ΔCD), which is unable to read its own mark and hence cannot propagate H3K9me2 (Nakayama et al., 2001; Zhang et al., 2008). If Clr4 propagates H3K9me2 spreading in the absence of Mst2, no H3K9me2 should be present in a *Clr4ΔCDmst2Δ* background, whereas residual H3K9me2 would point towards a recurrent recruitment of CLRC independently of its chromodomain, for example by the RNAi pathway. Unfortunately, Clr4ΔCD mutants show an extensive reduction of H3K9me2, which requires high sensitivity H3K9me2 chromatin immunoprecipitation (ChIP) experiments to allow functional dissection of the reader and writer functions of Clr4. Another experiment could address the dependence of heterochromatin propagation on transcription. CLRC deposits and propagates H3K9me2 independent of RNA production (Ragunathan et al., 2015), hence tethering of Clr4 to a transcriptionally silent locus should reveal if H3K9me2 starts to spread further upon deletion of *mst2*$^{+}$, which would point towards an RNA(i)-independent spreading mechanism.

Without the HP1 proteins being responsible to promote H3K9 methylation, one factor remains, which can propagate H3K9 methylation: the RITS complex, consisting of Chp1, Tas3 and Ago1. Importantly, Chp1 has the highest affinity for H3K9me2 of all chromodomain proteins and this affinity increases further upon binding to RNA (Ishida et al., 2012; Schalch et al., 2009). Unlike Swi6/Chp2, Chp1 has no chromoshadow domain and is unable to oligomerize on its own. However, oligomerization is achieved by the C-terminal domain of Tas3 and is essential for initiation of heterochromatin (Li et al., 2009b). Supporting the hypothesis of RITS-mediated spreading of H3K9me2 in a *swi6Δ* or *mst2Δ*, H3K9me2 levels are reduced upon mutating Tas3 to the oligomerization mutant Tas3* at IRC1R (see Figure 21B and Stunnenberg et al., 2015). Additionally, deletion of *mst2*$^{+}$ renders the entire RNAi machinery dispensable for heterochromatin maintenance with the exception of Tas3, in whose absence heterochromatin levels drop almost completely at the centromere (see Figure 21C). This underlines the fundamental role of Tas3 in

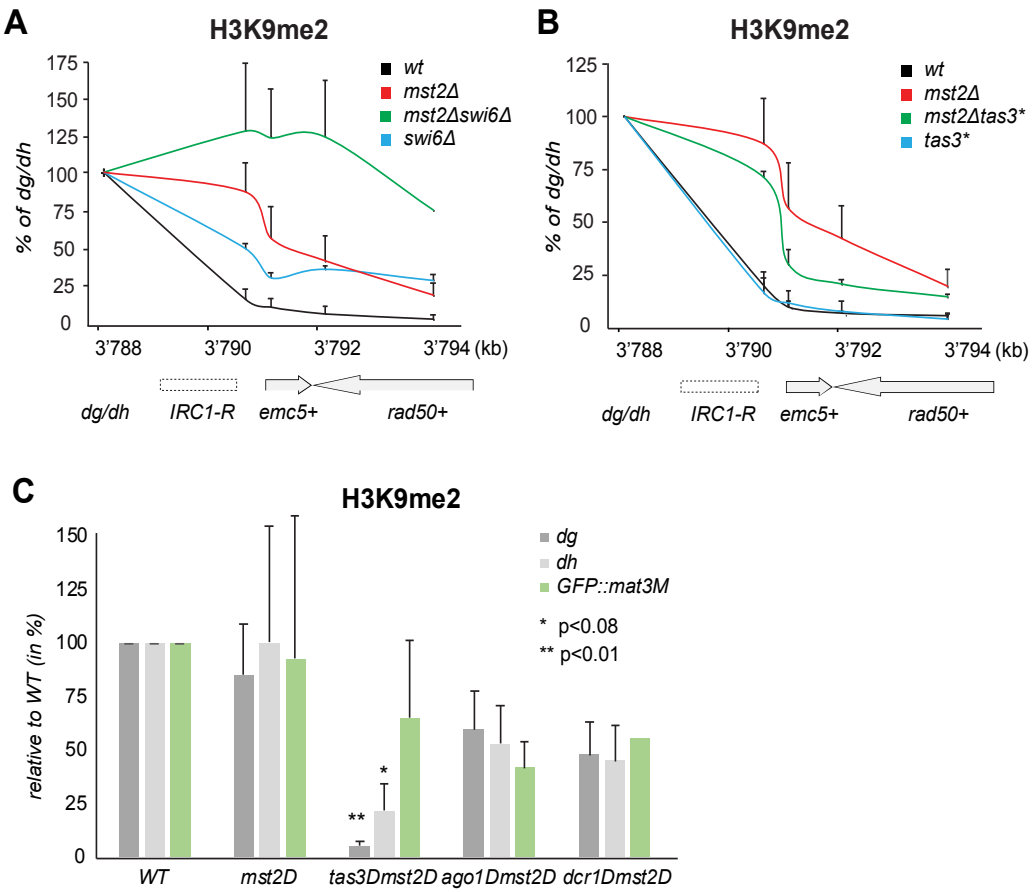

Figure 21: Mechanism of H3K9me2 spreading. **A**, ChIP showing that the spreading of H3K9me2 at IRC1R in *mst2*Δ is not Swi6-dependent but rather has an additive effect. **B**, spreading of H3K9me2 in *mst2*Δ is compromised upon mutation of Tas3 to the oligomerization mutant. **C**, unlike other RNAi components such as Dcr1 or Ago1, Tas3 is essential for maintenance of centromeric heterochromatin also in *mst2*Δ cells.

nucleation and maintenance of RNAi-dependent centromeric heterochromatin, but also in nucleation of facultative heterochromatin (Hiriart et al., 2012).

In summary, these results suggest that in the absence of Mst2, enhanced spreading of RITS (and/or Clr4) results in high levels of H3K9 methylation. Due to Chp1's high affinity to H3K9me2 and RNA, Swi6/Chp2 could be prevented from nucleosome binding. In this model, I would expect only weak silencing despite high H3K9me2, because without Swi6/Chp2 binding neither Cid14 nor SHREC2 may be recruited to mediate CTGS or TGS, respectively. Consequently, I propose Swi6, Chp1/Tas3 ChIP(-seq) experiments to test if RITS binding is increased and/or starts to spread upon deletion of *mst2*$^{+}$ and if Swi6 binding is decreased in a *mst2*Δ*paf1** background. To further investigate the silencing role of Swi6/Chp2, I suggest tethering experiments of Swi6 to the *ade6*$^{+}$ reporter to see if such tethering induces silencing of the transcripts.

Another explanation could be that RITS itself promotes degradation of the transcript and that this action would be compromised in *mst2*Δ cells. Indeed, Chp1 contains a PIN (endonuclease) domain, which is important for subtelomeric silencing (Schalch et al., 2011). Although the PIN domain of Chp1 lacks endonucleolytic activity, it could still serve as a platform for the exosome complex, similar to Rrp44 (Schneider et al., 2009). In this regard, the RITS complex would act in two modes, either propagating H3K9 methylation or orchestrating the processing of transcripts into siRNAs. Such a model would comply with the observed reduced siRNA levels in *mst2*Δ cells, but clearly more experiments are necessary to follow up on this exciting model. First experiments could involve random mutagenesis of RITS subunits to identify separation of function-alleles, which disconnect H3K9 methylation and siRNA biogenesis. Investigation of structural changes upon deletion of *mst2*$^{+}$ or of post-transcriptional modifications on RITS with/without Mst2 could also reveal exciting findings.

In the paragraph above, I propose that in the absence of Mst2 the RITS complex starts to spread across chromatin and propagates H3K9 methylation, but only weak silencing. In this case, how is RITS-mediated propagation of H3K9me2 stopped? Notably, Chp1 and Clr4 cannot bind to H3K9me2 peptides with concomitant acetylated H3K4, which leads to an inhibition of Chp1/Clr4-mediated H3K9 methylation (Xhemalce and Kouzarides, 2010). I speculate that H3K14 acetylation might have a similar function, because H3K4 and H3K14 each reside five residues next to H3K9 and chromodomain proteins may bind in two “mirrored” orientations. We observe this for the HP1 protein Rhino in *D. melanogaster*, as its chromodomain recognizes H3K9me2 in combination with H3K4Ac, but also H3K14Ac (Fabio Mohn, *unpublished*). Furthermore, recent results from our group identified the H3K4 KAT Mst1 to enhance the phenotype in *mst2*Δ cells, corroborating the inhibitory role of H3K4 and H3K14 acetylation in spreading of H3K9me2 (Yukiko Shimada, *unpublished*). In this case, acetylated histones on the *ade6*$^{+}$-neighboring genes would impair spreading of H3K9 methylation in *paf1*mst2*$^{+}$ cells, which is consistent with what we observe.

Fine-tuning of HULC impairs *de novo* heterochromatin formation

Whereas the H3K14 acetylation model discussed above fits with the observed spreading of H3K9 methylation, reduced siRNA production, and weak transcriptional repression upon deletion of *mst2*$^{+}$, it is still not sufficient to explain the efficient initiation of silencing in *mst2*Δ cells. This is because Mst2C rather localizes to the body or 3'-end of genes, where only low levels of H3K14ac exist. Further supporting a function beyond H3K14 acetylation are also studies that report unchanged H3K14ac levels in *mst2*Δ due to the redundant acetylation by the other H3K14 KAT, Gcn5 (Hirota et al., 2007; Nugent et al., 2010; Wang et al., 2012).

Indeed, no ectopic H3K9 methylation was observed in *gnc5*Δ cells and initiation of silencing in a *gcn5*Δ*paf1** is similar to a *paf1** single mutant. However, once established, spreading of H3K9me2 downstream of the nucleation site could be observed (Valentin Flury, *unpublished*). These phenotypes place Gcn5 in between the phenotype of *paf1** and *paf1*mst2*Δ mutants and may look inconsistent. However, another major function of Gcn5-containing SAGA is deubiquitination of H2B, which is lost upon deletion of *gcn5*$^{+}$ and results in higher H2B ubiquitination levels (Vlaming et al., 2016, data not shown). Increased H2Bub levels may prevent efficient nucleation of heterochromatin, whereas reduced acetylation of histones may facilitate spreading, partially explaining the reduced initiation frequency of *paf1*gcn5*Δ cells. This could be tested by specifically mutating the active site of Gcn5 (Gcn5-E191Q; Wang et al., 1998), thus creating an intact complex without acetyltransferase activity, or vice versa by deleting the SAGA deubiquitinase Ubp8, which does not affect the activity of Gcn5.

Because of this intriguing connection of H2B deubiquitination and increased silencing, I would like to postulate a second, alternative model, which involves Brl1, another Mst2 substrate identified in this thesis, and H2B, the so far only identified substrate of Brl1. My results demonstrate that Mst2-mediated acetylation of Brl1 stimulates H2B ubiquitination. Furthermore, the Mst2C anchor H3K36me3 overlaps remarkably well with the indirect Mst2C target H2Bub

across the gene body, which supports a potential crosstalk. Intriguingly, H2Bub has been linked multiple times to the protection of genes from silencing in *S. pombe*: 1) Deletion of HULC subunits strengthens silencing, whereas overexpression of HULC subunits leads to a loss of silencing of a heterochromatic reporter (Zofall and Grewal, 2007). 2) All Paf1C mutants that allow silencing *in trans* by RNAi show reduced H2Bub levels (Kowalik et al., 2015; Mbogning et al., 2013). 3) H2BK119R mutants show increased H3K9me2 at the central core of the centromere, which usually lacks repressive signals and contains the histone variant Cnp1 instead of histone H3 (Sadeghi et al., 2014). Notably, also total H3 levels were increased, suggesting that H2Bub is important for depletion of H3 histones from the central core to protect it from ectopic H3K9 methylation.

Paradoxically, both deletion of Brl1 or mutation of H2BK119 prevent silencing (data not shown). This may be explained due to the additional functions of H2Bub in promoter repression and in the DNA damage response (Batta et al., 2011; Giannattasio et al., 2005), which may prevent or mask silencing. Hence, fine-tuning of HULC activity and localization may be important to prevent silencing and may be directly regulated by Paf1C and Mst2C, which stimulate HULC localization and activity in the gene body, respectively (see Results, Van Oss et al., 2016). In this case, solely reduced H2Bub levels within the gene body may allow silencing. Amongst the Paf1C subunits, only the *leo1*∆ null mutant maintains reduced H2Bub levels, whereas all other subunits show strongly reduced (*paf1*∆) or absent H2B ubiquitination (Mbogning et al., 2013). Similarly, only *leo1*∆ cells allow silencing, whereas all other Paf1C null mutants do not silence anymore (Kowalik et al., 2015). To support this model, it would be exciting to investigate H2Bub and its distribution across the gene in *leo1Δ* and *paf1*∆ cells.

Hence, I postulate a model, where H2B ubiquitination in the gene body prevents nucleation of heterochromatin and that the ratio of H2B ubiquitination levels between the TSS and the gene body dictates the elongation (and potentially termination) efficiency, thus preventing RITS binding to the nascent transcript (see model in Figure 22).

Although H2B ubiquitination is the only identified substrate of HULC so far, acetylated Brl1 could also ubiquitinate a different substrate or even have an ubiquitin-independent function to counteract nucleation of heterochromatin. In this way, ubiquitinomics (*i.e.* the identification of all ubiquitinated lysines in the proteome) would be an unbiased way to identify endogenous Brl1 targets and to assess a potential alteration of Brl1 specificity depending on its acetylation state. Indeed, Bre1p (the Brl1 homologue in *S. cerevisiae*) was shown to ubiquitinate the Set1/COMPASS component Swd2p, which is needed for H3K4 trimethylation (Vitaliano-Prunier et al., 2008). Sequence alignments show that the two ubiquitinated lysines of Swd2p (K68 & 69) are conserved between *S. cerevisiae, S. pombe,* and human (data not shown). Therefore, it would be interesting to confirm potential ubiquitination of those residues by ubiquitinomics and to perform follow-up experiments investigating K68/9R mutants, which should mimic a non-ubiquitinated form of Swd2.

Excitingly, the budding yeast protein Swd2p is also involved in transcription termination and lack of H2B ubiquitination leads to mRNA export defects and increased RNAPII pausing at transcription termination sites (Harlen and Churchman, 2017; Vitaliano-Prunier et al., 2012). Hence, its potential homologue in *S. pombe* would be interesting to examine for a potential role in transcription termination.

It still remains to be determined, which enzyme removes the acetylation mark on Brl1. Acetylomics experiments of different KDAC mutants (*e.g.* Clr3 and Sir2) may reveal if they deacetylate Brl1. Intriguingly, a suppressor mutation in a *paf1** strain maps to Mit1, a subunit of SHREC, which also contains Clr3, a major KDAC (data not shown). This mutant shows increased H2Bub levels and does not silence anymore, thereby indirectly phenocopying a Brl1-K242Q mutant. In addition, Clr3 also acts in euchromatin (Paula Georgescu, *unpublished*) implying the possibility that SHREC directly regulates the euchromatic feedback loop by modulating histone and Brl1-K242 acetylation levels. Clearly, further experiments, such as acetylomics and measuring H2B ubiquitin levels in KDAC mutants are needed to strengthen this hypothesis.

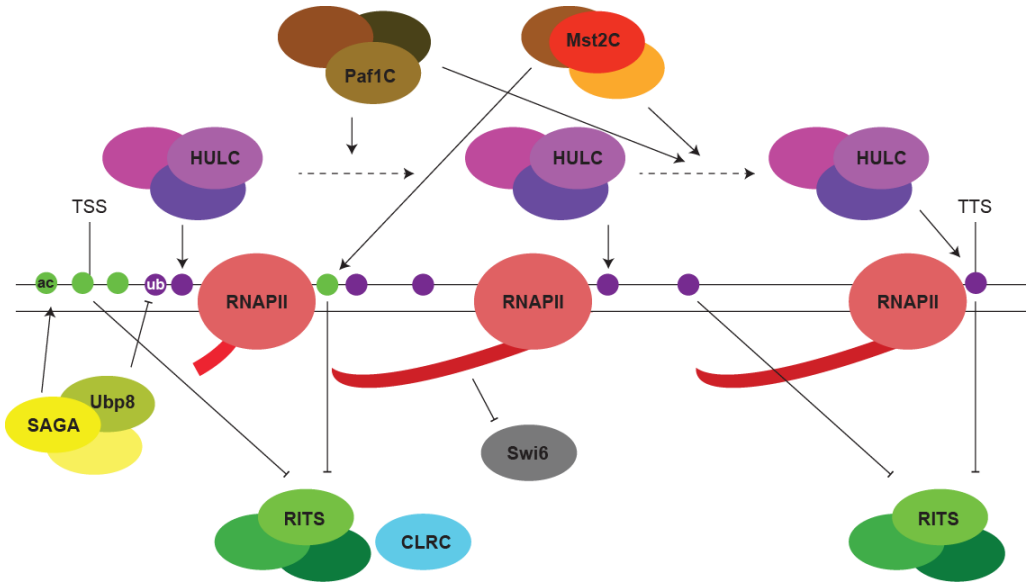

Figure 22: Speculative model for euchromatic repression of de novo heterochromatin formation. Multiple transcription-coupled chromatin marks prevent binding of the RITS complex to the nascent transcript. Both Paf1C and Mst2C promote HULC occupancy/activity in the body and the 3'-UTR of the transcribed gene leading to high H2B ubiquitination. This enhances elongation and termination efficiency, thus preventing RITS complex binding on a kinetic level, but also sterically. Furthermore, acetylation of H3K4/14 may also impair spreading of the RITS complex and CLRC, representing a second layer of repression. Since also Swi6 cannot bind to transcribed regions due to RNA-mediated eviction, all H3K9me2-recognizing and stabilizing proteins are prevented from binding to euchromatic loci, unless specifically recruited.

Transcription termination and heterochromatin nucleation

In the previous paragraphs, I elaborated how Mst2C and Paf1C modulate the chromatin context to prevent ectopic heterochromatin formation, presumably through H2B ubiquitination and H3K14 acetylation. However, the role of transcription itself is crucial in determining the fate of the transcript. Whereas the above-mentioned chromatin marks may impede the binding to or propagation of H3K9me2, the initial step of RNAi-directed heterochromatin formation is still dependent on a window of opportunity for the RITS complex to bind to the nascent transcript (Shimada et al., 2016).

Numerous findings hint towards a model where efficient transcription termination is crucial for preventing heterochromatin formation. Analysis of facultative heterochromatin islands in *S. pombe* on meiotic genes revealed that H3K9me2 levels peak at the 3'-end of genes, a

phenotype which is recapitulated on the *ade6*$^{+}$ reporter (Zofall et al., 2012, see Manuscript). Furthermore, *cis*-acting signals on euchromatic transcripts, presumably 3'-end processing signals or polyadenylation sites prevent action of the RNAi pathway (Yu et al., 2014). Vice versa, heterochromatic transcripts were shown to undergo inefficient transcription termination and termination sites coincide with high siRNA levels (Zaratiegui et al., 2011). This is corroborated by findings from our group, which propose the inefficient transcription termination in Paf1 mutants to provide a binding opportunity for the RITS complex (Kowalik et al., 2015). Also *trans*-acting factors were identified such as the 5' - 3' exonuclease Dhp1, which can induce premature transcription termination to nucleate heterochromatin (Chalamcharla et al., 2015; Tucker et al., 2016). Although those studies used temperature-sensitive (*ts)* alleles of the essential Dhp1 protein, the link of transcription termination to *de novo* heterochromatin formation is exciting.

Transcription termination has been studied extensively and the *cis*-acting signals on the nascent transcripts and the *trans*-acting factors involved in transcript processing, such as the CPF complex, are well-studied (see Introduction). However, if and how the chromatin context regulates transcription termination is largely unclear. Nevertheless, two major histone PTMs, H3K36me3 and H2Bub, are present at the end of the gene body and 3'-UTR, thus evoking the exciting possibility that these two modifications modulate transcription termination and prevent RITS complex or CLRC assembly on chromatin (see Figure 22). Experiments addressing the RNAPII occupancy at transcription termination sites, such as RNAPII ChIP or Native elongating transcript-sequencing (NET-Seq), in HULC, Set2, or Mst2 mutants may reveal novel functions of H2Bub and/or H3K36me3 in directing transcription termination.

How could these histone modifications prevent binding of the RITS complex? Similar to *S. cerevisiae*, binding of repressing complexes might be prevented by steric interference. Especially the ubiquitin moiety is almost as big as a histone protein itself and thereby may profoundly affect nucleosome accessibility. The nucleosome contains an acidic patch, which

contains parts of H2A and H2B. This region is gaining more and more attention as it becomes evident that histone readers not only recognize their respective mark on the histone tail, but also contact the nucleosome via the acidic patch (McGinty et al., 2014). Hence, an intriguing model could be that the bulkiness of the ubiquitin moiety sterically blocks the access of chromatin binders to the acidic patch. Amongst the precluded factors would be Chp1, which was recently shown to contact the acidic patch with its chromodomain (Zocco et al., 2016). Also HULC contacts the acidic patch in order to ubiquitinate H2B, and is thus guided to non-ubiquitinated nucleosomes (Cucinotta et al., 2015). This suggests a competition between HULC and Chp1 to bind the nucleosome, therefore (genome-wide) Chp1 ChIP experiments in HULC or H2BK119R mutants could address this question. In such mutants, Chp1 binding should be increased and potential low levels of H3K9me2 may be expected.

According to the model above, deubiquitination of H2Bub would be a prerequisite for *de novo* heterochromatin formation. Indeed, the subunit Sgf73 of the SAGA deubiquitination module was shown to interact with RITS and to assist in maintenance of centromeric silencing. Hence, I speculate that the RITS-DUB interaction may deubiquitinate H2Bub to allow efficient binding of RITS (Deng et al., 2015). Therefore, I would test *sgf73*Δ cells for their ability to initiate heterochromatin formation. Because all other SAGA DUB module subunits, including Ubp8, did not show any perturbations in heterochromatin, Sgf73 may recruit a different deubiquitinase or function via a completely different mechanism. Indeed, the Sgf73 homologue in *D. melanogaster*, Ataxin-7, modulates H2Bub differently than the other SAGA subunits (Mohan et al., 2014). In budding yeast, Sgf73p is involved in telomeric silencing via a direct interaction with the KDAC Sir2, however with context-dependent effects (McCormick et al., 2014). Furthermore, Sgf73p and Ubp8p form a SAGA-independent DUB module, which can deubiquitinate H2Bub outside of the SAGA complex and has been linked to promote mRNA export (Lim et al., 2013). Therefore it seems plausible that deubiquitination in *S. pombe* is also a prerequisite for heterochromatin formation, but might be orchestrated by multiple deubiquitinases.

It should be noted that besides HULC, multiple ubiquitin ligases and proteases were reported to affect heterochromatin stability in *S. pombe*. Amongst them are ubiquitin conjugating E2 enzymes such as Ubc15, Ubc3, and HULC subunit Rhp6; E3 ubiquitin ligases such as Brl1 and Msc1; and ubiquitin proteases such as Ubp3 (Choi et al., 2002; Lawrence and Volpe, 2009; Nielsen et al., 2002; Reyes-Turcu et al., 2011; Zofall and Grewal, 2007). Furthermore, Rhp6 ubiquitinates histone-like protein Obr1, which is crucial in mating-type region silencing and loss of silencing can be propagated even in the absence of Obr1 (Naresh et al., 2003).

Also CLRC is a CRL-type E3 ubiquitin ligase, whose activity is important for heterochromatin assembly (Hong et al., 2005; Jia et al., 2005). Notably, a purified CLRC complex can polyubiquitinate H2B *in vitro*, providing a potential mechanism to displace (monoubiquitinated?) H2B in heterochromatin (Horn et al., 2005). However, other groups did not report such activity (Buscaino et al., 2012; Jia et al., 2005). Also non-histone substrates could be targeted by the CLRC complex for polyubiquitination, as it was shown for a different CRL-type E3 ligase, the Cul4-Ddb1^{Ctd2} complex, which polyubiquitinates Epe1 in heterochromatin (Braun et al., 2011).

In summary, despite the important functions of ubiquitin in chromatin regulation, they are still barely understood on a molecular level. Therefore, I propose to use ubiquitinomics to dissect the roles of CLRC with a special focus on Raf1 due to its role as possible substrate receptor (Kuscu et al., 2014). Additionally, ubiquitinomics for other ubiquitination-related factors affecting heterochromatin structures may be an elegant first experimental step to get novel insights into ubiquitin-mediated chromatin regulation.

Physiological role of hetero- and euchromatic feedback loops

Unicellular organisms have the remarkable ability to adapt to changes in environmental conditions. Because *S. pombe* has a functional RNAi pathway, it is an excellent model organism to study potential siRNA-mediated adaptation to environmental changes (see Figure 23). For example, RNAi has been linked to adaption under heat shock conditions: Under normal temperatures, RNAi represses stress genes in a Dcr1-dependent manner (Woolcock et al., 2012). Upon heat shock however, Dcr1 is exported and aggregates in the cytoplasm, which leads to a derepression of these stress genes. At the same time, Heat shock protein 104 disaggregates Dcr1 in the cytoplasm, which leads to its reimport into the nucleus and to the repression of the stress genes, but also of the Hsp104 locus (Oberti et al., 2015). This constitutes a negative feedback loop, which buffers environmental changes by reducing the influence of RNAi-related gene expression changes.

Evolution of such a sophisticated feedback loop suggests a modulatory function of RNAi in adaptation to environmental changes. This is further supported by unpublished data from our group, which shows that the RNAi pathway is involved in directing survival under high cobalt chloride conditions (see Figure 23). Intriguingly, a deletion library screen found *mst2*Δ cells to survive better under high cobalt chloride conditions (Ryuko et al., 2012). The same study also identified ubiquitin donor gene Ubi3 and the potentially ubiquitinated Set1/COMPASS subunit Swd2, implying that an imperfect euchromatic feedback loop could lead to faster adaption to stress conditions due to changed plasticity. Mst2 itself may be directly regulated environmentally, since a former PhD student in our group identified a shortened protein isoform of $mst2^{+}$ under heat shock conditions (Kasia Kowalik, *unpublished*). This phenotype lets us speculate that RNAi and Mst2C represent major players in regulating epigenetic plasticity, especially during elevated temperatures.

Intriguingly, Pdp3 is acetylated and phosphorylated on multiple residues, suggesting extensive regulation of the Mst2 complex anchor (Kettenbach et al., 2015). Furthermore in a

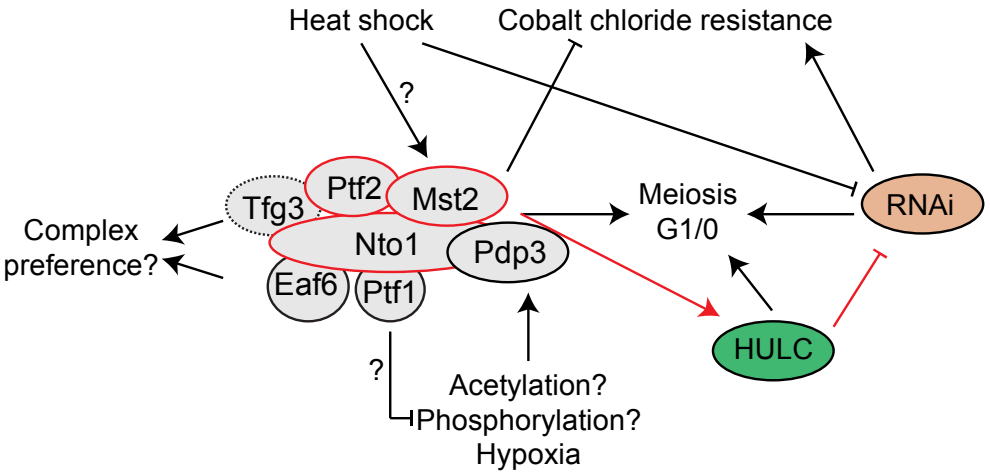

Figure 23: Interplay between Mst2C, HULC and RNAi machinery and their physiological roles. Tfg3 and Eaf6 are annotated to be present in multiple complexes, which may affect Mst2 specificity and activity. Ptf1 has an annotated phosphatase domain, which could counteract the phosphorylation of Pdp3 and affect chromatin binding. Pdp3 is also acetylated which also may alter its function. HULC also has additional acetylation sites, which may be regulated by other KATs. Red color depicts newly discovered genetic interactions in this thesis and indicates future directions of research. See text for further information.

global localization study in *S. cerevisiae*, Pdp3p was found to localize to the cytoplasm upon hypoxia (Dastidar et al., 2012), which could imply that without Pdp3p, NuA3b may localize to silent regions such as subtelomeres and activate subtelomeric genes. This is what we observe for Mst2C in *pdp3*Δ in *S. pombe* and since the subtelomeric genes are regulated in a nutrient-dependent manner (Mata et al., 2002), I propose that alteration of Pdp3 localization upon hypoxia or altered Mst2 interactions upon heat shock may lead to a metabolic shift to directly respond to environmental cues. Indeed, overexpression of *S. cerevisiae* Pdp3p or its human homologue, the oncogene NSD3s, leads to a metabolic shift from respiration to fermentation, a characteristic of cancer cells (Rona et al., 2016). This switch is dependent on Sas3p, implying a relevant function of Sas3p in metabolic control. In *S. pombe*, overexpression of Pdp3 has been annotated to be lethal, but has not been tested in more detail (Arita et al., 2011).

Not only stress conditions induce gene expression changes, but also the developmental switch between mitotic and meiotic (sexual) reproduction. Nitrogen starvation is one of the major signals that promote sexual reproduction in *S. pombe*. Upon removal of all nitrogen sources, yeast cells stop in cell cycle phase G1 and express pheromones in order to conjugate with a yeast cell

of the opposite mating type (reviewed in van Werven and Amon, 2011). In case of no mating partners, cells arrest in G1 (also called G0). Despite low transcriptional activity, nitrogen-starved G1 cells show very high levels of H3K36me3, which seems contradictory (Pai et al., 2014). One explanation for this discrepancy is that either H3K36me3 solely recruits Clr6C to induce transcriptional silencing, whereas Mst2C is precluded from H3K36me3 binding or that Mst2C binds these genes, but they are not (yet) transcribed. The latter hypothesis could attribute a poising function to Mst2C in priming cells to undergo meiosis upon conjugation. Indeed, in *S. cerevisiae* such a switch from a KDAC to a KAT system was proposed to shift nitrogen-starved cells from asexual to sexual reproduction (Pnueli et al., 2004). In this way, increased H2B ubiquitination due to Mst2-mediated acetylation of Brl1 may mark these genes for immediate (or efficient) transcription upon meiotic entry. Hence, it would be interesting to further investigate the role of Mst2C in this switch, potentially also looking at Brl1 and H2B ubiquitination. In addition, RNAi seems to play an essential role for cell survival upon prolonged starvation, which is proposed to work via ectopic heterochromatin formation (Joh et al., 2016; Roche et al., 2016). Altogether, this underlines the importance RNAi and Mst2C in regulating epigenetic plasticity to environmental cues.

In meiosis, *mst2*Δ cells suffer from abnormal ascospore formation and chromosome missegregation (Gómez et al., 2005). Furthermore, *paf1** single mutants initiate the ectopic silencing of the *ade6*$^{+}$ reporter very efficiently during meiosis, indicating a more potent RNAi pathway (Kowalik et al., 2015), whereas *paf1*mst2*Δ hardly survive meiosis (data not shown). This suggests that RNAi becomes more powerful during meiosis and hence, investigation of RNAi during meiosis may reveal novel, interesting insights. Intriguingly, meiotic genes are repressed in a RITS-dependent manner and Chp1 is released (or ejected) from chromatin very quickly upon nitrogen starvation (Hiriart et al., 2012). In addition, recent studies show that concomitant deletion of RNAi and Dhp1 leads to haploid meiosis and *dhp1-1* mutants mimic the *mst2*Δ phenotype in

ascospore formation, suggesting that RNAi, CTGS and Mst2 are linked in fine-tuning meiotic entry in G1-arrested cells (Chalamcharla et al., 2015; Tucker et al., 2016).

These indications motivated me to investigate meiosis more closely and I already established protocols to do so. However, biochemical analysis of meiotic events is hampered by the asynchronous entry of a cell population from G1 into the premeiotic S phase. This problem has been solved in previous years by using a temperature-sensitive mutant of Pat1, the main inhibitory kinase of meiotic entry (Iino and Yamamoto, 1985). New advances significantly improved this technique by specifically mutating the ATP-binding pocket of Pat1, which renders it sensitive to bulky ATP analogues such as 1- NM-PP1 (Cipak et al., 2012, 2014). Addition of this small molecule specifically inhibits the Pat1-as2 mutant, guaranteeing a synchronous entry into meiosis without the need of increased temperature and no effect on other kinases (see Figure 24). Therefore, in collaboration with an undergraduate student I established this protocol, which is enabling us to investigate epigenetic process during meiosis by biochemical and genetic approaches. Next, we will investigate the roles of Mst2C, Paf1C, and histone marks during meiosis to elucidate the importance of epigenetic plasticity during sexual differentiation.

These experiments will enable us for the first time to dissect the meiotic function of heterochromatin formation and prevention and could have a major impact for understanding germline-induced phenotypes and diseases in human cells.

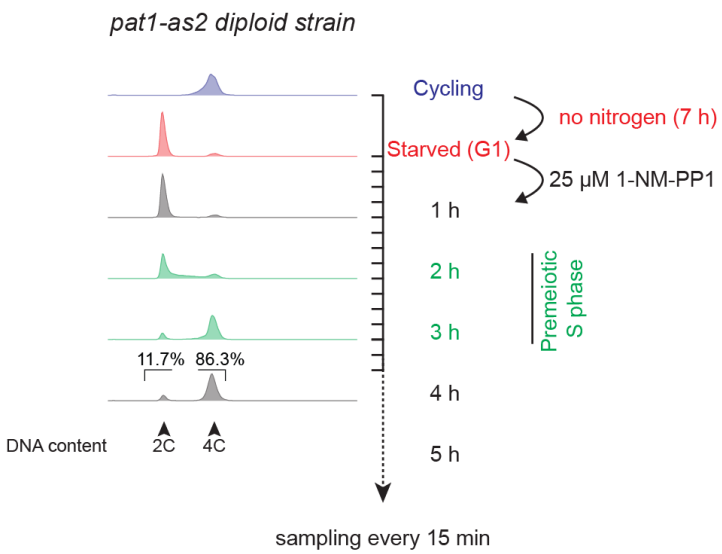

Figure 24: Synchronous meiosis using the 1-NM-PP1 sensitive pat1-as2 strain. Cycling diploid cells (blue) usually harbor four copies of the genome, which can be quantified using FACS. Starved cells (red) reside in G1 phase with only two copies. Addition of the Pat1-as2 inhibitor 1-NM-PP1 leads to a synchronous entry (<1 h difference) into premeiotic S phase, where again four copies are present after replication (green). This synchrony makes it possible to sample the entire meiotic process (~8 h) in 15 min intervals and analyze global properties on siRNA, RNA and protein level. Figure adapted from the Master thesis of T. Kuzdere.

Conservation to other organisms

Role of H3K36me3 and H2Bub in preventing silencing

It is firmly established that acetylation counteracts nucleation and spreading of heterochromatin, by directly changing biochemical properties of nucleosomes, but also by providing binding platforms for activating proteins or preventing binding of repressive complexes (see Introduction). However, a direct crosstalk between H2Bub and H3K36me3 has not been reported so far, although both euchromatic marks counteract heterochromatin in all here discussed organisms. Notably, although both marks counteract heterochromatin formation, there is no evidence for specific action of H3K36me3/H2Bub in counteracting RNAi pathways in other organisms, such as the piRNA pathway in animals or siRNA-dependent DNA methylation in *A. thaliana*. Also in *S. pombe*, wherein RNAi-independent heterochromatin formation in the absence of Mst2 has been reported (Wang et al., 2015), H3K36me3/H2Bub counteract heterochromatin independently of RNAi. However, this could not be addressed in my experiments due to the dependence of *de novo* heterochromatin formation on siRNAs targeting the *ade6*$^{+}$-reporter gene. Furthermore, mechanisms of initiation of heterochromatin formation and its repression by euchromatic factors have not been addressed in many organisms because it is inherently difficult due to powerful feedback loops, which impair a clear dissection of events.

In *S. cerevisiae*, H3K36me3 is sufficient to impair spreading of Sir2/3/4 independently of the KDAC Rpd3S, which suggests an additional role of H3K36me3 (Tompa and Madhani, 2007). Also H2Bub counteracts spreading of Sir2/3/4 in *S. cerevisiae* indirectly by promoting H3K79 methylation (Behrouzi et al., 2016). This mark impedes binding of Sir3p to nucleosomes and concomitant acetylation of H4K16 completely abrogates Sir3p binding. Furthermore, active deubiquitination is necessary to promote efficient spreading, attributing an essential role for low H2Bub in repressed regions (Sun and Allis, 2002). Indeed, Sir4p interacts with deubiquitinase Ubp10p and *ubp10* mutants show compromised silencing (Gardner et al., 2005). Ubp10p has

been further implicated to also deubiquitinate H2Bub in the gene body of long genes together with Ubp8p, which primarily deubiquitinates H2B at the start of the gene (Schulze et al., 2011). It could well be that the homologues of Ubp8/10p, Ubp8/16 also act redundantly in *S. pombe.* Such redundant functions would also partially explain why it is still unclear if deubiquitination of H2B is a prerequisite for heterochromatin assembly. Thus, I would test both genes as single/double deletions for their potential role in promoting heterochromatin formation.

Due to the euchromatin-preserving functions of H3K36me3 and H2Bub, a potential conservation of the identified euchromatic feedback loop seems possible. Although the identified acetylation site K242 in Brl1 is not conserved to Bre1p in *S. cerevisiae*, other acetylated residues in close proximity have been identified (K191, K194, K231), but not tested for biological relevance (Downey et al., 2015). Yet, other acetylomics studies did not identify these residues, maybe due to low abundance or technical differences (Henriksen et al., 2012; Weinert et al., 2014).

Notably, all investigated acetylomics studies in *S. cerevisiae* identified an acetylated lysine residue on Sgf73 (K33) with increased acetylation upon deletion of KDAC Rpd3p (Henriksen et al., 2012). The acetylated residue lies within the interaction motif of Sgf73p with Ubp8p (Köhler et al., 2010), suggesting that acetylation of K33 may impair association of Sgf73p with Ubp8p and thus reduce H2B deubiquitination. Such action would imply a potential divergence of the acetylation specificity of NuA3b, which targets the deubiquitination instead of the ubiquitination process. Although the responsible KAT remains to be identified (potentially NuA3b), such unusual divergent conservation would assign an important role of KAT/KDACs in the regulation of H2Bub levels. It would be therefore interesting to investigate the homologue of Rpd3p, Clr6 (or its non-essential subunit Alp13) in the search of the KDAC, which deacetylates Brl1.

In *A. thaliana*, deubiquitination of H2B by UBP26 is essential to allow spreading of H3K9me2 and DNA methylation (Sridhar et al., 2007) and H3K36me3 inhibits facultative heterochromatin formation via H3K27me3 on FLC (Yang et al., 2014). Ubiquitination of H2B and H3K36me3 both are important to fully activate FLC expression and hence delay flowering (Cao et al., 2008; Gu et

al., 2009; Zhao et al., 2005). Notably, the H3K36me3-reader proteins MRG1/2 both bind to H3K36me3 and are also required for full activation of FLC (Xu et al., 2014). This activation likely occurs via recruitment of the KATs HAM1/2, which acetylate H4K5, thus mimicking the mode of recruitment of Mst2 in *S. pombe*. Yet, also H3K4me3 levels change in MRG1/2 mutants, thus precluding a clear distinction between H4K5ac being a cause or a consequence of FLC activation. Hence, acetylomics of KAT mutants, especially HAM1/2 may reveal novel substrates.

Also deubiquitination of H2B seems to be important to regulate flowering time, as deletion of UBP26 also leads to early flowering, similarly to the phenotypes of the H2B ubiquitination machinery mutants (Schmitz et al., 2009). This finding implies that the turnover of ubiquitination on H2B could be important to activate gene expression. Yet, limited direct evidence such as ChIP experiments are available because most studies focused on genetic interactions, which do not allow a functional dissection of events.

In *D. melanogaster*, the Ubp10p homologue Scrawny also deubiquitinates H2Bub and is required for gene silencing and stem cell maintenance, whereas UBP7 deubiquitinates H2Bub for efficient PRC2-mediated facultative heterochromatin formation (Buszczak et al., 2009; Van Der Knaap et al., 2005). Conversely, the SAGA deubiquitinase *non-stop* and the DUB subunit SGF11 impair heterochromatin spreading, which suggests that the DUB module of SAGA rather prevents heterochromatin formation (Zhao et al., 2008). Another subunit of the DUB module, Ataxin-7 (the homologue of the previously introduced Sgf73 protein in yeast) plays a different role: Unlike in yeast, deletion of Ataxin-7 does not render the DUB module inactive, but rather hyperactive and reduces H2B ubiquitination levels (Mohan et al., 2014). It would be interesting to test if Sgf73 in *S. pombe* rather acts as its homologue in budding yeast or if its function is similar to metazoan Ataxin-7.

Also H3K36me3 has been linked to repressing PRC2 activity and hence facultative heterochromatin formation (Schmitges et al., 2011). Furthermore, full transcriptional activation of the single X chromosome in male flies, also known as dosage compensation, partially relies on

H3K36me3 (Bell et al., 2008). H3K36me3 recruits the male-specific lethal (MSL) complex with the KAT MOF via the potential H3K36me3-reader MSL3 to these regions, which leads to hyperacetylation of H4K16 and thus resembles recruitment of Mst2C in *S. pombe* and HAM1/2 in *A. thaliana*. Intriguingly, H4K16ac levels only correlate with H3K36me3 on the X chromosome, whereas they anticorrelate on autosomes. Such inconsistence could be explained by additional substrates of MOF, which are chromatin-context dependent. Furthermore, *in vitro* data suggests that MOF directly acetylates MSL3 to regulate spreading of the complex (Buscaino et al., 2003). Hence, acetylomics experiments may confirm or reveal additional substrates of MOF.

In summary, H3K36me3 and H2B ubiquitination protect genes from silencing and are required for full transcriptional activity in plants and flies. However, a direct link between these two marks is missing and only limited literature is available about regulation of both marks (especially H2B ubiquitination). Although acetylome studies have been performed, their coverage is limited and only identified a few hundred acetylation sites (Finkemeier et al., 2011; Weinert et al., 2011).

In mammals, H2Bub was shown to prevent heterochromatin spreading, such as at the human β-globin locus, where H2B ubiquitination demarcates a protective boundary (Ma et al., 2011). Furthermore, similar to *S. pombe*, H2Bub is important for centromere integrity, especially at the central core (Sadeghi et al., 2014). However, there is only limited data available about H2B ubiquitination preventing heterochromatin. As observed in *D. melanogaster*, H3K36me3 prevents PRC2 activity also in mammals (Lu et al., 2016; Yuan et al., 2011). Furthermore, H3K36me3 is recognized by the *de novo* DNA methyltransferases Dnmt3A and B1, which methylate DNA in the gene bodies and suppress cryptic transcription initiation events (Baubec et al., 2015; Neri et al., 2017). DNA methylation is quite persistent and can be propagated through cell division, serving potentially as a memory function. It could well be that also metazoans acquired some sort of transcriptional memory involving DNA methylation, thereby using a similar model to *S. pombe*.

Conserved to *D. melanogaster*, the MSL complex with its KAT MOF (KAT8 in mammals) is important for H4K16 acetylation (Dou et al., 2005). Fascinatingly, the human MSL complex contains the E3 ligase MSL2, which ubiquitinates H2BK34 and promotes H3K4 and H3K79 methylation (Wu et al., 2011). The authors propose a dual function of the MSL complex to activate gene expression both by acetylation of H4K16, but also by ubiquitination of H2BK34, thus strongly resembling the function of Mst2C in *S. pombe*.

Notably, the lysine K242 of Brl1 is conserved to the human homologue Bre1A but not to Bre1B, despite similar conservation in general, which is quite low with 14 % (data not shown). However, acetylome analysis did not reveal this specific residue or residues in close proximity to be acetylated (Svinkina et al., 2015). In general, in order to understand the role of acetylated lysines in the N-terminal part of Brl1 or its homologues, structural information might be crucial. Because this region is predicted *in silico* to be quite stable due to many coiled-coil motifs (data not shown), crystallization attempts might be successful and provide useful insights in how acetylation of Brl1 may affect its structure, interactions and activity.

On a physiological level, low levels of H2Bub are required to maintain stem cell identity in mammals and fruit flies, which is catalyzed by the activity of deubiquitinases, such as USP44 (Fuchs et al., 2012a). During differentiation, USP44 expression is reduced to increase H2Bub levels and induce optimal gene activation, especially for long genes. Along these lines, H2Bub peaks during differentiation, but is again strongly reduced in terminally differentiated cells such as myotubes (Karpiuk et al., 2012; Vethantham et al., 2012). Similarly, H3K36me3 promotes cell differentiation and exists at low levels in mouse embryonic stem cells (Zhang et al., 2014).

As a final point, H3K36me3 and H2Bub are also both deregulated in cancer. For example Setd2, a human homologue of Set2, is mutated in multiple cancer forms and many different cancer types are associated with a complete loss of H2B ubiquitination (Cole et al., 2015; Dalgliesh et al., 2010; Fontebasso et al., 2013; Hahn et al., 2012). Interestingly, a mutation of the H3K36 residue itself (H3K36M) has a dominant-negative effect on H3K36 methylation by sequestering

the responsible methyltransferases and might be causal for sarcomas (Lu et al., 2016). This sequestering abolishes H3K36me3, leads to increased H3K27me3 by PRC2, and reduced differentiation, further corroborating the antagonistic actions of H3K36me3 and H3K27me3.

In brief, both H2Bub and H3K36me3 protect genes from being silenced, actively prevent heterochromatin spreading and facultative heterochromatin formation, and are important for complete gene activation in multiple organisms. These functions are important during differentiation and promote genome stability, which counteracts development of cancer. However, it remains unknown if there is a direct crosstalk and self-enforcing feedback loop between H3K36me3 and H2B ubiquitination in other organisms than *S. pombe*.

Function of Mst2C

The homologue of Mst2 in *S. cerevisiae*, Sas3p, was postulated to be a promoter-associated KAT that acts redundantly with SAGA to activate transcription (Taverna et al., 2006). The double deletion of Sas3p and Gcn5p is synthetic lethal in *S. cerevisiae*, but not in *S. pombe*, suggesting divergence of these complexes. Interestingly, recent research shows that in *S. cerevisiae*, an alternative subcomplex called NuA3b localizes to gene bodies via its newly identified subunit Pdp3p, which complies with my data in fission yeast (see Figure 25 left panel, Gilbert et al., 2014; Martin et al., 2017). Furthermore, NuA3 does not show high activity on H3K14 unless Gcn5p is deleted (Vicente-Muñoz et al., 2014). Deletion of Pdp3p and Gcn5p is not synthetic lethal, suggesting a different role of this complex and hence it would be interesting to identify Sas3p targets by acetylomics to check if the H3K36me3(-Sas3p)-H2Bub signaling cascade is conserved.

Intriguingly, Pdp3p-mediated NuA3b localization is especially important for efficient elongation on longer genes (Martin et al., 2017). This could be conserved to *S. pombe*, where I see increased cryptic antisense transcription on longer genes in *paf1*mst2*Δ cells (data not shown). Hence, it would be interesting to investigate if long genes are more prone to ectopic

heterochromatin formation and show increased H3K9me2 in a *paf1*mst2*Δ or *paf1*pdp3*Δ background. This could be tested by H3K9me2 ChIP-Seq and would also reveal other loci with *de novo* heterochromatin formation. Furthermore, budding yeast Pdp3p pull-down experiments identified Rpb1, FACT and deubiquitinating enzymes (Vicente-Muñoz et al., 2014), suggesting that NuA3b might interact with these components to promote transcriptional elongation directly or indirectly via H2Bub.

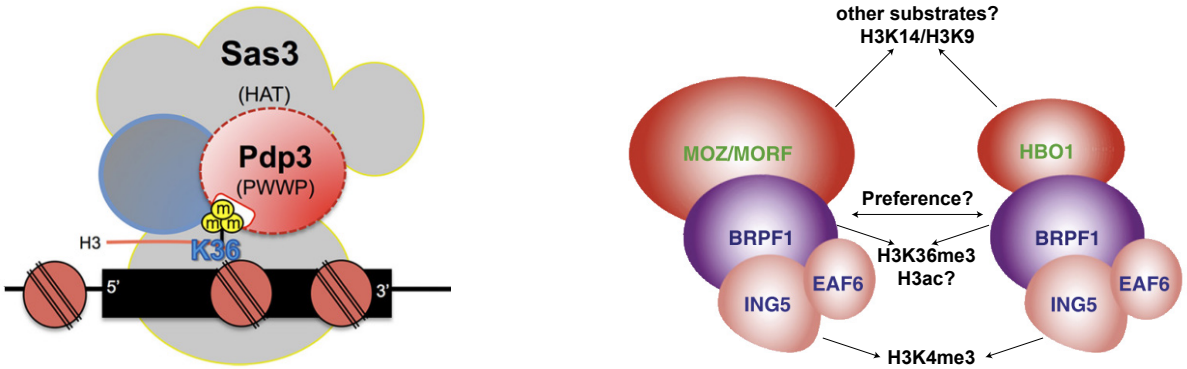

Figure 25: Conservation and composition of Mst2C homologues. Left panel: NuA3b is the recently identified homologue of Mst2C including H3K36me3 reader Pdp3p. Also in *S. cerevisiae*, NuA3b is believed to have additional substrates to H3K14. Picture taken from Gilbert et al., 2014.
Right panel: In mammals, multiple Mst2C homologues can acetylate H3K14. However, the exact preferences are unknown and may depend on complex composition. BRPF1 is an essential subunit for complex integrity and specificity and has multiple histone reader domains. Alternatively, HBO1 can also associate with JADE1, a scaffold protein similar to BRPF1. ING5 can be replaced by ING4 and is the homologue of *S. cerevisiae* Yng1p. Picture adapted from Yang, 2015.

Mst2C is also conserved in mammals, but it is difficult to assign a clear homologue (see Figure 25, right panel). Multiple KATs are known to acetylate H3K14, the main histone target of Mst2C, which are KAT6A, KAT6B and KAT7 (also known as MOZ, MORF and HBO1). They acetylate H3K14, but also H3K9 (Dreveny et al., 2014; Kueh et al., 2011). All three KATs exist in complexes, in which several members resemble Mst2C subunits, such as EAF6 and BRPF1, which also contains a H3K36me3-recognizing PWWP domain like Pdp3 (Vezzoli et al., 2010). Besides the PWWP domain, BRPF1 contains multiple DNA and histone-recognizing domains and likely acts as a scaffold protein, but also controls substrate specificity such as H3 acetylation for KAT7 (Lalonde et al., 2013). This suggests that BRPF1 orchestrates the localization and substrate specificity of multiple KATs and thus makes it a key player in directing histone acetylation by

KAT6A/B/7. It would be therefore crucial to investigate the role of BRPF1 and its regulation, potentially via PTMs. Besides that, KAT7 was shown to protect the central core of centromeres from excessive H3K9me3 and to promote incorporation of CENP-A (the mammalian Cnp1 homologue), which resembles the role of H2Bub in *S. pombe* (Ohzeki et al., 2016).

During mouse development, KAT7 is the major H3K14 KAT and KAT7 knockout (KO) mice die at E10.5, unlike KAT6A and 6B KO mice, which die at E14.5 or postnatally, respectively (Katsumoto et al., 2006; Kueh et al., 2011; Thomas et al., 2000). Furthermore, KAT6A/B KO mice show severe morphological phenotypes, mostly affecting senescence, neural stem cell proliferation, and craniofacial properties (Perez-Campo et al., 2014; Sheikh et al., 2012). Senescence might be directly affected by acetylation of key regulator p53, which was shown to be mediated by KAT6A (Rokudai et al., 2013). Furthermore, all three potential Mst2 homologues are implicated in cancer and neuronal disorders (reviewed in Yang, 2015). These phenotypes illustrate the important function of KATs in controlling gene expression and genome stability, but have not yet been clearly assigned to the individual KATs.

While I focused on potential Mst2 homologues in mammals by looking at the same substrate H3K14, it could well be that the substrate specificity changed during evolution. Therefore, I would like to point out that the *bona fide* H4K16 KAT MOF as part of the MSL complex shows an intriguing similarity to the Mst2 complex. Multiple reports attribute a role of the MSL in stimulating transcriptional elongation, an anchoring role for H3K36me3 via MSL3 and a direct link to stimulate H2B ubiquitination via E3 ligase MSL2 (Bell et al., 2007; Larschan et al., 2007; Wu et al., 2011).

Summarizing, the function and composition of NuA3b in *S. cerevisiae* is similar to Mst2C and would be interesting to follow up on, focusing particularly on possible feedback loops. The mammalian complexes are however much less characterized, which first demands a clear assignment of an actual Mst2C homologue by looking at its genomic distribution via ChIP-Seq, before following up a potential role in protecting euchromatin and regulation of H2Bub.

Conclusions

Within this thesis, I discovered a euchromatic feedback loop, which involves an unusual histone writer crosstalk across the gene body, involving the KAT Mst2 and the euchromatic hallmarks H3K36me3 and ubiquitinated H2BK119. Since H2Bub directs H3K4 methylation, also a hallmark of transcription initiation, this loop ultimately closes the circle to transcriptional activity. Speculating, such a self-enforcing loop can serve multiple purposes:

1) It creates some sort of transcriptional memory, which reduces transcriptional noise and enhances epigenetic robustness. Indeed, H3K4me3 has been linked to provide such memory in re-expression of stress response genes in *A thaliana* (Ding et al., 2012). Similarly, H3K36me3 has been proposed to act as memory mark for parentally transcribed genes in the transcriptionally silent embryonic germ cells of *C. elegans*, which is absolutely essential to develop a functional germline in the offspring (Furuhashi et al., 2010).

2) It protects euchromatic genes from ectopic heterochromatin formation by inhibiting the binding of heterochromatin factors. This is likely to occur in a competitive manner, wherein transcriptional kinetics dictate the outcome and hence represent the initial discrimination between heterochromatic and euchromatic transcription. Indeed, mutants with hampered initiation and elongation kinetics also show no ectopic heterochromatin formation in a *paf1** background anymore, suggesting that RNAPII/nascent transcripts need to accumulate at the transcription termination sites to allow RNAi to nucleate heterochromatin. On the other hand, individual deletion of multiple transcription-associated factors, such as Mst2, Tfs1, mRNA export protein Mlo3, and Mediator subunit Med1 allows simultaneous deletion of RNAi factors such as Dcr1 without losing heterochromatin (Reddy et al., 2011; Reyes-Turcu et al., 2011). This suggests that transcription can also be shifted towards a condition favoring heterochromatin assembly.

3) Feedback loops give epigenetic robustness to the organism to maintain genomic stability in stress conditions and ensure accurate inheritance of the genetic material. At the same time, feedback loops maintain a certain plasticity and modulation, which allows the organism to adapt

to environmental changes. Since multiple protein complexes are involved in maintaining feedback loops, they offer a great variety for regulation, as changing the abundance, activity, or localization of a single member might be sufficient to alter or inactivate the feedback loop. Besides multiple identified and characterized heterochromatic feedback loops (Figures 12, 14 - 17), the identification of a euchromatic feedback loop (Figure 19) during my PhD adds another layer of complexity, but also increases the options for the organism to cope with challenges.

The role of H2B ubiquitination is fascinating. Given that various multisubunit complexes regulate H2Bub, such as Paf1C, Mst2C, and RNAPII, and that H2Bub is essential to install H3K4me3 (and H3K79me3 in other organisms), implies a central role of ubiquitination in chromatin regulation. This also makes sense on a structural level due to the bulkiness of ubiquitin, which suggests that ubiquitin may hinder chromatin effector proteins from binding to the nucleosome. Hence, I speculate that ubiquitin keeps chromatin in an intermediate, plastic state, which prevents (cryptic) transcription initiation, but also heterochromatin formation. Therefore, it is not surprising that H2B ubiquitination levels increase during differentiation, whereas being low in undifferentiated or terminally differentiated cells, suggesting that the increased plasticity during differentiation may rely on increased H2Bub levels and chromatin decompaction. In undifferentiated stem cells, H2Bub levels are kept low by the action of by multiple proteases perhaps in order not to create too much plasticity, which would result in uncontrolled differentiation.

As already mentioned above, the initial discrimination between heterochromatin and euchromatic transcription may rely on transcription kinetics. Whereas it is conceivable that high transcriptional activity interferes with heterochromatin initiation (Shimada et al., 2016), I believe that rather the transcriptional elongation speed dictates the fate of the transcript. High transcriptional activity has to lead to an increased elongation speed in order to avoid RNAPII collisions and this increased elongation rate primarily interferes with *de novo* heterochromatin

formation. Therefore, I would like to introduce a new term describing transcriptional kinetics, the "transcriptional efficiency". Whereas transcriptional activity rather describes how often RNAPII transcribes a gene and correlates well with H3K4me3 and H3K36me3, transcriptional efficiency describes how fast RNAPII proceeds through the gene body. This efficiency is orchestrated by a multitude of RNAPII-associated factors, such as Paf1C, FACT and HULC. Intriguingly, H2B ubiquitination plays an essential role and perhaps constitutes the actual histone mark associated with high transcriptional efficiency due to its stimulatory role on FACT and chromatin remodelers.

Although this model is a wild speculation, a few examples hint in this direction. For a long time the transcriptional elongation rate has been determined by run-on experiments. However, these experiments also take into account how many RNAPII molecules are loaded onto a particular gene and therefore mirror transcriptional activity as well. Recently, different methods such as 4sUDRB-Seq or BruDRB-Seq have been established (Fuchs et al., 2014a; Veloso et al., 2014). These methods use a block of early elongation by DRB to then measure how fast 4sU- or BrU-labelled nucleotides are incorporated after the release of this block. Although also this technique relies on the use of a drug and may induce artefacts, it is interesting that H2B ubiquitination seems to correlate very well with the respective elongation speed, whereas H3K36me3 correlates less (Fuchs et al., 2014b). Furthermore, such a model would partially explain the intimate link of H3K4me3 with H2B ubiquitination, since this would provide an essential crosstalk, wherein the transcriptional machinery, perhaps Paf1C, fine-tunes transcriptional initiation and elongation kinetics.

I am aware that such a model requires more experimental evidence and it is unclear if H2Bub is cause or consequence of high elongation rates. More experiments addressing elongation speed and its interplay with chromatin marks are required to support such a model. Yet, I am fascinated by the versatility of biological systems using unusual crosstalks and feedback loops to fine-tune transcriptional kinetics. Furthermore, a still open question remains about the kinetics of transcription termination and the contribution of chromatin in that (m)RNA fate-determining process.

ACKNOWLEDGMENTS

First and foremost, I would like to thank Marc for giving me the opportunity to do my PhD in his lab and being an outstanding boss! He always supported and believed in me, suggested unanticipated and break-through experiments, but also always gave me the freedom to pursue unexpected findings. His enthusiasm for science is just great and contagious and will serve me as a prime example for my future career in academia. I would like to further thank my thesis committee members Sigurd Braun and Helge Grosshans for fruitful discussions, excellent ideas and great support. Thanks also to Antoine Peters for chairing my PhD defense.

Furthermore, I would like to thank Sigurd and Paula for collaborating with me on the Mst2 project, a truly fruitful, engaged and stimulating collaboration! Along the same line, I would like to thank Sigurd for accepting not only to be co-referee, but also for hosting me in his lab for a few weeks. I enjoyed a lot this quick change of scene in Munich.

A big THANK YOU! goes to the entire lab, including current and former lab members, for creating a truly awesome working atmosphere, wherein overtime and weekend hours simply do not really count. Big thanks to the lab masters Yuki and Motty for providing an ideal lab environment and also always having an open ear for PhD student issues. I would specially like to acknowledge Claudi for introducing me to all the yeast methods, Alex for proofreading my thesis and Tahsin for his collaborative efforts on a new exciting project.

Furthermore, a huge thanks to our awesome facilities at the FMI, especially the Protein Analysis Facility and the Genomics Facility, which I used extensively. Special thanks to Vytautas and Jan, who helped me establishing acetylomics in the lab and Kirsten and Stéphane for countless preparations of (small)RNA libraries.

Personally, I feel truly privileged and humbled to have worked in such a great lab and found true friends, with whom I spent many hours in- and outside of the lab, be it chilling, grilling, and swimming at/in the Rhine, multiple house warming and keeping it warm parties (some are still

pending!), concerts, festivals, playing beach volleyball or skiing in winter. Special thanks to Vroni and Rieke, who became good friends during this time also outside of the lab.

My deepest gratitude also extends to my old and new friends outside of the Bühler lab, who distracted and supported me in difficult times: Old friends from my hometown and from the scouts, the “Soledurner Fasnacht” crowd, the former “Bernese” fellow students, the “Basel crew”, the “1st year baby PhD students with PhD mommy Elida”, the “Portuguese mafia” and the “Kitchen ravers” aka the flat mates ☺.

As usual, I would like to acknowledge some awesome music, which made me go and go and go during late stays in the lab, in the office and while writing this thesis. Therefore big up for Pendulum, Zeds dead, Kidnap Kid, Elke Kleijn, BBC Radio 1, UKF D’n’B, and Mixmag!

Last but not least, I would like to thank my family for their endless support and love: my mom and dad, Alex, and my sister with her family. This thesis would not have been possible without Lena, who continuously and infinitely supported me during all times and who just made my life so much better! Muito obrigado, amorzinha!

REFERENCES

Adelman, K., Wei, W., Ardehali, M.B., Werner, J., Zhu, B., Reinberg, D., and Lis, J.T. (2006). Drosophila Paf1 modulates chromatin structure at actively transcribed genes. Mol. Cell. Biol. *26*, 250–260.

Akoulitchev, S., Chuikov, S., and Reinberg, D. (2000). TFIIH is negatively regulated by cdk8-containing mediator complexes. Nature *407*, 102–106.

Al-Sady, B., Madhani, H.D., and Narlikar, G.J. (2013). Division of labor between the chromodomains of HP1 and Suv39 methylase enables coordination of heterochromatin spread. Mol. Cell *51*, 80–91.

Allen, B.L., and Taatjes, D.J. (2015). The Mediator complex: a central integrator of transcription. Nat. Rev. Mol. Cell Biol. *16*, 155–166.

Allfrey, V.G., Faulkner, R., and Mirsky, A.E. (1964). Acetylation and Methylation of Histones and Their Possible Role in the Regulation of Rna Synthesis. Proc. Natl. Acad. Sci. U. S. A. *51*, 786–794.

Allis, C.D., Berger, S.L., Cote, J., Dent, S., Jenuwien, T., Kouzarides, T., Pillus, L., Reinberg, D., Shi, Y., Shiekhattar, R., et al. (2007). New nomenclature for chromatin-modifying enzymes. Cell *131*, 633–636.

Allison, L.A., Moyle, M., Shales, M., and Ingles, C.J. (1985). Extensive homology among the largest subunits of eukaryotic and prokaryotic RNA polymerases. Cell *42*, 599–610.

Allshire, R.C., Javerzat, J.-P., Redhead, N.J., and Cranston, G. (1994). Position effect variegation at fission yeast centromeres. Cell *76*, 157–169.

Allshire, R.C., Nimmo, E.R., Ekwall, K., Javerzat, J.P., and Cranston, G. (1995). Mutations derepressing silent centromeric domains in fission yeast disrupt chromosome segregation. Genes Dev. *9*, 218–233.

Angel, A., Song, J., Dean, C., and Howard, M. (2011). A Polycomb-based switch underlying quantitative epigenetic memory. Nature *476*, 105–108.

Aoyagi, S., and Archer, T.K. (2007). Dynamic Histone Acetylation/Deacetylation with Progesterone Receptor-Mediated Transcription. Mol. Endocrinol. *21*, 843–856.

Aranda, A., and Proudfoot, N. (2001). Transcriptional termination factors for RNA polymerase II in yeast. Mol. Cell *7*, 1003–1011.

Aravin, A., Gaidatzis, D., Pfeffer, S., Lagos-Quintana, M., Landgraf, P., Iovino, N., Morris, P., Brownstein, M.J., Kuramochi-Miyagawa, S., Nakano, T., et al. (2006). A novel class of small RNAs bind to MILI protein in mouse testes. Nature *442*, 203–207.

Aravin, A.A., Lagos-Quintana, M., Yalcin, A., Zavolan, M., Marks, D., Snyder, B., Gaasterland, T., Meyer, J., and Tuschl, T. (2003). The small RNA profile during Drosophila melanogaster development. Dev. Cell *5*, 337–350.

Aravin, A.A., Sachidanandam, R., Bourc'his, D., Schaefer, C., Pezic, D., Toth, K.F., Bestor, T., and Hannon, G.J. (2008). A piRNA pathway primed by individual transposons is linked to de novo DNA methylation in mice. Mol. Cell *31*, 785–799.

Arita, Y., Nishimura, S., Matsuyama, A., Yashiroda, Y., Usui, T., Boone, C., and Yoshida, M. (2011). Microarray-based target identification using drug hypersensitive fission yeast expressing ORFeome. Mol. Biosyst. *7*, 1463–1472.

Aygün, O., Mehta, S., and Grewal, S.I.S. (2013). HDAC-mediated suppression of histone turnover promotes epigenetic stability of heterochromatin. Nat. Struct. Mol. Biol. *20*, 547–554.

Batta, K., Zhang, Z., Yen, K., Goffman, D.B., and Pugh, B.F. (2011). Genome-wide function of H2B ubiquitylation in promoter and genic regions. Genes Dev. *25*, 2254–2265.

REFERENCES

Baubec, T., Colombo, D.F., Wirbelauer, C., Schmidt, J., Burger, L., Krebs, A.R., Akalin, A., and Schübeler, D. (2015). Genomic profiling of DNA methyltransferases reveals a role for DNMT3B in genic methylation. Nature *520*, 243–247.

Bayne, E.H., White, S.A., Kagansky, A., Bijos, D.A., Sanchez-Pulido, L., Hoe, K.L., Kim, D.U., Park, H.O., Ponting, C.P., Rappsilber, J., et al. (2010). Stc1: A Critical Link between RNAi and Chromatin Modification Required for Heterochromatin Integrity. Cell *140*, 666–677.

Becker, J.S., Nicetto, D., and Zaret, K.S. (2016). H3K9me3-Dependent Heterochromatin: Barrier to Cell Fate Changes. Trends Genet. *32*, 29–41.

Behrouzi, R., Lu, C., Currie, M.A., Jih, G., Iglesias, N., and Moazed, D. (2016). Heterochromatin assembly by interrupted Sir3 bridges across neighboring nucleosomes. Elife *5*, 209–217.

Bell, O., Wirbelauer, C., Hild, M., Scharf, A.N.D., Schwaiger, M., MacAlpine, D.M., Zilbermann, F., van Leeuwen, F., Bell, S.P., Imhof, A., et al. (2007). Localized H3K36 methylation states define histone H4K16 acetylation during transcriptional elongation in Drosophila. EMBO J. *26*, 4974–4984.

Bell, O., Conrad, T., Kind, J., Wirbelauer, C., Akhtar, A., and Schübeler, D. (2008). Transcription-coupled methylation of histone H3 at lysine 36 regulates dosage compensation by enhancing recruitment of the MSL complex in Drosophila melanogaster. Mol. Cell. Biol. *28*, 3401–3409.

Bell, O., Tiwari, V.K., Thomä, N.H., and Schübeler, D. (2011). Determinants and dynamics of genome accessibility. Nat. Rev. Genet. *12*, 554–564.

Belotserkovskaya, R., Oh, S., Bondarenko, V.A., Orphanides, G., Studitsky, V.M., and Reinberg, D. (2003). FACT facilitates transcription-dependent nucleosome alteration. Science *301*, 1090–1093.

Bentley, D.L. (2014). Coupling mRNA processing with transcription in time and space. Nat. Rev. Genet. *15*, 163–175.

Berger, S.L., Kouzarides, T., Shiekhattar, R., and Shilatifard, A. (2009). An operational definition of epigenetics. Genes Dev. *23*, 781–783.

Bernstein, B.E., Mikkelsen, T.S., Xie, X., Kamal, M., Huebert, D.J., Cuff, J., Fry, B., Meissner, A., Wernig, M., Plath, K., et al. (2006). A bivalent chromatin structure marks key developmental genes in embryonic stem cells. Cell *125*, 315–326.

Berry, S., and Dean, C. (2015). Environmental perception and epigenetic memory: Mechanistic insight through FLC. Plant J. *83*, 133–148.

Birney, E., Stamatoyannopoulos, J.A., Dutta, A., oacute, R.G., Gingeras, T.R., Margulies, E.H., Weng, Z., Snyder, M., Dermitzakis, E.T., Thurman, R.E., et al. (2007). Identification and analysis of functional elements in 1% of the human genome by the ENCODE pilot project. Nature *447*, 799–816.

Blackledge, N.P., Farcas, A.M., Kondo, T., King, H.W., McGouran, J.F., Hanssen, L.L.P., Ito, S., Cooper, S., Kondo, K., Koseki, Y., et al. (2014). Variant PRC1 Complex-Dependent H2A Ubiquitylation Drives PRC2 Recruitment and Polycomb Domain Formation. Cell *157*, 1445–1459.

Blewitt, M.E., Vickaryous, N.K., Hemley, S.J., Ashe, A., Bruxner, T.J., Preis, J.I., Arkell, R., and Whitelaw, E. (2005). An N-ethyl-N-nitrosourea screen for genes involved in variegation in the mouse. Proc. Natl. Acad. Sci. U. S. A. *102*, 7629–7634.

Böhmdorfer, G., Sethuraman, S., Rowley, M.J., Krzyszton, M., Rothi, M.H., Bouzit, L., and Wierzbicki, A.T. (2016). Long non-coding RNA produced by RNA polymerase V determines boundaries of heterochromatin. Elife *5*, 1–24.

Bonnet, J., Devys, D., and Tora, L. (2014). Histone H2B ubiquitination: Signaling not scrapping. Drug Discov. Today Technol. *12*, 19–27.

REFERENCES

Booth, G.T., Wang, I.X., Cheung, V.G., and Lis, J.T. (2016). Divergence of a conserved elongation factor and transcription regulation in budding and fission yeast. Genome Res. *26*, 799–811.

Bortvin, A., and Winston, F. (1996). Evidence that Spt6p controls chromatin structure by a direct interaction with histones. Science *272*, 1473–1476.

Bosco, G., Campbell, P., Leiva-Neto, J.T., and Markow, T.A. (2007). Analysis of Drosophila Species Genome Size and Satellite DNA Content Reveals Significant Differences Among Strains as Well as Between Species. Genetics *177*, 1277–1290.

Braun, S., Garcia, J.F., Rowley, M., Rougemaille, M., Shankar, S., and Madhani, H.D. (2011). The Cul4-Ddb1Cdt2 ubiquitin ligase inhibits invasion of a boundary-associated antisilencing factor into heterochromatin. Cell *144*, 41–54.

Braunstein, M., Rose, A.B., Holmes, S.G., Allis, C.D., and Broach, J.R. (1993). Transcriptional silencing in yeast is associated with reduced nucleosome acetylation. Genes Dev. *7*, 592–604.

Brennecke, J., Aravin, A.A., Stark, A., Dus, M., Kellis, M., Sachidanandam, R., and Hannon, G.J. (2007). Discrete small RNA-generating loci as master regulators of transposon activity in Drosophila. Cell *128*, 1089–1103.

Brown, C.J., Ballabio, A., Rupert, J.L., Lafreniere, R.G., Grompe, M., Tonlorenzi, R., and Willard, H.F. (1991). A gene from the region of the human X inactivation centre is expressed exclusively from the inactive X chromosome. Nature *349*, 38–44.

Brown, J.L., Mucci, D., Whiteley, M., Dirksen, M.L., and Kassis, J.A. (1998). The Drosophila Polycomb group gene pleiohomeotic encodes a DNA binding protein with homology to the transcription factor YY1. Mol. Cell *1*, 1057–1064.

Brown, J.L., Fritsch, C., Mueller, J., and Kassis, J.A. (2003). The Drosophila pho-like gene encodes a YY1-related DNA binding protein that is redundant with pleiohomeotic in homeotic gene silencing. Development *130*, 285–294.

Buhler, M., and Gasser, S.M. (2009). Silent chromatin at the middle and ends: lessons from yeasts. Embo J *28*, 2149–2161.

Bühler, M., Verdel, A., and Moazed, D. (2006). Tethering RITS to a Nascent Transcript Initiates RNAi- and Heterochromatin-Dependent Gene Silencing. Cell *125*, 873–886.

Bühler, M., Haas, W., Gygi, S.P., and Moazed, D. (2007). RNAi-Dependent and -Independent RNA Turnover Mechanisms Contribute to Heterochromatic Gene Silencing. Cell *129*, 707–721.

Bühler, M., Spies, N., Bartel, D.P., and Moazed, D. (2008). TRAMP-mediated RNA surveillance prevents spurious entry of RNAs into the Schizosaccharomyces pombe siRNA pathway. Nat. Struct. Mol. Biol. *15*, 1015–1023.

Buker, S.M., Iida, T., Bühler, M., Villén, J., Gygi, S.P., Nakayama, J.-I., and Moazed, D. (2007). Two different Argonaute complexes are required for siRNA generation and heterochromatin assembly in fission yeast. Nat. Struct. Mol. Biol. *14*, 200–207.

Buscaino, A., Köcher, T., Kind, J.H., Holz, H., Taipale, M., Wagner, K., Wilm, M., and Akhtar, A. (2003). MOF-regulated acetylation of MSL-3 in the Drosophila dosage compensation complex. Mol. Cell *11*, 1265–1277.

Buscaino, A., White, S.A., Houston, D.R., Lejeune, E., Simmer, F., de Lima Alves, F., Diyora, P.T., Urano, T., Bayne, E.H., Rappsilber, J., et al. (2012). Raf1 is a DCAF for the Rik1 DDB1-like protein and has separable roles in siRNA generation and chromatin modification. PLoS Genet. *8*, 1–14.

REFERENCES

Buscaino, A., Lejeune, E., Audergon, P., Hamilton, G., Pidoux, A., and Allshire, R.C. (2013). Distinct roles for Sir2 and RNAi in centromeric heterochromatin nucleation, spreading and maintenance. EMBO J. *32*, 1250–1264.

Buszczak, M., Paterno, S., and Spradling, A.C. (2009). Drosophila stem cells share a common requirement for the histone H2B ubiquitin protease scrawny. Science *323*, 248–251.

Cam, H.P., Sugiyama, T., Chen, E.S., Chen, X., Fitzgerald, P.C., and Grewal, S.I.S. (2005). Comprehensive analysis of heterochromatin- and RNAi- mediated epigenetic control of the fission yeast genome. Nat. Genet. *37*, 809–820.

Campos, E.I., and Reinberg, D. (2009). Histones: annotating chromatin. Annu. Rev. Genet. *43*, 559–599.

Canzio, D., Chang, E.Y., Shankar, S., Kuchenbecker, K.M., Simon, M.D., Madhani, H.D., Narlikar, G.J., and Al-Sady, B. (2011). Chromodomain-Mediated Oligomerization of HP1 Suggests a Nucleosome-Bridging Mechanism for Heterochromatin Assembly. Mol. Cell *41*, 67–81.

Cao, Y., Dai, Y., Cui, S., and Ma, L. (2008). Histone H2B monoubiquitination in the chromatin of FLOWERING LOCUS C regulates flowering time in Arabidopsis. Plant Cell *20*, 2586–2602.

Carlberg, C., and Molnár, F. (2014). Mechanisms of Gene Regulation (Dordrecht: Springer Netherlands).

Carrozza, M.J., Li, B., Florens, L., Suganuma, T., Swanson, S.K., Lee, K.K., Shia, W.J., Anderson, S., Yates, J., Washburn, M.P., et al. (2005). Histone H3 methylation by Set2 directs deacetylation of coding regions by Rpd3S to suppress spurious intragenic transcription. Cell *123*, 581–592.

Chalamcharla, V.R., Folco, H.D., Dhakshnamoorthy, J., and Grewal, S.I.S. (2015). Conserved factor Dhp1/Rat1/Xrn2 triggers premature transcription termination and nucleates heterochromatin to promote gene silencing. Proc. Natl. Acad. Sci. *112*, 201522127.

Chen, E.S., Zhang, K., Nicolas, E., Cam, H.P., Zofall, M., and Grewal, S.I. (2008). Cell cycle control of centromeric repeat transcription and heterochromatin assembly. Nature *451*, 734–737.

Cho, E.J., Kobor, M.S., Kim, M., Greenblatt, J., and Buratowski, S. (2001). Opposing effects of Ctk1 kinase and Fcp1 phosphatase at Ser 2 of the RNA polymerase II C-terminal domain. Genes Dev. *15*, 3319–3329.

Choi, E.S., Kim, H.S., Jang, Y.K., Hong, S.H., and Park, S.D. (2002). Two ubiquitin-conjugating enzymes, Rhp6 and UbcX, regulate heterochromatin silencing in Schizosaccharomyces pombe. Mol. Cell. Biol. *22*, 8366–8374.

Choi, J., Hyun, Y., Kang, M.-J., In Yun, H., Yun, J.-Y., Lister, C., Dean, C., Amasino, R.M., Noh, B., Noh, Y.-S., et al. (2009). Resetting and regulation of Flowering Locus C expression during Arabidopsis reproductive development. Plant J. *57*, 918–931.

Chu, Y., Simic, R., Warner, M.H., Arndt, K.M., and Prelich, G. (2007). Regulation of histone modification and cryptic transcription by the Bur1 and Paf1 complexes. EMBO J. *26*, 4646–4656.

Cipak, L., Hyppa, R.W., Smith, G.R., and Gregan, J. (2012). ATP analog-sensitive Pat1 protein kinase for synchronous fission yeast meiosis at physiological temperature. Cell Cycle *11*, 1626–1633.

Cipak, L., Polakova, S., Hyppa, R.W., Smith, G.R., and Gregan, J. (2014). Synchronized fission yeast meiosis using an ATP analog-sensitive Pat1 protein kinase. Nat. Protoc. *9*, 223–231.

Cole, A.J., Clifton-Bligh, R., and Marsh, D.J. (2015). Histone H2B monoubiquitination: Roles to play in human malignancy. Endocr. Relat. Cancer *22*, T19–T33.

REFERENCES

Colmenares, S.U., Buker, S.M., Buhler, M., Dlakić, M., and Moazed, D. (2007). Coupling of Double-Stranded RNA Synthesis and siRNA Generation in Fission Yeast RNAi. Mol. Cell *27*, 449–461.

Cordaux, R., and Batzer, M.A. (2009). The impact of retrotransposons on human genome evolution. Nat. Rev. Genet. *10*, 691–703.

Creamer, K.M., Job, G., Shanker, S., Neale, G. a, Lin, Y., Bartholomew, B., and Partridge, J.F. (2014). The Mi-2 homolog Mit1 actively positions nucleosomes within heterochromatin to suppress transcription. Mol. Cell. Biol. *34*, 2046–2061.

Cucinotta, C.E., Young, A.N., Klucevsek, K.M., and Arndt, K.M. (2015). The Nucleosome Acidic Patch Regulates the H2B K123 Monoubiquitylation Cascade and Transcription Elongation in Saccharomyces cerevisiae. PLoS Genet. *11*, 1–25.

Cuddapah, S., Jothi, R., Schones, D.E., Roh, T.-Y., Cui, K., and Zhao, K. (2009). Global analysis of the insulator binding protein CTCF in chromatin barrier regions reveals demarcation of active and repressive domains. Genome Res. *19*, 24–32.

Czermin, B., Schotta, G., Hülsmann, B.B., Brehm, A., Becker, P.B., Reuter, G., and Imhof, A. (2001). Physical and functional association of SU(VAR)3-9 and HDAC1 in Drosophila. EMBO Rep. *2*, 915–919.

Czudnochowski, N., Bösken, C. a., and Geyer, M. (2012). Serine-7 but not serine-5 phosphorylation primes RNA polymerase II CTD for P-TEFb recognition. Nat. Commun. *3*, 842.

Dalgliesh, G.L., Furge, K., Greenman, C., Chen, L., Bignell, G., Butler, A., Davies, H., Edkins, S., Hardy, C., Latimer, C., et al. (2010). Systematic sequencing of renal carcinoma reveals inactivation of histone modifying genes. Nature *463*, 360–363.

Dastidar, R.G., Hooda, J., Shah, A., Cao, T.M., Henke, R.M., and Zhang, L. (2012). The nuclear localization of SWI/SNF proteins is subjected to oxygen regulation. Cell Biosci. *2*, 1.

David, C.J., Boyne, A.R., Millhouse, S.R., and Manley, J.L. (2011). The RNA polymerase II C-terminal domain promotes splicing activation through recruitment of a U2AF65-Prp19 complex. Genes Dev. *25*, 972–983.

Davidovich, C., and Cech, T.R. (2015). The recruitment of chromatin modifiers by long noncoding RNAs: lessons from PRC2. RNA *21*, 2007–2022.

Deans, C., and Maggert, K.A. (2015). What Do You Mean, “Epigenetic”? Genetics *199*, 887–896.

Debelouchina, G.T., Gerecht, K., and Muir, T.W. (2016). Ubiquitin utilizes an acidic surface patch to alter chromatin structure. Nat. Chem. Biol. *13*, 1–9.

DeGennaro, C.M., Alver, B.H., Marguerat, S., Stepanova, E., Davis, C.P., Bahler, J., Park, P.J., and Winston, F. (2013). Spt6 Regulates Intragenic and Antisense Transcription, Nucleosome Positioning, and Histone Modifications Genome-Wide in Fission Yeast. Mol. Cell. Biol. *33*, 4779–4792.

Deng, X., Zhou, H., Zhang, G., Wang, W., Mao, L., Zhou, X., Yu, Y., and Lu, H. (2015). Sgf73, a subunit of SAGA complex, is required for the assembly of RITS complex in fission yeast. Sci. Rep. *5*, 14707.

Dermody, J.L., and Buratowski, S. (2010). Leo1 subunit of the yeast paf1 complex binds RNA and contributes to complex recruitment. J. Biol. Chem. *285*, 33671–33679.

Dhalluin, C., Carlson, J.E., Zeng, L., He, C., Aggarwal, A.K., and Zhou, M.M. (1999). Structure and ligand of a histone acetyltransferase bromodomain. Nature *399*, 491–496.

Dilworth, D.J., Tackett, A.J., Rogers, R.S., Yi, E.C., Christmas, R.H., Smith, J.J., Siegel, A.F., Chait, B.T., Wozniak, R.W., and Aitchison, J.D. (2005). The mobile nucleoporin Nup2p and chromatin-bound Prp20p function in endogenous NPC-mediated transcriptional control. J. Cell Biol. *171*, 955 LP-965.

REFERENCES

Ding, Y., Fromm, M., and Avramova, Z. (2012). Multiple exposures to drought “train” transcriptional responses in Arabidopsis. Nat. Commun. *3*, 740.

Dion, M.F., Altschuler, S.J., Wu, L.F., and Rando, O.J. (2005). Genomic characterization reveals a simple histone H4 acetylation code. Proc. Natl. Acad. Sci. U. S. A. *102*, 5501–5506.

Djebali, S., Davis, C.A., Merkel, A., Dobin, A., Lassmann, T., Mortazavi, A., Tanzer, A., Lagarde, J., Lin, W., Schlesinger, F., et al. (2012). Landscape of transcription in human cells. Nature *489*, 101–108.

Domcke, S., Bardet, A.F., Adrian Ginno, P., Hartl, D., Burger, L., and Schübeler, D. (2015). Competition between DNA methylation and transcription factors determines binding of NRF1. Nature *528*, 575–579.

Donze, D., and Kamakaka, R.T. (2001). RNA polymerase III and RNA polymerase II promoter complexes are heterochromatin barriers in Saccharomyces cerevisiae. EMBO J. *20*, 520–531.

Dou, Y., Milne, T.A., Tackett, A.J., Smith, E.R., Fukuda, A., Wysocka, J., Allis, C.D., Chait, B.T., Hess, J.L., and Roeder, R.G. (2005). Physical association and coordinate function of the H3 K4 methyltransferase MLL1 and the H4 K16 acetyltransferase MOF. Cell *121*, 873–885.

Downey, M., Johnson, J.R., Davey, N.E., Newton, B.W., Johnson, T.L., Galaang, S., Seller, C.A., Krogan, N., and Toczyski, D.P. (2015). Acetylome Profiling Reveals Overlap in the Regulation of Diverse Processes by Sirtuins, Gcn5, and Esa1. Mol. Cell. Proteomics *14*, 162–176.

Dreveny, I., Deeves, S.E., Fulton, J., Yue, B., Messmer, M., Bhattacharya, A., Collins, H.M., and Heery, D.M. (2014). The double PHD finger domain of MOZ/MYST3 induces α-helical structure of the histone H3 tail to facilitate acetylation and methylation sampling and modification. Nucleic Acids Res. *42*, 822–835.

Du, J., Zhong, X., Bernatavichute, Y. V, Stroud, H., Feng, S., Caro, E., Vashisht, A.A., Terragni, J., Chin, H.G., Tu, A., et al. (2012). Dual binding of chromomethylase domains to H3K9me2-containing nucleosomes directs DNA methylation in plants. Cell *151*, 167–180.

Dutrow, N., Nix, D. a, Holt, D., Milash, B., Dalley, B., Westbroek, E., Parnell, T.J., and Cairns, B.R. (2008). Dynamic transcriptome of Schizosaccharomyces pombe shown by RNA-DNA hybrid mapping. Nat. Genet. *40*, 977–986.

Ebert, A., Schotta, G., Lein, S., Kubicek, S., Krauss, V., Jenuwein, T., and Reuter, G. (2004). Su(var) genes regulate the balance between euchromatin and heterochromatin in Drosophila. Genes Dev. *18*, 2973–2983.

Egan, E.D., Braun, C.R., Gygi, S.P., and Moazed, D. (2014). Post-transcriptional regulation of meiotic genes by a nuclear RNA silencing complex Post-transcriptional regulation of meiotic genes by a nuclear RNA silencing complex. *2014*, 867–881.

Egel, R. (1984). Two tightly linked silent cassettes in the mating-type region of Schizosaccharomyces pombe. Curr. Genet. *8*, 199–203.

Eissenberg, J.C., Morris, G.D., Reuter, G., and Hartnett, T. (1992). The heterochromatin-associated protein HP-1 is an essential protein in Drosophila with dosage-dependent effects on position-effect variegation. Genetics *131*, 345 LP-352.

Ekwall, K., Nielsen, O., and Ruusala, T. (1991). Repression of a mating type cassette in the fission yeast by four DNA elements. Yeast *7*, 745–755.

Ekwall, K., Javerzat, J.P., Lorentz, A., Schmidt, H., Cranston, G., and Allshire, R. (1995). The chromodomain protein Swi6: a key component at fission yeast centromeres. Science (80-.). *269*, 1429 LP-1431.

REFERENCES

Ekwall, K., Cranston, G., and Allshire, R.C. (1999). Fission Yeast Mutants That Alleviate Transcriptional Silencing in Centromeric Flanking Repeats and Disrupt Chromosome Segregation. Genetics *153*, 1153 LP-1169.

Elgin, S.C.R., and Reuter, G. (2013). Position-effect variegation, heterochromatin formation, and gene silencing in Drosophila. Cold Spring Harb. Perspect. Biol. *5*.

De Fazio, S., Bartonicek, N., Di Giacomo, M., Abreu-Goodger, C., Sankar, A., Funaya, C., Antony, C., Moreira, P.N., Enright, A.J., and O'Carroll, D. (2011). The endonuclease activity of Mili fuels piRNA amplification that silences LINE1 elements. Nature *480*, 259–263.

Fierz, B., Chatterjee, C., McGinty, R.K., Bar-Dagan, M., Raleigh, D.P., and Muir, T.W. (2011). Histone H2B ubiquitylation disrupts local and higher-order chromatin compaction. Nat Chem Biol *7*, 113–119.

Filippakopoulos, P., Qi, J., Picaud, S., Shen, Y., Smith, W.B., Fedorov, O., Morse, E.M., Keates, T., Hickman, T.T., Felletar, I., et al. (2010). Selective inhibition of BET bromodomains. Nature *468*, 1067–1073.

Finkemeier, I., Laxa, M., Miguet, L., Howden, A.J.M., and Sweetlove, L.J. (2011). Proteins of diverse function and subcellular location are lysine acetylated in Arabidopsis. Plant Physiol. *155*, 1779–1790.

Fleming, A.B., Kao, C.-F., Hillyer, C., Pikaart, M., and Osley, M.A. (2008). H2B Ubiquitylation Plays a Role in Nucleosome Dynamics during Transcription Elongation. Mol. Cell *31*, 57–66.

Fontebasso, A.M., Schwartzentruber, J., Khuong-Quang, D.-A., Liu, X.-Y., Sturm, D., Korshunov, A., Jones, D.T.W., Witt, H., Kool, M., Albrecht, S., et al. (2013). Mutations in SETD2 and genes affecting histone H3K36 methylation target hemispheric high-grade gliomas. Acta Neuropathol. *125*, 659–669.

Forsburg, S.L. (2001). The art and design of genetic screens: yeast. Nat. Rev. Genet. *2*, 659–668.

Fuchs, G., and Oren, M. (2014). Writing and reading H2B monoubiquitylation. Biochim. Biophys. Acta *1839*, 694–701.

Fuchs, G., Shema, E., Vesterman, R., Kotler, E., Wolchinsky, Z., Wilder, S., Golomb, L., Pribluda, A., Zhang, F., Haj-Yahya, M., et al. (2012a). RNF20 and USP44 Regulate Stem Cell Differentiation by Modulating H2B Monoubiquitylation. Mol. Cell *46*, 662–673.

Fuchs, G., Voichek, Y., Benjamin, S., Gilad, S., Amit, I., and Oren, M. (2014a). 4sUDRB-seq: measuring genomewide transcriptional elongation rates and initiation frequencies within cells. Genome Biol. *15*, R69.

Fuchs, G., Hollander, D., and Voichek, Y. (2014b). Co-transcriptional histone H2B monoubiquitylation is tightly coupled with RNA polymerase II elongation rate Co-transcriptional histone H2B monoubiquitylation is tightly coupled with RNA polymerase II elongation rate. Genome Res. *24*, 1572–1583.

Fuchs, S.M., Kizer, K.O., Braberg, H., Krogan, N.J., and Strahl, B.D. (2012b). RNA Polymerase II Carboxyl-terminal Domain Phosphorylation Regulates Protein Stability of the Set2 Methyltransferase and Histone H3 Di- and Trimethylation at Lysine 36. J. Biol. Chem. *287*, 3249–3256.

Furuhashi, H., Takasaki, T., Rechtsteiner, A., Li, T., Kimura, H., Checchi, P.M., Strome, S., and Kelly, W.G. (2010). Trans-generational epigenetic regulation of C. elegans primordial germ cells. Epigenetics Chromatin *3*, 15.

García-González, E., Escamilla-Del-Arenal, M., Arzate-Mejía, R., and Recillas-Targa, F. (2016). Chromatin remodeling effects on enhancer activity. Cell. Mol. Life Sci. *73*, 2897–2910.

Gardner, K.A., Rine, J., and Fox, C.A. (1999). A region of the Sir1 protein dedicated to recognition of a silencer and required for interaction with the Orc1 protein in saccharomyces cerevisiae. Genetics *151*, 31–44.

REFERENCES

Gardner, R.G., Nelson, Z.W., and Gottschling, D.E. (2005). Ubp10/Dot4p regulates the persistence of ubiquitinated histone H2B: distinct roles in telomeric silencing and general chromatin. Mol. Cell. Biol. *25*, 6123–6139.

Gartenberg, M.R., and Smith, J.S. (2016). The Nuts and Bolts of Transcriptionally Silent Chromatin in Saccharomyces cerevisiae. Genetics *203*, 1563–1599.

Gerace, E.L., Halic, M., and Moazed, D. (2010). The methyltransferase activity of Clr4Suv39h triggers RNAi independently of histone H3K9 methylation. Mol. Cell *39*, 360–372.

Gerasimova, T.I., Gdula, D.A., Gerasimov, D. V, Simonova, O., and Corces, V.G. (1995). A drosophila protein that imparts directionality on a chromatin insulator is an enhancer of position-effect variegation. Cell *82*, 587–597.

Giannattasio, M., Lazzaro, F., Plevani, P., and Muzi-Falconi, M. (2005). The DNA damage checkpoint response requires histone H2B ubiquitination by Rad6-Bre1 and H3 methylation by Dot1. J. Biol. Chem. *280*, 9879–9886.

Gilbert, T.M., McDaniel, S.L., Byrum, S.D., Cades, J.A., Dancy, B.C.R., Wade, H., Tackett, A.J., Strahl, B.D., and Taverna, S.D. (2014). A PWWP domain-containing protein targets the NuA3 acetyltransferase complex via histone H3 lysine 36 trimethylation to coordinate transcriptional elongation at coding regions. Mol. Cell. Proteomics *13*, 2883–2895.

Glover-Cutter, K., Larochelle, S., Erickson, B., Zhang, C., Shokat, K., Fisher, R.P., and Bentley, D.L. (2009). TFIIH-Associated Cdk7 Kinase Functions in Phosphorylation of C-Terminal Domain Ser7 Residues, Promoter-Proximal Pausing, and Termination by RNA Polymerase II. Mol. Cell. Biol. *29*, 5455–5464.

Godde, J.S., and Widom, J. (1992). Chromatin structure of Schizosaccharomyces pombe. J. Mol. Biol. *226*, 1009–1025.

Gómez, E.B., Espinosa, J.M., and Forsburg, S.L. (2005). Schizosaccharomyces pombe mst2+ encodes a MYST family histone acetyltransferase that negatively regulates telomere silencing. Mol. Cell. Biol. *25*, 8887–8903.

Goriaux, C., Desset, S., Renaud, Y., Vaury, C., and Brasset, E. (2014). Transcriptional properties and splicing of the flamenco piRNA cluster. EMBO Rep. *15*, 411 LP-418.

Govind, C.K., Qiu, H., Ginsburg, D.S., Ruan, C., Hofmeyer, K., Hu, C., Swaminathan, V., Workman, J.L., Li, B., and Hinnebusch, A.G. (2010). Phosphorylated Pol II CTD Recruits Multiple HDACs, Including Rpd3C(S), for Methylation-Dependent Deacetylation of ORF Nucleosomes. Mol. Cell *39*, 234–246.

Grant, P.A., Schieltz, D., Pray-Grant, M.G., Steger, D.J., Reese, J.C., Yates, J.R., and Workman, J.L. (1998). A subset of TAF(II)s are integral components of the SAGA complex required for nucleosome acetylation and transcriptional stimulation. Cell *94*, 45–53.

Greer, E.L., and Shi, Y. (2012). Histone methylation: a dynamic mark in health, disease and inheritance. Nat. Rev. Genet. *13*, 343–357.

Grewal, S.I.S., and Jia, S. (2007). Heterochromatin revisited. Nat. Rev. Genet. *8*, 35–46.

Grewal, S.I.S., and Klar, A.J.S. (1997). A Recombinationally Repressed Region between Mat2 and Mat3 Loci Shares Homology to Centromeric Repeats and Regulates Directionality of Mating-Type Switching in Fission Yeast. Genetics *146*, 1221–1238.

Grewal, S.I.S., Bonaduce, M.J., and Klar, A.J.S. (1998). Histone Deacetylase Homologs Regulate Epigenetic Inheritance of Transcriptional Silencing and Chromosome Segregation in Fission Yeast. Genetics *150*, 563 LP-576.

Groh, S., and Schotta, G. (2017). Silencing of endogenous retroviruses by heterochromatin. Cell. Mol. Life Sci. *0*, 0.

REFERENCES

Gu, X., Jiang, D., Wang, Y., Bachmair, A., and He, Y. (2009). Repression of the floral transition via histone H2B monoubiquitination. Plant J. *57*, 522–533.

Haag, J.R., Ream, T.S., Marasco, M., Nicora, C.D., Norbeck, A.D., Pasa-Tolic, L., and Pikaard, C.S. (2012). In vitro transcription activities of Pol IV, Pol V and RDR2 reveal coupling of Pol IV and RDR2 for dsRNA synthesis in plant RNA silencing. Mol. Cell *48*, 811–818.

Hahn, M.A., Dickson, K.-A., Jackson, S., Clarkson, A., Gill, A.J., and Marsh, D.J. (2012). The tumor suppressor CDC73 interacts with the ring finger proteins RNF20 and RNF40 and is required for the maintenance of histone 2B monoubiquitination. Hum. Mol. Genet. *21*, 559–568.

Halic, M., and Moazed, D. (2010). Dicer-Independent Primal RNAs Trigger RNAi and Heterochromatin Formation. Cell *140*, 504–516.

Harigaya, Y., Tanaka, H., Yamanaka, S., Tanaka, K., Watanabe, Y., Tsutsumi, C., Chikashige, Y., Hiraoka, Y., Yamashita, A., and Yamamoto, M. (2006). Selective elimination of messenger RNA prevents an incidence of untimely meiosis. Nature *442*, 45–50.

Harlen, K.M., and Churchman, L.S. (2017). Subgenic Pol II interactomes identify region-specific transcription elongation regulators. Mol. Syst. Biol. *13*, 900.

Harlen, K.M., Trotta, K.L., Smith, E.E., Mosaheb, M.M., Fuchs, S.M., and Churchman, L.S. (2016). Comprehensive RNA Polymerase II Interactomes Reveal Distinct and Varied Roles for Each Phospho-CTD Residue. Cell Rep. *15*, 2147–2158.

Harris, J.K., Kelley, S.T., Spiegelman, G.B., and Pace, N.R. (2003). The Genetic Core of the Universal Ancestor. Genome Res. *13*, 407–412.

Hartzog, G.A., and Fu, J. (2013). The Spt4-Spt5 complex: A multi-faceted regulator of transcription elongation. Biochim. Biophys. Acta - Gene Regul. Mech. *1829*, 105–115.

Havecker, E.R., Wallbridge, L.M., Hardcastle, T.J., Bush, M.S., Kelly, K.A., Dunn, R.M., Schwach, F., Doonan, J.H., and Baulcombe, D.C. (2010). The Arabidopsis RNA-Directed DNA Methylation Argonautes Functionally Diverge Based on Their Expression and Interaction with Target Loci. Plant Cell *22*, 321–334.

Hawkins, R.D., Hon, G.C., Lee, L.K., Ngo, Q., Lister, R., Pelizzola, M., Edsall, L.E., Kuan, S., Luu, Y., Klugman, S., et al. (2010). Distinct epigenomic landscapes of pluripotent and lineage-committed human cells. Cell Stem Cell *6*, 479–491.

Hayashi, A., Ishida, M., Kawaguchi, R., Urano, T., Murakami, Y., and Nakayama, J. (2012). Heterochromatin protein 1 homologue Swi6 acts in concert with Ers1 to regulate RNAi-directed heterochromatin assembly. Proc. Natl. Acad. Sci. U. S. A. *109*, 6159–6164.

Hecht, A., Strahl-Bolsinger, S., and Grunstein, M. (1996). Spreading of transcriptional repressor SIR3 from telomeric heterochromatin. Nature *383*, 92–96.

Heitz, E. (1928). Das Heterochromatin der Moose. Jahrb Wiss Bot. *69*, 762–818.

Hengartner, C.J., Myer, V.E., Liao, S.-M., Wilson, C.J., Koh, S.S., and Young, R.A. (1998). Temporal Regulation of RNA Polymerase II by Srb10 and Kin28 Cyclin-Dependent Kinases. Mol. Cell *2*, 43–53.

Henriksen, P., Wagner, S. a., Weinert, B.T., Sharma, S., Bacinskaja, G., Rehman, M., Juffer, A.H., Walther, T.C., Lisby, M., and Choudhary, C. (2012). Proteome-wide analysis of lysine acetylation suggests its broad regulatory scope in Saccharomyces cerevisiae. Mol. Cell. Proteomics *11*, 1510–1522.

Henry, K.W., Wyce, A., Lo, W.-S., Duggan, L.J., Emre, N.C.T., Kao, C.-F., Pillus, L., Shilatifard, A., Osley, M.A., and Berger, S.L. (2003). Transcriptional activation via sequential histone H2B ubiquitylation and deubiquitylation, mediated by SAGA-associated Ubp8. Genes Dev. *17*, 2648–2663.

REFERENCES

Hiriart, E., Vavasseur, A., Touat-Todeschini, L., Yamashita, A., Gilquin, B., Lambert, E., Perot, J., Shichino, Y., Nazaret, N., Boyault, C., et al. (2012). Mmi1 RNA surveillance machinery directs RNAi complex RITS to specific meiotic genes in fission yeast. EMBO J. *31*, 2296–2308.

Hirota, K., Mizuno, K. -i., Shibata, T., and Ohta, K. (2007). Distinct Chromatin Modulators Regulate the Formation of Accessible and Repressive Chromatin at the Fission Yeast Recombination Hotspot ade6-M26. Mol. Biol. Cell *19*, 1162–1173.

Holoch, D., and Moazed, D. (2015a). RNA-mediated epigenetic regulation of gene expression. Nat. Rev Genet *16*, 71–84.

Holoch, D., and Moazed, D. (2015b). Small-RNA loading licenses Argonaute for assembly into a transcriptional silencing complex. Nat. Struct. Mol. Biol. *22*, 328–335.

Holstege, F.C., van der Vliet, P.C., and Timmers, H.T. (1996). Opening of an RNA polymerase II promoter occurs in two distinct steps and requires the basal transcription factors IIE and IIH. EMBO J. *15*, 1666–1677.

Hong, E.-J.E., Villén, J., Gerace, E.L., Gygi, S.P., and Moazed, D. (2005). A cullin E3 ubiquitin ligase complex associates with Rik1 and the Clr4 histone H3-K9 methyltransferase and is required for RNAi-mediated heterochromatin formation. RNA Biol. *2*, 106–111.

Horn, P.J., Bastie, J.-N., and Peterson, C.L. (2005). A Rik1-associated, cullin-dependent E3 ubiquitin ligase is essential for heterochromatin formation. Genes Dev. *19*, 1705–1714.

Howe, L., Auston, D., Grant, P., John, S., Cook, R.G., Workman, J.L., and Pillus, L. (2001). Histone H3 specific acetyltransferases are essential for cell cycle progression. Genes Dev. *15*, 3144–3154.

Huang, H., Lin, S., Garcia, B.A., and Zhao, Y. (2015). Quantitative Proteomic Analysis of Histone Modifications. Chem. Rev. *115*, 2376–2418.

Huarte, M., Lan, F., Kim, T., Vaughn, M.W., Zaratiegui, M., Martienssen, R.A., Buratowski, S., and Shi, Y. (2007). The fission yeast Jmj2 reverses histone H3 lysine 4 trimethylation. J. Biol. Chem. *282*, 21662–21670.

Iida, T., Nakayama, J. ichi, and Moazed, D. (2008). siRNA-Mediated Heterochromatin Establishment Requires HP1 and Is Associated with Antisense Transcription. Mol. Cell *31*, 178–189.

Iino, Y., and Yamamoto, M. (1985). Negative control for the initiation of meiosis in Schizosaccharomyces pombe. Proc. Natl. Acad. Sci. U. S. A. *82*, 2447–2451.

Imbalzano, A.N., Zaret, K.S., and Kingston, R.E. (1994). Transcription factor (TF) IIB and TFIIA can independently increase the affinity of the TATA-binding protein for DNA. J. Biol. Chem. *269*, 8280–8286.

Ishida, M., Shimojo, H., Hayashi, A., Kawaguchi, R., Ohtani, Y., Uegaki, K., Nishimura, Y., and Nakayama, J.I. (2012). Intrinsic Nucleic Acid-Binding Activity of Chp1 Chromodomain Is Required for Heterochromatic Gene Silencing. Mol. Cell *47*, 228–241.

Jacobson, R.H., Ladurner, A.G., King, D.S., and Tjian, R. (2000). Structure and function of a human TAFII250 double bromodomain module. Science *288*, 1422–1425.

Jaehning, J.A. (2010). The Paf1 complex: Platform or player in RNA polymerase II transcription? Biochim. Biophys. Acta - Gene Regul. Mech. *1799*, 379–388.

Jain, R., Iglesias, N., and Moazed, D. (2016). Distinct Functions of Argonaute Slicer in siRNA Maturation and Heterochromatin Formation. Mol. Cell *63*, 191–205.

Jain, A. K. and Barton, M.C. (2016). Bromodomain Histone Readers and Cancer. J. Mol. Biol. 1–8.

REFERENCES

James, T.C., and Elgin, S.C. (1986). Identification of a nonhistone chromosomal protein associated with heterochromatin in Drosophila melanogaster and its gene. Mol. Cell. Biol. *6*, 3862–3872.

Jeronimo, C., Collin, P., and Robert, F. (2016). The RNA Polymerase II CTD: The Increasing Complexity of a Low-Complexity Protein Domain. J. Mol. Biol. *428*, 2607–2622.

Jia, S., Noma, K., and Grewal, S.I.S. (2004). RNAi-independent heterochromatin nucleation by the stress-activated ATF/CREB family proteins. Science *304*, 1971–1976.

Jia, S., Kobayashi, R., and Grewal, S.I.S. (2005). Ubiquitin ligase component Cul4 associates with Clr4 histone methyltransferase to assemble heterochromatin. Nat Cell Biol *7*, 1007–1013.

Job, G., Brugger, C., Xu, T., Lowe, B.R., Pfister, Y., Qu, C., Shanker, S., Baños Sanz, J.I., Partridge, J.F., and Schalch, T. (2016). SHREC Silences Heterochromatin via Distinct Remodeling and Deacetylation Modules. Mol. Cell *62*, 207–221.

Joh, R.I., Khanduja, J.S., Calvo, I.A., Mistry, M., Palmieri, C.M., Savol, A.J., Ho Sui, S.J., Sadreyev, R.I., Aryee, M.J., and Motamedi, M. (2016). Survival in Quiescence Requires the Euchromatic Deployment of Clr4/SUV39H by Argonaute-Associated Small RNAs. Mol. Cell *64*, 1088–1101.

Johnsson, A., Durand-Dubief, M., Xue-Franzén, Y., Rönnerblad, M., Ekwall, K., and Wright, A. (2009). HAT-HDAC interplay modulates global histone H3K14 acetylation in gene-coding regions during stress. EMBO Rep. *10*, 1009–1014.

Kadonaga, J.T. (2012). Perspectives on the RNA polymerase II core promoter. Wiley Interdiscip Rev Dev Biol. *1*, 40–51.

Kadosh, D., and Struhl, K. (1997). Repression by Ume6 involves recruitment of a complex containing Sin3 corepressor and Rpd3 histone deacetylase to target promoters. Cell *89*, 365–371.

Kagansky, A., Folco, H.D., Almeida, R., Pidoux, A.L., Boukaba, A., Simmer, F., Urano, T., Hamilton, G.L., and Allshire, R.C. (2009). Synthetic heterochromatin bypasses RNAi and centromeric repeats to establish functional centromeres. Science *324*, 1716–1719.

Kalb, R., Latwiel, S., Baymaz, H.I., Jansen, P.W.T.C., Müller, C.W., Vermeulen, M., and Müller, J. (2014). Histone H2A monoubiquitination promotes histone H3 methylation in Polycomb repression. Nat Struct Mol Biol *21*, 569–571.

Kanoh, J., and Ishikawa, F. (2001). spRap1 and spRif1, recruited to telomeres by Taz1, are essential for telomere function in fission yeast. Curr. Biol. *11*, 1624–1630.

Kanoh, J., Sadaie, M., Urano, T., and Ishikawa, F. (2005). Telomere binding protein Taz1 establishes Swi6 heterochromatin independently of RNAi at telomeres. Curr. Biol. *15*, 1808–1819.

Karpiuk, O., Najafova, Z., Kramer, F., Hennion, M., Galonska, C., König, A., Snaidero, N., Vogel, T., Shchebet, A., Begus-Nahrmann, Y., et al. (2012). The Histone H2B Monoubiquitination Regulatory Pathway Is Required for Differentiation of Multipotent Stem Cells. Mol. Cell *46*, 705–713.

Kato, H., Goto, D.B., Martienssen, R.A., Urano, T., Furukawa, K., and Murakami, Y. (2005). RNA Polymerase II Is Required for RNAi-Dependent Heterochromatin Assembly. Science (80-.). *309*, 467 LP-469.

Katsumoto, T., Aikawa, Y., Iwama, A., Ueda, S., Ichikawa, H., Ochiya, T., and Kitabayashi, I. (2006). MOZ is essential for maintenance of hematopoietic stem cells. Genes Dev. *20*, 1321–1330.

Kawakami, K., Hayashi, A., Nakayama, J.I., and Murakami, Y. (2012). A novel RNAi protein, Dsh1, assembles RNAi machinery on chromatin to amplify heterochromatic siRNA. Genes Dev. *26*, 1811–1824.

Keller, C., Adaixo, R., Stunnenberg, R., Woolcock, K.J., Hiller, S., and Bühler, M. (2012). HP1 Swi6 Mediates the Recognition and Destruction of Heterochromatic RNA Transcripts. Mol. Cell *47*, 215–227.

REFERENCES

Keller, C., Kulasegaran-Shylini, R., Shimada, Y., Hotz, H.-R., and Bühler, M. (2013). Noncoding RNAs prevent spreading of a repressive histone mark. Nat. Struct. Mol. Biol. *20*, 994–1000.

Kettenbach, A.N., Deng, L., Wu, Y., Baldissard, S., Adamo, M.E., Gerber, S.A., and Moseley, J.B. (2015). Quantitative phosphoproteomics reveals pathways for coordination of cell growth and division by the conserved fission yeast kinase pom1. Mol. Cell. Proteomics *14*, 1275–1287.

Kettenberger, H., Armache, K.-J., and Cramer, P. (2003). Architecture of the RNA Polymerase II-TFIIS Complex and Implications for mRNA Cleavage. Cell *114*, 347–357.

Kiely, C.M., Marguerat, S., Garcia, J.F., Madhani, H.D., Bähler, J., and Winston, F. (2011). Spt6 is required for heterochromatic silencing in the fission yeast Schizosaccharomyces pombe. Mol. Cell. Biol. *31*, 4193–4204.

Kim, Y.Z. (2014). Altered histone modifications in gliomas. Brain Tumor Res. Treat. *2*, 7–21.

Kim, T., and Buratowski, S. (2007). Two Saccharomyces cerevisiae JmjC Domain Proteins Demethylate Histone H3 Lys36 in Transcribed Regions to Promote Elongation. J. Biol. Chem. *282*, 20827–20835.

Kim, H.S., Choi, E.S., Shin, J.A., Jang, Y.K., and Park, S.D. (2004a). Regulation of Swi6/HP1-dependent heterochromatin assembly by cooperation of components of the mitogen-activated protein kinase pathway and a histone deacetylase Clr6. J. Biol. Chem. *279*, 42850–42859.

Kim, J., Hake, S.B., and Roeder, R.G. (2005). The Human Homolog of Yeast BRE1 Functions as a Transcriptional Coactivator through Direct Activator Interactions. Mol. Cell *20*, 759–770.

Kim, M., Krogan, N.J., Vasiljeva, L., Rando, O.J., Nedea, E., Greenblatt, J.F., and Buratowski, S. (2004b). The yeast Rat1 exonuclease promotes transcription termination by RNA polymerase II. Nature *432*, 517–522.

Kimmerly, W., Buchman, A., Kornberg, R., and Rine, J. (1988). Roles of two DNA-binding factors in replication, segregation and transcriptional repression mediated by a yeast silencer. EMBO J. *7*, 2241–2253.

Kimura, A., Umehara, T., and Horikoshi, M. (2002). Chromosomal gradient of histone acetylation established by Sas2p and Sir2p functions as a shield against gene silencing. Nat Genet *32*, 370–377.

Kizer, K.O., Phatnani, H.P., Shibata, Y., Hall, H., Greenleaf, A.L., and Strahl, B.D. (2005). A novel domain in Set2 mediates RNA polymerase II interaction and couples histone H3 K36 methylation with transcript elongation. Mol. Cell. Biol. *25*, 3305–3316.

Kloc, A., Zaratiegui, M., Nora, E., and Martienssen, R. (2008). RNA Interference Guides Histone Modification during the S Phase of Chromosomal Replication. Curr. Biol. *18*, 490–495.

Van Der Knaap, J.A., Kumar, B.R.P., Moshkin, Y.M., Langenberg, K., Krijgsveld, J., Heck, A.J.R., Karch, F., and Verrijzer, C.P. (2005). GMP synthetase stimulates histone H2B deubiquitylation by the epigenetic silencer USP7. Mol. Cell *17*, 695–707.

Köhler, A., Zimmerman, E., Schneider, M., Hurt, E., and Zheng, N. (2010). Structural Basis for Assembly and Activation of the Heterotetrameric SAGA Histone H2B Deubiquitinase Module. Cell *141*, 606–617.

Kostrewa, D., Zeller, M.E., Armache, K., Seizl, M., Leike, K., Thomm, M., and Cramer, P. (2009). RNA polymerase II–TFIIB structure and mechanism of transcription initiation. Nature *462*, 323–330.

Kowalik, K.M., Shimada, Y., Flury, V., Stadler, M.B., Batki, J., and Bühler, M. (2015). The Paf1 complex represses small-RNA-mediated epigenetic gene silencing. Nature *520*, 248–252.

REFERENCES

Kueh, A.J., Dixon, M.P., Voss, A.K., and Thomas, T. (2011). HBO1 is required for H3K14 acetylation and normal transcriptional activity during embryonic development. Mol. Cell. Biol. *31*, 845–860.

Kuramochi-Miyagawa, S., Watanabe, T., Gotoh, K., Totoki, Y., Toyoda, A., Ikawa, M., Asada, N., Kojima, K., Yamaguchi, Y., Ijiri, T.W., et al. (2008). DNA methylation of retrotransposon genes is regulated by Piwi family members MILI and MIWI2 in murine fetal testes. Genes Dev. *22*, 908–917.

Kurdistani, S.K., Tavazoie, S., and Grunstein, M. (2004). Mapping global histone acetylation patterns to gene expression. Cell *117*, 721–733.

Kuscu, C., Zaratiegui, M., Kim, H.S., Wah, D.A., Martienssen, R.A., Schalch, T., and Joshua-Tor, L. (2014). CRL4-like Clr4 complex in Schizosaccharomyces pombe depends on an exposed surface of Dos1 for heterochromatin silencing. Proc. Natl. Acad. Sci. U. S. A. *111*, 1795–1800.

Kwak, H., and Lis, J.T. (2013). Control of transcriptional elongation. Annu. Rev. Genet. *47*, 483–508.

Kwon, S.H., and Workman, J.L. (2011). The changing faces of HP1: From heterochromatin formation and gene silencing to euchromatic gene expression. BioEssays *33*, 280–289.

Lalonde, M.-E., Avvakumov, N., Glass, K.C., Joncas, F.-H., Saksouk, N., Holliday, M., Paquet, E., Yan, K., Tong, Q., Klein, B.J., et al. (2013). Exchange of associated factors directs a switch in HBO1 acetyltransferase histone tail specificity. Genes Dev. *27*, 2009–2024.

Larschan, E., Alekseyenko, A.A., Gortchakov, A.A., Peng, S., Li, B., Yang, P., Workman, J.L., Park, P.J., and Kuroda, M.I. (2007). MSL complex is attracted to genes marked by H3K36 trimethylation using a sequence-independent mechanism. Mol. Cell *28*, 121–133.

Law, J.A., Du, J., Hale, C.J., Feng, S., Krajewski, K., Palanca, A.M.S., Strahl, B.D., Patel, D.J., and Jacobsen, S.E. (2013). Polymerase IV occupancy at RNA-directed DNA methylation sites requires SHH1. Nature *498*, 385–389.

Lawrence, R.J., and Volpe, T. a (2009). Msc1 links dynamic Swi6/HP1 binding to cell fate determination. Proc. Natl. Acad. Sci. U. S. A. *106*, 1163–1168.

Lee, N.N., Chalamcharla, V.R., Reyes-Turcu, F., Mehta, S., Zofall, M., Balachandran, V., Dhakshnamoorthy, J., Taneja, N., Yamanaka, S., Zhou, M., et al. (2013). Mtr4-like Protein Coordinates Nuclear RNA Processing for Heterochromatin Assembly and for Telomere Maintenance. Cell *155*, 1061–1074.

Lemay, J.-F., Larochelle, M., Marguerat, S., Atkinson, S., Bähler, J., and Bachand, F. (2014). The RNA exosome promotes transcription termination of backtracked RNA polymerase II. Nat Struct Mol Biol *21*, 919–926.

Lewis, E.B. (1978). A gene complex controlling segmentation in Drosophila. Nature *276*, 565–570.

Li, E., and Zhang, Y. (2014). DNA methylation in mammals. Cold Spring Harb. Perspect. Biol. *6*, a019133.

Li, B., Jackson, J., Simon, M.D., Fleharty, B., Gogol, M., Seidel, C., Workman, J.L., and Shilatifard, A. (2009a). Histone H3 lysine 36 dimethylation (H3K36me2) is sufficient to recruit the Rpd3s histone deacetylase complex and to repress spurious transcription. J. Biol. Chem. *284*, 7970–7976.

Li, F., Huarte, M., Zaratiegui, M., Vaughn, M.W., Shi, Y., Martienssen, R., and Cande, W.Z. (2008). Lid2 Is Required for Coordinating H3K4 and H3K9 Methylation of Heterochromatin and Euchromatin. Cell *135*, 272–283.

Li, H., Motamedi, M.R., Yip, C.K., Wang, Z., Walz, T., Patel, D.J., and Moazed, D. (2009b). An Alpha Motif at Tas3 C Terminus Mediates RITS cis Spreading and Promotes Heterochromatic Gene Silencing. Mol. Cell *34*, 155–167.

REFERENCES

Liang, G., Lin, J.C.Y., Wei, V., Yoo, C., Cheng, J.C., Nguyen, C.T., Weisenberger, D.J., Egger, G., Takai, D., Gonzales, F.A., et al. (2004). Distinct localization of histone H3 acetylation and H3-K4 methylation to the transcription start sites in the human genome. Proc. Natl. Acad. Sci. U. S. A. *101*, 7357–7362.

Licatalosi, D.D., Geiger, G., Minet, M., Schroeder, S., Cilli, K., McNeil, J.B., and Bentley, D.L. (2002). Functional Interaction of Yeast Pre-mRNA 3′ End Processing Factors with RNA Polymerase II. Mol. Cell *9*, 1101–1111.

Lim, S., Kwak, J., Kim, M., and Lee, D. (2013). Separation of a functional deubiquitylating module from the SAGA complex by the proteasome regulatory particle. Nat. Commun. *4*, 2641.

Liou, G.G., Tanny, J.C., Kruger, R.G., Walz, T., and Moazed, D. (2005). Assembly of the SIR complex and its regulation by O-acetyl-ADP-ribose, a product of NAD-dependent histone deacetylation. Cell *121*, 515–527.

Liu, X., Bushnell, D.A., Silva, D.-A., Huang, X., and Kornberg, R.D. (2011). Initiation complex structure and promoter proofreading. Science *333*, 633–637.

Lu, C., Jain, S.U., Hoelper, D., Bechet, D., Molden, R.C., Ran, L., Murphy, D., Venneti, S., Hameed, M., Pawel, B.R., et al. (2016). Histone H3K36 mutations promote sarcomagenesis through altered histone methylation landscape. Science *352*, 844–849.

De Lucia, F., Crevillen, P., Jones, A.M.E., Greb, T., and Dean, C. (2008). A PHD-polycomb repressive complex 2 triggers the epigenetic silencing of FLC during vernalization. Proc. Natl. Acad. Sci. U. S. A. *105*, 16831–16836.

Lunde, B.M., Reichow, S.L., Kim, M., Suh, H., Leeper, T.C., Yang, F., Mutschler, H., Buratowski, S., Meinhart, A., and Varani, G. (2010). Cooperative interaction of transcription termination factors with the RNA polymerase II C-terminal domain. Nat. Struct. Mol. Biol. *17*, 1195–1201.

Lyon, M.F. (1961). Gene action in the X-chromosome of the mouse (Mus musculus L.). Nature *190*, 372–373.

Ma, M.K.-W., Heath, C., Hair, A., and West, A.G. (2011). Histone crosstalk directed by H2B ubiquitination is required for chromatin boundary integrity. PLoS Genet. *7*, e1002175.

MacKellar, A.L., and Greenleaf, A.L. (2011). Cotranscriptional association of mRNA export factor Yra1 with C-terminal domain of RNA polymerase II. J. Biol. Chem. *286*, 36385–36395.

Marasovic, M., Zocco, M., and Halic, M. (2013). Argonaute and Triman Generate Dicer-Independent priRNAs and Mature siRNAs to Initiate Heterochromatin Formation. Mol. Cell *52*, 173–183.

Margueron, R., Justin, N., Ohno, K., Sharpe, M.L., Son, J., Drury III, W.J., Voigt, P., Martin, S.R., Taylor, W.R., De Marco, V., et al. (2009). Role of the polycomb protein EED in the propagation of repressive histone marks. Nature *461*, 762–767.

Martienssen, R., and Moazed, D. (2015). RNAi and Heterochromatin Assembly. Cold Spring Harb. Perspect. Biol. *7*, a019323.

Martin, B.J.E., McBurney, K.L., Maltby, V.E., Jensen, K.N., Brind'Amour, J., and Howe, L.J. (2017). Histone H3K4 and H3K36 Methylation Independently Recruit the NuA3 Histone Acetyltransferase in Saccharomyces cerevisiae. Genetics *205*, genetics.116.199422.

Martinez-Rucobo, F.W., Kohler, R., van de Waterbeemd, M., Heck, A.J.R., Hemann, M., Herzog, F., Stark, H., and Cramer, P. (2015). Molecular Basis of Transcription-Coupled Pre-mRNA Capping. Mol. Cell *58*, 1079–1089.

Martinez-Rucobo, F.W., Sainsbury, S., Cheung, A.C.M., and Cramer, P. (2011). Architecture of the RNA polymerase–Spt4/5 complex and basis of universal transcription processivity. EMBO J. *30*, 1302 LP-1310.

REFERENCES

Mata, J., Lyne, R., Burns, G., and Bähler, J. (2002). The transcriptional program of meiosis and sporulation in fission yeast. Nat. Genet. *32*, 143–147.

Mathis, D.J., and Chambon, P. (1981). The SV40 early region TATA box is required for accurate in vitro initiation of transcription. Nature *290*, 310–315.

Mayer, A., Heidemann, M., Lidschreiber, M., Schreieck, A., Sun, M., Hintermair, C., Kremmer, E., Eick, D., and Cramer, P. (2012). CTD tyrosine phosphorylation impairs termination factor recruitment to RNA polymerase II. Science *336*, 1723–1725.

Mbogning, J., Nagy, S., Pagé, V., Schwer, B., Shuman, S., Fisher, R.P., and Tanny, J.C. (2013). The PAF Complex and Prf1/Rtf1 Delineate Distinct Cdk9-Dependent Pathways Regulating Transcription Elongation in Fission Yeast. PLoS Genet. *9*, 29–31.

McCormick, M.A., Mason, A.G., Guyenet, S.J., Dang, W., Garza, R.M., Ting, M.K., Moller, R.M., Berger, S.L., Kaeberlein, M., Pillus, L., et al. (2014). The SAGA Histone Deubiquitinase Module Controls Yeast Replicative Lifespan via Sir2 Interaction. Cell Rep. *8*, 477–486.

McGinty, R.K., Henrici, R.C., and Tan, S. (2014). Crystal structure of the PRC1 ubiquitylation module bound to the nucleosome. Nature *514*, 591–596.

Mellone, B.G., Ball, L., Suka, N., Grunstein, M.R., Partridge, J.F., and Allshire, R.C. (2003). Centromere Silencing and Function in Fission Yeast Is Governed by the Amino Terminus of Histone H3. Curr. Biol. *13*, 1748–1757.

Mendenhall, E.M., Koche, R.P., Truong, T., Zhou, V.W., Issac, B., Chi, A.S., Ku, M., and Bernstein, B.E. (2010). GC-Rich Sequence Elements Recruit PRC2 in Mammalian ES Cells. PLOS Genet. *6*, e1001244.

Moazed, D., Kistler, A., Axelrod, A., Rine, J., and Johnson, A.D. (1997). Silent information regulator protein complexes in Saccharomyces cerevisiae: a SIR2/SIR4 complex and evidence for a regulatory domain in SIR4 that inhibits its interaction with SIR3. Proc. Natl. Acad. Sci. U. S. A. *94*, 2186–2191.

Mohan, R.D., Dialynas, G., Weake, V.M., Liu, J., Martin-Brown, S., Florens, L., Washburn, M.P., Workman, J.L., and Abmayr, S.M. (2014). Loss of Drosophila Ataxin-7, a SAGA subunit, reduces H2B ubiquitination and leads to neural and retinal degeneration. Genes Dev. *28*, 259–272.

Mohn, F., Sienski, G., Handler, D., and Brennecke, J. (2014). The Rhino-Deadlock-Cutoff Complex Licenses Noncanonical Transcription of Dual-Strand piRNA Clusters in Drosophila. Cell *157*, 1364–1379.

Mohn, F., Handler, D., and Brennecke, J. (2015). Noncoding RNA. piRNA-guided slicing specifies transcripts for Zucchini-dependent, phased piRNA biogenesis. Science *348*, 812–817.

Morgan, T.H. (1910). SEX LIMITED INHERITANCE IN DROSOPHILA. Science *32*, 120–122.

Morgan, M.T., and Wolberger, C. (2017). Recognition of ubiquitinated nucleosomes. Curr. Opin. Struct. Biol. *42*, 75–82.

Morris, S. a, Shibata, Y., Noma, K., Tsukamoto, Y., Warren, E., Temple, B., Grewal, S.I.S., and Strahl, B.D. (2005). Histone H3 K36 methylation is associated with transcription elongation in Schizosaccharomyces pombe. Eukaryot. Cell *4*, 1446–1454.

Motamedi, M.R., Verdel, A., Colmenares, S.U., Gerber, S.A., Gygi, S.P., and Moazed, D. (2004). Two RNAi complexes, RITS and RDRC, physically interact and localize to noncoding centromeric RNAs. Cell *119*, 789–802.

Motamedi, M.R., Hong, E.J.E., Li, X., Gerber, S., Denison, C., Gygi, S., and Moazed, D. (2008). HP1 Proteins Form Distinct Complexes and Mediate Heterochromatic Gene Silencing by Nonoverlapping Mechanisms. Mol. Cell *32*, 778–790.

REFERENCES

Muller, H. (1930). Types of visible variations induced by X-rays in Drosophila. J. Genet. 299–334.

Nakahigashi, K., Jasencakova, Z., Schubert, I., and Goto, K. (2005). The Arabidopsis heterochromatin protein1 homolog (TERMINAL FLOWER2) silences genes within the euchromatic region but not genes positioned in heterochromatin. Plant Cell Physiol. *46*, 1747–1756.

Nakayama, J., Rice, J.C., Strahl, B.D., Allis, C.D., and Grewal, S.I.S. (2001). Role of Histone H3 Lysine 9 Methylation in Epigenetic Control of Heterochromatin Assembly. Science (80-.). *292*, 110–113.

Nakayama, J. ichi, Xiao, G., Noma, K. ichi, Malikzay, A., Bjerling, P., Ekwall, K., Kobayashi, R., and Grewal, S.I.S. (2003). Alp13, an MRG family protein, is a component of fission yeast Clr6 histone deacetylase required for genomic integrity. EMBO J. *22*, 2776–2787.

Nanney, D.L. (1958). EPIGENETIC CONTROL SYSTEMS. Proc. Natl. Acad. Sci. U. S. A. *44*, 712–717.

Naresh, A., Saini, S., and Singh, J. (2003). Identification of Uhp1, a ubiquitinated histone-like protein, as a target/mediator of Rhp6 in mating-type silencing in fission yeast. J. Biol. Chem. *278*, 9185–9194.

Naumann, K., Fischer, A., Hofmann, I., Krauss, V., Phalke, S., Irmler, K., Hause, G., Aurich, A.-C., Dorn, R., Jenuwein, T., et al. (2005). Pivotal role of AtSUVH2 in heterochromatic histone methylation and gene silencing in Arabidopsis. EMBO J. *24*, 1418–1429.

Nechaev, S., and Adelman, K. (2011). Pol II waiting in the starting gates: Regulating the transition from transcription initiation into productive elongation. Biochim. Biophys. Acta *1809*, 34–45.

Neri, F., Rapelli, S., Krepelova, A., Incarnato, D., Parlato, C., Basile, G., Maldotti, M., Anselmi, F., and Oliviero, S. (2017). Intragenic DNA methylation prevents spurious transcription initiation. Nature *543*, 72–77.

Ng, H.H., Xu, R.-M., Zhang, Y., and Struhl, K. (2002). Ubiquitination of histone H2B by Rad6 is required for efficient Dot1-mediated methylation of histone H3 lysine 79. J. Biol. Chem. *277*, 34655–34657.

Ng, H.H., Robert, F., Young, R.A., and Struhl, K. (2003a). Targeted recruitment of Set1 histone methylase by elongating Pol II provides a localized mark and memory of recent transcriptional activity. Mol. Cell *11*, 709–719.

Ng, H.H., Dole, S., and Struhl, K. (2003b). The Rtf1 Component of the Paf1 Transcriptional Elongation Complex Is Required for Ubiquitination of Histone H2B. J. Biol. Chem. *278*, 33625–33628.

Nicolas, E., Yamada, T., Cam, H.P., Fitzgerald, P.C., Kobayashi, R., and Grewal, S.I. (2007). Distinct roles of HDAC complexes in promoter silencing, antisense suppression and DNA damage protection. Nat Struct Mol Biol *14*, 372–380.

Nielsen, I.S., Nielsen, O., Murray, J.M., and Thon, G. (2002). The fission yeast ubiquitin-conjugating enzymes UbcP3, Ubc15, and Rhp6 affect transcriptional silencing of the mating-type region. Eukaryot. Cell *1*, 613–625.

Noma, K., Sugiyama, T., Cam, H., Verdel, A., Zofall, M., Jia, S., Moazed, D., and Grewal, S.I.S. (2004). RITS acts in cis to promote RNA interference-mediated transcriptional and post-transcriptional silencing. Nat. Genet. *36*, 1174–1180.

Noma, K. ichi, Cam, H.P., Maraia, R.J., and Grewal, S.I.S. (2006). A Role for TFIIIC Transcription Factor Complex in Genome Organization. Cell *125*, 859–872.

Nonet, M., Sweetser, D., and Young, R.A. (1987). Functional redundancy and structural polymorphism in the large subunit of RNA polymerase II. Cell *50*, 909–915.

REFERENCES

Nordick, K., Hoffman, M.G., Betz, J.L., and Jaehning, J.A. (2008). Direct interactions between the Paf1 complex and a cleavage and polyadenylation factor are revealed by dissociation of Paf1 from RNA polymerase II. Eukaryot. Cell *7*, 1158–1167.

Nugent, R.L., Johnsson, A., Fleharty, B., Gogol, M., Xue-Franzén, Y., Seidel, C., Wright, A.P., and Forsburg, S.L. (2010). Expression profiling of S. pombe acetyltransferase mutants identifies redundant pathways of gene regulation. BMC Genomics *11*, 59.

Oberti, D., Biasini, A., Kirschmann, M.A., Genoud, C., Stunnenberg, R., Shimada, Y., and Bühler, M. (2015). Dicer and Hsp104 Function in a Negative Feedback Loop to Confer Robustness to Environmental Stress. Cell Rep. *10*, 47–61.

Ohzeki, J., Shono, N., Otake, K., Martins, N.M.C., Kugou, K., Kimura, H., Nagase, T., Larionov, V., Earnshaw, W.C., and Masumoto, H. (2016). KAT7/HBO1/MYST2 Regulates CENP-A Chromatin Assembly by Antagonizing Suv39h1-Mediated Centromere Inactivation. Dev. Cell *37*, 413–427.

Olins, A.L., and Olins, D.E. (1974). Spheroid chromatin units (v bodies). Science *183*, 330–332.

Onishi, M., Liou, G.-G., Buchberger, J.R., Walz, T., and Moazed, D. (2007). Role of the Conserved Sir3-BAH Domain in Nucleosome Binding and Silent Chromatin Assembly. Mol. Cell *28*, 1015–1028.

Van Oss, S.B., Shirra, M.K., Bataille, A.R., Wier, A.D., Yen, K., Vinayachandran, V., Byeon, I.-J.L., Cucinotta, C.E., Héroux, A., Jeon, J., et al. (2016). The Histone Modification Domain of Paf1 Complex Subunit Rtf1 Directly Stimulates H2B Ubiquitylation through an Interaction with Rad6. Mol. Cell *64*, 815–825.

Pai, C.-C., Deegan, R.S., Subramanian, L., Gal, C., Sarkar, S., Blaikley, E.J., Walker, C., Hulme, L., Bernhard, E., Codlin, S., et al. (2014). A histone H3K36 chromatin switch coordinates DNA double-strand break repair pathway choice. Nat. Commun. *5*, 4091.

Pane, A., Wehr, K., and Schüpbach, T. (2007). zucchini and squash encode two putative nucleases required for rasiRNA production in the Drosophila germline. Dev. Cell *12*, 851–862.

Partridge, J.F., Scott, K.S.C., Bannister, A.J., Kouzarides, T., and Allshire, R.C. (2002). cis-acting DNA from fission yeast centromeres mediates histone H3 methylation and recruitment of silencing factors and cohesin to an ectopic site. Curr. Biol. *12*, 1652–1660.

Pavri, R., Zhu, B., Li, G., Trojer, P., Mandal, S., Shilatifard, A., and Reinberg, D. (2006). Histone H2B Monoubiquitination Functions Cooperatively with FACT to Regulate Elongation by RNA Polymerase II. Cell *125*, 703–717.

Pei, Y., Hausmann, S., Ho, C.K., Schwer, B., and Shuman, S. (2001). The Length, Phosphorylation State, and Primary Structure of the RNA Polymerase II Carboxyl-terminal Domain Dictate Interactions with mRNA Capping Enzymes. J. Biol. Chem. *276*, 28075–28082.

Pei, Y., Schwer, B., and Shuman, S. (2003). Interactions between Fission Yeast Cdk9, Its Cyclin Partner Pch1, and mRNA Capping Enzyme Pct1 Suggest an Elongation Checkpoint for mRNA Quality Control. J. Biol. Chem. *278*, 7180–7188.

Perez-Campo, F.M., Costa, G., Lie-a-Ling, M., Stifani, S., Kouskoff, V., and Lacaud, G. (2014). MOZ-Mediated Repression of p16 INK 4 a Is Critical for the Self-Renewal of Neural and Hematopoietic Stem Cells. Stem Cells *32*, 1591–1601.

Peters, A.H.F.M., O'Carroll, D., Scherthan, H., Mechtler, K., Sauer, S., Schöfer, C., Weipoltshammer, K., Pagani, M., Lachner, M., Kohlmaier, A., et al. (2001). Loss of the Suv39h Histone Methyltransferases Impairs Mammalian Heterochromatin and Genome Stability. Cell *107*, 323–337.

Pikaard, C.S., and Mittelsten Scheid, O. (2014). Epigenetic regulation in plants. Cold Spring Harb. Perspect. Biol. *6*, a019315.

REFERENCES

Piro, A.S., Mayekar, M.K., Warner, M.H., Davis, C.P., and Arndt, K.M. (2012). Small region of Rtf1 protein can substitute for complete Paf1 complex in facilitating global histone H2B ubiquitylation in yeast. Proc. Natl. Acad. Sci. U. S. A. *109*, 10837–10842.

Piunti, A., and Shilatifard, A. (2016). Epigenetic balance of gene expression by Polycomb and COMPASS families. Science *352*, aad9780.

Pnueli, L., Edry, I., Cohen, M., and Kassir, Y. (2004). Glucose and nitrogen regulate the switch from histone deacetylation to acetylation for expression of early meiosis-specific genes in budding yeast. Mol. Cell. Biol. *24*, 5197–5208.

Porrua, O., and Libri, D. (2015). Transcription termination and the control of the transcriptome: why, where and how to stop. Nat Rev Mol Cell Biol *16*, 190–202.

Ptashne, M. (2013). Epigenetics: core misconcept. Proc. Natl. Acad. Sci. U. S. A. *110*, 7101–7103.

Qiu, H., Hu, C., Gaur, N.A., and Hinnebusch, A.G. (2012). Pol II CTD kinases Bur1 and Kin28 promote Spt5 CTR-independent recruitment of Paf1 complex. EMBO J. *31*, 3494 LP-3505.

Racine, A., Pagé, V., Nagy, S., Grabowski, D., and Tanny, J.C. (2012). Histone H2B ubiquitylation promotes activity of the intact Set1 histone methyltransferase complex in fission yeast. J. Biol. Chem. *287*, 19040–19047.

Ragunathan, K., Jih, G., and Moazed, D. (2015). Epigenetics. Epigenetic inheritance uncoupled from sequence-specific recruitment. Science *348*, 1258699.

Rakyan, V.K., Blewitt, M.E., Druker, R., Preis, J.I., and Whitelaw, E. (2002). Metastable epialleles in mammals. Trends Genet. *18*, 348–351.

Rando, O.J. (2012). Combinatorial complexity in chromatin structure and function: revisiting the histone code. Curr. Opin. Genet. Dev. *22*, 148–155.

Rasmussen, E.B., and Lis, J.T. (1993). In vivo transcriptional pausing and cap formation on three Drosophila heat shock genes. Proc. Natl. Acad. Sci. U. S. A. *90*, 7923–7927.

Rebollo, R., Karimi, M.M., Bilenky, M., Gagnier, L., Miceli-Royer, K., Zhang, Y., Goyal, P., Keane, T.M., Jones, S., Hirst, M., et al. (2011). Retrotransposon-Induced Heterochromatin Spreading in the Mouse Revealed by Insertional Polymorphisms. PLOS Genet. *7*, e1002301.

Reddy, B.D., Wang, Y., Niu, L., Higuchi, E.C., Marguerat, S.B., Bähler, J., Smith, G.R., and Jia, S. (2011). Elimination of a specific histone H3K14 acetyltransferase complex bypasses the RNAi pathway to regulate pericentric heterochromatin functions. Genes Dev. *25*, 214–219.

Reuter, G., and Wolff, I. (1981). Isolation of dominant suppressor mutations for position-effect variegation in Drosophila melanogaster. Mol. Gen. Genet. MGG *182*, 516–519.

Reyes-Turcu, F.E., Zhang, K., Zofall, M., Chen, E., and Grewal, S.I.S. (2011). Defects in RNA quality control factors reveal RNAi-independent nucleation of heterochromatin. Nat. Struct. Mol. Biol. *18*, 1132–1138.

Riising, E.M., Comet, I., Leblanc, B., Wu, X., Johansen, J.V., and Helin, K. (2014). Gene Silencing Triggers Polycomb Repressive Complex 2 Recruitment to CpG Islands Genome Wide. Mol. Cell *55*, 347–360.

Roche, B., Arcangioli, B., and Martienssen, R.A. (2016). RNA interference is essential for cellular quiescence. Science *354*, aah5651.

Roguev, A., Schaft, D., Shevchenko, A., Pijnappel, W.W., Wilm, M., Aasland, R., and Stewart, A.F. (2001). The Saccharomyces cerevisiae Set1 complex includes an Ash2 homologue and methylates histone 3 lysine 4. EMBO J. *20*, 7137–7148.

REFERENCES

Rokudai, S., Laptenko, O., Arnal, S.M., Taya, Y., Kitabayashi, I., and Prives, C. (2013). MOZ increases p53 acetylation and premature senescence through its complex formation with PML. Proc. Natl. Acad. Sci. U. S. A. *110*, 3895–3900.

Rona, G.B., Almeida, D.S.G., Pinheiro, A.S., and Eleutherio, E.C.A. (2016). The PWWP domain of the human oncogene WHSC1L1/NSD3 induces a metabolic shift toward fermentation. Oncotarget.

Rougemaille, M., Braun, S., Coyle, S., Dumesic, P.A., Garcia, J.F., Isaac, R.S., Libri, D., Narlikar, G.J., and Madhani, H.D. (2012). Ers1 links HP1 to RNAi. Proc. Natl. Acad. Sci. U. S. A. *109*, 11258–11263.

Roy, A.L., and Singer, D.S. (2015). Core promoters in transcription: Old problem, new insights. Trends Biochem. Sci. *40*, 165–171.

Rozenblatt-Rosen, O., Nagaike, T., Francis, J.M., Kaneko, S., Glatt, K.A., Hughes, C.M., LaFramboise, T., Manley, J.L., and Meyerson, M. (2009). The tumor suppressor Cdc73 functionally associates with CPSF and CstF 3' mRNA processing factors. Proc. Natl. Acad. Sci. U. S. A. *106*, 755–760.

Rudolph, T., Yonezawa, M., Lein, S., Heidrich, K., Kubicek, S., Schäfer, C., Phalke, S., Walther, M., Schmidt, A., Jenuwein, T., et al. (2007). Heterochromatin formation in Drosophila is initiated through active removal of H3K4 methylation by the LSD1 homolog SU(VAR)3-3. Mol. Cell *26*, 103–115.

Ryan, K., Calvo, O., and Manley, J.L. (2004). Evidence that polyadenylation factor CPSF-73 is the mRNA 3' processing endonuclease. RNA *10*, 565–573.

Ryuko, S., Ma, Y., Ma, N., Sakaue, M., and Kuno, T. (2012). Genome-wide screen reveals novel mechanisms for regulating Cobalt uptake and detoxification in fission yeast. Mol. Genet. Genomics *287*, 651–662.

Sadaie, M., Kawaguchi, R., Ohtani, Y., Arisaka, F., Tanaka, K., Shirahige, K., and Nakayama, J.-I. (2008). Balance between distinct HP1 family proteins controls heterochromatin assembly in fission yeast. Mol. Cell. Biol. *28*, 6973–6988.

Sadeghi, L., Siggens, L., Svensson, J.P., and Ekwall, K. (2014). Centromeric histone H2B monoubiquitination promotes noncoding transcription and chromatin integrity. Nat. Struct. Mol. Biol. *21*, 236–243.

Sadeghi, L., Prasad, P., Ekwall, K., Cohen, A., and Svensson, J.P. (2015). The Paf1 complex factors Leo1 and Paf1 promote local histone turnover to modulate chromatin states in fission yeast. EMBO Rep. *16*, 1673–1687.

Saksouk, N., Simboeck, E., and Déjardin, J. (2015). Constitutive heterochromatin formation and transcription in mammals. Epigenetics Chromatin *8*, 3.

Sandell, L.L., and Zakian, V.A. (1992). Telomeric position effect in yeast. Trends Cell Biol. *2*, 10–14.

Sansó, M., Lee, K.M., Viladevall, L., Jacques, P.É., Pagé, V., Nagy, S., Racine, A., St. Amour, C. V., Zhang, C., Shokat, K.M., et al. (2012). A Positive Feedback Loop Links Opposing Functions of P-TEFb/Cdk9 and Histone H2B Ubiquitylation to Regulate Transcript Elongation in Fission Yeast. PLoS Genet. *8*.

Santos-Rosa, H., Schneider, R., Bannister, A.J., Sherriff, J., Bernstein, B.E., Emre, N.C.T., Schreiber, S.L., Mellor, J., and Kouzarides, T. (2002). Active genes are tri-methylated at K4 of histone H3. Nature *419*, 407–411.

Sawadogo, M., and Roeder, R.G. (1985). Factors involved in specific transcription by human RNA polymerase II: analysis by a rapid and quantitative in vitro assay. Proc. Natl. Acad. Sci. U. S. A. *82*, 4394–4398.

REFERENCES

Schalch, T., Job, G., Noffsinger, V.J., Shanker, S., Kuscu, C., Joshua-Tor, L., and Partridge, J.F. (2009). High-Affinity Binding of Chp1 Chromodomain to K9 Methylated Histone H3 Is Required to Establish Centromeric Heterochromatin. Mol. Cell *34*, 36–46.

Schalch, T., Job, G., Shanker, S., Partridge, J.F., and Joshua-Tor, L. (2011). The Chp1–Tas3 core is a multifunctional platform critical for gene silencing by RITS. Nat. Struct. Mol. Biol. *18*, 1351–1357.

Schmitges, F.W., Prusty, A.B., Faty, M., Stützer, A., Lingaraju, G.M., Aiwazian, J., Sack, R., Hess, D., Li, L., Zhou, S., et al. (2011). Histone Methylation by PRC2 Is Inhibited by Active Chromatin Marks. Mol. Cell *42*, 330–341.

Schmitz, R.J., Tamada, Y., Doyle, M.R., Zhang, X., and Amasino, R.M. (2009). Histone H2B deubiquitination is required for transcriptional activation of FLOWERING LOCUS C and for proper control of flowering in Arabidopsis. Plant Physiol. *149*, 1196–1204.

Schneider, C., Leung, E., Brown, J., and Tollervey, D. (2009). The N-terminal PIN domain of the exosome subunit Rrp44 harbors endonuclease activity and tethers Rrp44 to the yeast core exosome. Nucleic Acids Res. *37*, 1127–1140.

Schotta, G., Ebert, A., Krauss, V., Fischer, A., Hoffmann, J., Rea, S., Jenuwein, T., Dorn, R., and Reuter, G. (2002). Central role of Drosophila SU(VAR)3-9 in histone H3-K9 methylation and heterochromatic gene silencing. EMBO J. *21*, 1121–1131.

Schotta, G., Lachner, M., Sarma, K., Ebert, A., Sengupta, R., Reuter, G., Reinberg, D., and Jenuwein, T. (2004). A silencing pathway to induce H3-K9 and H4-K20 trimethylation at constitutive heterochromatin. Genes Dev. *18*, 1251–1262.

Schultz, J. (1950). Interrelations of factors affecting heterochromatin-induced variegation in Drosophila. Genetics *35*, 134.

Schultz, D.C., Ayyanathan, K., Negorev, D., Maul, G.G., and Rauscher, F.J. (2002). SETDB1: a novel KAP-1-associated histone H3, lysine 9-specific methyltransferase that contributes to HP1-mediated silencing of euchromatic genes by KRAB zinc-finger proteins. Genes Dev. *16*, 919–932.

Schulze, J.M., Hentrich, T., Nakanishi, S., Gupta, A., Emberly, E., Shilatifard, A., and Kobor, M.S. (2011). Splitting the task: Ubp8 and Ubp10 deubiquitinate different cellular pools of H2BK123. Genes Dev. *25*, 2242–2247.

Schwer, B., Sanchez, A.M., and Shuman, S. (2015). RNA polymerase II CTD phospho-sites Ser5 and Ser7 govern phosphate homeostasis in fission yeast. RNA *21*, 1770–1780.

Scott, K.C., Merrett, S.L., and Willard, H.F. (2006). A heterochromatin barrier partitions the fission yeast centromere into discrete chromatin domains. Curr. Biol. *16*, 119–129.

Shankaranarayana, G.D., Motamedi, M.R., Moazed, D., and Grewal, S.I.S. (2003). Sir2 Regulates Histone H3 Lysine 9 Methylation and Heterochromatin Assembly in Fission Yeast. Curr. Biol. *13*, 1240–1246.

Sheikh, B.N., Dixon, M.P., Thomas, T., and Voss, a. K. (2012). Querkopf is a key marker of self-renewal and multipotency of adult neural stem cells. J. Cell Sci. *125*, 295–309.

Shimada, Y., Mohn, F., and Bühler, M. (2016). The RNA-induced transcriptional silencing complex targets chromatin exclusively via interacting with nascent transcripts. Genes Dev. *30*, 1–10.

Sienski, G., Dönertas, D., and Brennecke, J. (2012). Transcriptional silencing of transposons by Piwi and maelstrom and its impact on chromatin state and gene expression. Cell *151*, 964–980.

Sienski, G., Batki, J., Senti, K., Dönertas, D., Tirian, L., Meixner, K., and Brennecke, J. (2015). Silencio / CG9754 connects the Piwi – piRNA complex to the cellular heterochromatin machinery. Genes Dev. *29*, 1–14.

REFERENCES

Sigova, A., Rhind, N., and Zamore, P.D. (2004). A single Argonaute protein mediates both transcriptional and posttranscriptional silencing in Schizosaccharomyces pombe. Genes Dev. *18*, 2359–2367.

Simmer, F., Buscaino, A., Kos-Braun, I.C., Kagansky, A., Boukaba, A., Urano, T., Kerr, A.R.W., and Allshire, R.C. (2010). Hairpin RNA induces secondary small interfering RNA synthesis and silencing in trans in fission yeast. EMBO Rep. *11*, 112–118.

Simon, J., Chiang, A., Bender, W., Shimell, M.J., and O'Connor, M. (1993). Elements of the Drosophila bithorax complex that mediate repression by Polycomb group products. Dev. Biol. *158*, 131–144.

Smolle, M., Venkatesh, S., Gogol, M.M., Li, H., Zhang, Y., Florens, L., Washburn, M.P., and Workman, J.L. (2012). Chromatin remodelers Isw1 and Chd1 maintain chromatin structure during transcription by preventing histone exchange. Nat Struct Mol Biol *19*, 884–892.

Sridhar, V. V, Kapoor, A., Zhang, K., Zhu, J.J.-K., Zhou, T., Hasegawa, P.M., Bressan, R. a, and Zhu, J.J.-K. (2007). Control of DNA methylation and heterochromatic silencing by histone H2B deubiquitination. Nature *447*, 735–738.

van Steensel, B., Smogorzewska, A., and de Lange, T. (1998). TRF2 protects human telomeres from end-to-end fusions. Cell *92*, 401–413.

Steinmetz, E.J., Warren, C.L., Kuehner, J.N., Panbehi, B., Ansari, A.Z., and Brow, D.A. (2006). Genome-Wide Distribution of Yeast RNA Polymerase II and Its Control by Sen1 Helicase. Mol. Cell *24*, 735–746.

Strahl, B.D., and Allis, C.D. (2000). The language of covalent histone modifications. Nature *403*, 41–45.

Strahl, B.D., Ohba, R., Cook, R.G., and Allis, C.D. (1999). Methylation of histone H3 at lysine 4 is highly conserved and correlates with transcriptionally active nuclei in Tetrahymena. Proc. Natl. Acad. Sci. *96*, 14967–14972.

Stunnenberg, R., Kulasegaran-Shylini, R., Keller, C., Kirschmann, M.A., Gelman, L., and Bühler, M. (2015). H3K9 methylation extends across natural boundaries of heterochromatin in the absence of an HP1 protein. EMBO J. *34*, 2789–2803.

Sugiyama, T., Cam, H.P., Sugiyama, R., Noma, K. ichi, Zofall, M., Kobayashi, R., and Grewal, S.I.S. (2007). SHREC, an Effector Complex for Heterochromatic Transcriptional Silencing. Cell *128*, 491–504.

Sun, Z.-W., and Allis, C.D. (2002). Ubiquitination of histone H2B regulates H3 methylation and gene silencing in yeast. Nature *418*, 104–108.

Suzuki, S., Kato, H., Suzuki, Y., Chikashige, Y., Hiraoka, Y., Kimura, H., Nagao, K., Obuse, C., Takahata, S., and Murakami, Y. (2016). Histone H3K36 trimethylation is essential for multiple silencing mechanisms in fission yeast. Nucleic Acids Res. *44*, 4147–4162.

Svinkina, T., Gu, H., Silva, J.C., Mertins, P., Qiao, J., Fereshetian, S., Jaffe, J.D., Kuhn, E., Udeshi, N.D., and Carr, S.A. (2015). Deep, quantitative coverage of the lysine acetylome using novel anti-acetyl-lysine antibodies and an optimized proteomic workflow. Mol. Cell. Proteomics *14*, 2429–2440.

Takahashi, K., Murakami, S., Chikashige, Y., Niwa, O., and Yanagida, M. (1991). A large number of tRNA genes are symmetrically located in fission yeast centromeres. J. Mol. Biol. *218*, 13–17.

Takahashi, K., Chen, E.S., and Yanagida, M. (2000). Requirement of Mis6 centromere connector for localizing a CENP-A-like protein in fission yeast. Science *288*, 2215–2219.

Talbert, P.B., and Henikoff, S. (2016). Histone variants on the move: substrates for chromatin dynamics. Nat. Rev. Mol. Cell Biol. *18*, 115–126.

REFERENCES

Tanny, J.C. (2014). Chromatin modification by the RNA Polymerase II elongation complex. Transcription *5*, e988093.

Tanny, J.C., and Moazed, D. (2001). Coupling of histone deacetylation to NAD breakdown by the yeast silencing protein Sir2: Evidence for acetyl transfer from substrate to an NAD breakdown product. Proc. Natl. Acad. Sci. U. S. A. *98*, 415–420.

Tanny, J.C., Erdjument-Bromage, H., Tempst, P., and Allis, C.D. (2007). Ubiquitylation of histone H2B controls RNA polymerase II transcription elongation independently of histone H3 methylation. Genes Dev. *21*, 835–847.

Taverna, S.D., Ilin, S., Rogers, R.S., Tanny, J.C., Lavender, H., Li, H., Baker, L., Boyle, J., Blair, L.P., Chait, B.T., et al. (2006). Yng1 PHD Finger Binding to H3 Trimethylated at K4 Promotes NuA3 HAT Activity at K14 of H3 and Transcription at a Subset of Targeted ORFs. Mol. Cell *24*, 785–796.

Tchasovnikarova, I.A., Timms, R.T., Matheson, N.J., Wals, K., Antrobus, R., Göttgens, B., Dougan, G., Dawson, M.A., and Lehner, P.J. (2015). GENE SILENCING. Epigenetic silencing by the HUSH complex mediates position-effect variegation in human cells. Science *348*, 1481–1485.

Thomas, T., Voss, A.K., Chowdhury, K., and Gruss, P. (2000). Querkopf, a MYST family histone acetyltransferase, is required for normal cerebral cortex development. Development *127*, 2537–2548.

Thon, G., and Verhein-Hansen, J. (2000). Four chromo-domain proteins of Schizosaccharomyces pombe differentially repress transcription at various chromosomal locations. Genetics *155*, 551–568.

Tompa, R., and Madhani, H.D. (2007). Histone H3 lysine 36 methylation antagonizes silencing in Saccharomyces cerevisiae independently of the Rpd3S histone deacetylase complex. Genetics *175*, 585–593.

Tomson, B.N., and Arndt, K.M. (2013). The many roles of the conserved eukaryotic Paf1 complex in regulating transcription, histone modifications, and disease states. Biochim. Biophys. Acta - Gene Regul. Mech. *1829*, 166–126.

Trojer, P., and Reinberg, D. (2007). Facultative heterochromatin: is there a distinctive molecular signature? Mol. Cell *28*, 1–13.

Tu, S., Bulloch, E.M.M., Yang, L., Ren, C., Huang, W.-C., Hsu, P.-H., Chen, C., Liao, C.-L., Yu, H.-M., Lo, W.-S., et al. (2007). Identification of Histone Demethylases in Saccharomyces cerevisiae. J. Biol. Chem. *282*, 14262–14271.

Tucker, J.F., Ohle, C., Schermann, G., Bendrin, K., Zhang, W., Fischer, T., and Zhang, K. (2016). A Novel Epigenetic Silencing Pathway Involving the Highly Conserved 5'-3' Exoribonuclease Dhp1/Rat1/Xrn2 in Schizosaccharomyces pombe. PLOS Genet. *12*, e1005873.

Veloso, A., Kirkconnell, K.S., Magnuson, B., and Biewen, B. (2014). Rate of elongation by RNA polymerase II is associated with specific gene features and epigenetic modifications Rate of elongation by RNA polymerase II is associated with specific gene features and epigenetic modifications. 896–905.

Venkatesh, S., Smolle, M., Li, H., Gogol, M.M., Saint, M., Kumar, S., Natarajan, K., and Workman, J.L. (2012). Set2 methylation of histone H3 lysine 36 suppresses histone exchange on transcribed genes. Nature *489*, 452–455.

Venter, J.C., Adams, M.D., Myers, E.W., Li, P.W., Mural, R.J., Sutton, G.G., Smith, H.O., Yandell, M., Evans, C.A., Holt, R.A., et al. (2001). The sequence of the human genome. Science *291*, 1304–1351.

Verdel, A., and Moazed, D. (2005). RNAi-directed assembly of heterochromatin in fission yeast. FEBS Lett. *579*, 5872–5878.

Verdel, A., Jia, S., Gerber, S., Sugiyama, T., Gygi, S., Grewal, S.I.S., and Moazed, D. (2004). RNAi-mediated targeting of heterochromatin by the RITS complex. Science *303*, 672–676.

REFERENCES

Vermeulen, M., and Timmers, H.M. (2010). Grasping trimethylation of histone H3 at lysine 4. Epigenomics *2*, 395–406.

Verrier, L., Taglini, F., Barrales, R.R., Webb, S., Urano, T., Braun, S., and Bayne, E.H. (2015). Global regulation of heterochromatin spreading by Leo1. Open Biol. *5*, 150045-.

Vethantham, V., Yang, Y., Bowman, C., Asp, P., Lee, J.-H., Skalnik, D.G., and Dynlacht, B.D. (2012). Dynamic loss of H2B ubiquitylation without corresponding changes in H3K4 trimethylation during myogenic differentiation. Mol. Cell. Biol. *32*, 1044–1055.

Vezzoli, A., Bonadies, N., Allen, M.D., Freund, S.M. V, Santiveri, C.M., Kvinlaug, B.T., Huntly, B.J.P., Gottgens, B., and Bycroft, M. (2010). Molecular basis of histone H3K36me3 recognition by the PWWP domain of Brpf1. Nat Struct Mol Biol *17*, 617–619.

Vicente-Muñoz, S., Romero, P., Magraner-Pardo, L., Martinez-Jimenez, C.P., Tordera, V., and Pamblanco, M. (2014). Comprehensive analysis of interacting proteins and genome-wide location studies of the Sas3-dependent NuA3 histone acetyltransferase complex. FEBS Open Bio *4*, 996–1006.

Viladevall, L., St. Amour, C. V, Rosebrock, A., Schneider, S., Zhang, C., Allen, J.J., Shokat, K.M., Schwer, B., Leatherwood, J.K., and Fisher, R.P. (2009). TFIIH and P-TEFb Coordinate Transcription with Capping Enzyme Recruitment at Specific Genes in Fission Yeast. Mol. Cell *33*, 738–751.

Vitaliano-Prunier, A., Menant, A., Hobeika, M., Geli, V., Gwizdek, C., and Dargemont, C. (2008). Ubiquitylation of the COMPASS component Swd2 links H2B ubiquitylation to H3K4 trimethylation. Nat Cell Biol *10*, 1365–1371.

Vitaliano-Prunier, A., Babour, A., Hérissant, L., Apponi, L., Margaritis, T., Holstege, F.C.P., Corbett, A.H., Gwizdek, C., and Dargemont, C. (2012). H2B ubiquitylation controls the formation of export-competent mRNP. Mol. Cell *45*, 132–139.

Vlaming, H., Molenaar, T.M., van Welsem, T., Poramba-Liyanage, D.W., Smith, D.E., Velds, A., Hoekman, L., Korthout, T., Hendriks, S., Altelaar, A.M., et al. (2016). Direct screening for chromatin status on DNA barcodes in yeast delineates the regulome of H3K79 methylation by Dot1. Elife *5*, e18919.

Volpe, T.A., Kidner, C., Hall, I.M., Teng, G., Grewal, S.I.S., Martienssen, R.A., Henikoff, S., Grewal, S.I., Elgin, S.C., Wallrath, L.L., et al. (2002). Regulation of heterochromatic silencing and histone H3 lysine-9 methylation by RNAi. Science *297*, 1833–1837.

Wang, H., Wang, L., Erdjument-Bromage, H., Vidal, M., Tempst, P., Jones, R.S., and Zhang, Y. (2004). Role of histone H2A ubiquitination in Polycomb silencing. Nature *431*, 873–878.

Wang, J., Tadeo, X., Hou, H., Tu, P.G., Thompson, J., Yates, J.R., and Jia, S. (2013). Epe1 recruits BET family bromodomain protein Bdf2 to establish heterochromatin boundaries. Genes Dev. *27*, 1886–1902.

Wang, J., Lawry, S.T., Cohen, A.L., and Jia, S. (2014). Chromosome boundary elements and regulation of heterochromatin spreading. Cell. Mol. Life Sci. *71*, 4841–4852.

Wang, J., Reddy, B.D., and Jia, S. (2015). Rapid epigenetic adaptation to uncontrolled heterochromatin spreading. Elife *4*, 1–17.

Wang, J., Cohen, A.L., Letian, A., Tadeo, X., Moresco, J.J., Liu, J., Yates, J.R., Qiao, F., and Jia, S. (2016a). The proper connection between shelterin components is required for telomeric heterochromatin assembly. Genes Dev. *30*, 827–839.

Wang, J., Jia, S.T., and Jia, S. (2016b). New Insights into the Regulation of Heterochromatin. Trends Genet. *32*, 284–294.

REFERENCES

Wang, L., Liu, L., and Berger, S.L. (1998). Critical residues for histone acetylation by Gcn5, functioning in Ada and SAGA complexes, are also required for transcriptional function in vivo. Genes Dev. *12*, 640–653.

Wang, Y., Kallgren, S.P., Reddy, B.D., Kuntz, K., López-Maury, L., Thompson, J., Watt, S., Chun, M., Hou, H., Shi, Y., et al. (2012). Histone H3 lysine 14 acetylation is required for activation of a DNA damage checkpoint in fission yeast. J. Biol. Chem. *287*, 4386–4393.

Weinert, B.T., Wagner, S.A., Horn, H., Henriksen, P., Liu, W.R., Olsen, J. V, Jensen, L.J., and Choudhary, C. (2011). Proteome-wide mapping of the Drosophila acetylome demonstrates a high degree of conservation of lysine acetylation. Sci. Signal. *4*, ra48.

Weinert, B.T., Iesmantavicius, V., Moustafa, T., Schölz, C., Wagner, S.A., Magnes, C., Zechner, R., and Choudhary, C. (2014). Acetylation dynamics and stoichiometry in Saccharomyces cerevisiae. Mol. Syst. Biol. *10*, 1–12.

van Werven, F.J., and Amon, A. (2011). Regulation of entry into gametogenesis. Philos. Trans. R. Soc. Lond. B. Biol. Sci. *366*, 3521–3531.

Whitlock, J.P., and Simpson, R.T. (1976). Removal of histone H1 exposes a fifty base pair DNA segment between nucleosomes. Biochemistry *15*, 3307–3314.

Wieczorek, E., Brand, M., Jacq, X., and Tora, L. (1998). Function of TAFII-containing complex without TBP in transcription by RNA polymerase II. Nature *393*, 187–191.

Wier, A.D., Mayekar, M.K., Héroux, A., Arndt, K.M., and VanDemark, A.P. (2013). Structural basis for Spt5-mediated recruitment of the Paf1 complex to chromatin. Proc. Natl. Acad. Sci. U. S. A. *110*, 17290–17295.

Wierzbicki, A.T., Ream, T.S., Haag, J.R., and Pikaard, C.S. (2009). RNA polymerase V transcription guides ARGONAUTE4 to chromatin. Nat. Genet. *41*, 630–634.

Wilhelm, B.T., Marguerat, S., Watt, S., Schubert, F., Wood, V., Goodhead, I., Penkett, C.J., Rogers, J., and Bähler, J. (2008). Dynamic repertoire of a eukaryotic transcriptome surveyed at single-nucleotide resolution. Nature *453*, 1239–1243.

Wood, A., Schneider, J., Dover, J., Johnston, M., and Shilatifard, A. (2005). The Bur1/Bur2 Complex Is Required for Histone H2B Monoubiquitination by Rad6/Bre1 and Histone Methylation by COMPASS. Mol. Cell *20*, 589–599.

Wood, V., Gwilliam, R., Rajandream, M.A., Lyne, M., Lyne, R., Stewart, A., Sgouros, J., Peat, N., Hayles, J., Baker, S., et al. (2002). The genome sequence of Schizosaccharomyces pombe. Nature *415*, 871–880.

Woolcock, K.J., Gaidatzis, D., Punga, T., and Bühler, M. (2011). Dicer associates with chromatin to repress genome activity in Schizosaccharomyces pombe. Nat. Struct. Mol. Biol. *18*, 94–99.

Woolcock, K.J., Stunnenberg, R., Gaidatzis, D., Hotz, H.R., Emmerth, S., Barraud, P., and Bühler, M. (2012). RNAi keeps Atf1-bound stress response genes in check at nuclear pores. Genes Dev. *26*, 683–692.

Wu, L., Zee, B.M., Wang, Y., Garcia, B.A., and Dou, Y. (2011). The RING Finger Protein MSL2 in the MOF Complex Is an E3 Ubiquitin Ligase for H2B K34 and Is Involved in Crosstalk with H3 K4 and K79 Methylation. Mol. Cell *43*, 132–144.

Wyce, A., Xiao, T., Whelan, K.A., Kosman, C., Walter, W., Eick, D., Hughes, T.R., Krogan, N.J., Strahl, B.D., and Berger, S.L. (2007). H2B ubiquitylation acts as a barrier to Ctk1 nucleosomal recruitment prior to removal by Ubp8 within a SAGA-related complex. Mol. Cell *27*, 275–288.

REFERENCES

Xhemalce, B., and Kouzarides, T. (2010). A chromodomain switch mediated by histone H3 Lys 4 acetylation regulates heterochromatin assembly. Genes Dev. *24*, 647–652.

Xiao, T., Hall, H., Kizer, K.O., Shibata, Y., Hall, M.C., Borchers, C.H., and Strahl, B.D. (2003). Phosphorylation of RNA polymerase II CTD regulates H3 methylation in yeast. Genes Dev. *17*, 654–663.

Xu, Y., Gan, E.-S., Zhou, J., Wee, W.-Y., Zhang, X., and Ito, T. (2014). Arabidopsis MRG domain proteins bridge two histone modifications to elevate expression of flowering genes. Nucleic Acids Res. *42*, 10960–10974.

Yamada, T., Fischle, W., Sugiyama, T., Allis, C.D., and Grewal, S.I.S. (2005). The nucleation and maintenance of heterochromatin by a histone deacetylase in fission yeast. Mol. Cell *20*, 173–185.

Yamada, T., Yamaguchi, Y., Inukai, N., Okamoto, S., Mura, T., and Handa, H. (2006). P-TEFb-Mediated Phosphorylation of hSpt5 C-Terminal Repeats Is Critical for Processive Transcription Elongation. Mol. Cell *21*, 227–237.

Yamanaka, S., Mehta, S., Reyes-Turcu, F.E., Zhuang, F., Fuchs, R.T., Rong, Y., Robb, G.B., and Grewal, S.I.S. (2013). RNAi triggered by specialized machinery silences developmental genes and retrotransposons. Nature *493*, 557–560.

Yamane, K., Mizuguchi, T., Cui, B., Zofall, M., Noma, K.I., and Grewal, S.I.S. (2011). Asf1/HIRA facilitate global histone deacetylation and associate with HP1 to promote nucleosome occupancy at heterochromatic loci. Mol. Cell *41*, 56–66.

Yang, X.J. (2015). MOZ and MORF acetyltransferases: Molecular interaction, animal development and human disease. Biochim. Biophys. Acta - Mol. Cell Res. *1853*, 1818–1826.

Yang, F., and Xi, R. (2017). Silencing transposable elements in the Drosophila germline. Cell. Mol. Life Sci. *74*, 435–448.

Yang, H., Howard, M., and Dean, C. (2014). Antagonistic roles for H3K36me3 and H3K27me3 in the cold-induced epigenetic switch at Arabidopsis FLC. Curr. Biol. *24*, 1793–1797.

Yoh, S.M., Cho, H., Pickle, L., Evans, R.M., and Jones, K.A. (2007). The Spt6 SH2 domain binds Ser2-P RNAPII to direct Iws1-dependent mRNA splicing and export. Genes Dev. *21*, 160–174.

Young, B., and Heath, J.W. (2000). Wheater's Functional Histology (Edinburgh: Harcourt publishers Limited).

Yu, R., Jih, G., Iglesias, N., and Moazed, D. (2014). Determinants of Heterochromatic siRNA Biogenesis and Function. Mol. Cell *53*, 262–276.

Yu, Y., Gu, J., Jin, Y., Luo, Y., Preall, J.B., Ma, J., Czech, B., and Hannon, G.J. (2015). Panoramix enforces piRNA-dependent cotranscriptional silencing. Science *350*, 339–342.

Yuan, W., Xu, M., Huang, C., Liu, N., Chen, S., and Zhu, B. (2011). H3K36 methylation antagonizes PRC2-mediated H3K27 methylation. J. Biol. Chem. *286*, 7983–7989.

Yuan, W., Luo, X., Li, Z., Yang, W., Wang, Y., Liu, R., Du, J., and He, Y. (2016). A cis cold memory element and a trans epigenome reader mediate Polycomb silencing of FLC by vernalization in Arabidopsis. Nat. Genet. *48*, 1527–1534.

Zaborowska, J., Egloff, S., and Murphy, S. (2016). The pol II CTD: new twists in the tail. Nat Struct Mol Biol *23*, 771–777.

Zaratiegui, M., Castel, S.E., Irvine, D. V, Kloc, A., Ren, J., Li, F., de Castro, E., Marín, L., Chang, A.-Y., Goto, D., et al. (2011). RNAi promotes heterochromatic silencing through replication-coupled release of RNA Pol II. Nature *479*, 135–138.

REFERENCES

Zhang, F., and Yu, X. (2011). WAC, a Functional Partner of RNF20/40, Regulates Histone H2B Ubiquitination and Gene Transcription. Mol. Cell *41*, 384–397.

Zhang, K., Mosch, K., Fischle, W., and Grewal, S.I.S. (2008). Roles of the Clr4 methyltransferase complex in nucleation, spreading and maintenance of heterochromatin. Nat. Struct. Mol. Biol. *15*, 381–388.

Zhang, K., Fischer, T., Porter, R.L., Dhakshnamoorthy, J., Zofall, M., Zhou, M., Veenstra, T., and Grewal, S.I.S. (2011). Clr4/Suv39 and RNA quality control factors cooperate to trigger RNAi and suppress antisense RNA. Science *331*, 1624–1627.

Zhang, T., Cooper, S., and Brockdorff, N. (2015). The interplay of histone modifications - writers that read. EMBO Rep. *16*, 1467–1481.

Zhang, X., Yazaki, J., Sundaresan, A., Cokus, S., Chan, S.W.-L., Chen, H., Henderson, I.R., Shinn, P., Pellegrini, M., Jacobsen, S.E., et al. (2006). Genome-wide high-resolution mapping and functional analysis of DNA methylation in arabidopsis. Cell *126*, 1189–1201.

Zhang, X., Clarenz, O., Cokus, S., Bernatavichute, Y. V, Pellegrini, M., Goodrich, J., and Jacobsen, S.E. (2007). Whole-genome analysis of histone H3 lysine 27 trimethylation in Arabidopsis. PLoS Biol. *5*, e129.

Zhang, Y., Xie, S., Zhou, Y., Xie, Y., Liu, P., Sun, M., Xiao, H., Jin, Y., Sun, X., Chen, Z., et al. (2014). H3K36 histone methyltransferase Setd2 is required for murine embryonic stem cell differentiation toward endoderm. Cell Rep. *8*, 1989–2002.

Zhao, Y., and Garcia, B.A. (2015). Comprehensive Catalog of Currently Documented Histone Modifications. Cold Spring Harb. Perspect. Biol. *7*, a025064.

Zhao, Y., Lang, G., Ito, S., Bonnet, J., Metzger, E., Sawatsubashi, S., Suzuki, E., Le Guezennec, X., Stunnenberg, H.G., Krasnov, A., et al. (2008). A TFTC/STAGA module mediates histone H2A and H2B deubiquitination, coactivates nuclear receptors, and counteracts heterochromatin silencing. Mol. Cell *29*, 92–101.

Zhao, Z., Yu, Y., Meyer, D., Wu, C., and Shen, W.-H. (2005). Prevention of early flowering by expression of FLOWERING LOCUS C requires methylation of histone H3 K36. Nat. Cell Biol. *7*, 1256–1260.

Zilio, N., Codlin, S., Vashisht, A. a, Bitton, D. a, Head, S.R., Wohlschlegel, J. a, Bähler, J., and Boddy, M.N. (2014). A novel histone deacetylase complex in the control of transcription and genome stability. Mol. Cell. Biol. *34*, 3500–3514.

Zocco, M., Marasovic, M., Pisacane, P., Bilokapic, S., and Halic, M. (2016). The Chp1 chromodomain binds the H3K9me tail and the nucleosome core to assemble heterochromatin. Cell Discov. *2*, 16004.

Zofall, M., and Grewal, S.I.S. (2006). Swi6/HP1 Recruits a JmjC Domain Protein to Facilitate Transcription of Heterochromatic Repeats. Mol. Cell *22*, 681–692.

Zofall, M., and Grewal, S.I.S. (2007). HULC, a histone H2B ubiquitinating complex, modulates heterochromatin independent of histone methylation in fission yeast. J. Biol. Chem. *282*, 14065–14072.

Zofall, M., Yamanaka, S., Reyes-Turcu, F.E., Zhang, K., Rubin, C., Grewal, S.I.S., Henikoff, S., Jenuwein, T., Allis, C.D., Grewal, S.I., et al. (2012). RNA elimination machinery targeting meiotic mRNAs promotes facultative heterochromatin formation. Science *335*, 96–100.

APPENDIX

Manuscript 1: The Paf1 complex represses small-RNA-mediated epigenetic gene silencing

Manuscript 2: The histone acetyltransferase Mst2 protects active chromatin from epigenetic silencing by acetylating the ubiquitin ligase Brl1

APPENDIX

Manuscript 1: The Paf1 complex represses small-RNA-mediated epigenetic gene silencing

LETTER

doi:10.1038/nature14337

The Paf1 complex represses small-RNA-mediated epigenetic gene silencing

Katarzyna Maria Kowalik[1,2]*, Yukiko Shimada[1,2]*, Valentin Flury[1,2], Michael Beda Stadler[1,2,3], Julia Batki[4] & Marc Bühler[1,2]

RNA interference (RNAi) refers to the ability of exogenously introduced double-stranded RNA to silence expression of homologous sequences. Silencing is initiated when the enzyme Dicer processes the double-stranded RNA into small interfering RNAs (siRNAs). Small RNA molecules are incorporated into Argonaute-protein-containing effector complexes, which they guide to complementary targets to mediate different types of gene silencing, specifically post-transcriptional gene silencing and chromatin-dependent gene silencing[1]. Although endogenous small RNAs have crucial roles in chromatin-mediated processes across kingdoms, efforts to initiate chromatin modifications *in trans* by using siRNAs have been inherently difficult to achieve in all eukaryotic cells. Using fission yeast, here we show that RNAi-directed heterochromatin formation is negatively controlled by the highly conserved RNA polymerase-associated factor 1 complex (Paf1C). Temporary expression of a synthetic hairpin RNA in Paf1C mutants triggers stable heterochromatin formation at homologous loci, effectively silencing genes *in trans*. This repressed state is propagated across generations by the continual production of secondary siRNAs, independently of the synthetic hairpin RNA. Our data support a model in which Paf1C prevents targeting of nascent transcripts by the siRNA-containing RNA-induced transcriptional silencing complex and thereby epigenetic gene silencing, by promoting efficient transcription termination and rapid release of the RNA from the site of transcription. We show that although compromised transcription termination is sufficient to initiate the formation of bi-stable heterochromatin by *trans*-acting siRNAs, impairment of both transcription termination and nascent transcript release is imperative to confer stability to the repressed state. Our work uncovers a novel mechanism for small-RNA-mediated epigenome regulation and highlights fundamental roles for Paf1C and the RNAi machinery in building epigenetic memory.

In the fission yeast *Schizosaccharomyces pombe*, a functional RNAi pathway is required for the formation and stable propagation of constitutive heterochromatin found at pericentromeric repeat sequences. *S. pombe* contains single genes encoding for an Argonaute and a Dicer protein, called *ago1*+ and *dcr1*+, respectively. Centromeres of *ago1*Δ or *dcr1*Δ cells have markedly reduced histone 3 lysine 9 (H3K9) methylation, which is a hallmark of heterochromatin, and defective chromosome segregation and heterochromatic gene silencing[2]. Ago1 is loaded with endogenous small RNAs corresponding to heterochromatic repeats, and interacts with Chp1 and Tas3 to form the RNA-induced transcriptional silencing (RITS) complex[3]. Current models propose that Ago1-bound small RNAs target RITS to centromeres via base-pairing interactions with nascent, chromatin-associated non-coding transcripts. Consequently, RITS recruits the RNA-dependent RNA polymerase complex (RDRC) to initiate double-stranded RNA synthesis and siRNA amplification, as well as the cryptic loci regulator complex (CLRC) to facilitate methylation of histone H3K9 (ref. 4). Chp1 reinforces the heterochromatin association of RITS by binding methylated H3K9 with high affinity[5], thereby creating a positive-feedback loop between siRNA biogenesis, RITS localization and H3K9 methylation. Hence, siRNA-programmed RITS acts as a specificity determinant for the recruitment of other RNAi complexes and chromatin-modifying enzymes to centromeres. However, an outstanding question is whether synthetic siRNAs can also function in this context, and thereby be used to trigger *de novo* formation of heterochromatin, particularly outside of centromeric repeats, to stably silence gene expression at will[1].

Small RNAs have crucial roles in endogenous chromatin-mediated processes also in plants, *Caenorhabditis elegans*, *Drosophila melanogaster* and ciliates. Their role in chromatin silencing can also be extended to mammalian cells, although the mechanisms and physiological pathways are less clear[1,6]. Yet, efforts to initiate chromatin modifications *in trans* by using siRNAs have been inherently difficult to achieve in all organisms. In plants, this is because the ability of siRNAs to induce DNA methylation at gene promoters is context-dependent and sensitive to pre-existing chromatin modifications[7]. And although siRNAs have been shown to promote DNA methylation *in trans* on homologous reporter transgenes in tobacco and *Arabidopsis*[8], it is unclear whether this is a general phenomenon for endogenous promoters. In mammalian cells, the introduction of siRNAs or hairpin RNAs has been reported to promote the modification of DNA and histones[9–11]. However, most small RNAs seem to mediate post-transcriptional gene silencing exclusively, and siRNA-mediated silencing of transcription does not necessarily require chromatin modification[12,13]. Consequently, the potential of synthetic siRNAs to trigger long-lasting gene repression in mammalian cells is debated. Similarly, although studies in *S. pombe* have shown that RNA-hairpin-derived siRNAs can promote H3K9 methylation *in trans* at a small number of loci[14,15], it is inefficient, locus-dependent, and the silent state observed is weak and highly unstable[14]. Rather, endogenous protein-coding genes seem to be refractory to siRNA-directed repression *in trans* in wild-type cells (Extended Data Figs 1 and 2). Therefore, it has been proposed that the ability of siRNAs to direct *de novo* formation of heterochromatin *in trans* is under strict control by mechanisms that have thus far remained elusive.

To identify putative suppressors of siRNA-mediated heterochromatin formation, we designed a small-RNA-mediated silencing (sms) forward genetic screen. We constructed a reporter strain (sms0), which expresses an RNA hairpin (ade6-hp) that is complementary to 250 nucleotides of *ade6*+ (Fig. 1a and Extended Data Fig. 1). We chose *ade6*+ as a reporter because *ade6* mutant cells form red colonies on limiting adenine indicator plates, whereas *ade6*+ cells appear white. Although the ade6-hp construct generated siRNAs complementary to *ade6*+ messenger RNAs, no red colonies were visible, demonstrating that *ade6*+ siRNAs cannot silence the *ade6*+ gene *in trans* in sms0 cells (Extended Data Figs 1b and 2). To screen for mutants that would enable *ade6*+ siRNAs to act *in trans*, we mutagenized sms0 cells with ethylmethansulfonate (EMS). This revealed five *sms* mutants that are highly susceptible to *de novo* formation of heterochromatin and stable gene silencing by siRNAs that are acting *in trans* (Extended Data Fig. 3).

[1]Friedrich Miescher Institute for Biomedical Research, Maulbeerstrasse 66, 4058 Basel, Switzerland. [2]University of Basel, Petersplatz 10, 4003 Basel, Switzerland. [3]Swiss Institute of Bioinformatics, Maulbeerstrasse 66, 4058 Basel, Switzerland. [4]Eötvös Loránd University, Faculty of Sciences, Institute of Chemistry, 1/A Pázmány Péter sétány, Budapest 1117, Hungary.
*These authors contributed equally to this work.

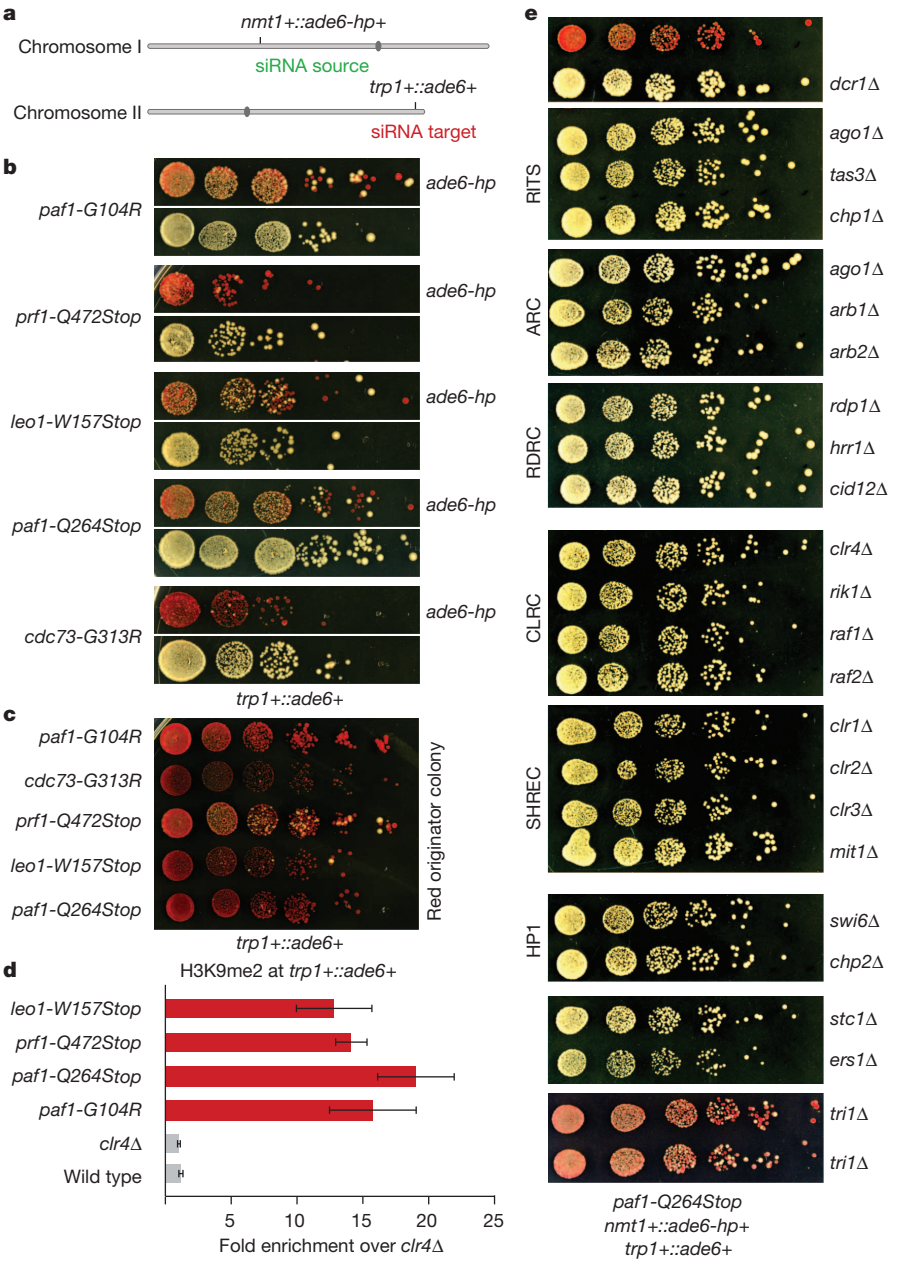

Figure 1 | siRNA-directed *de novo* formation of heterochromatin. **a**, The ade6-hp RNA producing locus and siRNA target *in trans* in the sms0 strain. **b**, Silencing assay performed with freshly generated Paf1C mutants. **c**, Silencing assay performed with red colonies from **b**. **d**, *ade6+* siRNAs direct the methylation of H3K9 *in trans* at the *trp1+::ade6+* locus in Paf1C mutant cells. Error bars, s.e.m.; $n = 3$ technical replicates. **e**, Gene silencing at the *trp1+::ade6+* locus depends on the same factors as constitutive heterochromatin at centromeric repeats. ARC, Argonaute siRNA chaperone complex.

To map the mutations in *sms* mutants, we re-sequenced the genomes of sms0 and backcrossed *sms* mutants using whole-genome next-generation sequencing. We mapped missense or nonsense mutations in the genes SPBC651.09c, SPAC664.03, SPBC13E7.08c and SPBC17G9.02c (Extended Data Fig. 3), whose homologues in budding yeast encode for protein subunits of the Paf1 complex. We therefore named SPAC664.03, SPBC13E7.08c and SPBC17G9.02c after the *S. cerevisiae* homologues *paf1+*, *leo1+* and *cdc73+*, respectively. SPBC651.09c has already been named as *prf1+* (ref. 16). To validate these as the causative mutations, we reconstituted the candidate point mutations in Paf1, Leo1, Cdc73 and Prf1 in sms0 cells. All five point mutations recapitulated the *sms* mutant phenotype in cells expressing ade6-hp siRNAs (Fig. 1b, c). As expected from the red colour assays, *ade6+* mRNA levels were reduced in all mutant strains. siRNA-mediated *ade6+* silencing was also observed in cells that express a carboxy-terminally 3×Flag-tagged version of the fifth Paf1C subunit Tpr1, which acts as a hypomorphic allele (Extended Data Fig. 4). Therefore, we have identified mutant alleles for the homologues of all five subunits of Paf1C that enable siRNAs to induce gene silencing *in trans*.

We next analysed whether other genes could also be silenced *in trans* in the Paf1C mutants. We first selected the endogenous *ura4+* gene, as this has been shown to be refractory to silencing by siRNAs acting *in trans*[14,15,17]. The *paf1-Q264Stop* mutation was introduced in a strain expressing *ura4+* siRNAs from a *ura4+* hairpin integrated at the *nmt1+* locus[15]. *ura4+* repression was monitored by growing cells on media containing 5-fluoroorotic acid (5-FOA), which is toxic to *ura4+* expressing cells. As expected, *paf1+* cells did not grow on 5-FOA-containing media, indicating that the *ura4+* gene is expressed. However, *paf1-Q264Stop* cells formed colonies on 5-FOA containing media, demonstrating siRNA-directed silencing of the endogenous *ura4+* locus (Extended Data Fig. 5a). Similarly, siRNAs generated at the heterochromatic *ura4+::5BoxB* locus[18] were able to silence a *leu1Δ::ura4+* reporter *in trans* in *paf1-Q264Stop* but not *paf1+* cells (Extended Data Fig. 5b), demonstrating that siRNAs generated from sources other than RNA stem–loop structures also direct *trans*-silencing in *paf1+* mutant cells. Finally, we also observed silencing of the endogenous *ade6+* gene when ade6-hp siRNAs were expressed from the *nmt1+* locus in *paf1-Q264Stop* cells (Extended Data Fig. 5c). In summary, Paf1C mutations

enabled siRNA-directed silencing *in trans* at all euchromatic loci that we tested.

The foregoing results indicated that *de novo* formation of heterochromatin was mediated by *trans*-acting siRNAs. Indeed, Paf1C mutants showed high H3K9 methylation at all *ade6+* siRNA target loci (Fig. 1d and Extended Data Fig. 6a–c), demonstrating that Paf1C prevents *trans*- as well as *cis*-acting siRNAs from directing methylation of H3K9. Further corroborating the formation of bona fide heterochromatin at the *ade6+* target locus, *ade6+* repression was dependent on components of SHREC (Snf2/histone deacetylase (HDAC) repressor complex) and CLRC, as well as the heterochromatin protein 1 (HP1) proteins Swi6 and Chp2, which are known to facilitate constitutive heterochromatin formation at centromeres (Fig. 1e). Finally, the formation of heterochromatin reduced transcriptional activity of the *ade6+* gene as evidenced by reduced H3K36 tri-methylation and RNA polymerase (Pol) II occupancy (Extended Data Fig. 6d, e). From these results we conclude that siRNAs can initiate the formation of heterochromatin and gene silencing, but that this is under strict negative control by Paf1C. This explains previous unsuccessful attempts to induce stable heterochromatin formation *in trans* using synthetic siRNAs.

Consistent with the formation of an epigenetically distinct chromatin domain at the siRNA target loci, cells in a population of freshly generated Paf1C mutants were either fully red or fully white. The latter gradually became red with increasing numbers of mitotic divisions, and once established, the silent state was remarkably stable (Fig. 1b, c). The fact that not all cells in a population of naive Paf1C mutant cells turned red immediately allowed us to determine the frequency of initiation of heterochromatin formation quantitatively. This analysis revealed that silencing in mitotic cells was efficiently established in *leo1-W157Stop* mutant cells, whereas *cdc73-G313R* cells were the least efficient (Fig. 2a). Descendants of a red colony switched to the white phenotype only sporadically in all Paf1C mutants, demonstrating that maintenance of heterochromatin is very robust in these cells (Fig. 2b). Interestingly, siRNA-directed *de novo* formation of heterochromatin was most efficient in meiosis. In 70% of all crosses between a naive *paf1-Q264Stop* mutant (white) and a *paf1+* cell, at least one of two *paf1-Q264Stop* spores had initiated *ade6+* repression (red) (Fig. 2c and Extended Data Fig. 7). We also observed highly efficient propagation of the silent state through meiosis, but only in descendants of spores that inherited the Paf1C mutation (Fig. 2d). Thus, siRNAs are sufficient to initiate the formation of very stable heterochromatin when Paf1C function is impaired.

Notably, assembly of heterochromatin at the *ade6+* target gene was accompanied by the production of novel *ade6+* siRNAs that are not encoded in the ade6-hp and that accumulated to high levels (Fig. 2e). Thus, primary ade6-hp siRNAs trigger the production of highly abundant secondary *ade6+* siRNAs in Paf1C mutants. To test whether continuous production of siRNAs is necessary for sustaining the repressed state, we deleted genes encoding for RNAi factors and found that *ade6+* silencing was completely abolished in all canonical RNAi mutants. Deletion of *tri1+* resulted in moderate derepression of *ade6+* silencing, suggesting a minor contribution of this exonuclease to siRNA-mediated heterochromatin silencing (Fig. 1e). To test whether secondary siRNAs produced at the *ade6+* target locus are sufficient to maintain heterochromatin, we crossed a *trp1+::ade6+ paf1-Q264Stop ade6-hp+* strain (red) with a *trp1+::ade6+ paf1-Q264Stop* (white) strain. These crosses regularly produced spores that gave rise to red cells even in the absence of the *nmt1+::ade6-hp+* allele. The red phenotype was still visible after replica plating, demonstrating that heterochromatin can be maintained in the absence of the primary siRNAs for hundreds of mitotic cell divisions (Fig. 2f). These results demonstrate that siRNAs can induce an epigenetic change in gene expression in meiotic and mitotic cells, and that secondary siRNA production is sufficient to propagate the repressed state for many mitotic cell divisions independently of the primary siRNAs that triggered the epigenetic switch.

The highly conserved Paf1C is well known for promoting RNA Pol II transcription elongation and RNA 3′-end processing (Fig. 3a). Paf1C also governs transcription-coupled histone modifications and has connections to DNA damage repair, cell cycle progression, and other processes[19]. Given this broad function, we assessed the effect of our Paf1C mutations on genome expression. This analysis revealed that *paf1-G104R*, *paf1-Q264Stop*, *prf1-Q472Stop* and *leo1-W157Stop* impair repression of heterochromatin formation, without affecting RNA expression globally (Supplementary Information and Extended Data Fig. 8). This is consistent with our observation that *ade6+* expression is unaffected in Paf1C mutants in the absence of siRNAs (Fig. 1b). We did, however, detect a reduction in H3K36 tri-methylation and an increase in RNA Pol II occupancy on the *ade6+* gene in *paf1-Q264Stop* cells (Fig. 3b, c). This is consistent with the role of Paf1C in promoting transcription, and suggests that decelerated transcription kinetics in Paf1C mutants enables siRNA-directed epigenetic gene silencing. To dissect which of Paf1C's activities are most critical to prevent RNAi-mediated heterochromatin assembly, we interfered with transcription elongation, termination

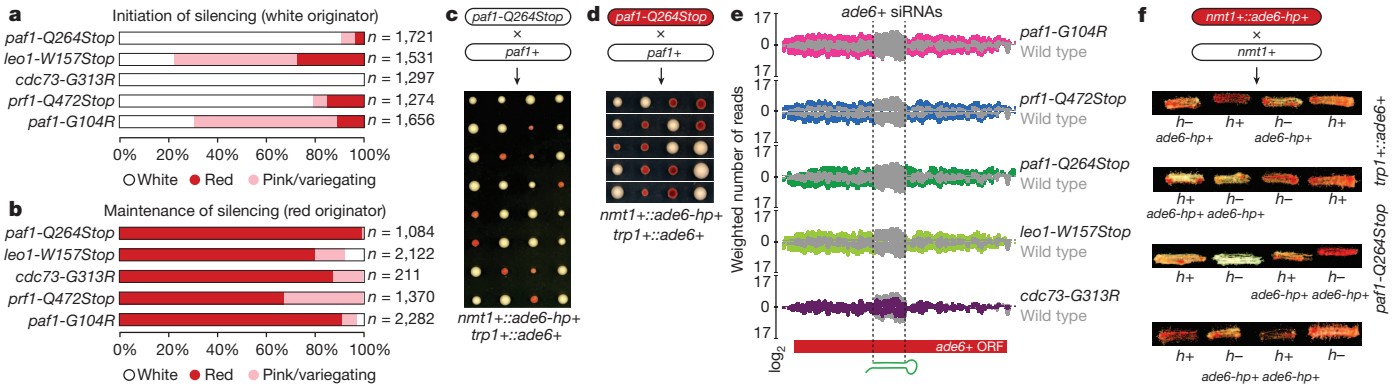

Figure 2 | siRNA-mediated epigenetic gene silencing. **a**, Percentage of naive Paf1C mutant cells that establish heterochromatin within 20–30 mitotic divisions. *n*, number of scored colonies. **b**, Stability of ectopic heterochromatin in mitotic cells. *n*, number of scored colonies. **c**, Initiation of heterochromatin formation during meiosis. Naive *paf1-Q264Stop* cells (white) were crossed with *paf1+* cells. Spore dissection of eight crosses is shown. **d**, Red *paf1-Q264Stop* cells (heterochromatic *ade6+*) were crossed with *paf1+* cells to assess stability of ectopic heterochromatin through meiosis. White descendants are *paf1+*. **e**, siRNA reads mapping to the *ade6+* locus in wild-type (grey) and Paf1C mutant (coloured) strains. Read counts were normalized to library size and are shown in $\log_2$ scale. Dashed lines mark the *ade6+* fragment targeted by the hairpin. **f**, Red *paf1-Q264Stop* cells (heterochromatic *ade6+*) carrying the *ade6+*-targeting hairpin (*ade6-hp+*) were crossed with *paf1-Q264Stop* cells without the hairpin to test hairpin requirement after initiation of silencing. Four spores derived from the cross were struck on yeast extract (YE) plates to assess the silencing phenotype. *h+* and *h−* denote mating types and *ade6-hp+* marks cells carrying the hairpin.

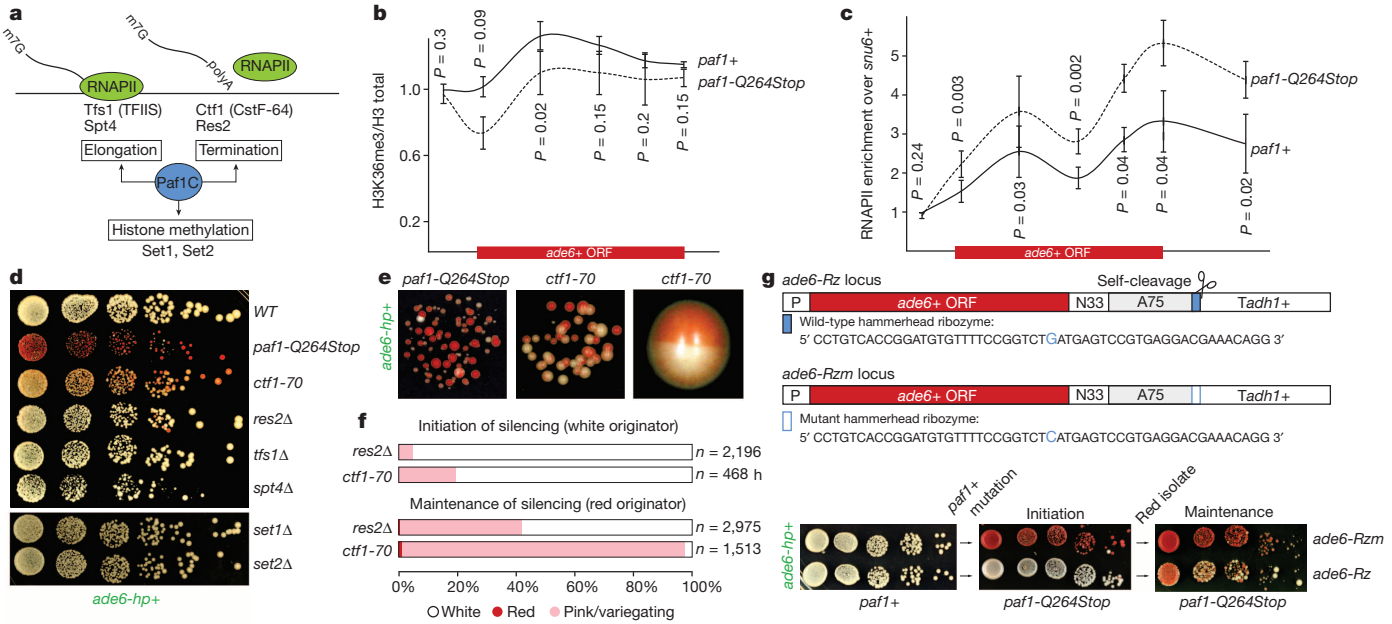

Figure 3 | Mechanism of repression. **a**, Paf1C governs RNA Pol II (RNAPII) transcription elongation, RNA 3′-end processing, and transcription-coupled histone modifications. **b**, **c**, Chromatin immunoprecipitation experiments to assess *ade6+* transcriptional activity in Paf1C mutant cells. H3K36me3 levels were normalized to total H3 levels. *snu6+* is transcribed by RNAPIII and serves as background control. ORF, open-reading frame. Error bars, s.e.m.; $n = 3$ independent biological replicates; *P* values were calculated using one-tailed Student's *t*-test. **d**, **e**, Silencing assays showing that *ade6+* siRNAs can initiate repression of *ade6+* in transcription termination mutants. Note the bi-stable state of repression in *ctf1-70* cells. Cells were grown on YE plates. WT, wild type. **f**, Percentage of naive transcription termination defective cells (white originator) that establish heterochromatin within 20–30 mitotic divisions (initiation) and stability of ectopic heterochromatin in descendants thereof (maintenance). *n*, number of scored colonies. **g**, A 52-nucleotide wild-type or mutant hammerhead ribozyme sequence preceded by a templated polyA(75)-tail was integrated 33 nucleotides downstream of the *ade6+* stop codon (*ade6-Rz* or *ade6-Rzm*, respectively). **h**, Silencing assay showing that *ade6+* siRNAs stably repress *ade6-Rzm* but not *ade6-Rz* in *paf1* mutant cells. Note that *ade6-Rz* produces fully functional mRNA in *paf1+* cells.

or co-transcriptional histone modification directly by mutating genes encoding elongation factors (Tfs1 and Spt4), termination factors (Ctf1 and Res2), or histone methyltransferases (Set1 and Set2)[20,21] (Fig. 3a). We observed siRNA-mediated initiation of *ade6+* silencing in *ctf1-70* and *res2Δ* cells, but not in *tfs1Δ*, *spt4Δ*, *set1Δ* and *set2Δ* cells (Fig. 3d–f), demonstrating that impaired transcription termination but not elongation is sufficient to allow siRNA-directed repression. Notably, although impaired transcription termination in *ctf1-70* and *res2Δ* cells was sufficient to initiate silencing, the silent state was less stable than in *paf1-Q264Stop* mutant cells (Fig. 3e, f). This explains why our screen did not reveal mutations in transcription termination factors.

In *ctf1-70* cells, although RNA Pol II fails to terminate, the nascent RNA is still properly processed and released from the site of transcription[21]. This probably accounts for the less stable silencing in *ctf1-70* cells and suggests that the more severe phenotype of Paf1C mutants is due to the combined effects of impaired termination and nascent transcript release. Therefore, we tested whether artificially releasing the nascent transcript from the site of transcription partially alleviates siRNA-mediated heterochromatin formation in Paf1C mutant cells. To this end, we inserted a 52-nucleotide hammerhead ribozyme (Rz), preceded by a templated polyA (A_{75}) tail, downstream of the *ade6+* open reading frame (*ade6-Rz*) to induce self-cleavage of nascent *ade6+* transcripts (Fig. 3g). Indeed, initiation of silencing at the *ade6-Rz* locus was inefficient and the repressed state was poorly propagated in *paf1-Q264Stop* mutant cells. By contrast, silencing was very effective in cells that contain a single base change in the catalytic site of the ribozyme (*ade6-Rzm*) that abolishes self-cleavage (Fig. 3h). Thus, retaining the nascent transcript on chromatin is critical to stabilize the repressed state.

These results are consistent with a kinetic model for Paf1C function and demonstrate that proper transcription termination is crucial to prevent *de novo* formation of heterochromatin by siRNAs (Extended Data Fig. 9). This is further supported by the recent observation that termination sequences in the 3′ untranslated region of the *ura4+* gene inhibit the ability of siRNAs to promote heterochromatin formation[17] and is reminiscent of enhanced silencing phenotype (*esp*) mutations in *Arabidopsis thaliana*, which are in genes that encode for members of the cleavage polyadenylation specificity factor and cleavage stimulation factor complexes[22]. Importantly, our results show that impairment of both transcription termination and nascent transcript release is imperative to confer stability to the repressed state, although compromised transcription termination is sufficient to initiate the formation of bi-stable heterochromatin by *trans*-acting siRNAs.

Besides Dcr1-dependent siRNAs, Ago1 associates with Dcr1-independent small RNAs referred to as primal RNAs (priRNAs). priRNAs seem to be degradation products of abundant transcripts and could potentially trigger siRNA amplification and uncontrolled heterochromatic gene silencing[23]. Therefore, we speculated that the physiological function of Paf1C is to protect the genome from spurious priRNA-mediated heterochromatin formation. To investigate this we analysed whether Paf1C mutants would disclose genomic regions that could be potentially assembled into facultative heterochromatin by endogenous small RNAs. On the basis of our results, loci at which facultative heterochromatin forms in an RNAi-dependent manner are expected to show reduced RNA expression with a concomitant increase in siRNA production. As expected, the *nmt1+::ade6-hp+*, *trp1+::ade6+* and *ade6-704* loci fulfilled this criteria (Extended Data Fig. 10a). Moreover, we observed repression and siRNA production for genes flanking these loci, indicating spreading of heterochromatin into neighbouring genes, which occurred up to 6 kilobases (kb) up or downstream of the ade6-hp siRNA target sites. Indeed, we observed H3K9 methylation in this region in *leo1Δ* cells specifically (Extended Data Fig. 10b, c). In addition to these regions, we observed siRNA-directed silencing signatures at different, non *ade6+*-linked genomic loci, indicating that Paf1C may indeed function to protect the genome from illegitimate repression of protein coding genes by endogenous priRNAs. However, we did not recover the same sites repeatedly in the different Paf1C mutants

(Supplementary Table 1). This indicates that initiation of silencing at these sites occurred stochastically and that there are no specific sites primed for the formation of facultative heterochromatin in mitotic cells that are grown under standard laboratory conditions. Therefore, we conclude that Paf1C protects protein-coding genes from unwanted long-term silencing that might occur by chance, thereby restraining phenotypic variation and conferring epigenetic robustness to the organism.

In summary, we discovered that synthetic siRNAs are highly effective in directing locus-independent assembly of heterochromatin that can be stably maintained through mitosis and meiosis only when Paf1C activity is impaired. A remarkable observation of our study is that the newly established heterochromatin was inherited for hundreds of cell divisions across generations in Paf1C mutant cells, even in the absence of the primary siRNAs that triggered the assembly of heterochromatin. This phenomenon complies with the classical definition of epigenetics[24] (that is, that it is heritable even in the absence of the initiating signal) and highlights fundamental roles of Paf1C and the RNAi machinery in building up epigenetic memory. This mechanism is also reminiscent of RNA-mediated epigenetic phenomena in higher eukaryotes such as paramutation[25] and RNA-induced epigenetic silencing (RNAe)[26]. RNAe is a phenomenon in which small RNAs of the *C. elegans* Piwi pathway can initiate transgene silencing that is extremely stable across generations even in the absence of the initiating Piwi protein. Yet, not all Piwi pathway RNAs trigger RNAe (ref. 27). Similarly, generation of siRNAs is necessary but not sufficient for paramutation in maize[28]. Thus, Paf1C may also have a regulatory role in paramutation and/or RNAe. Notably, Paf1C is known to help maintain expression of transcription factors required for pluripotency in human and mouse embryonic stem cells and prevent expression of genes involved in lineage specification[29,30], which may also involve small RNAs and chromatin regulation.

The ability to induce long-lasting and sequence specific gene silencing by transient delivery of synthetic siRNAs without changing the underlying DNA sequence will not only enable fundamental research on mechanisms that confer epigenetic memory, but may also open up new avenues in biotechnology and broaden the spectrum of the potential applications of RNAi-based therapeutics. Epigenetic control over gene expression is of particular interest in plant biotechnology, as this would circumvent the generation of genetically modified organisms.

Online Content Methods, along with any additional Extended Data display items and Source Data, are available in the online version of the paper; references unique to these sections appear only in the online paper.

Received 2 October 2014; accepted 16 February 2015.
Published online 25 March 2015.

1. Moazed, D. Small RNAs in transcriptional gene silencing and genome defence. *Nature* **457,** 413–420 (2009).
2. Volpe, T. A. *et al.* Regulation of heterochromatic silencing and histone H3 lysine-9 methylation by RNAi. *Science* **297,** 1833–1837 (2002).
3. Verdel, A. *et al.* RNAi-mediated targeting of heterochromatin by the RITS complex. *Science* **303,** 672–676 (2004).
4. Motamedi, M. R. *et al.* Two RNAi complexes, RITS and RDRC, physically interact and localize to noncoding centromeric RNAs. *Cell* **119,** 789–802 (2004).
5. Schalch, T. *et al.* High-affinity binding of Chp1 chromodomain to K9 methylated histone H3 is required to establish centromeric heterochromatin. *Mol. Cell* **34,** 36–46 (2009).
6. Castel, S. E. & Martienssen, R. A. RNA interference in the nucleus: roles for small RNAs in transcription, epigenetics and beyond. *Nature Rev. Genet.* **14,** 100–112 (2013).
7. Chan, S. W., Zhang, X., Bernatavichute, Y. V. & Jacobsen, S. E. Two-step recruitment of RNA-directed DNA methylation to tandem repeats. *PLoS Biol.* **4,** e363 (2006).
8. Mette, M. F., Aufsatz, W., van der Winden, J., Matzke, M. A. & Matzke, A. J. Transcriptional silencing and promoter methylation triggered by double-stranded RNA. *EMBO J.* **19,** 5194–5201 (2000).
9. Ting, A. H., Schuebel, K. E., Herman, J. G. & Baylin, S. B. Short double-stranded RNA induces transcriptional gene silencing in human cancer cells in the absence of DNA methylation. *Nature Genet.* **37,** 906–910 (2005).
10. Morris, K. V., Chan, S. W., Jacobsen, S. E. & Looney, D. J. Small interfering rna-induced transcriptional gene silencing in human cells. *Science* **305,** 1289–1292 (2004).
11. Kim, D. H., Villeneuve, L. M., Morris, K. V. & Rossi, J. J. Argonaute-1 directs siRNA-mediated transcriptional gene silencing in human cells. *Nature Struct. Mol. Biol.* **13,** 793–797 (2006).
12. Janowski, B. A. *et al.* Involvement of AGO1 and AGO2 in mammalian transcriptional silencing. *Nature Struct. Mol. Biol.* **13,** 787–792 (2006).
13. Napoli, S., Pastori, C., Magistri, M., Carbone, G. M. & Catapano, C. V. Promoter-specific transcriptional interference and c-myc gene silencing by siRNAs in human cells. *EMBO J.* **28,** 1708–1719 (2009).
14. Simmer, F. *et al.* Hairpin RNA induces secondary small interfering RNA synthesis and silencing in *trans* in fission yeast. *EMBO Rep.* **11,** 112–118 (2010).
15. Iida, T., Nakayama, J. & Moazed, D. siRNA-mediated heterochromatin establishment requires HP1 and is associated with antisense transcription. *Mol. Cell* **31,** 178–189 (2008).
16. Mbogning, J. *et al.* The PAF complex and Prf1/Rtf1 delineate distinct Cdk9-dependent pathways regulating transcription elongation in fission yeast. *PLoS Genet.* **9,** e1004029 (2013).
17. Yu, R., Jih, G., Iglesias, N. & Moazed, D. Determinants of heterochromatic siRNA biogenesis and function. *Mol. Cell* **53,** 262–276 (2014).
18. Bühler, M., Verdel, A. & Moazed, D. Tethering RITS to a nascent transcript initiates RNAi- and heterochromatin-dependent gene silencing. *Cell* **125,** 873–886 (2006).
19. Tomson, B. N. & Arndt, K. M. The many roles of the conserved eukaryotic Paf1 complex in regulating transcription, histone modifications, and disease states. *Biochim. Biophys. Acta* **1829,** 116–126 (2013).
20. Cheung, A. C. & Cramer, P. A movie of RNA polymerase II transcription. *Cell* **149,** 1431–1437 (2012).
21. Aranda, A. & Proudfoot, N. Transcriptional termination factors for RNA polymerase II in yeast. *Mol. Cell* **7,** 1003–1011 (2001).
22. Herr, A. J., Molnar, A., Jones, A. & Baulcombe, D. C. Defective RNA processing enhances RNA silencing and influences flowering of *Arabidopsis*. *Proc. Natl Acad. Sci. USA* **103,** 14994–15001 (2006).
23. Halic, M. & Moazed, D. Dicer-independent primal RNAs trigger RNAi and heterochromatin formation. *Cell* **140,** 504–516 (2010).
24. Ptashne, M. On the use of the word 'epigenetic'. *Curr. Biol.* **17,** R233–R236 (2007).
25. Chandler, V. L. Paramutation: from maize to mice. *Cell* **128,** 641–645 (2007).
26. Luteijn, M. J. & Ketting, R. F. PIWI-interacting RNAs: from generation to transgenerational epigenetics. *Nature Rev. Genet.* **14,** 523–534 (2013).
27. Luteijn, M. J. *et al.* Extremely stable Piwi-induced gene silencing in *Caenorhabditis elegans*. *EMBO J.* **31,** 3422–3430 (2012).
28. Chandler, V. L. Paramutation's properties and puzzles. *Science* **330,** 628–629 (2010).
29. Ding, L. *et al.* A genome-scale RNAi screen for Oct4 modulators defines a role of the Paf1 complex for embryonic stem cell identity. *Cell Stem Cell* **4,** 403–415 (2009).
30. Ponnusamy, M. P. *et al.* RNA polymerase II associated factor 1/PD2 maintains self-renewal by its interaction with Oct3/4 in mouse embryonic stem cells. *Stem Cells* **27,** 3001–3011 (2009).

Supplementary Information is available in the online version of the paper.

Acknowledgements We thank T. Iida for providing the plasmid encoding the ade6-hp construct, N. Laschet and R. Tsuji for technical assistance, S. Thiry for hybridizing tiling arrays, K. Jacobeit and S. Dessus-Babus for small RNA sequencing, T. Roloff for archiving data sets, M. Kirschmann for developing the Matlab script for colony counting, and A. Tuck for comments on the manuscript. This work was supported by funds from the Swiss National Science Foundation, the European Research Council, and the Boehringer Ingelheim Fonds. The Friedrich Miescher Institute for Biomedical Research is supported by the Novartis Research Foundation.

Author Contributions Y.S., K.M.K., V.F. and J.B. generated strains and performed experiments; Y.S. performed the sms screen; the genome-wide small RNA and gene expression data were analysed by K.M.K.; M.B.S. designed and performed the computational analysis of the mutant genome resequencing data; M.B. designed experiments and prepared the manuscript. All authors discussed the results and commented on the manuscript.

Author Information Genome-wide data sets are deposited at GEO under the accession number GSE59171. Reprints and permissions information is available at www.nature.com/reprints. The authors declare competing financial interests: details are available in the online version of the paper. Readers are welcome to comment on the online version of the paper. Correspondence and requests for materials should be addressed to M.B. (marc.buehler@fmi.ch).

METHODS

Strains and plasmids. Fission yeast strains were grown at 30 °C in YES medium. All strains were constructed following a PCR-based protocol[31] or by standard mating and sporulation. Plasmids and strains generated in this study are shown in Supplementary Tables 2 and 3.

EMS mutagenesis, hit selection and backcrossing. Exponentially growing *sms0* (SPB464) cells were washed and resuspended in 50 mM K-phosphate buffer (pH 7.0) and treated with EMS (final concentration 2.5%) for 150 min. An equal volume of freshly prepared 10% sodium thiosulfate was then added. Cells were washed with water and subsequently resuspended in YES. EMS treatment resulted in ~50% cell viability. To screen for mutants in which *ade6+* expression was silenced, cells were spread on YE plates. About 350,000 colonies were examined and pink colonies were selected for further evaluation. Positive hits were backcrossed four times with the parental strains SPB464 or SPB1788, depending on mating type.

Silencing assays. To assess *ura4+* expression, serial tenfold dilutions of the respective strains were plated on PMGc (non-selective, NS) or on PMGc plates containing 2 mg ml^{-1} 5-FOA. To assess *ade6+* expression, serial tenfold dilutions of the respective strains were plated on YES and YE plates.

Assessment of initiation versus maintenance of ectopic heterochromatin formation. Mutant strains were seeded on YE plates and single-cell-derived red or white colonies were selected. Colonies were resuspended in water and 100–500 cells were seeded on YE plates, which were then incubated at 30 °C for 3 days. Images of the plates were acquired after one night at 4 °C and colonies were counted automatically using Matlab (The MathWorks) and ImageJ Software (National Institutes of Health).

RNA isolation and cDNA synthesis. RNA isolation and cDNA synthesis was performed as described previously[32].

Quantitative real-time PCR. Real-time PCR on cDNA samples and ChIP DNA was performed as described[33] using a Bio-Rad CFX96 Real-Time System using SsoAdvanced SYBR Green supermix (Bio-Rad). Primer sequences are given in Supplementary Table 4.

Chromatin immunoprecipitation. Chromatin immunoprecipitation (ChIP) experiments were performed as previously described[33] with minor modifications. In brief, *S. pombe* cells were fixed with 1% formaldehyde for 15 min and then lysed in buffer containing 50 mM HEPES/KOH, pH 7.5, 140 mM NaCl, 1 mM EDTA, 1% Triton X-100, 0.1% sodium deoxycholate, 1 mM phenylmethylsulfonyl fluoride (PMSF) and protease inhibitor cocktail. Chromatin was sheared with a Bioruptor (Diagenode). The following antibodies were used in this study: histone H3K9me2-specific mouse monoclonal antibody from Wako (MABI0307), histone H3-specific rabbit polyclonal antibody from Abcam (ab1791), histone H3K36me3-specific rabbit polyclonal antibody from Abcam (ab9050), and RNA polymerase II mouse monoclonal antibody from Covance (8WG16).

Small RNA sequencing. Total RNA was isolated from exponentially growing cells using the hot phenol method[34]. The RNA was fractionated using RNeasy Midi columns (Qiagen) following the RNA cleanup protocol provided by the manufacturer. The flow-through fraction was precipitated ('small RNA' fraction). Aliquots (25 μg) of the small RNA fraction were separated by 17.5% PAGE and the 18–28-nucleotide population purified. Libraries were prepared using the Illumina TruSeqTM small RNA preparation protocol (RS-930-1012). The 145–160-nucleotide population was isolated and the library sequenced on an Illumina HiSeq2000. Small RNA reads were aligned as described previously[32] with two mismatches allowed.

Whole-genome sequencing. Cells from an overnight culture were collected, washed once with water and flash frozen in liquid nitrogen. Cells were spheroplasted in spheroplast buffer (1.2 M sorbitol, 100 mM $KHPO_4$, pH 7.5, 0.5 mg ml^{-1} zymolyase (Zymo Research), 1 mg ml^{-1} lysing enzyme from *Trichoderma harzianum* (Sigma)). Genomic DNA was isolated using the DNeasy Blood and Tissue Kit (Qiagen). Barcoded genomic DNA libraries for Illumina next-generation sequencing were prepared from 50 ng genomic DNA using the Nextera DNA Sample Preparation Kit (Illumina). Libraries were pooled equimolarly and sequenced on one lane of a HiSeq2000 machine (Illumina). Basecalling was done with RTA 1.13.48 (Illumina) software and for the demultiplexing CASAVA_v1.8.0 (Illumina) was used. For each strain, between 8.7 and 25.5 million (mean of 14.2 million) 50-nucleotide reads were generated and aligned to the *Schizosaccharomyces pombe* 972h- genome assembly (obtained on 17 September 2008 from http://www.broad.mit.edu/annotation/genome/schizosaccharomyces_group/MultiDownloads.html) using 'bwa' (ref. 35, version 0.7.4) with default parameters, but only retaining single-hit alignments ('bwa samse -n 1' and selecting alignments with 'X0:i:1'), resulting in a genome coverage between 26 and 85-fold (mean of 44-fold). The alignments were converted to BAM format, sorted and indexed using 'samtools' (ref. 36, version 0.1.19). Potential PCR duplicates were removed using 'MarkDuplicates' from 'Picards' (http://picard.sourceforge.net/, version 1.92). Sequence variants were identified using GATK (ref. 37, version 2.5.2) indel realignment and base quality score recalibration using a set of high confidence variants identified in an initial step as known variants, followed by single nucleotide polymorphism (SNP) and INDEL discovery and genotyping for each individual strain using standard hard filtering parameters, resulting in a total of 270–274 sequence variations (mean of 280) in each strain compared to the reference genome (406 unique variations in total over all strains). Finally, variations were filtered to retain only high quality single nucleotide variations (QUAL $\geq$ 50) of EMS type (G|C to A|T) with an alellic balance $\geq$ 0.9 (homozygous) that were not also identified in the parental strain (sms0), reducing the number of variations per strain to a number between 2 and 8 (mean of 4.6).

Expression profiling. RNA was isolated from cells collected at an attenuance (*D*) of 600 nm of 0.5 ($D_{600\,nm} = 0.5$) using the hot phenol method[34]. The isolated RNA was processed according to the GeneChip Whole Transcript Double-Stranded Target Assay Manual from Affymetrix using the GeneChip *S. pombe* Tiling 1.0FR. All tiling arrays were processed in R[38] using bioconductor[39] and the packages tilingArray[40] and preprocessCore. The arrays were RMA background-corrected, quantile-normalized, and $\log_2$-transformed on the oligonucleotide level using the following command: expr <−log$_2$(normalize.quantiles(rma.background.correct(exprs(readCel2eSet (filenames,rotated = TRUE))))). Oligonucleotide coordinates were intersected with the genome annotation and used to calculate average expression levels for individual genomic features (excluding those with <10 oligonucleotides) as well as broader annotation categories. In the latter case, multimapping oligonucleotides were counted only once per category (avoiding multiple counts from the same oligonucleotide).

Gene nomenclature. The proteins PAF1p, CDC73p, RTF1p, LEO1p and CTR9p form a stable complex in *S. cerevisiae* (Paf1C). The systematic IDs of the genes encoding the *S. pombe* homologues of these proteins are SPAC664.03, SPBC17G9.02c, SPBC651.09c, SPBC13E7.08c and SPAC27D7.14c, respectively. The *CTR9* homologue SPAC27D7.14c is currently annotated as Tpr1. The RTF1 homologue SPBC651.09c is currently annotated as PAF-related factor 1 (*prf1+*), because *rtf1+* is already used for an unrelated gene (SPAC22F8.07c). Therefore, we refer to SPAC664.03, SPBC17G9.02c, SPBC651.09c, SPBC13E7.08c and SPAC27D7.14c as *paf1+*, *cdc73+*, *prf1+*, *leo1+* and *tpr1+*, respectively, in this paper.

Statistics. A one-tailed Student's *t*-test was used, with $P < 0.05$ as the significance level. No statistical methods were used to predetermine sample size.

31. Bähler, J. *et al.* Heterologous modules for efficient and versatile PCR-based gene targeting in *Schizosaccharomyces pombe*. *Yeast* **14,** 943–951 (1998).
32. Emmerth, S. *et al.* Nuclear retention of fission yeast dicer is a prerequisite for RNAi-mediated heterochromatin assembly. *Dev. Cell* **18,** 102–113 (2010).
33. Keller, C. *et al.* HP1(Swi6) mediates the recognition and destruction of heterochromatic RNA transcripts. *Mol. Cell* **47,** 215–227 (2012).
34. Leeds, P., Peltz, S. W., Jacobson, A. & Culbertson, M. R. The product of the yeast UPF1 gene is required for rapid turnover of mRNAs containing a premature translational termination codon. *Genes Dev.* **5,** 2303–2314 (1991).
35. Li, H. & Durbin, R. Fast and accurate short read alignment with Burrows–Wheeler transform. *Bioinformatics* **25,** 1754–1760 (2009).
36. Li, H. *et al.* The sequence alignment/map format and SAMtools. *Bioinformatics* **25,** 2078–2079 (2009).
37. DePristo, M. A. *et al.* A framework for variation discovery and genotyping using next-generation DNA sequencing data. *Nature Genet.* **43,** 491–498 (2011).
38. Ihaka, R. & Gentleman, R. R: a language for data analysis and graphics. *J. Comput. Graph. Stat.* **5,** 299–314 (1996).
39. Gentleman, R. C. *et al.* Bioconductor: open software development for computational biology and bioinformatics. *Genome Biol.* **5,** R80 (2004).
40. Huber, W., Toedling, J. & Steinmetz, L. M. Transcript mapping with high-density oligonucleotide tiling arrays. *Bioinformatics* **22,** 1963–1970 (2006).
41. Bühler, M., Haas, W., Gygi, S. P. & Moazed, D. RNAi-dependent and -independent RNA turnover mechanisms contribute to heterochromatic gene silencing. *Cell* **129,** 707–721 (2007).

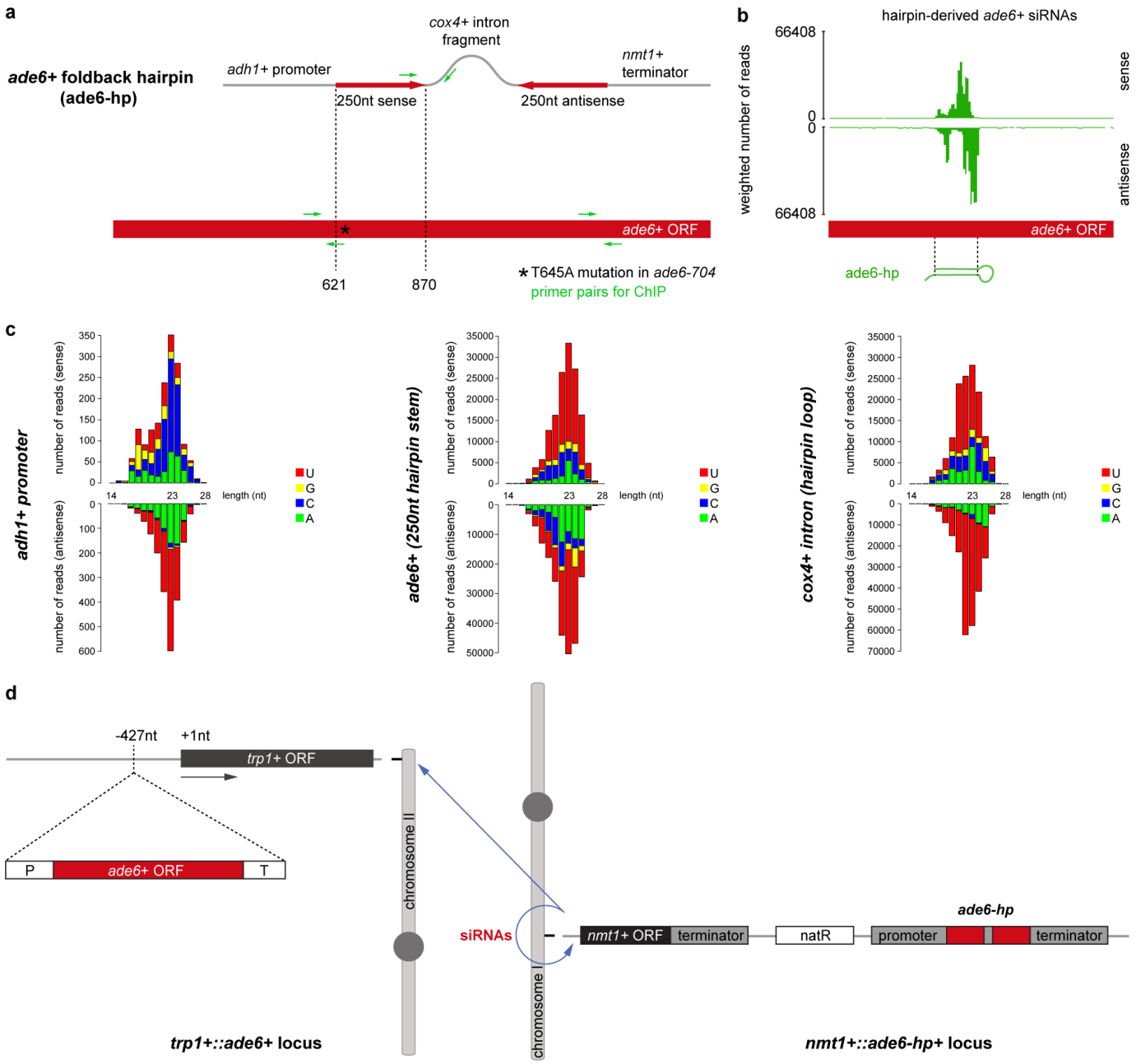

Extended Data Figure 1 | Design of the *ade6+* RNA hairpin (ade6-hp) construct that expresses abundant sense and antisense (primary) siRNAs. **a**, The RNA stem–loop construct consists of a 250-nucleotide-long *ade6+* fragment, followed by a *cox4+* intronic sequence and the reverse complement of the *ade6+* fragment. The promoter sequence of the *adh1+* gene drives expression of the RNA hairpin. Transcription of the construct is terminated by the termination signals of the *nmt1+* gene. The construct was provided by T. Iida. **b**, **c**, Small RNA sequencing revealed that the RNA stem is converted into sense and antisense siRNAs covering the 250-nucleotide stretch from the *ade6+* open reading frame (nucleotides 621–870). Furthermore, sense and antisense siRNAs mapping to the *cox4+* intronic and *adh1+* promoter sequences are also generated when this construct is expressed in wild-type cells. ORF, open reading frame. Asterisk denotes the point mutation (Thr645Ala) in the *ade6-704* loss of function allele. Green arrows indicate forward and reverse primers that were used for PCR in ChIP experiments. **d**, Schematic diagram depicting origin and target(s) of synthetic ade6-hp siRNAs. The ade6-hp expression cassette (**a**) was inserted into the *nmt1+* locus on chromosome I by homologous recombination. The ade6-hp-containing plasmid was linearized with *PmlI*, which cuts in the middle of the *nmt1+* terminator sequence, and transformed into *ade6-704* cells. Thereby, the ade6-hp construct was inserted downstream of the *nmt1+* gene. The nourseothricin (Nat)-resistance cassette linked to the ade6-hp construct allowed selection of positive transformants. It also allows assessment of spreading of repressive heterochromatin that is nucleated by the ade6-hp siRNAs *in cis* (see Extended Data Fig. 7b). A wild-type copy of the *ade6+* gene was inserted upstream of the *trp1+* gene on chromosome II by homologous recombination. Because the endogenous *ade6-704* allele is non-functional, positive transformants could be selected by growth in the absence of adenine. In Paf1C mutant cells, ade6-hp-derived siRNAs either act *in cis* to assemble heterochromatin at the *nmt1+* locus (chromosome I), or *in trans* to direct the formation of heterochromatin at the *trp1+::ade6+* (chromosome II) and *ade6-704* (chromosome III) loci.

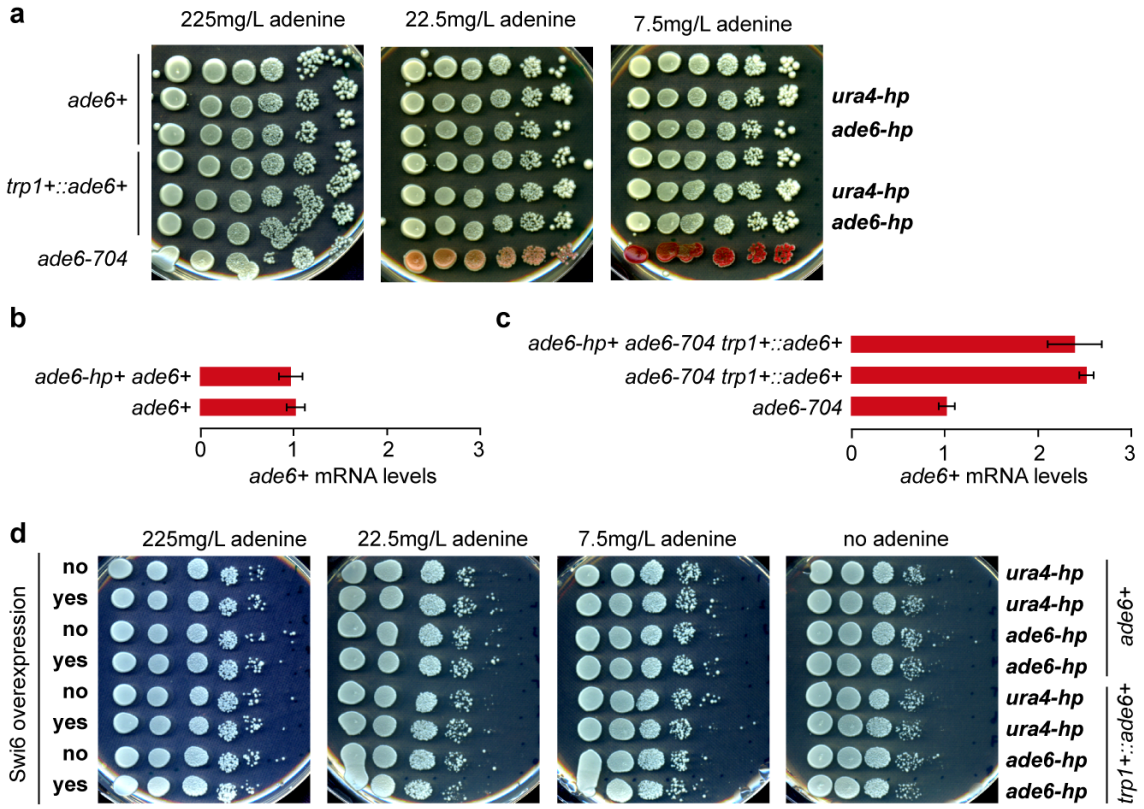

Extended Data Figure 2 | Silencing assays demonstrating the inability of synthetic siRNAs to act *in trans* in Paf1C wild-type cells. **a**, *ade6+* silencing assays were performed with cells expressing synthetic ade6-hp siRNAs, ura4-hp siRNAs or no siRNAs. The ability of ade6-hp siRNAs to silence either the endogenous *ade6+* gene or the *trp1+::ade6+* reporter gene was assessed at different adenine concentrations. *ade6-704* cells were used as positive control. **b**, **c**, *ade6+* mRNA levels were determined by quantitative RT–PCR and normalized to *act1+* mRNA. One representative biological replicate is shown. Error bars, s.d. **d**, *ade6+* silencing assays demonstrating that neither the endogenous *ade6+* gene nor the *trp1+::ade6+* reporter gene becomes repressed by *trans-acting* ade6-hp siRNAs, even upon overexpression of the heterochromatin protein Swi6.

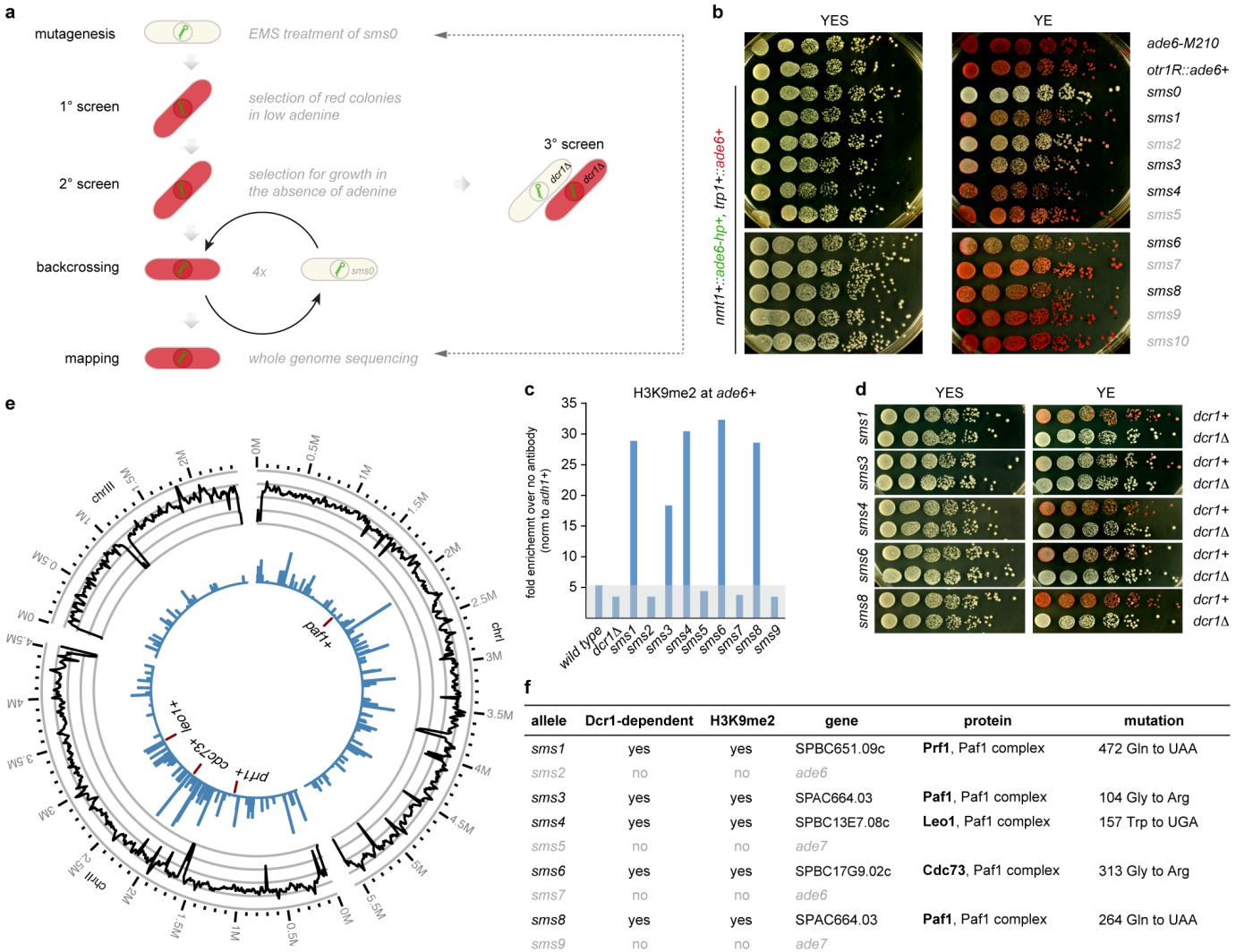

f

allele	Dcr1-dependent	H3K9me2	gene	protein	mutation
sms1	yes	yes	SPBC651.09c	**Prf1**, Paf1 complex	472 Gln to UAA
sms2	no	no	*ade6*		
sms3	yes	yes	SPAC664.03	**Paf1**, Paf1 complex	104 Gly to Arg
sms4	yes	yes	SPBC13E7.08c	**Leo1**, Paf1 complex	157 Trp to UGA
sms5	no	no	*ade7*		
sms6	yes	yes	SPBC17G9.02c	**Cdc73**, Paf1 complex	313 Gly to Arg
sms7	no	no	*ade6*		
sms8	yes	yes	SPAC664.03	**Paf1**, Paf1 complex	264 Gln to UAA
sms9	no	no	*ade7*		

Extended Data Figure 3 | Sms forward genetic screen identifies five true positive hits that enable siRNAs to methylate H3K9 at the *ade6+* gene *in trans*. **a**, Workflow of the EMS mutagenesis screen. We mutagenized sms0 cells, which express abundant siRNAs complementary to the *ade6+* gene (indicated by green hairpin), with EMS (primary screen). Subsequently, we tested the positive red colonies for growth in the absence of adenine to select against loss-of-function mutations in the adenine biosynthesis pathway (secondary screen). In hits that remained positive after the secondary screen, *dcr1+* was deleted to identify truly siRNA-dependent hits (tertiary screen). For mapping of causative mutations by whole-genome next-generation sequencing, positive hits were backcrossed four times. **b**, *sms1-10* mutants show the red *ade6+* silencing phenotype on YE plates, which segregated through four successive backcrosses for all 10 mutants. The *ade6-M210* loss-of-function allele and *ade6+* inserted within centromeric heterochromatin (*otr1R::ade6+*) serve as positive controls. **c**, ChIP experiment demonstrating methylation of H3K9 at the *ade6+* target loci in *sms1*, *3*, *4*, *6* and *8*. One representative biological replicate is shown. **d**, *ade6+* silencing in *sms1*, *3*, *4*, *6* and *8* is Dcr1-dependent. **e**, Resequencing of EMS-mutagenized *S. pombe* strains. From outside to inside, the tracks show the genomic location, the average coverage per window of 10 kb (black line, scale from 0 to 30), the number of sequence variations identified before filtering in all strains per window of 10 kb (blue bars, scale from 0 to 90) and the five mutations that passed the filtering and overlapped with Paf1C genes (red lines, the two mutations in Paf1 are too close to be resolved individually). **f**, Table lists mutations mapped by whole-genome sequencing. In Dcr1-dependent mutants, we mapped mutations in the genes SPBC651.09c, SPAC664.03, SPBC13E7.08c and SPBC17G9.02c whose homologues in budding yeast encode for protein subunits of the Paf1 complex.

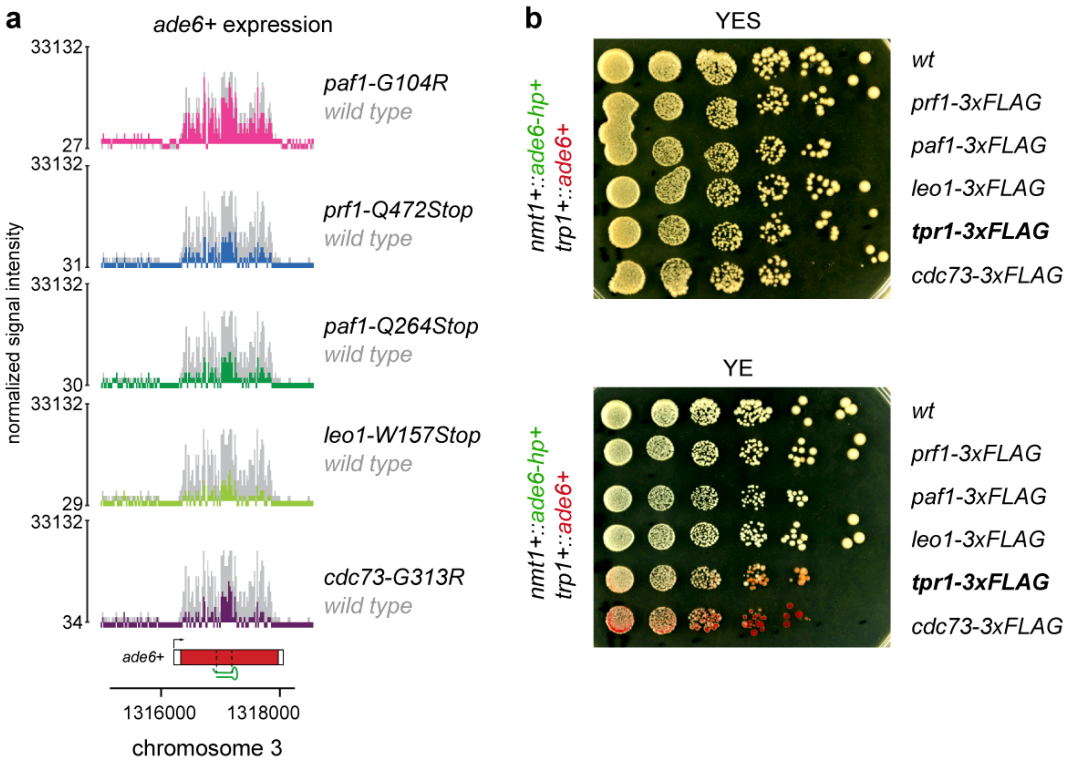

Extended Data Figure 4 | Mutant alleles for the homologues of all five subunits of Paf1C enable siRNAs to induce gene silencing *in trans*. **a**, *ade6+* siRNAs reduce *ade6+* mRNA levels in all Paf1C mutant strains identified in this study. Whole-genome tiling arrays were used to assess gene expression in the mutant cells indicated. *y* axis is in linear scale. **b**, C-terminally tagged Tpr1 and Cdc73 are hypomorphic. Full deletions of the *tpr1+* and *cdc73+* genes cause retarded growth phenotypes (Extended Data Fig. 8c). By contrast, *tpr1-3xFLAG* and *cdc73-3xFLAG* grow normally, and display ade6-hp siRNA-mediated repression of the *ade6+* gene.

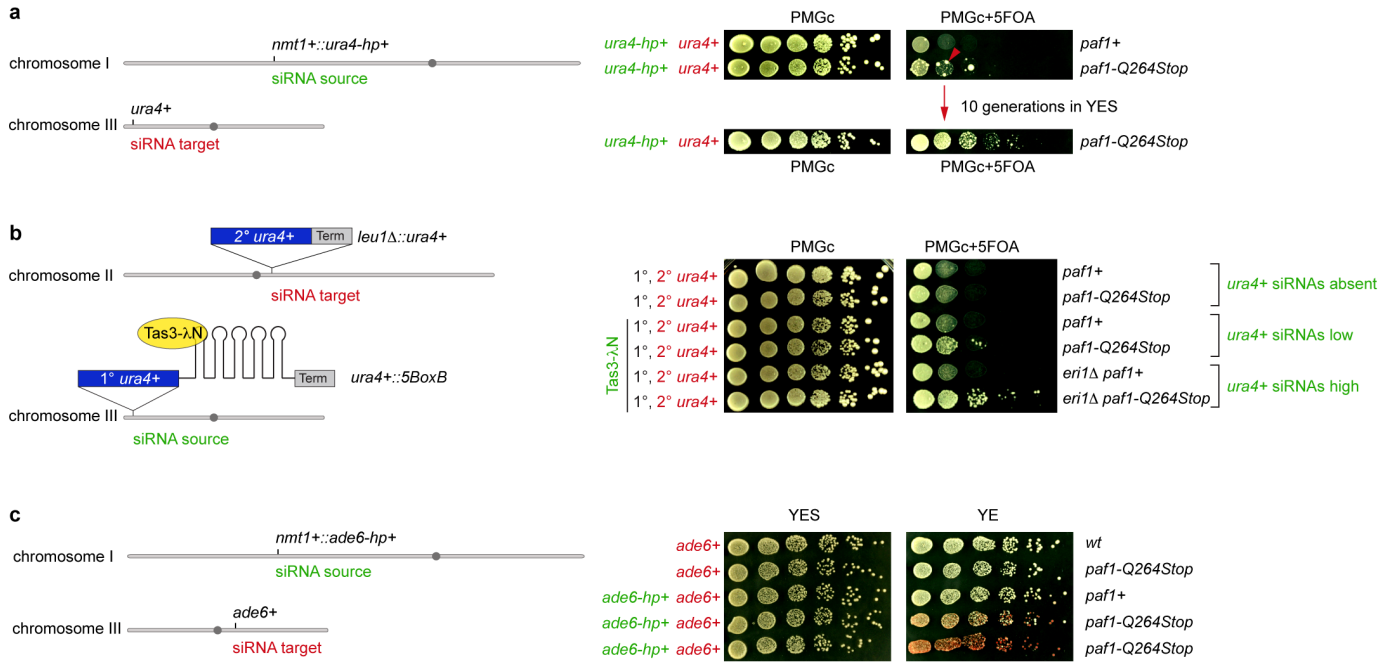

Extended Data Figure 5 | Expression of synthetic siRNAs in *paf1-Q264Stop* cells is sufficient to trigger stable repression of protein coding genes *in trans*. **a**, Left, the *paf1-Q264Stop* mutation was introduced into cells that express synthetic ura4-hp siRNAs[15]. Right, wild-type (*paf1+*) and *paf1-Q264Stop* were grown in the presence or absence of 5-FOA. Red arrow indicates *paf1-Q264Stop* colonies growing on FOA-containing medium. Note that these colonies could be propagated in non-selective medium without losing the repressed state. **b**, In *S. pombe*, artificial tethering of the RITS complex to mRNA expressed from the endogenous *ura4+* locus using the phage λN protein results in *de novo* generation of *ura4+* siRNAs. These siRNAs load onto RITS and are necessary to establish heterochromatin at the *ura4+* locus *in cis*. However, like ura4-hp siRNAs, they are incapable of triggering the repression of a second *ura4+* locus *in trans*[18]. To test whether *ura4+* siRNAs produced as a result of Tas3λN tethering to *ura4+::5BoxB* mRNA (chromosome III) can act *in trans* to silence a second *ura4+* allele (*leu1Δ::ura4+*, chromosome II), *paf1+* was mutated and *ura4+* repression was assessed by FOA silencing assays. Whereas 5-FOA was toxic to both *paf1+* and *paf1-Q264Stop* cells in the absence of *ura4+* siRNAs (Tas3 not fused to λN), FOA-resistant colonies appeared upon Tas3-λN tethering, demonstrating that siRNAs generated from the *ura4+::5BoxB* locus can initiate repression of the second *ura4+* copy expressed from the *leu1+* locus. Notably, siRNA-mediated *ura4+* repression *in trans* was more pronounced in the absence of the RNase Eri1. We have previously shown that the levels of *ura4+::5BoxB*-derived siRNA are higher in *eri1Δ* cells[41]. We note that *trans*-silencing of the second *ura4+* allele occasionally occurs in *paf1+* cells in the absence of Eri1 (ref. 18). However, in contrast to *paf1-Q264Stop* cells, the repressed state of *ura4+* is not stably propagated. Hairpin symbols downstream of the *ura4+* ORF denote BoxB sequences. They form stem–loop structures when transcribed and are bound by the λN protein. **c**, *ade6+* silencing assay demonstrating that also the endogenous *ade6+* gene is repressed if ade6-hp siRNAs are expressed from the *nmt1+* locus in *paf1-Q264Stop* cells. Silencing assay was performed with two freshly generated (naive) *paf1-Q264Stop* mutant strains. A few white colonies in which heterochromatin has not yet formed are discernable. Such white colonies were picked to determine heterochromatin initiation frequencies shown in Fig. 2.

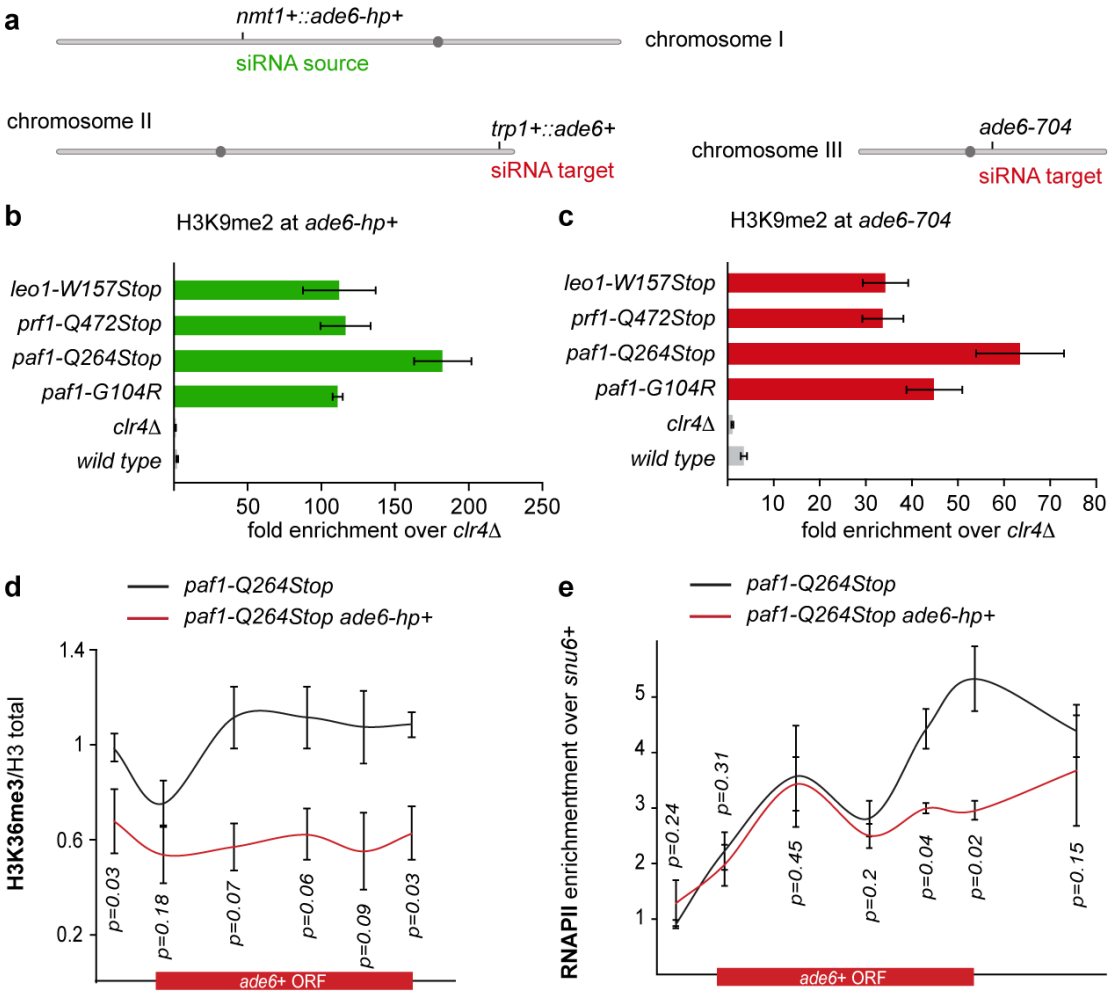

Extended Data Figure 6 | *ade6+* siRNAs trigger *de novo* methylation of H3K9 at homologous *ade6+* sequences *in cis* and *in trans*. **a**, ade6-hp RNA producing locus and siRNA target loci *in trans* in the sms0 strain. *ade6-704* is a loss-of-function allele of the endogenous *ade6+* gene and serves as a positive control in the silencing assays. **b**, **c**, *ade6+* siRNAs direct the methylation of H3K9 at *ade6* targets *in cis* (green) and *in trans* (red) in Paf1C mutant cells. H3K9me2 for *trp1+::ade6+* is shown in Fig. 1d. Quantitative PCR was performed with locus-specific primers. Error bars, s.e.m.; $n = 3$ technical replicates. **d**, **e**, ChIP experiments to assess *ade6+* transcriptional activity. H3K36me3 levels were normalized to total H3 levels. *snu6+* is transcribed by RNAPIII and serves as background control. Error bars, s.e.m.; $n = 3$ independent biological replicates; *P* values were calculated using the one-tailed Student's *t*-test.

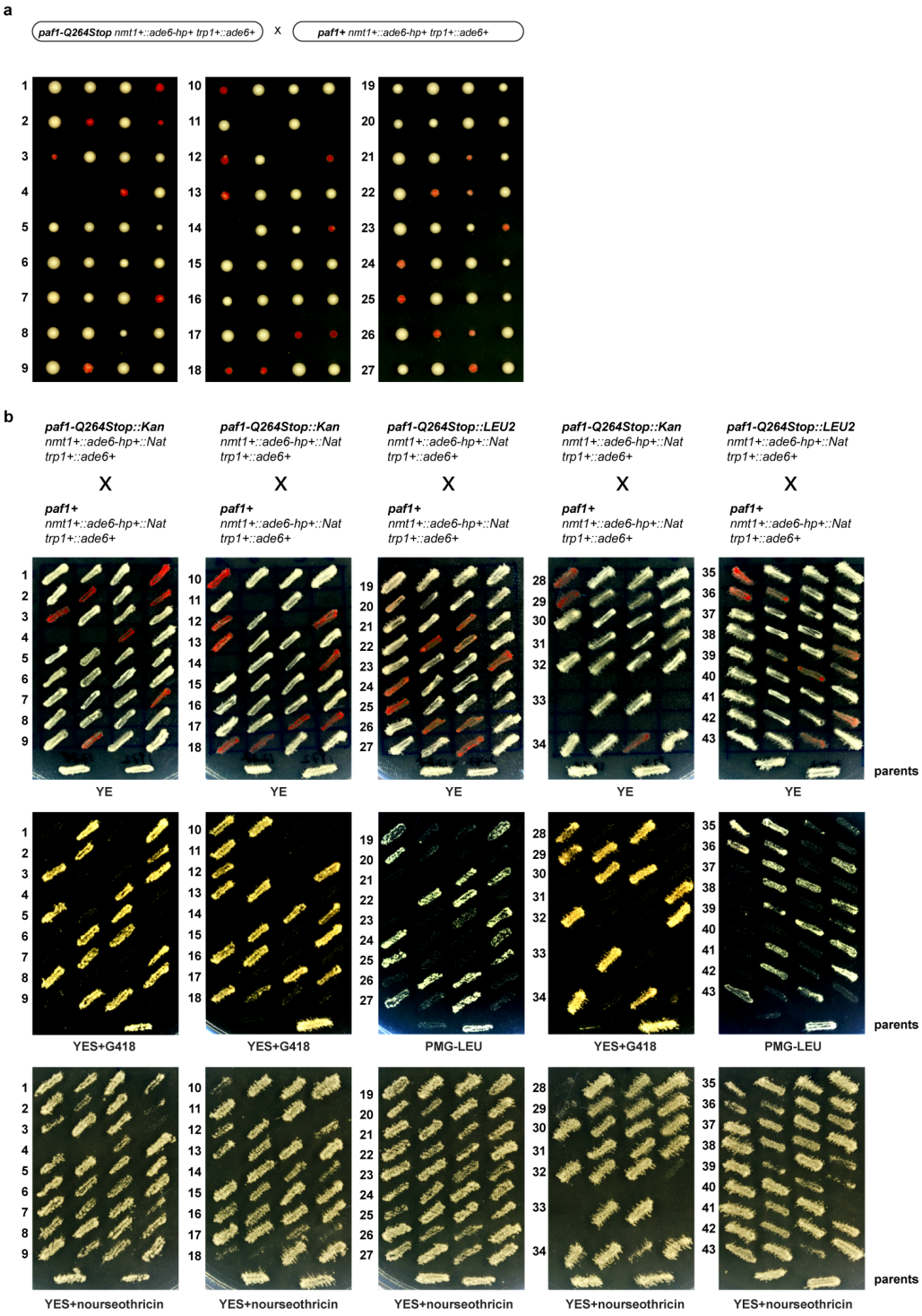

Extended Data Figure 7 | Pronounced siRNA-directed heterochromatin formation *in trans* during meiosis. **a**, White (naive) cells that had not yet established heterochromatin at the *trp1+::ade6+* locus were isolated from populations of freshly generated *paf1-Q264Stop* strains and crossed with *paf1+* cells. Both mating partners expressed ade6-hp siRNAs and contained the same *trp1+::ade6+* reporter. Spores were dissected on YE plates and incubated for 3–4 days at 30 °C. Note the non-Mendelian inheritance pattern of the parental white phenotype and the high incidence of heterochromatin formation (red phenotype) in *paf1-Q264Stop* cells after meiosis. **b**, Spores from 43 tetrads were dissected in total. Colonies formed by the individual spores (**a**) were then struck on YE plates and incubated for 3–4 days at 30 °C, followed by replica-plating onto YES-G418 and YES+nourseothricin (Nat) plates for genotyping. Thus, the cells visible on the YE plates have gone through roughly 50–80 mitotic divisions after mating and sporulation. This analysis shows that *de novo* formation of heterochromatin by *trans*-acting siRNAs during meiosis occurs more frequently than in mitosis. However, once established, heterochromatin is remarkably stable in mitotic cells (see also Fig. 2). Notably, growth of some *paf1-Q264Stop* descendants was reduced on YES+Nat plates, demonstrating spreading of heterochromatin into the neighbouring Nat-resistance cassette that marks the *nmt1+::ade6-hp+* locus (see Extended Data Fig. 1). Note that genes repressed by heterochromatin can be derepressed under strong negative selection. Thus, this observation indicates extraordinary repressive activity of the heterochromatin that forms *in cis* at the ade6-hp siRNA-producing locus. Finally, *paf1+* cells (no growth on YES-G418 or PMG-LEU) never turned red, demonstrating the high repressive activity of Paf1. This explains unsatisfactory results of previous attempts to induce the formation of stable heterochromatin *in trans* by expressing synthetic siRNAs.

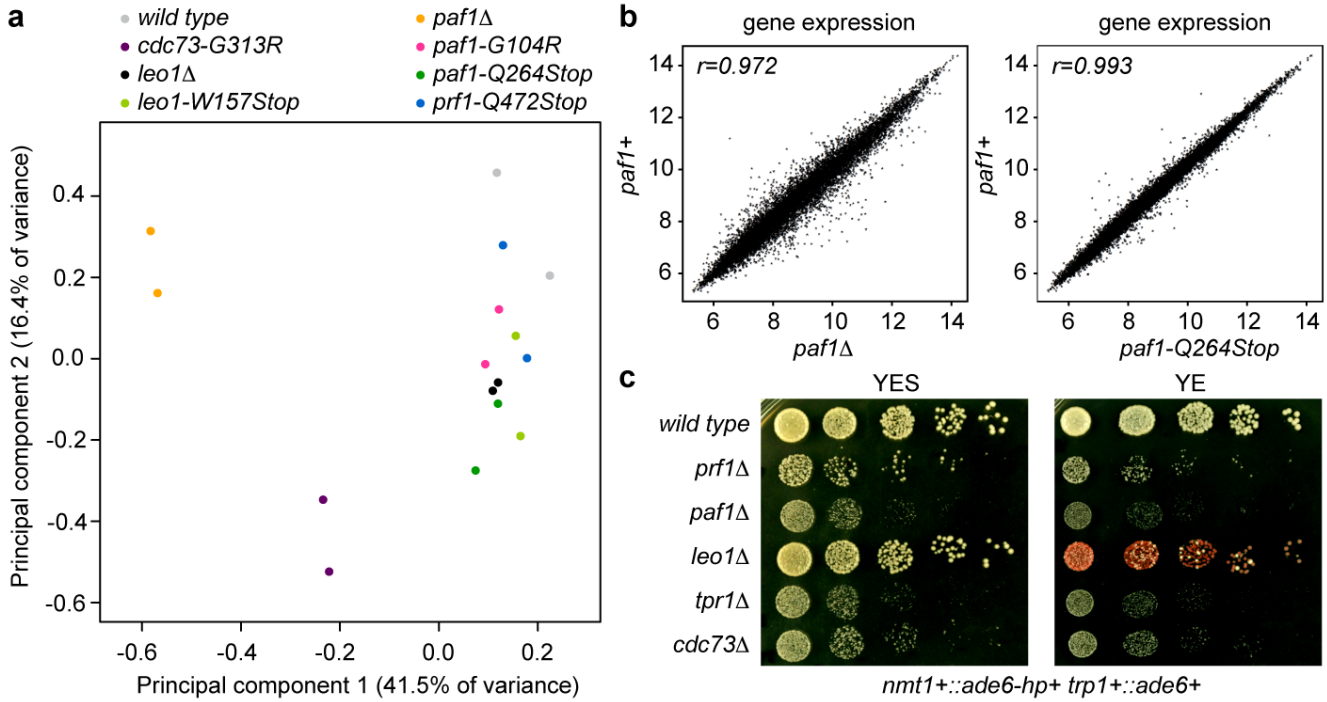

Extended Data Figure 8 | Effect of Paf1C mutations on global gene expression and silencing. **a**, The effect of the Paf1C mutations on genome expression was assessed by hybridizing total RNA to whole-genome tiling arrays. The parental wild-type strain, all Paf1C point mutations discovered in the screen, and full deletions of the *paf1+* and *leo1+* genes were included in the analysis. To compare the genome-wide expression profiles of the mutants with the wild-type strain, a principal component analysis (PCA) was performed on the data obtained for two biological replicates of each strain. Principal component (PC) 1 and 2 explained 41.5% and 16.4% of the variance between samples and were selected for visualization, revealing that *cdc73-G313R* and *paf1Δ* cells are most different from wild-type cells. All the other mutants clustered together in a group of samples that also includes wild type, demonstrating that RNA steady-state levels are only minimally affected in these mutants. Note that *leo1Δ* is more similar to wild type than *paf1Δ*, as well as that *paf1Δ* clusters separately from the Paf1C point mutants. **b**, Pairwise comparisons of gene expression between wild-type and *paf1* mutant strains. **c**, *leo1Δ* cells have no growth defect but are susceptible for *de novo* formation of heterochromatin by siRNAs acting *in trans*. These results suggest that Leo1 might be a bona fide repressor of small-RNA-mediated heterochromatin formation.

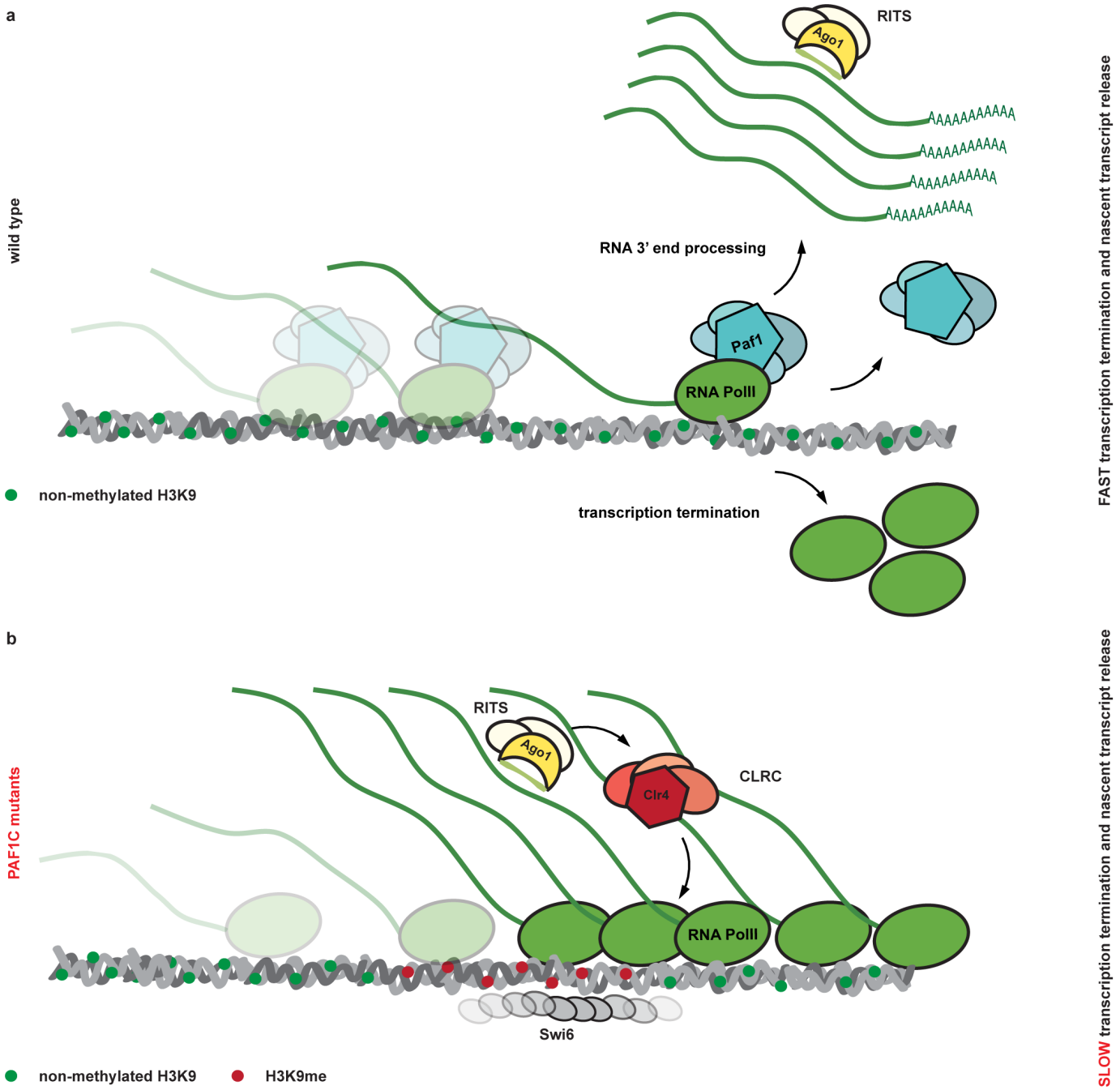

Extended Data Figure 9 | Kinetic model for Paf1C-mediated repression of siRNA-directed heterochromatin formation. **a**, Paf1C facilitates rapid transcription and release of the nascent transcript from the DNA template. Because the kinetics of transcription termination and RNA 3′ end processing is faster than RITS binding and CLRC recruitment, stable heterochromatin and long-lasting gene silencing cannot be established. **b**, In Paf1C mutant cells identified in this study, elongation of RNA polymerase II, termination of transcription, and the release of the nascent transcript from the site of transcription is decelerated. This results in an accumulation of RNA polymerases that are associated with nascent transcripts, opening up a window of opportunity for the siRNA-guided RITS complex to base-pair with nascent transcripts and recruit CLRC. Consequently, highly stable and repressive heterochromatin is assembled, which is accompanied by the generation of secondary siRNAs covering the entire locus (not depicted in this scheme). Notably, our results demonstrate that impaired transcription termination but not elongation is sufficient to allow silencing. However, to confer robustness to the repressed state, both transcription termination and release of the RNA transcript from the site of transcription must be impaired concomitantly.

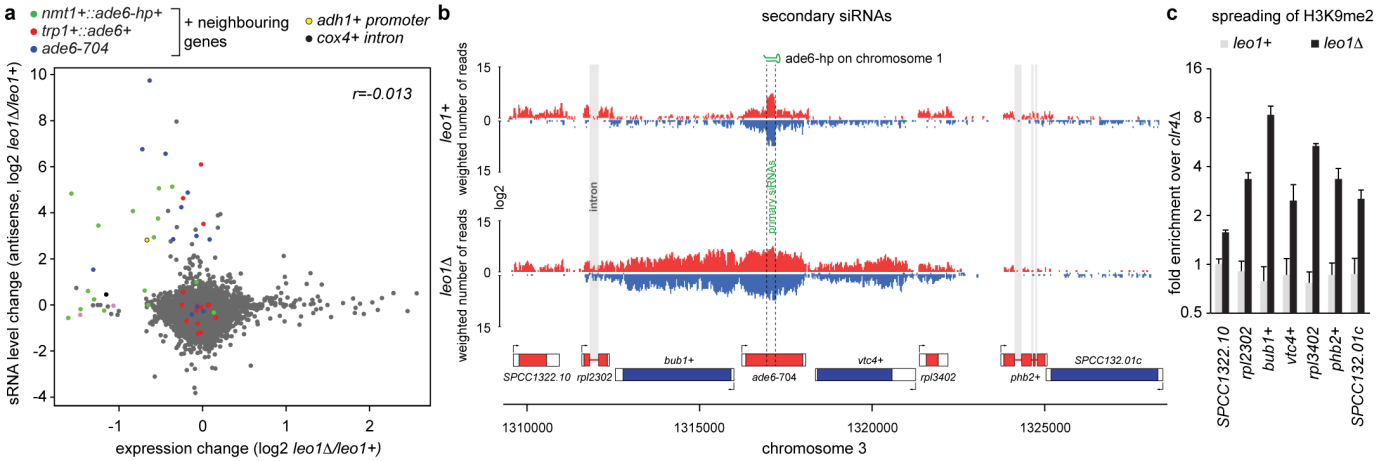

Extended Data Figure 10 | Formation of ectopic heterochromatin. **a**, Differential gene expression compared to differential antisense siRNA expression in *leo1*Δ. Gene expression profiles were obtained with whole-genome tiling arrays and small RNA profiles by deep sequencing. Genes neighbouring the *nmt1+::ade6-hp+*, *trp1+::ade6+* and *ade6-704* loci are marked in colour (see also Supplementary Table 1). **b**, siRNA reads mapping to the *ade6-704* locus in *leo1+* and *leo1*Δ strains. Red, plus strand; blue, minus strand. Intronic *rpl2302* siRNAs in *leo1*Δ cells indicate co-transcriptional double-stranded RNA synthesis by RDRC before splicing. **c**, ChIP experiment showing H3K9me2 enrichments on genes surrounding the *ade6-704* locus in *leo1+* and *leo1*Δ cells. Enrichments were calculated relative to background levels obtained in *clr4*Δ cells and normalized to *adh1+*. Error bars, s.d.; mean of $n = 2$ independent biological replicates.

APPENDIX

Manuscript 2: The histone acetyltransferase Mst2 protects active chromatin from epigenetic silencing by acetylating the ubiquitin ligase Brl1

Article

Molecular Cell

The Histone Acetyltransferase Mst2 Protects Active Chromatin from Epigenetic Silencing by Acetylating the Ubiquitin Ligase Brl1

Graphical Abstract

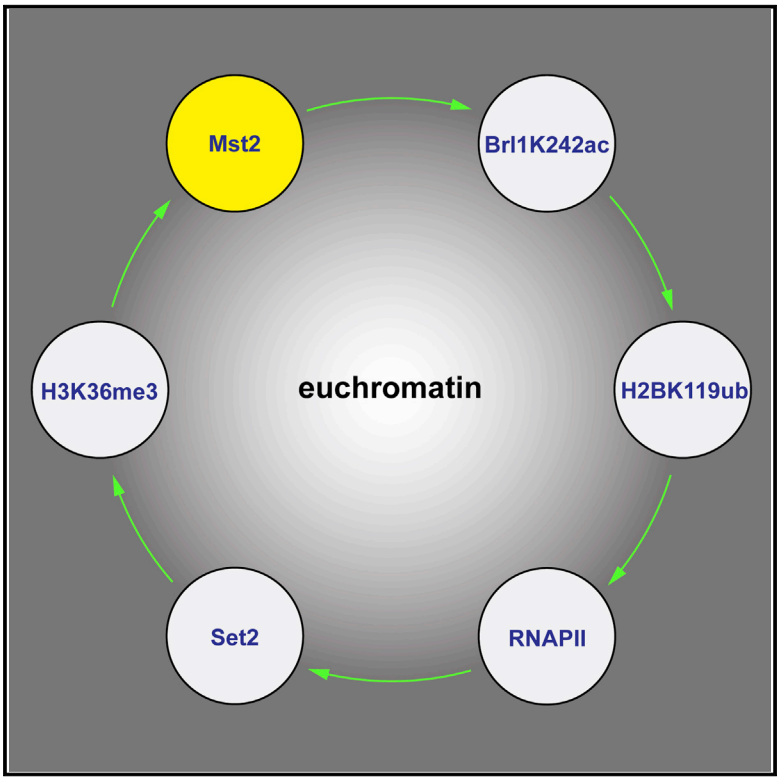

Highlights

- A positive feedback loop maintains euchromatic genes in an active state
- The histone acetyltransferase Mst2 acetylates the ubiquitin ligase Brl1
- Brl1 acetylation inhibits initiation of RNAi-directed heterochromatin formation
- H3K36me3 sequesters Mst2 to prevent illegitimate activation of heterochromatin

Authors

Valentin Flury,
Paula Raluca Georgescu,
Vytautas Iesmantavicius,
Yukiko Shimada, Tahsin Kuzdere,
Sigurd Braun, Marc Bühler

Correspondence

sigurd.braun@bmc.med.lmu.de (S.B.),
marc.buehler@fmi.ch (M.B.)

In Brief

The partitioning of distinct chromatin states is crucial for maintaining cellular identity. Flury et al. demonstrate that anchoring an acetyltransferase complex to actively transcribed genes protects euchromatin from transformation into heterochromatin. This mechanism acts through a positive feedback loop that involves acetylation of a non-histone target, which in turn mediates histone ubiquitylation.

Flury et al., 2017, Molecular Cell 67, 1–14
July 20, 2017
http://dx.doi.org/10.1016/j.molcel.2017.05.026

CellPress

Molecular Cell
Article

The Histone Acetyltransferase Mst2 Protects Active Chromatin from Epigenetic Silencing by Acetylating the Ubiquitin Ligase Brl1

Valentin Flury,[1,2] Paula Raluca Georgescu,[3] Vytautas Iesmantavicius,[1,2] Yukiko Shimada,[1,2] Tahsin Kuzdere,[1] Sigurd Braun,[3,*] and Marc Bühler[1,2,4,*]
[1]Friedrich Miescher Institute for Biomedical Research, Maulbeerstrasse 66, 4058 Basel, Switzerland
[2]University of Basel, Petersplatz 10, 4003 Basel, Switzerland
[3]Biomedical Center Munich, Physiological Chemistry, Ludwig-Maximilians-Universität München, Großhaderner Str. 9, 82152 Planegg-Martinsried, Germany
[4]Lead Contact
*Correspondence: sigurd.braun@bmc.med.lmu.de (S.B.), marc.buehler@fmi.ch (M.B.)
http://dx.doi.org/10.1016/j.molcel.2017.05.026

SUMMARY

Faithful propagation of functionally distinct chromatin states is crucial for maintaining cellular identity, and its breakdown can lead to diseases such as cancer. Whereas mechanisms that sustain repressed states have been intensely studied, regulatory circuits that protect active chromatin from inactivating signals are not well understood. Here we report a positive feedback loop that preserves the transcription-competent state of RNA polymerase II-transcribed genes. We found that Pdp3 recruits the histone acetyltransferase Mst2 to H3K36me3-marked chromatin. Thereby, Mst2 binds to all transcriptionally active regions genome-wide. Besides acetylating histone H3K14, Mst2 also acetylates Brl1, a component of the histone H2B ubiquitin ligase complex. Brl1 acetylation increases histone H2B ubiquitination, which positively feeds back on transcription and prevents ectopic heterochromatin assembly. Our work uncovers a molecular pathway that secures epigenome integrity and highlights the importance of opposing feedback loops for the partitioning of chromatin into transcriptionally active and inactive states.

INTRODUCTION

Chromatin exists in different states that are intimately linked with gene activity. Active chromatin is associated with histone H3 lysine 36 (H3K36) methylation in all eukaryotes. H3K36-specific methyltransferases contain a catalytic SET domain, but they have varying preferences to catalyze mono-, di-, or trimethylation of H3K36. In yeast, the conserved SET domain-containing protein 2 (Set2) performs all H3K36 methylation and is recruited to chromatin co-transcriptionally via direct interaction with RNA polymerase II (Wagner and Carpenter, 2012). Specific reader proteins that interact with histone deacetylases (HDACs) recognize methylated H3K36, which is necessary for HDAC activity within active genes (Drouin et al., 2010; Govind et al., 2010; Nicolas et al., 2007). This compensates for transcription-coupled disruption and hyperacetylation of chromatin, which would otherwise activate cryptic promoters within coding sequences (Carrozza et al., 2005; Nicolas et al., 2007). H3K36me2 is sufficient for localized HDAC activity on protein-coding genes in both *Saccharomyces cerevisiae* and *Schizosaccharomyces pombe* (Li et al., 2009; Suzuki et al., 2016), suggesting that H3K36me3 may have a distinct function.

How the active chromatin state is maintained and protected from aberrant inactivation is not well understood. In contrast, we have a detailed understanding of how repressed heterochromatin is maintained due largely to genetic studies in *S. pombe* and other model organisms. *S. pombe* shares many of the heterochromatin-specific histone modifications (H3K9 methylation and histone hypoacetylation) and protein components with animals and plants. Constitutive heterochromatin is found at the pericentromeric DNA repeats, telomeres, and the silent mating-type loci in *S. pombe*. As in all other eukaryotes studied, *cis*-acting DNA elements have evolved to specify the assembly of these heterochromatic regions (Beisel and Paro, 2011; Moazed, 2011). Additionally, the RNAi pathway is directly involved in the formation of heterochromatin at these loci, and it is indispensable for the stable propagation of pericentromeric heterochromatin (Grewal, 2010). The RNA-induced transcriptional silencing complex (RITS), which includes the RNAi protein Ago1, is directed to chromatin co-transcriptionally via base pairing of the Ago1-bound small RNA with complementary sequences in RNA polymerase II-generated nascent transcripts (Shimada et al., 2016). RITS recruits the sole *S. pombe* H3K9 methyltransferase Clr4 (Bayne et al., 2010), which methylates H3K9 to form a binding site for heterochromatin protein 1 (HP1) homologs. RITS also helps recruit an RNA-dependent RNA polymerase-containing complex to amplify the process by generating more double-stranded RNA substrate for Dcr1 (Motamedi et al., 2004; Sugiyama et al., 2005). This creates a positive feedback loop on centromeric repeats, guaranteeing

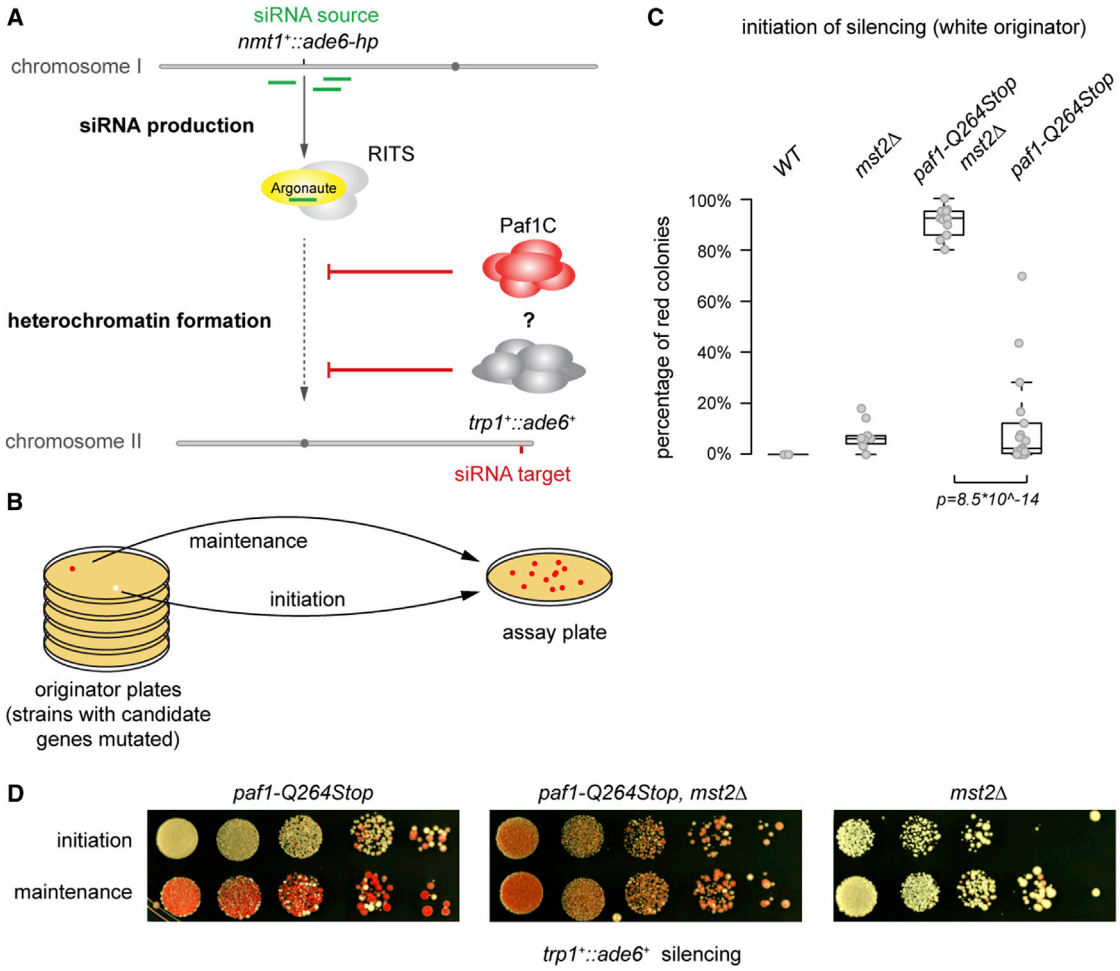

Figure 1. Mst2 Counteracts siRNA-Directed De Novo Heterochromatin Assembly

(A) Scheme: de novo silencing in *trans* by siRNAs from a hairpin RNA-producing locus is repressed by Paf1C and other protein complexes.

(B) Experimental setup: white (expressed) or red (silenced) colonies were selected, and their descendants were analyzed for initiation and maintenance of the silenced state, respectively.

(C) Descendants were categorized by color, and the percentage of colonies containing non-white (red) cells was calculated. The p value was calculated using the two-sided, two-sample Student's t test ($n \geq 3$ individual white colonies). Exact numbers are listed in the STAR Methods.

(D) Silencing assays were performed with indicated mutant strains to illustrate the difference between initiation and maintenance of silencing. A representative experiment is shown. Note that quantification shown in (C) was not based on this assay, because individual colonies cannot be clearly distinguished. For (C) and (D), see the STAR Methods for details.

high levels of H3K9 methylation and rapid turnover of centromeric RNAs into small interfering RNAs (siRNAs) to maintain a repressive chromatin state.

H3K9 methylation also promotes the recruitment of the class II HDAC Clr3, which deacetylates H3K14 and restricts the access of RNA polymerase II to heterochromatin, thus limiting transcription (Bjerling et al., 2002; Fischer et al., 2009; Motamedi et al., 2008; Sugiyama et al., 2007). In contrast, acetylation of H3K14 is associated with active chromatin, and it is mediated by the Gcn5 and Mst2 histone acetyltransferases (HATs). Interestingly, deletion of the *mst2*$^+$ gene strengthens heterochromatin silencing at telomeres (Gómez et al., 2005), and it bypasses the requirement of RNAi to maintain centromeric heterochromatin (Reddy et al., 2011). Mst2 also potentiates the phenotype of cells lacking Epe1, which is a putative H3K9 demethylase (Wang et al., 2015). These results indicate that Mst2 antagonizes heterochromatin silencing; however, the underlying mechanisms are unknown.

Whereas we have an advanced understanding of RNAi-mediated maintenance of heterochromatin, relatively little is known about de novo formation of heterochromatin because this is repressed by the RNA polymerase II-associated factor 1 complex (Paf1C). In Paf1C mutant cells, siRNAs initiate gene silencing in an all-or-nothing fashion characteristic of an epigenetic silencing response. Once established, the OFF state is stably propagated even in the absence of the primary siRNAs (Kowalik et al., 2015; Shimada et al., 2016). Yet, the rate at which individual cells initiate silencing is quite low, implying the existence of additional repressive activities (Figure 1A). To isolate factors that are specifically involved in initiating heterochromatin

assembly, but not maintenance, we tested previously described chromatin regulators in combination with Paf1C mutants, and we identified the HAT Mst2. We show that Mst2 represses RNAi-mediated heterochromatin formation specifically during the initiation phase of heterochromatin assembly. This is achieved by H3K36me3-dependent sequestration of Mst2 on actively transcribed genes, which is mediated by its interaction partner Pdp3. By restricting Mst2 activity to transcribed protein-coding genes, H3K36me3 maintains those in a euchromatic state. Surprisingly, we discovered that Mst2 acetylates a specific lysine in Brl1, a component of the histone H2B ubiquitin ligase complex (HULC), revealing insights into the mechanism by which Mst2 antagonizes the assembly of ectopic heterochromatin and secures epigenome integrity.

RESULTS

Mst2 Counteracts Small RNA-Directed Initiation of Heterochromatin Assembly

Ectopic heterochromatin formation in *S. pombe* can be triggered by the temporary expression of *trans*-acting primary siRNAs in cells harboring mutations in Paf1C subunits; however, the frequency of de novo silencing is low (Kowalik et al., 2015). To identify additional repressors of RNAi-directed heterochromatin assembly, we tested candidate proteins that have previously been implicated in chromatin regulation. We used a reporter strain expressing an RNA hairpin (*ade6-hp*) complementary to 250 nt of *ade6*$^+$ and harboring a nonsense mutation in the *paf1*$^+$ gene (*paf1-Q264Stop*) (Kowalik et al., 2015). We chose *ade6*$^+$ as a reporter gene because it allowed us to quantify the initiation of silencing in individual colonies that derived from single cells. When grown on limiting adenine indicator plates, cells with active or inactive *ade6*$^+$ form white or red colonies, respectively. To determine the frequency of initiation of silencing, we grew single- and double-mutant strains of *paf1-Q264Stop* alone or in combination with a deleted candidate gene on low-adenine originator plates, selected white colonies, and seeded a given number of (white) cells at single-cell density on low-adenine assay plates (Figure 1B). Subsequent counting of the colonies containing red cells allowed us to calculate the percentage of cells that had initiated *ade6*$^+$ silencing since they were seeded.

This analysis revealed that deletion of the *mst2*$^+$ gene, which encodes one of two MYST family HATs (Gómez et al., 2005), dramatically increased the rate at which *paf1-Q264Stop* cells silenced the *ade6*$^+$ reporter gene: 11% of *paf1-Q264Stop* cells formed red colonies (inactive *ade6*$^+$), whereas more than 90% of the *mst2Δ paf1-Q264Stop* double-mutant cells inactivated *ade6*$^+$ (Figure 1C). Importantly, although deletion of *mst2*$^+$ alone did enable *ade6*$^+$ silencing (Figure 1C), the repressed state was poorly maintained (Figure 1D). In contrast, *ade6*$^+$ silencing was stably propagated in *mst2Δ paf1-Q264Stop* double-mutant cells (Figure 1D).

Therefore, we have identified Mst2 as a repressor of RNAi-mediated heterochromatin formation. Mst2 acts specifically during the initiation phase of heterochromatin assembly as, in contrast to Paf1C, it does not disrupt heterochromatin once it has been established (Figure 1D and results described hereafter).

Mst2 Prevents RNAi-Dependent Spreading of Heterochromatin

The siRNAs trigger de novo formation of heterochromatin by guiding the H3K9 methylation machinery to complementary target sites (Kowalik et al., 2015). Consistent with this, we observed high levels of H3K9me2 at the endogenous *ade6*$^+$ locus in both *paf1-Q264Stop* single and *mst2Δ paf1-Q264Stop* double mutants, but not in wild-type cells (Figure 2A). As reported previously, H3K9me2 was not restricted to *ade6*$^+$ but spread into neighboring regions (Kowalik et al., 2015; Shimada et al., 2016), resulting in gene repression (Figures 2A and S1A). Remarkably, this spreading was greatly enhanced in the double-mutant strain. Whereas H3K9me2 enrichments dropped to wild-type levels in *paf1-Q264Stop* cells within a few kilobases (kb) around *ade6*$^+$, concomitant deletion of *mst2*$^+$ led to a substantial increase and extensive spreading of H3K9 methylation and gene silencing up to 30 kb downstream of *ade6*$^+$ (Figure 2A).

Another characteristic of RNAi-induced de novo formation of heterochromatin is the subsequent production of secondary siRNAs complementary to the target locus (Jain et al., 2016; Kowalik et al., 2015; Shimada et al., 2016; Simmer et al., 2010). By sequencing small RNAs, we observed that these secondary siRNAs were also more abundant in *paf1-Q264Stop mst2Δ* cells compared to the *paf1-Q264Stop* single mutant, particularly beyond the nucleation site targeted by the *trans*-acting primary siRNAs (Figure 2A). This suggests that de novo targeting of RITS to the neighboring genes via *cis*-acting secondary siRNAs mediates H3K9me2 spreading. However, H3K9me2 was still strongly enriched 20 kb downstream of the *ade6*$^+$ gene in the double-mutant cells, whereas secondary siRNAs mapping to this region were barely detectable. Thus, it is possible that H3K9me2 spreads independently of siRNAs in the absence of Mst2. Alternatively, very low levels of siRNAs might be sufficient to promote spreading of heterochromatin in *cis*. We could not distinguish between these two possibilities at the *ade6*$^+$ locus, because RNAi is absolutely necessary to maintain ectopic heterochromatin at this site (Kowalik et al., 2015; Shimada et al., 2016) (Figure S1B). Therefore, we analyzed the effect of *mst2*$^+$ deletion on the boundary of constitutive heterochromatin at centromere 1.

Similar to genes flanking *ade6*$^+$, we observed increased H3K9me2 at the centromeric heterochromatin *IRC1R* boundary and spreading to its proximal genes *emc5*$^+$ and *rad50*$^+$ in *mst2Δ* cells (Figure 2B). Thus, consistent with a previous study (Wang et al., 2015), Mst2 counteracts spreading of H3K9 methylation also at this locus. This is interesting because H3K9me2 levels are low in wild-type cells, despite abundant siRNAs that originate from the IRC1R boundary (Figure 2C) (Keller et al., 2013), indicating that Mst2 counteracts small RNA-directed initiation of H3K9 methylation at this locus as well. Notably, also here we observed H3K9me2 spreading into the more distal *emc5*$^+$ and *rad50*$^+$ genes without the concomitant production of high levels of secondary siRNAs (Figure 2C). Because the RNAi machinery is not required to maintain H3K9 methylation at pericentromeric *dg/dh* repeats in the absence of Mst2 (Reddy et al., 2011), we could delete *ago1*$^+$ and *dcr1*$^+$ in the *mst2Δ* background to test whether a functional RNAi pathway is necessary for the observed *cis*-spreading of H3K9me2. This revealed that RNAi is indeed essential for H3K9me2 spreading into the

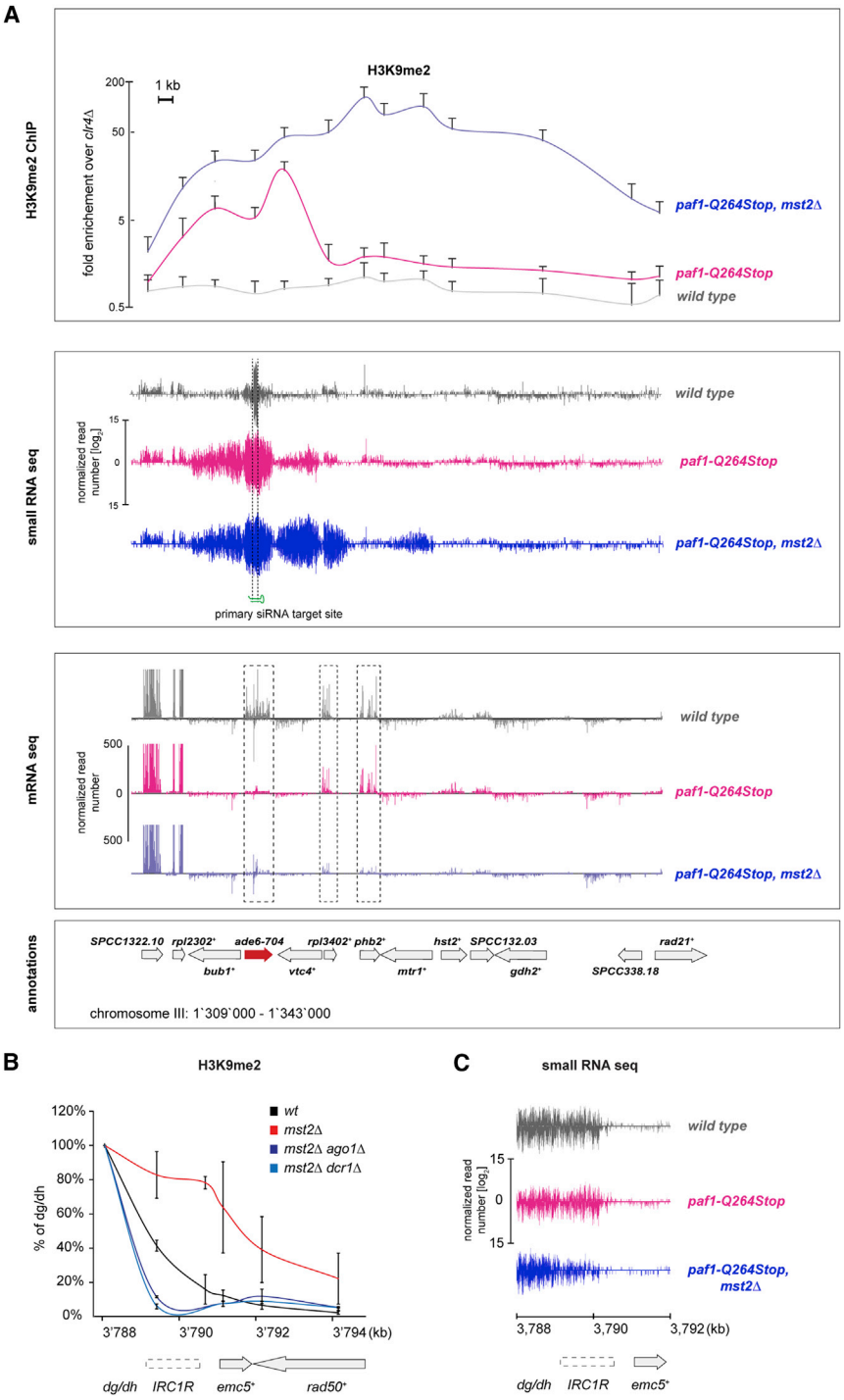

Figure 2. Large Heterochromatin Domains Form upon Removal of *mst2*$^+$

(A) Upper panel: ChIP analysis of H3K9me2 showing enrichments at the target gene *ade6-704* and neighboring regions. Error bars indicate SD ($n \geq 3$ independent biological replicates). The y axis is shown in logarithmic scale. Middle and lower panels: siRNAs (middle panel) and RNA (lower panel) reads mapping to the *ade6-M210* locus and neighboring regions in wild-type (gray), *paf1-Q264Stop* (red), and *paf1-Q264Stop mst2Δ* cells (blue), respectively, are shown. Read counts were normalized to the total read number and are depicted in $\log_2$ (middle panel) or linear scale (lower panel).

(B) H3K9me2 enrichments at the right centromere boundary of chromosome 1 (IRC1R). ChIP enrichments are shown relative to the centromeric repeats *dg/dh*, which was set at 100%. Error bars indicate SD (n = 2 or 3 independent biological replicates; *mst2Δ ago1Δ* and *mst2Δ dcr1Δ* or wild-type (WT) and *mst2Δ*, respectively).

(C) siRNAs mapping to IRC1R and neighboring regions in wild-type (gray), *paf1-Q264Stop* (red), and *paf1-Q264Stop mst2Δ* cells (blue). Read counts were normalized to the total read number and are depicted in $\log_2$ scale.

See also Figure S1.

adjacent euchromatic regions in the absence of Mst2 (Figures 2B and S1C). Together, our results reveal that Mst2 prevents RNAi-directed de novo assembly and spreading of heterochromatin.

Mst2 Is Excluded from Constitutive Heterochromatin

Because Mst2 prevents spreading of constitutive and synthetic heterochromatin, it is unlikely that Mst2 is recruited to heterochromatin boundaries in a sequence-specific manner. To assess the localization of Mst2 genome-wide in wild-type cells, we used DNA adenine methyltransferase identification (DamID), a sensitive chromatin-profiling technique that we and others have previously adapted for use in *S. pombe* (Steglich et al., 2012; Woolcock et al., 2011). We generated strains that express Mst2 fused to DNA adenine methylase (Dam), and we assessed GATC methylation, and thereby Mst2 binding, throughout the *S. pombe* genome using tiling arrays.

Comparing Dam-Mst2-binding profiles with genome-wide H3K9 methylation data (Keller et al., 2013) revealed a striking anti-correlation (Figure 3A). Whereas Mst2 bound throughout the entire genome, it was strongly depleted from constitutive heterochromatin found at centromeres, telomeres, and the silent mating-type locus (Figure 3B). We did not observe specific Mst2 enrichment at the borders of constitutive heterochromatin, consistent with Mst2 not being a bona fide boundary factor (Figure 3C). In contrast, we observed a preferential enrichment of Mst2 on RNA polymerase II-transcribed protein-coding genes (Figure 3D). Of note, regions transcribed by RNA polymerases I and III, such as tRNA, small nucleolar RNAs (snoRNAs), and rRNAs, were depleted of Mst2, similar to heterochromatic regions. To validate these data with an alternative method, we performed chromatin immunoprecipitation (ChIP) with cells expressing C-terminally FLAG-tagged Mst2.

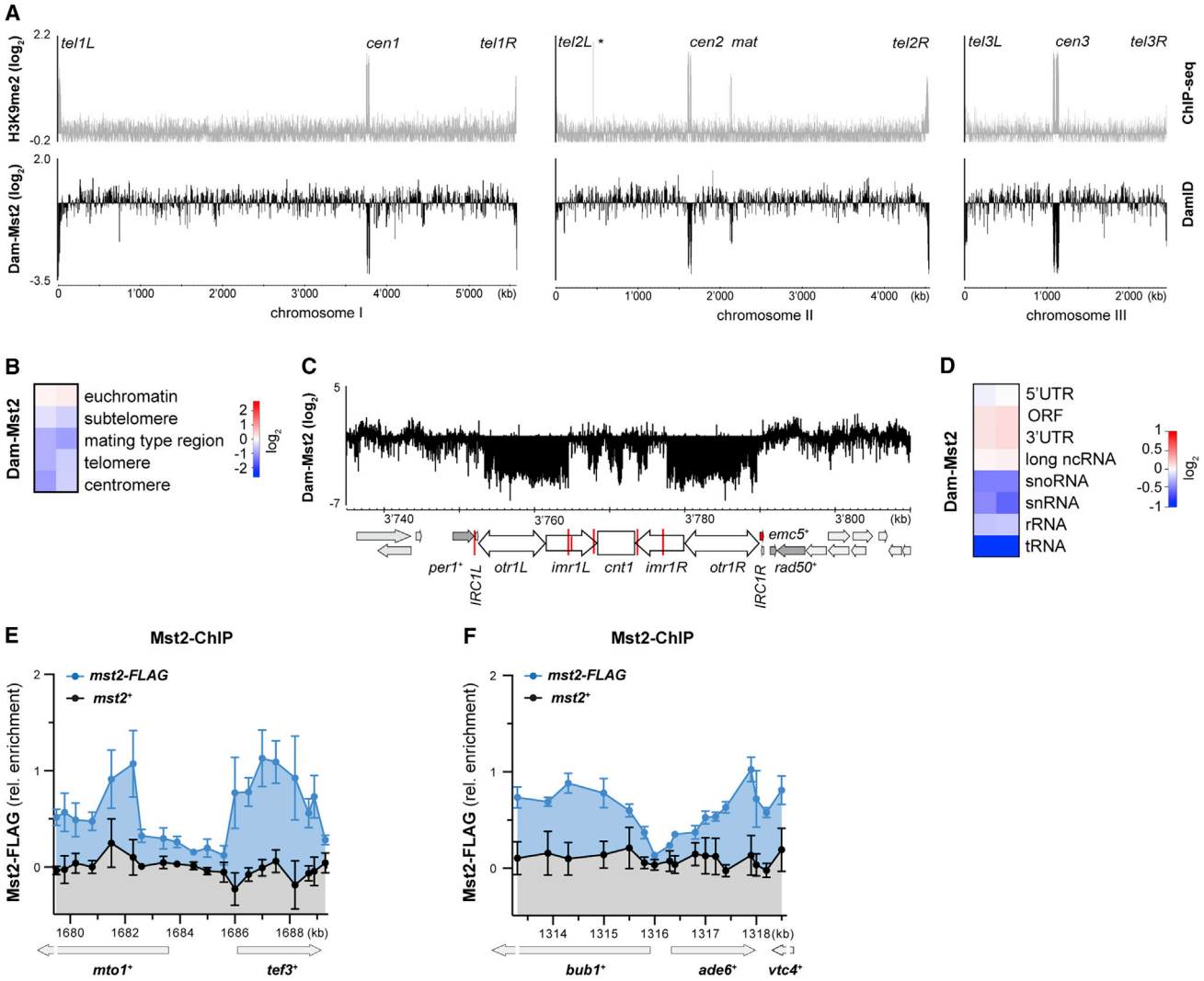

Figure 3. Mst2 Is Excluded from Constitutive Heterochromatin and Specifically Associates with Transcriptionally Active Chromatin

(A) Mst2 DamID maps for all three chromosomes (bottom) compared to previously generated H3K9me2 ChIP-sequencing data (top; Keller et al., 2013). The signal of Dam-Mst2 (normalized to Dam only) was averaged over 500 probes and is shown in $\log_2$ scale. The x axis shows position on chromosomes.

(B) Enrichment of Dam-Mst2 at different genomic regions. Two independent replicates are shown (scale in $\log_2$).

(C) Zoom of DamID map from (A) on centromere of chromosome 1.

(D) Enrichment of Dam-Mst2 at different euchromatic elements. Two independent replicates are shown (scale in $\log_2$).

(E and F) ChIP enrichment of Mst2-FLAG (blue) compared to untagged Mst2 (black) over the *mto1*$^+$/*tef3*$^+$ locus (E) and the *ade6-704* locus (F). ChIP data are shown relative to the mean of the untagged control with the background subtracted (n = 4 ± SEM).

Consistent with our DamID results, we observed Mst2 preferentially enriched on transcribed genes, including *bub1*$^+$, *ade6*$^+$, and *vtc4*$^+$ (Figures 3E and 3F), the region targeted for de novo formation of heterochromatin by primary *ade6* siRNAs in our initiation of silencing assays. Generally, Mst2 bound weakly to intergenic and promoter proximal regions and most strongly in the body of transcribed genes (Figures 3D–3F).

Pdp3 Binding to H3K36me3 Confines Mst2 to Euchromatin

How Mst2 is recruited to active genes is unclear. It is known to physically interact with a number of proteins to form a complex, which includes homologs of *S. cerevisiae* NuA3 HAT complex subunits (Wang et al., 2012). One of its subunits, Pdp3, contains a PWWP domain (Figure 4A), which binds methylated lysines and arginines (Adams-Cioaba and Min, 2009; Maurer-Stroh et al., 2003; Vermeulen et al., 2010). Interestingly, the *S. cerevisae* Pdp3 homolog recognizes H3K36me3 (Gilbert et al., 2014), which is enriched in the gene body and the 3′ UTR of active genes (Bell et al., 2007). This pattern is highly reminiscent of Mst2 localization (Figure 3D). Therefore, we speculated that Mst2 is targeted to transcribed genes via Pdp3 binding to H3K36me3. Indeed, we observed a positive correlation between our Dam-Mst2 and published H3K36me3 ChIP on microarray (ChIP-on-chip) data (Wilhelm

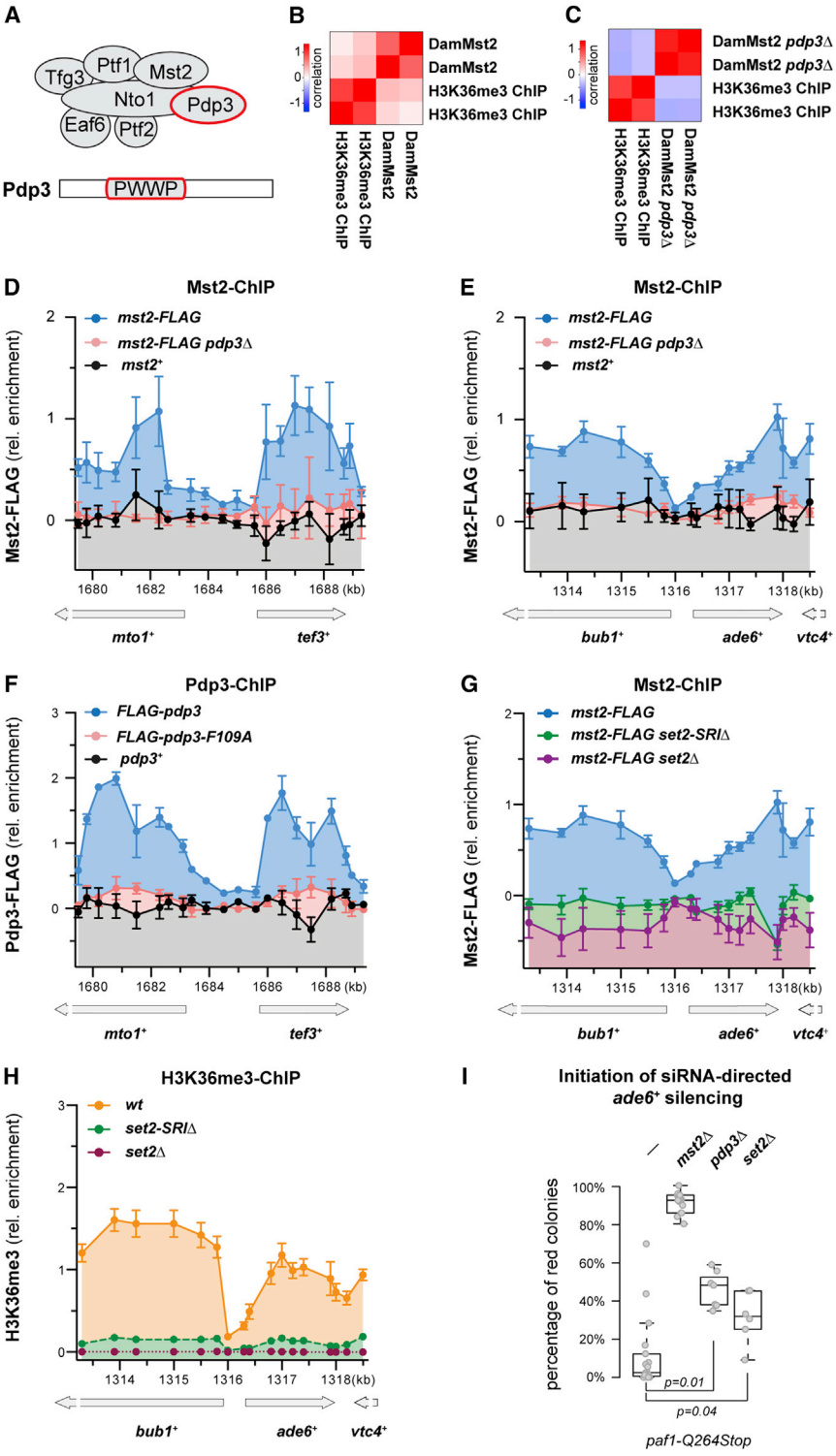

Figure 4. Pdp3 Anchors the Mst2 Complex to Euchromatin via H3K36me3

(A) Scheme of the Mst2 complex and protein domain organization of Pdp3.

(B and C) Correlation between enrichment of Dam-Mst2 and ChIP-on-chip data of H3K36me3 in wild-type (B) and *pdp3Δ* cells (C). Two independent biological replicates are shown (in $\log_2$ scale). ChIP-on-chip data are from Wilhelm et al. (2011).

(D and E) ChIP enrichment of Mst2-FLAG in WT (blue) or *pdp3Δ* (red) cells compared to an untagged wild-type strain (black) at the *mto1*$^+$/*tef3*$^+$ locus (D) or the *ade6-704* locus (E).

(F) ChIP enrichment of FLAG-Pdp3 (blue) or FLAG-Pdp3 mutant (*pdp3-F109A*, red) compared to untagged wild-type strain (black) at the *mto1*$^+$/*tef3*$^+$ locus.

(G) ChIP of Mst2-FLAG in WT (blue), *set2Δ* (purple), and *set2-SRIΔ* (green) cells at the *ade6-704* locus.

(H) ChIP of H3K36me3 in WT (orange), *set2Δ* (purple), and *set2-SRIΔ* (green) cells at the *ade6-704* locus. ChIP data in (D)–(G) are shown relative to the mean of the untagged control with the background subtracted; ChIP data in (H) are shown relative to the mean of WT over the entire chromatin region examined. All ChIP experiments have been performed with n = 3–4 ± SEM.

(I) Initiation frequencies in *paf1-Q264Stop* cells additionally deleted for *mst2*$^+$, *pdp3*$^+$, or *set2*$^+$ as in Figure 1D. The p values were calculated using the two-sided, two-sample Student's t test (n ≥ 4 independent white colonies). Exact numbers are listed in the STAR Methods.

et al., 2011) (Figure 4B; $R^2 = 0.25$). This positive correlation was completely lost upon deletion of the *pdp3*$^+$ gene (Figure 4C; $R^2 = -0.27$). Similarly, the enrichment of Mst2 on transcribed genes, including *bub1*$^+$, *ade6*$^+$, and *vtc4*$^+$, was abolished in *pdp3*Δ cells when interrogated by ChIP (Figures 4D and 4E). These results are consistent with Mst2 recruitment to transcribed genes via Pdp3. This is further supported by ChIP experiments with FLAG-tagged Pdp3, which revealed very similar binding patterns for Mst2 and Pdp3 on transcribed genes (Figures 4D and 4F). Importantly, Mst2 binding at the *ade6*$^+$ and *bub1*$^+$ genes was abolished in *set2Δ* mutants (Figure 4G), demonstrating that methylation of H3K36 is necessary for the recruitment of Mst2 to actively transcribed genes. Moreover, Pdp3 binding to chromatin was lost when we introduced a single point mutation (F109A) in the bona fide recognition site of the PWWP domain (Figure 4F).

H3K36me3 is deposited co-transcriptionally by the methyltransferase Set2 (Morris et al., 2005). Set2 is recruited to the transcribing RNA polymerase II through its conserved C-terminal Set2-Rpb1 interaction (SRI) domain (Kizer et al., 2005). Intriguingly, mutations in the SRI domain of *S. pombe* Set2 cause a specific loss of H3K36me3, without affecting H3K36me2 (Suzuki et al., 2016). This enabled us to determine whether Pdp3 is specific to H3K36me3 or whether it would also recognize H3K36me2.

Resembling Mst2 binding, H3K36me3 was enriched throughout the gene bodies of *ade6*$^+$ and *bub1*$^+$ but depleted from the intergenic region. As expected, H3K36me3 was completely abolished in *set2Δ* cells and in *set2-SRI*Δ cells (Figure 4H). Importantly, Mst2 binding at the *ade6*$^+$ and *bub1*$^+$ genes was also abolished in both mutants (Figure 4G). Together, these results reveal that Pdp3 specifically recognizes H3K36me3, but not H3K36me2, to recruit Mst2 to transcribed genes.

Thus far we have shown that the HAT Mst2 is recruited to transcribed genes via H3K36me3 and that it acts as a suppressor of RNAi-directed heterochromatin assembly and spreading. To assess whether these functions are connected, we quantified the initiation of *ade6*$^+$ silencing in mutants unable to recruit Mst2 to transcribed genes (i.e., *pdp3Δ* and *set2Δ* cells). Similar to *mst2*$^+$ deletion (*mst2Δ paf1-Q264Stop*), deletion of *pdp3*$^+$ (*pdp3Δ paf1-Q264Stop*) or *set2*$^+$ (*set2Δ paf1-Q264Stop*) also initiated silencing more frequently than the *paf1-Q264Stop* single mutant (Figure 4I). This demonstrates a functional link between H3K36 modification and RNAi-directed heterochromatin formation. Yet, we note that although phenocopying each other, *pdp3Δ* and *set2Δ* did not fully phenocopy an *mst2Δ* mutant in this assay. This indicates that Mst2 remains partially repressive in the absence of H3K36me3 binding.

H3K36me3 Preserves Euchromatin and Safeguards Heterochromatic Genes from Illegitimate Activation

The foregoing results establish Pdp3 as a reader of the H3K36me3 mark that recruits Mst2 to active genes. Nevertheless, in the absence of Pdp3 and Set2 there was residual Mst2 chromatin association above background (Figures 5A and S2A). Most prominently, Mst2 exclusion from constitutive heterochromatin was largely abolished in both *pdp3Δ* and *set2Δ* cells (Figures 5A and S2A). In contrast, deletion of *set1*$^+$, which encodes the histone methyltransferase that methylates H3K4, had no effect on Mst2 localization (Figure S2B).

These results suggest that H3K36me3-mediated recruitment of Mst2 to transcribed genes serves a dual function: it prevents RNAi-mediated heterochromatin formation in euchromatin, and it sequesters Mst2 away from heterochromatin to prevent aberrant activation of heterochromatic genes. In further support of the latter, it was previously reported that deletion of *set2*$^+$ or *pdp3*$^+$ alleviated heterochromatin silencing (Braun et al., 2011; Chen et al., 2008; Creamer et al., 2014; Matsuda et al., 2015; Suzuki et al., 2016) (Figure S2C). To test this more directly, we inhibited Mst2 recruitment to active genes using *pdp3*Δ cells, and we analyzed the effect on silencing of heterochromatic genes. We observed increased expression of centromeric repeats and subtelomeric genes in *pdp3Δ* cells, but not in *mst2Δ* cells (Figures 5B–5D). Importantly, these heterochromatin-silencing defects in the *pdp3Δ* background were rescued by deleting *mst2*$^+$ (Figures 5C, S2C, and S2D).

To further support our model that Mst2 recruitment to active genes prevents it from aberrantly activating heterochromatic genes, we fused the high-affinity DNA-binding protein LexA to wild-type Mst2 (LexA-Mst2) and catalytically inactive Mst2 (LexA-Mst2*[E274Q]) (Reddy et al., 2011), both expressed from the endogenous *mst2*$^+$ locus. In addition, we inserted an *ade6*$^+$ reporter gene linked to four LexA-binding sites into pericentromeric heterochromatin on chromosome 1 by homologous recombination (Figure 5E). Tethering of LexA-Mst2, but not LexA-Mst2*, caused a mild silencing defect of the heterochromatic *ade6*$^+$ reporter (Figure 5F). Because H3K36me3 ought to sequester LexA-Mst2 away from heterochromatin, we would expect a stronger silencing defect in cells lacking Pdp3 or Set2. Indeed, *ade6*$^+$ silencing was almost completely abolished in *pdp3Δ* (Figure 5G) and *set2Δ* cells (Figure 5H). Expression of the euchromatic *ade6-M* allele remained unaffected in those experiments (Figure S2E).

Therefore, we conclude that the Pdp3 subunit of the Mst2 complex serves two purposes: first, it focuses Mst2 activity on transcribed genes to maintain those in a euchromatic state; and second, it prevents Mst2 from functioning promiscuously and thereby safeguards heterochromatic genes from illegitimate activation.

Mst2 Acetylates Lysine 242 of the E3 Ubiquitin Protein Ligase Brl1

Mst2 is a MYST family HAT that specifically acetylates K14 on histone H3 in vitro and in vivo (Wang et al., 2012). However, H3K14 acetylation levels remained unchanged at centromeres, telomeres, or euchromatic protein-coding genes in *mst2Δ* cells (Figures S3A–S3C). Notably, Mst2 functions together with another HAT, Gcn5, to regulate global levels of H3K14ac (Wang et al., 2012). Thus, both HATs might interfere with the initiation of heterochromatin assembly through the acetylation of H3K14. However, we observed neither spreading of heterochromatin nor strongly enhanced initiation of heterochromatin assembly triggered by siRNAs in *gcn5Δ* cells (Figures S3D and S3E). Thus, the repressive effect on de novo formation of heterochromatin is unique to Mst2, and it appears to be mediated by an additional, unknown target of Mst2.

Therefore, we explored whether Mst2 also acetylates non-histone substrates using a liquid chromatography triple-stage mass spectrometry (LC-MS/MS/MS) approach (Aebersold and Mann, 2016; McAlister et al., 2014). Briefly, we extracted total protein from wild-type and HAT mutant cells and digested with Lys-C and Trypsin. The total protein digest was used to quantify global protein changes. Additionally, a fraction of the digest was enriched for peptides containing acetylated lysine using an anti-acetyl lysine-specific antibody. Before the LC-MS/MS/MS analysis on the Orbitrap Fusion Tribrid Mass spectrometer, samples were labeled with tandem mass tags (TMTs) and pooled (Figure 6A). MS-based analysis revealed that the *S. pombe* proteome remains largely unchanged in *mst2Δ* and *pdp3Δ* cells compared to wild-type cells (Figures S4A–S4C). The few proteins that changed in abundance were encoded by genes that reside in the vicinity of telomeric heterochromatin. As expected from our RNA measurements, protein levels of subtelomeric genes decreased in *mst2Δ* cells and increased in *pdp3Δ* cells (Figures S4A–S4C). In contrast, deletion of *gcn5*$^+$ caused substantial proteome-wide changes in protein abundance (Figure S4D). These results consolidate our findings described above and highlight that Gcn5 and Mst2 have distinct roles in controlling genome expression.

Intriguingly, quantification of the acetyl-lysine-enriched samples revealed widespread acetylome changes in *gcn5Δ* compared

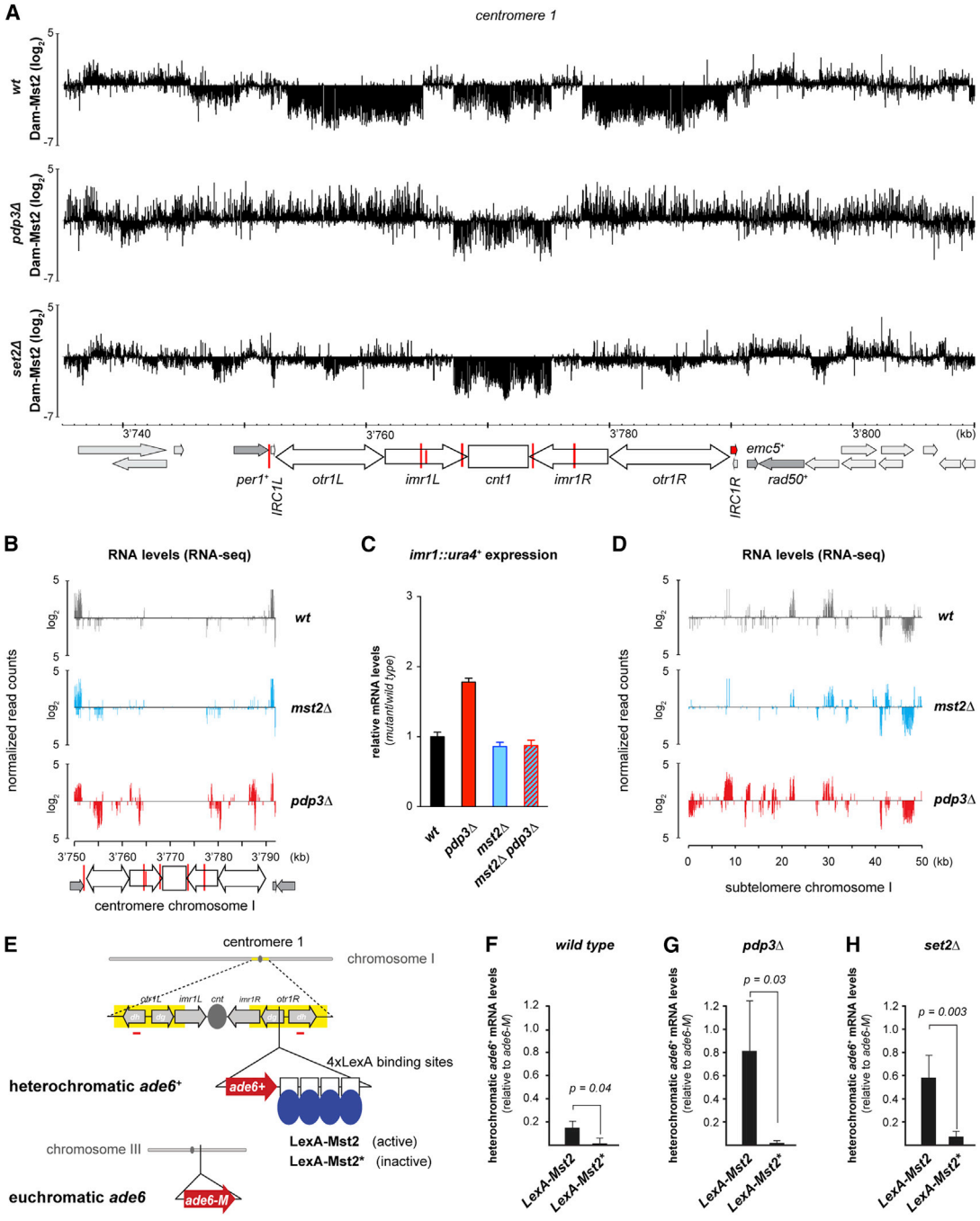

Figure 5. Promiscuous Mst2 Activity in the Absence of Pdp3 Attenuates Heterochromatin Silencing

(A) Mst2 DamID maps for the centromere of chromosome 1 in WT, *pdp3Δ*, and *set2Δ* cells. The signal of DamMst2 (normalized to Dam only) was averaged over 500 probes and is shown in $\log_2$ scale. The x axis shows position on chromosomes.

(B and D) RNA expression in WT, *pdp3Δ*, and *mst2Δ* cells at centromere 1 (B) and telomere 1L (D) assessed by RNA-seq. Relative read counts normalized to total read number (axis scale in $\log_2$) are shown.

(C) Relative RNA expression levels of *ura4*$^+$ (qRT-PCR analysis) at the innermost repeat (imr) in indicated mutants. Shown are the transcript levels relative to WT after normalization to *act1*$^+$. Data are represented as mean ± SEM from four independent biological experiments.

(E) Scheme of experimental setup for tethering Mst2 at heterochromatin: Four LexA-binding sites were inserted downstream of the *ade6*$^+$ reporter at the outermost repeat (otr) of chromosome 1 (top). The *ade6-M210* allele at the euchromatic endogenous locus of *ade6* (bottom) was used as a reference.

(F–H) Expression levels of heterochromatic *ade6*$^+$ reporter relative to euchromatic *ade6-M210* allele in WT (F), *pdp3Δ* (G), or *set2Δ* (H) cells. The p values were calculated using the two-sided, two-sample Student's t test. Error bars indicate SD ($n \geq 3$ independent biological replicates).

See also Figure S2.

to wild-type cells (Figure S4E). In contrast, only one lysine acetylation site was significantly decreased in *mst2Δ* cells (Figure 6B). We mapped this Mst2-dependent acetylation site to K242 of the E3 ubiquitin protein ligase Brl1 (Figure S4F). Importantly, Brl1 protein abundance remained unaffected in Mst2 and Pdp3 mutants (Figures S4A–S4C). Furthermore, acetylation of K242 was highly specific, because acetylation levels of other lysine residues in Brl1 (K339 and K138) remained unchanged in the absence of Mst2 (Figure 6B). Thus, in addition to H3K14 (Wang et al., 2012), Mst2 specifically acetylates the non-histone substrate Brl1 at lysine 242.

Brl1 Acetylation Antagonizes RNAi-Directed Heterochromatin Formation

Brl1 is an E3 ligase responsible for the ubiquitination of H2BK119 as part of the HULC complex, which promotes transcription and antagonizes heterochromatin silencing (Tanny et al., 2007; Zofall and Grewal, 2007). This raises the intriguing possibility that Mst2 regulates the activity of the HULC complex via the acetylation of Brl1. To test the role of Brl1 acetylation on H2B monoubiquitination directly, we substituted Brl1-K242 with glutamine (Q) or arginine (R) to mimic acetyl lysine or non-acetylated lysine, respectively. This revealed an overall reduction of H2B ubiquitination in *brl1-K242R* cells compared to wild-type or *brl1-K242Q* cells (Figures 6C and 6D). Confirming Brl1 as the sole H2B-ubiquitinating enzyme, H2BK119ub was undetectable in *brl1Δ* cells (Figure 6C). Moreover, H2BK119ub enrichment at the *ade6*$^+$ gene was depleted specifically upon expression of *ade6* siRNAs in *paf1-Q264Stop* cells (Figure S4G).

Next, we tested whether Brl1-K242 Q and R mutations would affect RNAi-directed heterochromatin formation. Mimicking an *mst2Δ* phenotype in the presence of a wild-type *paf1+* allele, *brl1-K242R* cells enabled primary siRNAs to initiate *ade6*$^+$ silencing. In contrast, *brl1-K242Q* cells were refractory to *ade6* siRNAs (Figure 6E). Remarkably, the *brl1-K242Q* allele completely disabled the initiation of *ade6*$^+$ silencing by *trans*-acting siRNAs in both *mst2Δ* single- (Figure 6E) and *paf1-Q264Stop mst2Δ* double-mutant cells (Figure 6F). In contrast, the initiation of siRNA-directed *ade6*$^+$ silencing in *paf1-Q264Stop mst2Δ* cells was not affected by the Brl1-K242 to R mutation (Figure 6F). We further observed secondary siRNAs covering the *ade6*$^+$ gene (Figure 6G), validating that the observed *ade6*$^+$ silencing was indeed mediated by RNAi.

In line with the abovementioned results that Mst2 does not disrupt heterochromatin once it is established, short-term maintenance of *ade6*$^+$ silencing remained largely unaffected in both Brl1-K242 Q and R mutants (Figure 6H). However, when cells were cultivated over several days, silencing was gradually lost in Brl1-K242Q, but not Brl1-K242R, mutant cells (Figures 6I and 6J). Hence, long-term maintenance of the silent state is impaired in the Brl1-K242Q mutant. We conclude that the Brl1-K242 Q mutation disables siRNA-directed re-initiation of *ade6*$^+$ silencing and, thus, affects consolidation of the silent state.

These results show that mimicking acetylation of a single lysine in Brl1 abrogates small RNA-directed initiation of epigenetic gene silencing. This places Brl1 at the center of a regulatory circuit that maintains protein-coding genes in an active state. Conjugation of mono-ubiquitin to H2B has been associated with active transcription by RNA polymerase II (Jason et al., 2002; Tanny, 2014). Thus, the observed stimulatory effect on H2B ubiquitination is expected to feed back positively on transcription. Indeed, we observed that overall H3K4me3 levels were slightly elevated in *brl1-K242Q* compared to wild-type or *brl1-K242R* cells, indicating augmented transcription initiation (Figures S4H and S4I). Thus, we have discovered an unexpected positive feedback loop that maintains transcriptionally active regions of the fission yeast genome in a euchromatic state. Because much of the enzymatic machinery involved is conserved from yeast to human, we anticipate that epigenome integrity is secured through similar mechanisms also in other organisms. Although not addressed in our study, it is possible that RNAi-independent pathways that assemble silent chromatin are equally counteracted.

DISCUSSION

Studies in a wide variety of eukaryotic systems have established the cooperation of sequence-dependent specificity factors with existing repressive histone marks to reinforce the silent chromatin state through positive feedback loops as a common principle (Gottschling, 2004; Moazed, 2011). Our study highlights that, like silent chromatin, maintenance of the active chromatin state equally depends on positive feedback. Because faithful propagation of active chromatin states through cell divisions is crucial to maintain cellular identity, we anticipate that multicellular organisms depend on similar mechanisms to shield specific cell types from differentiation signals. Below we discuss the implications of our findings on our understanding of how chromatin is partitioned into silent and active domains.

Reinforcement of the Active Chromatin State through Positive Feedback

Akin to positive feedback loops that reinforce silent chromatin states (Moazed, 2011), we propose a positive feedback system that maintains euchromatic genes in an active state that involves Paf1C and Mst2 (Figure 7A). Both Paf1C and Set2 are recruited to euchromatin co-transcriptionally through interactions with RNA polymerase II, which results in high levels of H3K36 methylation. H3K36me3 is recognized by Pdp3, leading to a high local concentration of Mst2, which acetylates K242 of the HULC subunit Brl1. HULC is required for the ubiquitination of histone H2B at lysine 119 (H2Bub), which is universally linked to active gene transcription, thereby closing the positive feedback loop. Acetylation of a non-histone protein by a HAT is intriguing and highlights that chromatin phenotypes in HAT or HDAC mutants may not necessarily be caused by histone acetylation. Because there is evidence from other systems that histone modifications deposited co-transcriptionally regulate the mechanisms that direct their formation (Tanny, 2014), we believe that consolidation of the active chromatin state through positive feedback is more prevalent than generally assumed.

High Activation Energy Warrants Stable Propagation of Euchromatic and Heterochromatic States

Our recent discovery of Paf1C as a repressor of siRNA-directed heterochromatin formation (Kowalik et al., 2015) and the results

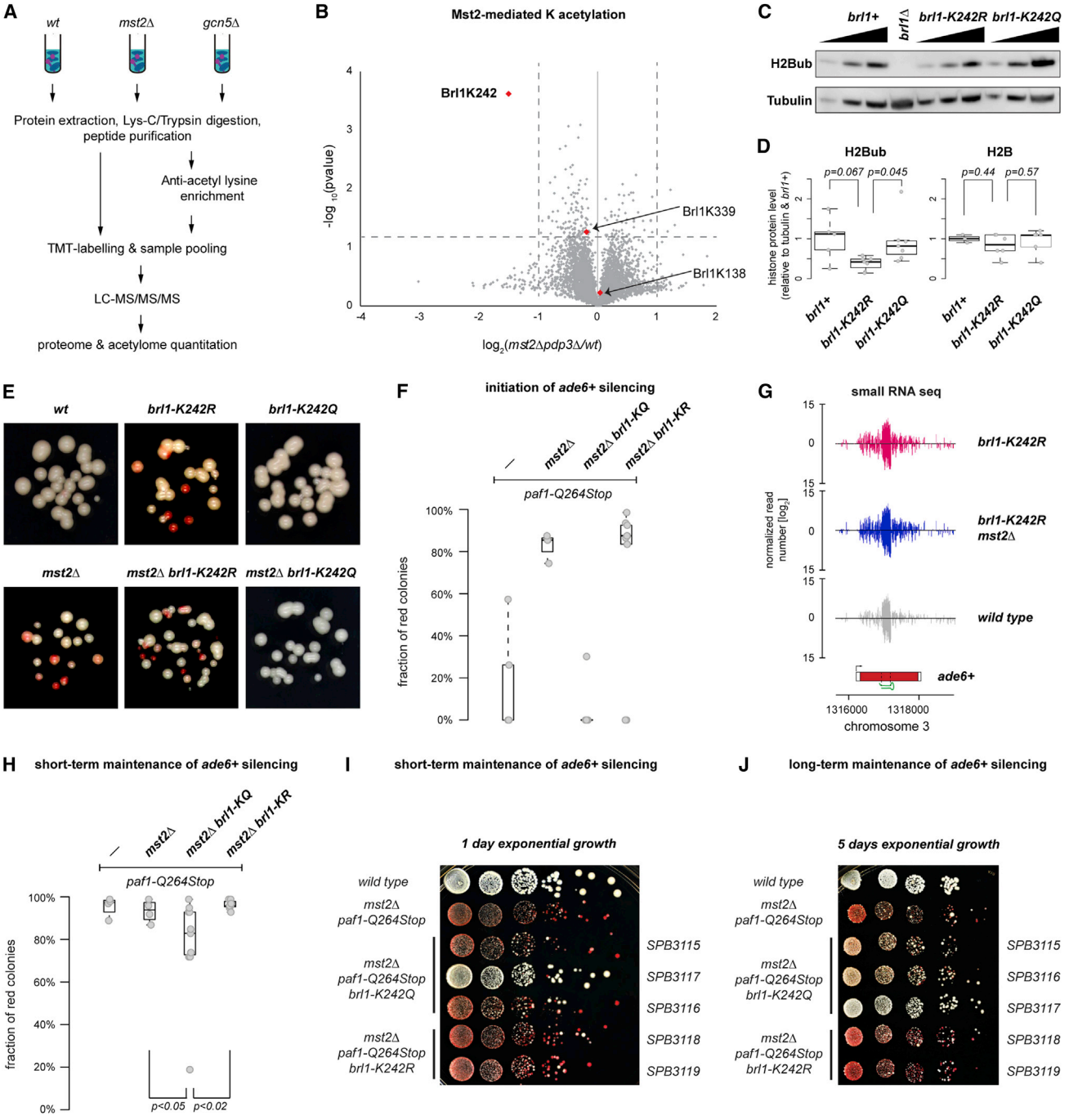

Figure 6. Mst2-Mediated Acetylation of Brl1 Represses Initiation of Heterochromatin Assembly

(A) Scheme: acetylomics workflow. Total peptides or peptides enriched for acetylation were labeled with TMT and subjected to LC-MS/MS/MS. We identified 8,926 acetylated peptides and quantified 3,933 proteins (Table S1). See the STAR Methods for more information.

(B) Volcano plot showing fold changes in *pdp3Δ mst2Δ* compared to WT cells. Identified acetylated Brl1 peptides are shown in red (n = 3 independent biological replicates). The x axis is shown in $\log_2$ scale.

(C) Immunodetection of H2BK119ub in different strains. Dilution series was 1/9, 1/3, and 1/1 of the respective protein extracts. Tubulin served as a loading control. A representative experiment is shown.

(D) Quantification of H2BK119ub (left) and H2B (right) levels normalized to tubulin and relative to WT (*brl1+*). Multiple independent biological replicates were for H2BK119ub (WT n = 5 and brl1-KR/KQ n = 7) and H2B (WT n = 3 and brl1-KR/KQ n = 6). The p values were calculated using the two-sided, two-sample Student's t test with equal/unequal variance according to prior evaluation with the F test.

(legend continued on next page)

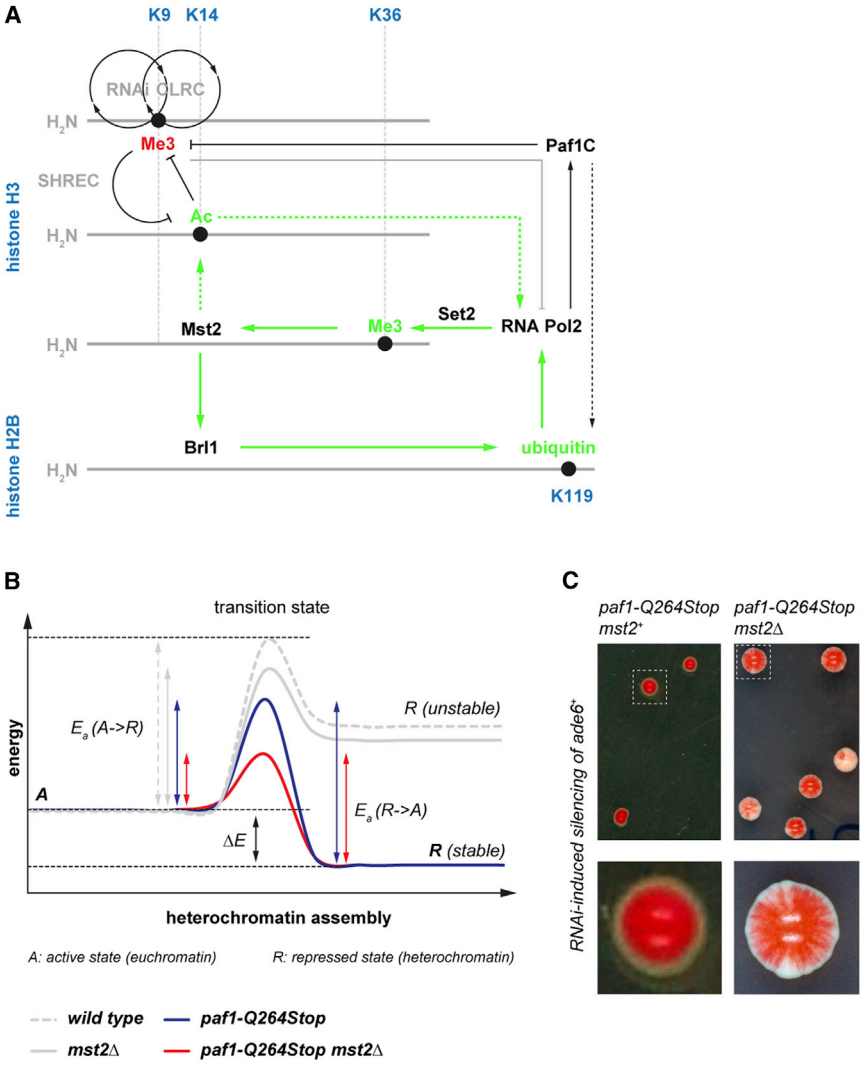

Figure 7. Mst2 Constitutes an Activation Barrier for Heterochromatin Assembly

(A) Scheme depicting the regulatory circuit that protects active chromatin from inactivating siRNAs (solid green arrows). Transcription by RNA polymerase II promotes Set2-mediated tri-methylation of H3K36 (Me3, green), which is recognized by Pdp3. This results in high local concentrations of Mst2 on actively transcribed genes. Mst2 acetylates Brl1 at lysine 242, which causes increased H2B ubiquitination and reinforced transcription. Black circles depict opposing feedback loops that maintain the inactive chromatin state (RNAi and CLRC). Relevant residues in the N-terminal tails of H3 and H2B are highlighted in blue. See the text for details.

(B) Model highlighting that a maximal transition state energy warranties stable propagation of euchromatic and heterochromatic states. Note that Mst2 and Paf1C repress distinct steps in the transition from euchromatin (*A*) to heterochromatin (*R*). The heterochromatin assembly reaction proceeds the fastest in *paf1 mst2* double-mutant cells, where the activation energy (E_a) is the lowest and heterochromatin eventually reaches a low-energy state (*R stable*). See the text for details.

(C) Mitotic propagation of siRNA-directed silencing of the *ade6*$^+$ gene monitored by red pigmentation of clones that grew on YE-Nat plates.

presented in this study demonstrate that siRNAs are sufficient to initiate the formation of heterochromatin independently of genomically encoded silencers, but only if repressive activities in the cell are constrained. Mst2 and Paf1C repress distinct steps in the transition from euchromatin to heterochromatin. This can be best illustrated in analogy to a chemical reaction with high activation energy (E_a) and where reactants (euchromatin) and products (heterochromatin) assume different energetic states (Figure 7B). In the absence of Mst2 or Paf1C, the energy level of the transition state is reduced so that the heterochromatin assembly reaction can proceed; but, only Paf1C mutant cells reach a heterochromatic state that is energetically lower than that of euchromatin, explaining why silencing is not stably maintained in *mst2* single mutants. The heterochromatin assembly reaction proceeds the fastest in *paf1 mst2* double-mutant cells, where the activation energy is the lowest and heterochromatin eventually reaches a low-energy state. Yet at the same time, E_a for the reverse reaction is smaller in double mutants compared to *paf1* single mutants, which predicts less stable inheritance of heterochromatin. Indeed, we observed a variegating silencing phenotype in *mst2 paf1* double, but not *paf1* single, mutants (Figure 7C).

This model highlights that a maximal transition state energy warranties stable propagation of both euchromatic and heterochromatic states. Thus, it does not seem surprising that previous

(E) Silencing assays of siRNA-directed de novo heterochromatin assembly (as described in Figure 1) in the strains indicated (close up). All strains contained a *paf1*$^+$ allele. A representative experiment is shown.

(F and H) Initiation (F) and maintenance (H) frequencies in *paf1-Q264Stop* cells with additional mutations in *mst2*$^+$ and *brl1*$^+$. Assessment of initiation/maintenance frequency was as in Figure 1D. The p values were calculated using two-sided, two-sample Student's t test (n ≥ 8 individual white colonies). Exact numbers are listed in the STAR Methods.

(G) siRNA reads mapping to the *ade6-M210* locus and neighboring regions in *brl1-K242R* (red) and *mst2Δbrl1-K242R* (blue) cells. Read counts were normalized to total read number and are depicted in $\log_2$ scale.

(I and J) Dilution assays showing gradual loss of ectopic silencing at the *trp1*$^+$*::ade6*$^+$ locus in *brl1-K242Q* mutants, but not in *brl1-K242R* mutants. Cells were grown exponentially for 1 day (I) or 5 days (J), and equal cell numbers were plated onto yeast extract-nourseothricin (YE-Nat). A representative experiment with independent strains is shown. Different yeast strains are depicted on the right.

See also Figures S3 and S4 and Table S1.

attempts to induce epigenetically stable gene silencing by using *trans*-acting siRNAs have failed under wild-type conditions (Bühler et al., 2006; Iida et al., 2008; Sigova et al., 2004; Simmer et al., 2010). It is the aforesaid self-reinforcing feedback regulation that possibly underlies the high activation energy of a heterochromatin assembly reaction. We speculate that E_a might be lowered under certain conditions, enabling the organism to establish facultative heterochromatin and, thus, adapt its gene expression program for optimal fitness. It will be a challenging but exciting task to find the putative enzymes that lower E_a in such a scenario.

Conservation of H3K36 Methylation-Mediated Anti-silencing

Certain post-transcriptional histone modifications are highly correlated with transcription. Yet, it is often unclear whether active chromatin marks are simply a consequence or rather a cause of transcriptional activity. The active H3K36me3 mark is generated by the SET domain containing proteins recruited by RNA polymerase II as a consequence of transcriptional activity. Our results suggest that, in *S. pombe*, H3K36me3 is also a cause of transcriptional activity. Importantly, it functions to sequester Mst2 on transcriptionally active genes, which serves a dual purpose: (1) it fuels the euchromatic positive feedback loop described above, and (2) it prevents Mst2 from acting promiscuously on constitutive heterochromatin. Thereby, H3K36me3 maintains euchromatic genes in an active state, and it concurrently safeguards constitutive heterochromatin from illegitimate activation by an invasion of Mst2, providing an explanation for the previously reported silencing defects in *set2*$^{+}$-deficient cells (Chen et al., 2008; Creamer et al., 2014; Matsuda et al., 2015; Suzuki et al., 2016).

In *S. cerevisiae*, the methylation of H3K36 by Set2 protects euchromatin from silencing by spreading of the Sir complex from neighboring silent chromatin independently of the Rpd3S HDAC complex (Tompa and Madhani, 2007). This highlights that H3K36 methylation functions through different effector mechanisms that may be conserved. Indeed, SETD2-mediated tri-methylation of H3K36 targets the de novo DNA methyltransferase DNMT3B to transcribed genes in mouse embryonic stem cells (Baubec et al., 2015). Similar to Pdp3-mediated recruitment of Mst2 to active genes in *S. pombe*, the PWWP domain of DNMT3B is likely to specify recruitment of DNA methylation activity to transcribed genes via interactions with methylated H3K36 (Baubec et al., 2015). The functional relevance of genic DNA methylation in mammalian cells is just being unraveled (Neri et al., 2017). If it had stimulatory effects on transcription, it would also constitute a positive feedback regulatory system. Finally, the polycomb repressive complex 2 (PRC2), reconstituted from humans, flies, mouse, and plants, is directly inhibited by H3K36 methylation (Schmitges et al., 2011; Yuan et al., 2011). Thus, it is tempting to speculate that methylation of H3K36 is an evolutionarily conserved strategy to maintain euchromatin in an active state. In light of this hypothesis, it is intriguing that human H3K36 methyltransferases have been implicated in a wide range of cancers (Papillon-Cavanagh et al., 2017; Schneider et al., 2002; Wagner and Carpenter, 2012). Moreover, the H3K36 to M mutation is seen in 95% of chondroblastomas and promotes sarcomagenesis through altering polycomb-mediated gene silencing (Behjati et al., 2013; Lu et al., 2016). Failure to partition chromatin into silent and active domains as a result of defective H3K36 methylation may, hence, contribute to the initiation and progression of human disease. Therefore, a detailed understanding of the mechanisms that control the active state of chromatin is extremely relevant to human health.

STAR★METHODS

Detailed methods are provided in the online version of this paper and include the following:

- KEY RESOURCES TABLE
- CONTACT FOR REAGENT AND RESOURCE SHARING
- EXPERIMENTAL MODEL AND SUBJECT DETAILS
- METHOD DETAILS
  - Strains and Plasmid Construction
  - Silencing Assays
  - Quantification of silencing frequency
  - ChIP-qPCR
  - small and poly(A)-RNA sequencing
  - DamID and Microarray analysis
  - RT-qPCR
  - Acetylomics
  - Western Blotting
- QUANTIFICATION AND STATISTICAL ANALYSIS
- DATA AND SOFTWARE AVAILABILITY

SUPPLEMENTAL INFORMATION

Supplemental Information includes four figures and two tables and can be found with this article online at http://dx.doi.org/10.1016/j.molcel.2017.05.026.

AUTHOR CONTRIBUTIONS

V.F. generated strains; performed H3K9me2-ChIP, western blot, DamID, proteomics, small RNA sequencing (RNA-seq), RNA-seq, and RT-PCR experiments; conducted silencing initiation/maintenance assays; and analyzed the data. P.R.G. generated strains; performed ChIP experiments (FLAG-Pdp3, Mst2-FLAG, H3, H3K36me3, and H3K14Ac), RT-PCR experiments, silencing assays, and western blot; and analyzed the data. V.I. performed proteomics with V.F. and acquired and analyzed data. Y.S. and T.K. generated strains. M.B. and S.B. conceived and supervised the study. S.B. analyzed ChIP data with P.R.G. V.F., P.R.G., S.B., and M.B. designed experiments and prepared figures. V.F. and M.B. wrote the manuscript. All authors discussed the results and commented on the manuscript.

ACKNOWLEDGMENTS

We thank F. Mohn and L. Kaaij for discussion and critical feedback on the manuscript and H. Pickersgill (Life Science Editors) for editorial assistance. We thank N. Laschet and Z. Sarkadi for excellent technical assistance. We would like to thank the FMI Functional Genomics facility for assistance in library construction and next-generation sequencing and Y. Murakami for providing a *set2ΔSRI* strain. This work was supported by funds from the European Research Council (ERC-StG-RNAiGenReg-280410 and ERC-CoG-REpiReg-681213 to M.B.), the European Union Network of Excellence EpiGeneSys (HEALTH-2010-257082 to S.B.), and the German Research

Foundation (BR 3511/3-1 to S.B.). The Friedrich Miescher Institute for Biomedical Research is supported by the Novartis Research Foundation.

Received: January 23, 2017
Revised: April 25, 2017
Accepted: May 23, 2017
Published: June 22, 2017

REFERENCES

Adams-Cioaba, M.A., and Min, J. (2009). Structure and function of histone methylation binding proteins. Biochem. Cell Biol. *87*, 93–105.

Aebersold, R., and Mann, M. (2016). Mass-spectrometric exploration of proteome structure and function. Nature *537*, 347–355.

Bähler, J., Wu, J.Q., Longtine, M.S., Shah, N.G., McKenzie, A., 3rd, Steever, A.B., Wach, A., Philippsen, P., and Pringle, J.R. (1998). Heterologous modules for efficient and versatile PCR-based gene targeting in Schizosaccharomyces pombe. Yeast *14*, 943–951.

Barrales, R.R., Forn, M., Georgescu, P.R., Sarkadi, Z., and Braun, S. (2016). Control of heterochromatin localization and silencing by the nuclear membrane protein Lem2. Genes Dev. *30*, 133–148.

Baubec, T., Colombo, D.F., Wirbelauer, C., Schmidt, J., Burger, L., Krebs, A.R., Akalin, A., and Schübeler, D. (2015). Genomic profiling of DNA methyltransferases reveals a role for DNMT3B in genic methylation. Nature *520*, 243–247.

Bayne, E.H., White, S.A., Kagansky, A., Bijos, D.A., Sanchez-Pulido, L., Hoe, K.-L., Kim, D.-U., Park, H.-O., Ponting, C.P., Rappsilber, J., and Allshire, R.C. (2010). Stc1: a critical link between RNAi and chromatin modification required for heterochromatin integrity. Cell *140*, 666–677.

Behjati, S., Tarpey, P.S., Presneau, N., Scheipl, S., Pillay, N., Van Loo, P., Wedge, D.C., Cooke, S.L., Gundem, G., Davies, H., et al. (2013). Distinct H3F3A and H3F3B driver mutations define chondroblastoma and giant cell tumor of bone. Nat. Genet. *45*, 1479–1482.

Beisel, C., and Paro, R. (2011). Silencing chromatin: comparing modes and mechanisms. Nat. Rev. Genet. *12*, 123–135.

Bell, O., Wirbelauer, C., Hild, M., Scharf, A.N.D., Schwaiger, M., MacAlpine, D.M., Zilbermann, F., van Leeuwen, F., Bell, S.P., Imhof, A., et al. (2007). Localized H3K36 methylation states define histone H4K16 acetylation during transcriptional elongation in Drosophila. EMBO J. *26*, 4974–4984.

Bjerling, P., Silverstein, R.A., Thon, G., Caudy, A., Grewal, S., and Ekwall, K. (2002). Functional divergence between histone deacetylases in fission yeast by distinct cellular localization and in vivo specificity. Mol. Cell. Biol. *22*, 2170–2181.

Braun, S., Garcia, J.F., Rowley, M., Rougemaille, M., Shankar, S., and Madhani, H.D. (2011). The Cul4-Ddb1(Cdt)^2 ubiquitin ligase inhibits invasion of a boundary-associated antisilencing factor into heterochromatin. Cell *144*, 41–54.

Bühler, M., Verdel, A., and Moazed, D. (2006). Tethering RITS to a nascent transcript initiates RNAi- and heterochromatin-dependent gene silencing. Cell *125*, 873–886.

Carrozza, M.J., Li, B., Florens, L., Suganuma, T., Swanson, S.K., Lee, K.K., Shia, W.-J., Anderson, S., Yates, J., Washburn, M.P., and Workman, J.L. (2005). Histone H3 methylation by Set2 directs deacetylation of coding regions by Rpd3S to suppress spurious intragenic transcription. Cell *123*, 581–592.

Chen, E.S., Zhang, K., Nicolas, E., Cam, H.P., Zofall, M., and Grewal, S.I.S. (2008). Cell cycle control of centromeric repeat transcription and heterochromatin assembly. Nature *451*, 734–737.

Creamer, K.M., Job, G., Shanker, S., Neale, G.A., Lin, Y.-C., Bartholomew, B., and Partridge, J.F. (2014). The Mi-2 homolog Mit1 actively positions nucleosomes within heterochromatin to suppress transcription. Mol. Cell. Biol. *34*, 2046–2061.

Drouin, S., Laramée, L., Jacques, P.-É., Forest, A., Bergeron, M., and Robert, F. (2010). DSIF and RNA polymerase II CTD phosphorylation coordinate the recruitment of Rpd3S to actively transcribed genes. PLoS Genet. *6*, e1001173.

Ekwall, K., Cranston, G., and Allshire, R.C. (1999). Fission yeast mutants that alleviate transcriptional silencing in centromeric flanking repeats and disrupt chromosome segregation. Genetics *153*, 1153–1169.

Fischer, T., Cui, B., Dhakshnamoorthy, J., Zhou, M., Rubin, C., Zofall, M., Veenstra, T.D., and Grewal, S.I.S. (2009). Diverse roles of HP1 proteins in heterochromatin assembly and functions in fission yeast. Proc. Natl. Acad. Sci. USA *106*, 8998–9003.

Gaidatzis, D., Lerch, A., Hahne, F., and Stadler, M.B. (2015). QuasR: quantification and annotation of short reads in R. Bioinformatics *31*, 1130–1132.

Gilbert, T.M., McDaniel, S.L., Byrum, S.D., Cades, J.A., Dancy, B.C.R., Wade, H., Tackett, A.J., Strahl, B.D., and Taverna, S.D. (2014). A PWWP domain-containing protein targets the NuA3 acetyltransferase complex via histone H3 lysine 36 trimethylation to coordinate transcriptional elongation at coding regions. Mol. Cell. Proteomics *13*, 2883–2895.

Gómez, E.B., Espinosa, J.M., and Forsburg, S.L. (2005). Schizosaccharomyces pombe mst2+ encodes a MYST family histone acetyltransferase that negatively regulates telomere silencing. Mol. Cell. Biol. *25*, 8887–8903.

Gottschling, D.E. (2004). Summary: epigenetics—from phenomenon to field. Cold Spring Harb. Symp. Quant. Biol. *69*, 507–519.

Govind, C.K., Qiu, H., Ginsburg, D.S., Ruan, C., Hofmeyer, K., Hu, C., Swaminathan, V., Workman, J.L., Li, B., and Hinnebusch, A.G. (2010). Phosphorylated Pol II CTD recruits multiple HDACs, including Rpd3C(S), for methylation-dependent deacetylation of ORF nucleosomes. Mol. Cell *39*, 234–246.

Grewal, S.I. (2010). RNAi-dependent formation of heterochromatin and its diverse functions. Curr. Opin. Genet. Dev. *20*, 134–141.

Iida, T., Nakayama, J., and Moazed, D. (2008). siRNA-mediated heterochromatin establishment requires HP1 and is associated with antisense transcription. Mol. Cell *31*, 178–189.

Jain, R., Iglesias, N., and Moazed, D. (2016). Distinct functions of Argonaute slicer in siRNA maturation and heterochromatin formation. Mol. Cell *63*, 191–205.

Jason, L.J.M., Moore, S.C., Lewis, J.D., Lindsey, G., and Ausió, J. (2002). Histone ubiquitination: a tagging tail unfolds? BioEssays *24*, 166–174.

Keller, C., Kulasegaran-Shylini, R., Shimada, Y., Hotz, H.-R., and Bühler, M. (2013). Noncoding RNAs prevent spreading of a repressive histone mark. Nat. Struct. Mol. Biol. *20*, 994–1000.

Kimura, H., Hayashi-Takanaka, Y., Goto, Y., Takizawa, N., and Nozaki, N. (2008). The organization of histone H3 modifications as revealed by a panel of specific monoclonal antibodies. Cell Struct. Funct. *33*, 61–73.

Kizer, K.O., Phatnani, H.P., Shibata, Y., Hall, H., Greenleaf, A.L., and Strahl, B.D. (2005). A novel domain in Set2 mediates RNA polymerase II interaction and couples histone H3 K36 methylation with transcript elongation. Mol. Cell. Biol. *25*, 3305–3316.

Knop, M., Siegers, K., Pereira, G., Zachariae, W., Winsor, B., Nasmyth, K., and Schiebel, E. (1999). Epitope tagging of yeast genes using a PCR-based strategy: more tags and improved practical routines. Yeast *15* (10B), 963–972.

Kowalik, K.M., Shimada, Y., Flury, V., Stadler, M.B., Batki, J., and Bühler, M. (2015). The Paf1 complex represses small-RNA-mediated epigenetic gene silencing. Nature *520*, 248–252.

Li, B., Jackson, J., Simon, M.D., Fleharty, B., Gogol, M., Seidel, C., Workman, J.L., and Shilatifard, A. (2009). Histone H3 lysine 36 dimethylation (H3K36me2) is sufficient to recruit the Rpd3s histone deacetylase complex and to repress spurious transcription. J. Biol. Chem. *284*, 7970–7976.

Lu, C., Jain, S.U., Hoelper, D., Bechet, D., Molden, R.C., Ran, L., Murphy, D., Venneti, S., Hameed, M., Pawel, B.R., et al. (2016). Histone H3K36 mutations promote sarcomagenesis through altered histone methylation landscape. Science *352*, 844–849.

Matsuda, A., Chikashige, Y., Ding, D.-Q., Ohtsuki, C., Mori, C., Asakawa, H., Kimura, H., Haraguchi, T., and Hiraoka, Y. (2015). Highly condensed chromatins are formed adjacent to subtelomeric and decondensed silent chromatin in fission yeast. Nat. Commun. *6*, 7753.

Maurer-Stroh, S., Dickens, N.J., Hughes-Davies, L., Kouzarides, T., Eisenhaber, F., and Ponting, C.P. (2003). The Tudor domain 'Royal Family': Tudor, plant Agenet, Chromo, PWWP and MBT domains. Trends Biochem. Sci. *28*, 69–74.

McAlister, G.C., Nusinow, D.P., Jedrychowski, M.P., Wühr, M., Huttlin, E.L., Erickson, B.K., Rad, R., Haas, W., and Gygi, S.P. (2014). MultiNotch MS3 enables accurate, sensitive, and multiplexed detection of differential expression across cancer cell line proteomes. Anal. Chem. *86*, 7150–7158.

Moazed, D. (2011). Mechanisms for the inheritance of chromatin states. Cell *146*, 510–518.

Morris, S.A., Shibata, Y., Noma, K., Tsukamoto, Y., Warren, E., Temple, B., Grewal, S.I.S., and Strahl, B.D. (2005). Histone H3 K36 methylation is associated with transcription elongation in Schizosaccharomyces pombe. Eukaryot. Cell *4*, 1446–1454.

Motamedi, M.R., Verdel, A., Colmenares, S.U., Gerber, S.A., Gygi, S.P., and Moazed, D. (2004). Two RNAi complexes, RITS and RDRC, physically interact and localize to noncoding centromeric RNAs. Cell *119*, 789–802.

Motamedi, M.R., Hong, E.-J.E., Li, X., Gerber, S., Denison, C., Gygi, S., and Moazed, D. (2008). HP1 proteins form distinct complexes and mediate heterochromatic gene silencing by nonoverlapping mechanisms. Mol. Cell *32*, 778–790.

Neri, F., Rapelli, S., Krepelova, A., Incarnato, D., Parlato, C., Basile, G., Maldotti, M., Anselmi, F., and Oliviero, S. (2017). Intragenic DNA methylation prevents spurious transcription initiation. Nature *543*, 72–77.

Nicolas, E., Yamada, T., Cam, H.P., Fitzgerald, P.C., Kobayashi, R., and Grewal, S.I.S. (2007). Distinct roles of HDAC complexes in promoter silencing, antisense suppression and DNA damage protection. Nat. Struct. Mol. Biol. *14*, 372–380.

Papillon-Cavanagh, S., Lu, C., Gayden, T., Mikael, L.G., Bechet, D., Karamboulas, C., Ailles, L., Karamchandani, J., Marchione, D.M., Garcia, B.A., et al. (2017). Impaired H3K36 methylation defines a subset of head and neck squamous cell carcinomas. Nat. Genet. *49*, 180–185.

Reddy, B.D., Wang, Y., Niu, L., Higuchi, E.C., Marguerat, S.B., Bähler, J., Smith, G.R., and Jia, S. (2011). Elimination of a specific histone H3K14 acetyltransferase complex bypasses the RNAi pathway to regulate pericentric heterochromatin functions. Genes Dev. *25*, 214–219.

Schmitges, F.W., Prusty, A.B., Faty, M., Stützer, A., Lingaraju, G.M., Aiwazian, J., Sack, R., Hess, D., Li, L., Zhou, S., et al. (2011). Histone methylation by PRC2 is inhibited by active chromatin marks. Mol. Cell *42*, 330–341.

Schneider, R., Bannister, A.J., and Kouzarides, T. (2002). Unsafe SETs: histone lysine methyltransferases and cancer. Trends Biochem. Sci. *27*, 396–402.

Schneider, C.A., Rasband, W.S., and Eliceiri, K.W. (2012). NIH Image to ImageJ: 25 years of image analysis. Nat Methods. *9*, 671–675.

Shimada, Y., Mohn, F., and Bühler, M. (2016). The RNA-induced transcriptional silencing complex targets chromatin exclusively via interacting with nascent transcripts. Genes Dev. *30*, 2571–2580.

Sigova, A., Rhind, N., and Zamore, P.D. (2004). A single Argonaute protein mediates both transcriptional and posttranscriptional silencing in Schizosaccharomyces pombe. Genes Dev. *18*, 2359–2367.

Simmer, F., Buscaino, A., Kos-Braun, I.C., Kagansky, A., Boukaba, A., Urano, T., Kerr, A.R.W., and Allshire, R.C. (2010). Hairpin RNA induces secondary small interfering RNA synthesis and silencing in trans in fission yeast. EMBO Rep. *11*, 112–118.

Steglich, B., Filion, G.J., van Steensel, B., and Ekwall, K. (2012). The inner nuclear membrane proteins Man1 and Ima1 link to two different types of chromatin at the nuclear periphery in S. pombe. Nucleus *3*, 77–87.

Sugiyama, T., Cam, H., Verdel, A., Moazed, D., and Grewal, S.I.S. (2005). RNA-dependent RNA polymerase is an essential component of a self-enforcing loop coupling heterochromatin assembly to siRNA production. Proc. Natl. Acad. Sci. USA *102*, 152–157.

Sugiyama, T., Cam, H.P., Sugiyama, R., Noma, K., Zofall, M., Kobayashi, R., and Grewal, S.I.S. (2007). SHREC, an effector complex for heterochromatic transcriptional silencing. Cell *128*, 491–504.

Suzuki, S., Kato, H., Suzuki, Y., Chikashige, Y., Hiraoka, Y., Kimura, H., Nagao, K., Obuse, C., Takahata, S., and Murakami, Y. (2016). Histone H3K36 trimethylation is essential for multiple silencing mechanisms in fission yeast. Nucleic Acids Res. *44*, 4147–4162.

Tanny, J.C. (2014). Chromatin modification by the RNA polymerase II elongation complex. Transcription *5*, e988093.

Tanny, J.C., Erdjument-Bromage, H., Tempst, P., and Allis, C.D. (2007). Ubiquitylation of histone H2B controls RNA polymerase II transcription elongation independently of histone H3 methylation. Genes Dev. *21*, 835–847.

Team, R.C. (2014). R: a language and environment for statistical computing. http://www.R-project.org/.

Tompa, R., and Madhani, H.D. (2007). Histone H3 lysine 36 methylation antagonizes silencing in Saccharomyces cerevisiae independently of the Rpd3S histone deacetylase complex. Genetics *175*, 585–593.

Vermeulen, M., Eberl, H.C., Matarese, F., Marks, H., Denissov, S., Butter, F., Lee, K.K., Olsen, J.V., Hyman, A.A., Stunnenberg, H.G., and Mann, M. (2010). Quantitative interaction proteomics and genome-wide profiling of epigenetic histone marks and their readers. Cell *142*, 967–980.

Wagner, E.J., and Carpenter, P.B. (2012). Understanding the language of Lys36 methylation at histone H3. Nat. Rev. Mol. Cell Biol. *13*, 115–126.

Wang, Y., Yang, F., Gritsenko, M.A., Wang, Y., Clauss, T., Liu, T., Shen, Y., Monroe, M.E., Lopez-Ferrer, D., Reno, T., et al. (2011). Reversed-phase chromatography with multiple fraction concatenation strategy for proteome profiling of human MCF10A cells. Proteomics *11*, 2019–2026.

Wang, Y., Kallgren, S.P., Reddy, B.D., Kuntz, K., López-Maury, L., Thompson, J., Watt, S., Ma, C., Hou, H., Shi, Y., et al. (2012). Histone H3 lysine 14 acetylation is required for activation of a DNA damage checkpoint in fission yeast. J. Biol. Chem. *287*, 4386–4393.

Wang, J., Reddy, B.D., and Jia, S. (2015). Rapid epigenetic adaptation to uncontrolled heterochromatin spreading. eLife *4*, 80.

Wilhelm, B.T., Marguerat, S., Aligianni, S., Codlin, S., Watt, S., and Bähler, J. (2011). Differential patterns of intronic and exonic DNA regions with respect to RNA polymerase II occupancy, nucleosome density and H3K36me3 marking in fission yeast. Genome Biol. *12*, R82.

Woods, A., Sherwin, T., Sasse, R., MacRae, T.H., Baines, A.J., and Gull, K. (1989). Definition of individual components within the cytoskeleton of Trypanosoma brucei by a library of monoclonal antibodies. J. Cell Sci. *93*, 491–500.

Woolcock, K.J., Gaidatzis, D., Punga, T., and Bühler, M. (2011). Dicer associates with chromatin to repress genome activity in Schizosaccharomyces pombe. Nat. Struct. Mol. Biol. *18*, 94–99.

Yuan, W., Xu, M., Huang, C., Liu, N., Chen, S., and Zhu, B. (2011). H3K36 methylation antagonizes PRC2-mediated H3K27 methylation. J. Biol. Chem. *286*, 7983–7989.

Zofall, M., and Grewal, S.I.S. (2007). HULC, a histone H2B ubiquitinating complex, modulates heterochromatin independent of histone methylation in fission yeast. J. Biol. Chem. *282*, 14065–14072.

STAR★METHODS

KEY RESOURCES TABLE

REAGENT or RESOURCE	SOURCE	IDENTIFIER
Antibodies		
anti-H3K9me2	(Kimura et al., 2008)	N/A
anti-FLAG	Sigma	Cat# F3165; RRID: AB_259529
anti-H3K14ac	Abcam	Cat# ab52946; RRID: AB_880442
anti-H3K36me3	Abcam	Cat# ab9050; RRID: AB_306966
anti-H3 (ChIP)	Active Motif	Cat# 61475
anti-H2B	Active Motif	Cat# 39238; RRID: AB_2631110
anti-H2BK119ub	Cell Signaling	Cat# 5546
anti-H3K4me3	Abcam	Cat# ab8580; RRID: AB_306649
anti-H3 (Western)	Abcam	Cat# ab1791; RRID: AB_302613
anti-tubulin	(Woods et al., 1989)	N/A
goat anti-mouse IgG (H + L)-HRP conjugate	Bio-Rad	Cat# 1706516; RRID: AB_11125547
Peroxidase AffiniPure Goat Anti-Mouse IgG (H+L)	Jackson Immunoresearch	Cat# 115-035-146; RRID: AB_2307392
Peroxidase AffiniPure Goat Anti-Rabbit IgG (H+L)	Jackson Immunoresearch	Cat# 111-035-144; RRID: AB_2307391
Acetyl-Lysine Motif Kit	Cell Signaling	Cat# 13416S
Chemicals, Peptides, and Recombinant Proteins		
5-Fluoroorotic Acid (FOA)	US biological, Thermo Fisher	Cat# 207291-8-4
nourseothricin dihydrogen sulfate (NAT)	Fisher or WERNER BioAgents GmbH	Cat# 5029426 or Cat# 5.0
G418 sulfate (Geneticin)	Roche or Invitrogen/Life Technologies	Cat# 04727878001-2 or Cat# 10131027
Hygromycin	Sigma or Invitrogen/Life Technologies	Cat# H7772 or Cat# 10687010
PrimeSTAR GXL DNA Polymerase	Clontech	Cat# R050A
Taq DNA Polymerase	NEB	Cat# M0267
Formaldehyde	Sigma or Carl Roth	Cat# F8775 or Cat# 4979
PMSF	Sigma	Cat# P7626
cOmplete Protease Inhibitor Cocktail	Roche	Cat# 11836145001
AEBSF (Pefabloc SC)	Roche	Cat# 11585916001
Dynabeads M-280 Sheep anti-mouse IgG	Thermo Fisher	Cat# 11202D
Dynabeads Protein G	Thermo Fisher/ Life Technologies	Cat# 10009D
Leupeptin hemisulfate	Carl Roth	Cat# CN33
Proteinase K	Roche	Cat# 3115879001
RNase A	Roche	Cat# 10109169001
SuperScript III	Thermo Fisher/ Life Technologies	Cat# 18080085
Acrylamid/BIS solution (30%) 37.5:1	Serva	Cat# 10688
Titriplex III (EDTA)	Merck Millipore	Cat# 108418
SsoAdvanced Universal SYBR Green Supermix	Bio-Rad	Cat# 172-5274
PowerUp SYBR Green Master Mix	Life Technologies	Cat# A25742
Zymolyase	Fischer	Cat# 6064819
Lysing enzyme from *Trichoderma harzianum*	Sigma	Cat# L1412
DpnI	NEB	Cat# R0176
DpnII	NEB	Cat# R0543
T4 DNA ligase	Roche	Cat# 10481220001

(*Continued on next page*)

Continued

REAGENT or RESOURCE	SOURCE	IDENTIFIER
Lys-C	Wako Chemicals	Cat# 125-05061
Trypsin	Thermo Fisher	Cat# 20233
SEP-PAK	Waters	Cat# WAT036790
YMC Triart C18 0.5 × 250 mm column	YMC Europe GmBH	Cat# TA12S0325J0AU
PepMap 100 C18 2 cm trap	Thermo Fisher	Cat# 164946
EASY-Spray C18 column	Thermo Fisher	Cat# ES801
Bolt 4-12% Bis-Tris Plus Gels	Thermo Fisher	Cat# NW04127BOX
Immobilon Western Chemiluminescent HRP Substrate	Millipore	Cat# WBKLS0500
Immobilon-P Membran, PVDF, 0,45 μm	Merck Millipore	Cat# IPVH00010
Critical Commercial Assays		
MasterPure Yeast RNA Purification Kit	Epicenter	Cat# MPY03100
Bio-Rad Protein Assay Dye Reagent Concentrate	Bio-Rad	Cat# 500-0006
TruSeq Small RNA library preparation kit	Illumina	Cat# RS-200-0012
TruSeq Stranded mRNA library preparation kit	Illumina	Cat# RS-122-2101
DNeasy Blood and Tissue Kit	QIAGEN	Cat# 69506
RNeasy Midi Kit	QIAGEN	Cat# 75144
GeneChip Hybridization, Wash, and Stain Kit	Affymetrix	Cat# 900720
Turbo DNA free	Thermo Fisher/ Life Technologies	Cat# AM1907
ChIP DNA Clean & Concentrator	Zymo Research	Cat# D5201
Deposited Data		
smallRNA and poly(A) mRNA sequencing data	This study	GEO: GSE93434
DamID data	This study	GEO: GSE93434
Mendeley Data dataset (original unprocessed Western Blot images)	This study	http://dx.doi.org/10.17632/98ywc24xv7.1
Mass spectrometry raw data	This study	ProteomeXchange: PXD005714
H3K36me3 ChIP-chip data	(Wilhelm et al., 2011)	ArrayExpress: E-TABM-946
Experimental Models: Organisms/Strains		
h⁻ leu1-32 ura4-D18 ade6-704 trp1⁺::ade6⁺ nmt1⁺::ade6-hp⁺::natMX	(Kowalik et al., 2015)	spb464
h⁺ leu1-32 ura4-D18 ade6-M210 trp1⁺::ade6⁺ nmt1⁺::ade6-hp⁺::natMX	(Kowalik et al., 2015)	spb1788
h⁻ leu1-32 ura4-D18 ade6-704 trp1⁺::ade6⁺ nmt1⁺::ade6-hp⁺::natMX paf1-sms8::LEU2	(Kowalik et al., 2015)	spb2047
h⁺ leu1-32 ura4-D18 ade6-704 or 210 trp1⁺::ade6⁺ nmt1⁺::ade6-hp⁺::natMX Paf1-SMS8::kanMX	(Kowalik et al., 2015)	spb2076
h⁻ leu1-32 ura4-D18 ade6-704 trp1⁺::ade6⁺ nmt1⁺::ade6-hp⁺::natMX paf1-sms8::LEU2 mst2Δ::kanMX	This study	spb2151
h⁺ leu1-32 ura4-D18 ade6-M210 or 704 trp1⁺::ade6⁺ nmt1⁺::ade6-hp⁺::natMX mst2Δ::kanMX paf1-sms8::LEU2	This study	spb2630
h⁺ leu1-32 ura4-D18 ade6-M210 trp1⁺::ade6⁺ nmt1⁺::ade6-hp⁺::natMX mst2Δ::kanMX	This study	spb2094
h⁺ leu1-32 ura4-D18 ade6-M210 trp1⁺::ade6⁺ nmt1⁺::ade6-hp⁺::natMX clr4Δ::hphMX	(Kowalik et al., 2015)	spb1950
h⁹⁰ mat3::GFP-natMX (ura4 promoter and adh1 terminator) ura4-DS/E leu1-32 ade6-M210 ncRNA.95Δ::URA3 (C. albicans) mst2Δ::hphMX	(Keller et al., 2013)	spb1591
h⁹⁰ mat3::GFP-natMX (ura4 promoter and adh1 terminator) ura4-DS/E leu1-32 ade6-M210 ncRNA.95Δ::URA (C. albicans) mst2Δ::hphMX	This study	spb1719

(*Continued on next page*)

Continued

REAGENT or RESOURCE	SOURCE	IDENTIFIER
h^{90} mat3::GFP-natMX (ura4 promoter and adh1 terminator) ura4-DS/E leu1-32 ade6-M210 ncRNA.95Δ::URA3 (C. albicans) mst2Δ::hphMX clr4Δ::kanMX	This study	spb1754
h^{90} mat3::GFP-natMX (ura4 promoter and adh1 terminator) ura4-DS/E leu1-32 ade6-M210 or M216 ncRNA.95Δ::URA3 (C. albicans) mst2Δ::hphMX dcr1Δ::kanMX	This study	spb1776
h? mat3::GFP-natMX (ura4 promoter and adh1 terminator) ura4-DS/E leu1-32 ade6-M210 or 216 ncRNA.95Δ::URA3 (C. albicans) mst2Δ::hphMX ago1Δ::kanMX	This study	spb1755
h^+ otr1R(SphI)::ura4$^+$ ura4-DS/E ade6-M210 leu1Δ::nmt1(81x)-dam-myc::kanMX	(Woolcock et al., 2011)	spb492
h^+ otr1R(SphI)::ura4$^+$ ura4-DS/E leu1-32 ade6-M210 leu1Δ::nmt1(81x)-dam-myc-mst2::kanMX	This study	spb2104
h^- leu1-32 ura4-D18 ade6-704 trp1$^+$::ade6$^+$	(Kowalik et al., 2015)	spb426 (PSB1782)
h^- leu1-32 ura4-D18 ade6-704 trp1$^+$::ade6$^+$ mst2-CBP-2xFLAG::natMX	This study	PSB1855
h^- leu1-32 ura4-D18 ade6-704 trp1$^+$::ade6$^+$ mst2-FLAG::natMX set2Δ::kanMX	This study	PSB1870
h^- leu1-32 ura4-D18 ade6-704 trp1$^+$::ade6$^+$ mst2-FLAG::natMX pdp3D::kanMX	This study	PSB1871
h^- leu1-32 ura4-D18 ade6-704 trp1$^+$::ade6$^+$ mst2-FLAG::natMX set2-SRIΔ::kanMX	This study	PSB1882
h^+ imr1L(NcoI)::ura4$^+$ otr1R(SphI)::ade6$^+$ leu1-32 ura4-DS/E ade6-M210	(Ekwall et al., 1999)	PSB65
h^+ imr1L(NcoI)::ura4$^+$ otr1R(SphI)::ade6$^+$ leu1-32 ura4-DS/E ade6-M210 natMX::CBP-2xFLAG-pdp3	This study	PSB1696
h^+ imr1L(NcoI)::ura4$^+$ otr1R(SphI)::ade6$^+$ leu1-32 ura4-DS/E ade6-M210 pdp3Δ::natMX::CBP-2xFLAG-pdp3_F109A	This study	PSB1698
h^+ otr1R(SphI)::ura4$^+$ ura4-DS/E leu1-32 ade6-M210 leu1Δ::nmt1(81x)-dam-myc-mst2::kanMX pdp3Δ::natMX	This study	spb2212
h? leu1-32 ura4-D18 ade6-704 or ade6M210 trp1+::ade6+ nmt1+::ade6-hp::natMX paf1-sms8::LEU2 pdp3Δ::kanMX	This study	spb2647
h? leu1-32 ura4-D18 ade6-704 or ade6M210 trp1+::ade6+ nmt1+::ade6-hp+::natMX paf1-sms8::LEU2 set2Δ::kanMX	This study	spb2646
h^+ otr1R(SphI)::ura4$^+$ ura4-DS/E leu1-32 ade6-M210 leu1Δ::nmt1(81x)-dam-myc-mst2::kanMX set2Δ::natMX	This study	spb2220
h^+ otr1R(SphI)::ura4$^+$ ura4-DS/E leu1-32 ade6-M210 leu1Δ::nmt1(81x)-dam-myc-mst2::kanMX set1Δ::natMX	This study	spb2239
h^+ leu1-32 ura4-D18 ade6-M210 trp1$^+$::ade6$^+$ nmt1$^+$::ade6-hp$^+$::natMX pdp3Δ::kanMX	This study	spb2319
h^- SPSQ (cyhR) SPL42 (cyhS) hphMX::cen1 imr1L(NcoI)::ura4$^+$ otr1R(SphI)::ade6$^+$ leu1-32 ura4-DS/E ade6-M210	(Barrales et al., 2016)	PSB582
h^- SPSQ (cyhR) SPL42 (cyhS) hphMX::cen1 imr1L(NcoI)::ura4$^+$ otr1R(SphI)::ade6$^+$ leu1-32 ura4-DS/E ade6-M210 pdp3Δ::natMX	This study	PSB689
h^- SPSQ (cyhR) SPL42 (cyhS) hphMX::cen1 imr1L(NcoI)::ura4$^+$ otr1R(SphI)::ade6$^+$ leu1-32 ura4-DS/E ade6-M210 mst2Δ::natMX	This study	PSB1122
h^- SPSQ (cyhR) SPL42 (cyhS) hphMX::cen1 imr1L(NcoI)::ura4$^+$ otr1R(SphI)::ade6$^+$ leu1-32 ura4-DS/E ade6-M210 pdp3D::natMX mst2Δ::kanMX	This study	PSB2099
h? otr1R(SphI)::ade6-4LexAb.s. (binding site) leu1-32 ura4-D18 or DS/E ade6-M210	This study	spb2835
h+ otr1R(SphI)::ade6-4LexAb.s. leu1-32 ura4-D18 or DS/E ade6-M210 LexA-mst2	This study	spb2821

(*Continued on next page*)

Continued

REAGENT or RESOURCE	SOURCE	IDENTIFIER
h+ otr1R(SphI)::ade6-4LexAb.s. leu1-32 ura4-D18 or DS/E ade6-M210 LexA-mst2(E274Q) cat.dead	This study	spb2822
h? otr1R(SphI)::ade6-4LexAb.s. leu1-32 ura4-D18 or DS/E ade6-M210 pdp3Δ::kanMX	This study	spb2836
h+ otr1R(SphI)::ade6-4LexAb.s. leu1-32 ura4-D18 or DS/E ade6-M210 LexA-Mst2 pdp3Δ::kanMX	This study	spb2804
h+ otr1R(SphI)::ade6-4LexAb.s. leu1-32 ura4-D18 or DS/E ade6-M210 LexA-mst2(E274Q) cat.dead pdp3Δ::kanMX	This study	spb2852
h- leu1-32 ura4-D18 or DS/E otr1R(SphI)::ade6-4LexAb.s. ade6-M210 set2Δ::kanMX	This study	spb2881
h+ otr1R(SphI)::ade6-4LexAb.s. leu1-32 ura4-D18 or DS/E ade6-M210 set2Δ::kanMX LexA-mst2	This study	spb2885
h? otr1R(SphI)::ade6-4LexAb.s. leu1-32 ura4-D18 or DS/E ade6-M210 set2Δ::kanMX LexA-mst2(E274Q) cat.dead	This study	spb2894
h^{90} mat3::GFP-natMX (ura4 promoter and adh1 terminator) ura4-DS/E leu1-32 ade6-M210 ncRNA.95Δ::URA3 (C. albicans) gcn5Δ::kanMX	This study	spb2101
h^{90} mat3::GFP-natMX (ura4 promoter and adh1 terminator) ura4-DS/E leu1-32 ade6-M210 ncRNA.95Δ::URA3 (C. albicans) pdp3Δ::kanMX	This study	spb2153
h^{90} mat3::GFP-natMX (ura4 promoter and adh1 terminator) ura4-DS/E leu1-32 ade6-M210 ncRNA.95Δ::URA3 (C. albicans) mst2Δ::hphMX pdp3Δ::kanMX	This study	spb2115
h^- leu1-32 ura4-D18 ade6-704 $trp1^+$::$ade6^+$ $nmt1^+$::ade6-hp^+::natMX brl1-K242R	This study	spb2982
h^- leu1-32 ura4-D18 ade6-704 $trp1^+$::$ade6^+$ $nmt1^+$::ade6-hp^+::natMX brl1-K242Q	This study	spb2983
h^+ leu1-32 ura4-D18 ade6-M210 $trp1^+$::$ade6^+$ $nmt1^+$::ade6-hp^+::natMX mst2Δ::kanMX brl1-K242Q	This study	spb2984
h^+ leu1-32 ura4-D18 ade6-M210 or ade6-704 $trp1^+$::$ade6^+$ $nmt1^+$::ade6-hp^+::natMX mst2Δ::kanMX brl1-K242R	This study	spb3023
h^- leu1-32 ura4-D18 ade6-M210 or ade6-704 $trp1^+$::$ade6^+$ $nmt1^+$::ade6-hp^+::natMX mst2Δ::kanMX paf1SMS8::LEU2 brl1-K242R	This study	spb3024
h^- leu1-32 ura4-D18 ade6-M210 or ade6-704 $trp1^+$::$ade6^+$ $nmt1^+$::ade6-hp^+::natMX paf1-sms8::LEU2 mst2Δ::kanMX brl1-K242Q	This study	spb2996
h^+ leu1-32 ura4-D18 ade6-M210 $trp1^+$::$ade6^+$ $nmt1^+$::ade6-hp^+::natMX mst2Δ::kanMX dcr1Δ::hphMX	This study	spb2364
h^+ leu1-32 ura4-D18 ade6-M210 $trp1^+$::$ade6^+$ $nmt1^+$::ade6-hp^+::natMX dcr1Δ::hphMX paf1sms8::LEU2 mst2Δ::kanMX	This study	spb2661
h^- leu1-32 ura4-D18 ade6-M210 $trp1^+$::$ade6^+$ $nmt1^+$::ade6-hp^+::natMX dcr1Δ::hphMX paf1sms8::LEU2 mst2Δ::kanMX	This study	spb2662
h^{90} mat3::GFP-natMX (ura4 promoter and adh1 terminator) ura4-DS/E leu1-32 ade6-M210 ncRNA.95Δ::URA3 (C. albicans) mst2Δ::hphMX arb2Δ::kanMX	This study	spb1739
h^{90} mat3::GFP-natMX (ura4 promoter and adh1 terminator) ura4-DS/E leu1-32 ade6-M210 ncRNA.95Δ::URA3 (C. albicans) mst2Δ::hphMX arb1Δ::kanMX	This study	spb1740
h^{90} mat3::GFP-natMX (ura4 promoter and adh1 terminator) ura4-DS/E leu1-32 ade6-M210 ncRNA.95Δ::URA3 (C. albicans) mst2Δ::hphMX cid12Δ::kanMX	This study	spb1741

(*Continued on next page*)

Continued

REAGENT or RESOURCE	SOURCE	IDENTIFIER
h^{90} mat3::GFP-natMX (ura4 promoter and adh1 terminator) ura4-DS/E leu1-32 ade6-M210 ncRNA.95Δ::URA3 (C. albicans) mst2Δ::hphMX ers1Δ::kanMX	This study	spb1745
h^{90} mat3::GFP-natMX (ura4 promoter and adh1 terminator) ura4-DS/E leu1-32 ade6-M210 ncRNA.95Δ::URA3 (C. albicans) mst2Δ::hphMX stc1Δ::kanMX	This study	spb1747
h? mat3::GFP-natMX (ura4 promoter and adh1 terminator) ura4-DS/E leu1-32 ade6-? ncRNA.95Δ::URA3 (C. albicans) mst2Δ::hphMX tas3Δ::kanMX	This study	spb1753
h? mat3::GFP-natMX (ura4 promoter and adh1 terminator) ura4-DS/E leu1-32 ade6-? ncRNA.95Δ::URA3 (C. albicans) mst2Δ::hphMX chp1Δ::kanMX	This study	spb1756
h? mat3::GFP-natMX (ura4 promoter and adh1 terminator) ura4-DS/E leu1-32 ade6-? ncRNA.95Δ::URA3 (C. albicans) mst2Δ::hphMX rik1Δ::kanMX	This study	spb1757
h? mat3::GFP-natMX (ura4 promoter and adh1 terminator) ura4-DS/E leu1-32 ade6-? ncRNA.95Δ::URA3 (C. albicans) mst2Δ::hphMXD hrr1Δ::kanMX	This study	spb1772
h90 mat3::GFP-natMX (ura4 promoter and adh1 terminator) ura4-DS/E leu1-32 ade6-M210 ncRNA.95Δ::URA3 (C. albicans) mst2Δ::hphMX rdp1Δ::kanMX	This study	spb1774
h? mat3::GFP-natMX (ura4 promoter and adh1 terminator) ura4-DS/E leu1-32 ade6-? ncRNA.95Δ::URA3 (C. albicans) mst2Δ::hphMX raf1Δ::kanMX	This study	spb1802
h? mat3::GFP-natMX (ura4 promoter and adh1 terminator) ura4-DS/E leu1-32 ade6-? ncRNA.95Δ::URA3 (C. albicans) mst2Δ::hphMX raf2Δ::kanMX	This study	spb1803
h^{+} SPSQ (cyhR) hphMX::cen1 imr1L(NcoI)::ura4^{+} otr1R(SphI)::ade6^{+} leu1-32 ura4-DS/E ade6-M210 clr3Δ::kanMX	This study	PSB1524
h^{-} leu1-32 ura4-D18 ade6-704 trp1^{+}::ade6^{+} nmt1^{+}::ade6-hp^{+}::natMX gcn5Δ::kanMX	This study	spb2404
h^{-} leu1-32 ura4-D18 ade6-704 trp1^{+}::ade6^{+} nmt1^{+}::ade6-hp^{+}::natMX gcn5Δ::kanMX paf1SMS8::LEU	This study	spb2443
h^{+} leu1-32 ura4-D18 ade6-M210 or ade6-704 trp1^{+}::ade6^{+} nmt1^{+}::ade6-hp^{+}::natMX paf1-sms8::LEU2 mst2Δ::kanMX brl1-K242Q	This study	spb3115
h^{+} leu1-32 ura4-D18 ade6-M210 or ade6-704 trp1^{+}::ade6^{+} nmt1^{+}::ade6-hp^{+}::natMX paf1-sms8::LEU2 mst2Δ::kanMX brl1-K242Q	This study	spb3116
h^{+} leu1-32 ura4-D18 ade6-M210 or ade6-704 trp1^{+}::ade6^{+} nmt1^{+}::ade6-hp^{+}::natMX paf1-sms8::LEU2 mst2Δ::kanMX brl1-K242Q	This study	spb3117
h^{+} leu1-32 ura4-D18 ade6-M210 or ade6-704 trp1^{+}::ade6^{+} nmt1^{+}::ade6-hp^{+}::natMX paf1-sms8::LEU2 mst2Δ::kanMX brl1-K242R	This study	spb3118
h^{+} leu1-32 ura4-D18 ade6-M210 or ade6-704 trp1^{+}::ade6^{+} nmt1^{+}::ade6-hp^{+}::natMX paf1-sms8::LEU2 mst2Δ::kanMX brl1-K242R	This study	spb3119
Oligonucleotides		
Primers	This study	Table S2
Recombinant DNA		
pFa6a 81xnmt1 - Dam - mst2	This study	pMB1436
pJR1 - 3xL - LexA - Mst2 gDNA	This study	pMB1636
pJR1 - 3xL - LexA - Mst2 mut (E274Q)-gDNA	This study	pMB1639

(*Continued on next page*)

Continued

REAGENT or RESOURCE	SOURCE	IDENTIFIER
Software and Algorithms		
ImageJ 1.47v	(Schneider et al., 2012)	N/A
R	(Team, 2014)	https://www.r-project.org/
QuasR	(Gaidatzis et al., 2015)	N/A
Proteome Discoverer 2.1 software	Thermo Fisher	Cat# IQLAAEGAB SFAKJMAUH
Other		
Illumina HiSeq2500	Illumina	N/A
GeneChip Scanner 3000 7G System	Affymetrix	Cat# 00-0213
Agilent 1100 system	Agilent	Cat# DE33201061
Orbitrap Fusion Tribrid	Thermo Fisher	Cat# IQLAAEGA APFADBMBCX
Easy nLC 1000 system	Thermo Fisher	Cat# LC-010190

CONTACT FOR REAGENT AND RESOURCE SHARING

Further information and requests for resources and reagents should be directed to and will be fulfilled by the Lead Contact, Marc Bühler (marc.buehler@fmi.ch).

EXPERIMENTAL MODEL AND SUBJECT DETAILS

Schizosaccharomyces pombe strains used in this study are derivatives of the standard laboratory strain 972 and are listed in the Key Resources Table. Cultures were grown at 30°C in liquid YES media (160 rpm, 12-24 hr) or at 30°C on solid YES agarose plates (for 3 days).

METHOD DETAILS

Strains and Plasmid Construction

All strains were constructed using the PCR-based protocol (Bähler et al., 1998) or by standard mating and sporulation. Brl1-K242R/Q point mutants were generated by first deleting the ORF with *URA3* from *Candida albicans* and then reinserting the mutated ORF into the same locus by FOA counter-selection. LexA-Mst2 and LexA-Mst2* strains were generated by deleting the *mst2*$^+$ ORF and reinserting *mst2(*)* fused LexA from a plasmid by homologous recombination. FLAG-Pdp3, FLAG-Pdp3-F109A point mutant and Mst2-FLAG were similarly generated by first deleting the respective ORF with a *kanMX* cassette; subsequently the *kanMX* cassette was replaced by inserting the FLAG-fusion together with a *natMX* selection marker. In case of Pdp3, the *natMX* marker is upstream of the 5′ UTR of *pdp3*$^+$. In the case of Mst2, the selection marker is downstream of the *mst2*$^+$ ORF (between the FLAG-tag ADH1 terminator and the 3′UTR of *mst2*$^+$). Western Blots to assess FLAG-tagged protein levels were deposited in Mendeley Data, http://dx.doi.org/10.17632/98ywc24xv7.1.

Silencing Assays

For *ade6*$^+$ reporter silencing assays, cells were spotted on YES and YE-Nat plates (containing 100 ug/mL nourseothricin) in a ten-fold serial dilution (initial seeded cell number 10^5 cells) and grown for four days. White colonies were picked to perform dilution assays for initiation of silencing, whereas red colonies were picked to visualize maintenance of silencing.

Serial dilutions of the strains indicated in Figure S1C were plated on PMGc (nonselective, NS) or on PMGc plates containing 2 mg/mL 5-Fluoroorotic Acid (FOA). For *ura4*$^+$ reporter assays in Figure S2C, cells were plated on EMM (non-selective, NS) or EMM containing 1 mg/mL FOA. The strains were grown at 30°C for three and four days, respectively.

Quantification of silencing frequency

In order to quantify the initiation and maintenance frequency of the silent state in different strains either a single cell-derived white (for initiation) or red (for maintenance) colony was selected. The single colony was resuspended in water and 50 - 500 cells were seeded on YE-Nat plates, which were incubated at 30°C for 5 days. Colonies were counted/categorized after an additional over night incubation at 4°C. Characterization distinguished between white and non-white cells (which could be either red, pink or variegating) and the relative percentage of white cells was used for visualization by boxplots. Multiple individual colonies were quantified for each

strain (= independent biological replicate): n = 3 (*wild-type*), n = 4 (*paf1-Q264Stop,pdp3Δ*; *paf1-Q264Stop,set2Δ*), n = 5 (*gcn5Δ*), n = 8 (*paf1Q-264Stop,brl1-K242R,mst2Δ*), n > 10 (*mst2Δ*; *paf1-Q264Stop*; *paf1-Q264Stop,mst2Δ*; *paf1-Q264Stop,gcn5Δ; paf1Q-264Stop,brl1K242Q,mst2Δ*).

ChIP-qPCR

ChIP experiments with H3K9me2 were performed as described in Bühler et al. (2006), using 2 μg of an anti-H3K9me2 antibody (Kimura et al., 2008). Briefly, 50 mL of exponentially growing cells were harvested at OD = 1.2 and crosslinked with 1% Formaldehyde for 15 min at room temperature. Cell pellets were lysed in ChIP lysis buffer (50 mM HEPES KOH pH 7.5, 140 mM NaCl, 1 mM EDTA, 1% Triton X-100, 0.1% Na-deoxycholate, 1 mM PMSF, 1x Roche cOMPLETE protease inhibitor cocktail) using a Bead-beater. Lysates were sonicated 13 × 30 s (60 s off) in a Bioruptor and centrifuged for 1x 5 min and 1x 15 min while proceeding with the supernatant. Protein concentration was determined using the Bio-Rad Assay and equal protein amounts were incubated with antibody for 2 hr and with 25 ug Dynabeads (Sheep anti-mouse IgG). Washes were performed three times with lysis buffer, once with wash buffer (10 mM Tris/HCl pH 8, 250 mM LiCl, 0.5% NP40, 0.5% sodium deoxycholate and 1 mM EDTA) and once with TE buffer. Eluates were de-crosslinked in TE and 1% SDS over night at 65°C and subsequently treated with RNase A (0.2 mg/mL) for 1 hr at 37°C and 0.1 mg protease K for 1 hr at 65°C. DNA was purified using phenol/chloroform extraction and real-time qPCR performed on the eluates using the SsoAdvanced Universal SYBR Green Supermix (Bio-Rad). Enrichment was calculated by normalization to the *adh1*$^{+}$ locus in the *clr4Δ* mutant that lacks H3K9me2.

ChIP experiments with FLAG-tagged Mst2 or Pdp3, H3K36me3, H3K14ac and H3 were essentially conducted as described in Barrales et al. (2016), using a Q800R1 sonicator (QSonica) for chromatin shearing (30 min, 30 s on /off cycles, 90% amplitude). For each IP, 2 μg of the following antibodies was used (cell lysates corresponding to different amounts of OD_{600} in brackets): anti-FLAG (Sigma F3165; 30 ODs); anti-H3K14ac (Abcam ab52946, 10 ODs); anti-H3K36me3 (Abcam ab9050, 5 ODs); anti-H3 (Active Motif 61475, 5 ODs). For ChIP experiments with Mst2-FLAG, 4 μg of anti-FLAG antibody and cell lysates corresponding to 50 OD_{600} were used. DNA was immunoprecipitated with Dynabeads Protein G (Life Technologies) and quantified by qPCR using the PowerUp SYBR Green Master Mix (Life Technologies) and a 7500 Fast Real-Time PCR System (Applied Biosystems). Datasets from each independent experiment (n = 3-4) were standardized using an experimental normalization by defining a global mean value for ChIP efficiency. This global mean value includes all qPCR amplicons (used for each tiling array) from the entire sample pool of strains (*wt* and mutant strains used in each experiment). For ChIP experiments with FLAG-tagged Mst2 and Pdp3, the raw values were first normalized against mitochondrial DNA as an internal control before applying the same calculations as above. The results are shown with the background subtracted. As background signal, we used for each amplicon the mean value of the untagged strain and the *pdp3Δ* (or *pdp3-F109A*) mutant, which significantly reduced the noise in the background-corrected data (as compared to the untagged control only). For ChIP with H3K14ac and H3, the raw values were also normalized against input and mitochondrial DNA; these normalized data are presented relative to the mean value of the wild-type for each amplicon.

small and poly(A)-RNA sequencing

Briefly, total RNA was isolated from exponentially growing cells with the hot phenol method. For small RNA-sequencing, the RNA was fractionated with RNeasy Midi columns (QIAGEN) according to the RNA cleanup protocol provided by the manufacturer. The flow-through fraction was precipitated ('small-RNA' fraction). The RNA retained on the column was eluted and ethanol-precipitated ('large-RNA' fraction). 25 ug of the small-RNA fraction was separated by 17.5% PAGE and the 15-28 nt fraction excised and purified. Libraries were prepared using the TruSeq Small RNA and TruSeq Stranded mRNA library preparation kits from Illumina for sRNA- and mRNA-Seq, respectively. Following the isolation of the 145-nt to 160-nt population, the libraries were sequenced on an Illumina HiSeq2500. Reads were processed, normalized and analyzed using QuasR (Gaidatzis et al., 2015) with two mismatches allowed.

DamID and Microarray analysis

DamID was performed as described in Woolcock et al. (2011). Briefly, strains expressing either unfused Dam or Dam fusion proteins were grown to OD = 0.4. Approximately 5.3 × 10^{7} cells were harvested, washed once with water and flash frozen in liquid nitrogen. Cells were spheroplasted in 500 μL spheroplast buffer (1.2 M sorbitol, 100 mM KHPO4, pH 7.5, 0.5 mg/ml Zymolyase (Zymo Research), 1 mg/ml lysing enzyme from Trichoderma harzianum (Sigma)). Genomic DNA was isolated using the DNeasy Blood and Tissue Kit (QIAGEN). gDNA was first digested with DpnI (NEB) before ligation of PCR adapters and subsequent DpnII digestion and final PCR amplification. Fragmentation and labeling was done using the GeneChip Whole Transcript Double-Stranded DNA Terminal Labeling Kit (Affymetrix). The fragmented and labeled DNA was hybridized to GeneChip *S. pombe* Tiling 1.0FR Arrays (Affymetrix). Average enrichment values were calculated for all oligos overlapping the major heterochromatic regions: mating type locus (chromosome 2, 2′114'000-2′137'000), telomeres (chromosome 1, 1-20'000 and 5′571'500-5′579'133; chromosome 2, 4'516'200-4'539'804), centromeres (chromosome 1, 3′753'687-3′789'421, chromosome 2, 1'602′264-1'644'747, chromosome 3, 1'070'904-1'137'003) and subtelomeres (chromosome1, 20'001-35'600 and 5′530'001-5′571'500; chromosome2, 1-15800 and 4497201-4516200). R scripts are available on request.

Microarray data was taken from Wilhelm et al. (2011) (ArrayExpress: E-TABM-946) and processed according to Woolcock et al. (2011), including a pseudocount of 64 to reduce background. R scripts are available upon request.

RT-qPCR

RNA isolation, reverse transcription and RT-qPCR were performed as described previously in Barrales et al. (2016) and Kowalik et al. (2015). For analysis, *act1*$^{+}$-normalized datasets were standardized against the mean of a sample pool of strains (*wt* and mutant strains) from each experiment. These results are shown as relative to the mean value of the wt (which is set to 1). qPCR primers used in this study are listed in Table S2.

Acetylomics

Experimental procedure

Briefly, 400 mL of indicated strains were grown to mid-late growth phase (OD = 1.5), harvested in lysis buffer (50 mM Tris, pH7.5, 150 mM NaCl, 1 mM EDTA, 1x mini complete protease inhibitor cocktail (Roche)) and frozen in liquid N2. Cells were ground in a liquid nitrogen-chilled steel container for 3 × 3 min at 30 Hz using a Retsch MM 400 Ball Mill (Retsch, Haan, Germany) in presence of 1% NP-40 and 0.1% Na-deoxycholate (final concentration). Cell lysates were incubated at 4°C for 15 min and then centrifuged for 15 min at 8'000 g. Proteins in the supernatant were precipitated with > 4 volumes of acetone overnight at −20°C. Protein pellets were re-suspended in 8M guanidine hydrochloride and 50 mM HEPES pH 8.5. Approximately 80-120 mg of proteins were reduced, alkylated and digested with Lys-C (Wako Chemicals) and Trypsin (Thermo Fisher) at 37°C. Peptides were purified using a SEP-PAK (Waters) and eluted in 50% acetonitrile in water. 15 mg of peptides were subjected to immunoprecipitation using the PTMScan Acetyl-Lysine Motif Kit from Cell Signaling Kit (13416S). Acetylated peptides were enriched and eluted according to the manufacturer's instructions. Eluted peptides were labeled with TMT 10plex isobaric labeling reagents (Thermo Fisher) as described in the manufacturer's instructions. To determine global proteome changes 20 μAc of each sample prior acetyl enrichment was labeled with TMT reagents. TMT labeled peptides were subjected to high pH offline fractionation on a YMC Triart C18 0.5 × 250 mm column (YMC Europe GmbH) using the Agilent 1100 system (Agilent Technologies). 72 fractions were collected for each experiment and concatenated into 24 fractions as previously described (Wang et al., 2011). For each LC-MS analysis, approximately 1 μg of peptides were loaded onto a PepMap 100 C18 2 cm trap (Thermo Fisher) using the Proxeon NanoLC-1000 system (Thermo Fisher). On-line peptide separation was performed on the 15 cm EASY-Spray C18 column (ES801, Thermo Fisher) by applying a linear gradient of increasing ACN concentration at a flow rate of 150 nL/min.

Spectra Acquisition

An Orbitrap Fusion Tribrid (Thermo Fisher) mass spectrometer was operated in a data-dependent mode and TMT reporter ions were quantified using a synchronous precursor selection (SPS)-based MS3 technology, as previously described (McAlister et al., 2014). In brief, the top 10 most intense precursor ions from the Orbitrap survey scan were selected for collision-induced dissociation (CID) fragmentation. The ion-trap analyzer was used to generate the MS2 CID spectrum from which the notches for the MS3 scan were selected. The MS3 spectrum was recorded using the Orbitrap analyzer at a resolution of 60000.

Data processing

Thermo RAW files were processed using Proteome Discoverer 2.1 software (Thermo Fisher), as described in the manufacturer's instruction. Briefly, the Sequest search engine was used to search the MS2 spectra against the *Schizosaccharomyces pombe* UniProt database (downloaded on 30/01/2015) supplemented with common contaminating proteins. For total proteome analysis, cysteine carbamidomethylation and TMT tags on lysine and peptide N-termini were set as static modifications, whereas oxidation of methionine residues and acetylation protein N-termini were set as variable modifications. For acetyl-lysine enriched sample analysis, lysine acetylation and lysine TMT tags were set as variable modifications, while other modifications were set the same as for the proteome analysis. The assignments of the MS2 scans were filtered to allow 1% FDR. For reporter quantification, the S/N values were corrected for isotopic impurities of the TMT reagent using the values provided by the manufacturer. The sums across all TMT reporter channels were normalized assuming equal total protein content in each sample for proteome analysis, whereas for acetylome analysis normalization was based on total amount of acetylated peptides. All identified peptides from the proteome and acetylome experiments in this study are listed in Table S1.

Western Blotting

For all proteins examined (unless otherwise indicated), total proteins from exponentially growing cells were extracted using TCA and resuspended in 1M Tris-HCl pH 8.0. Protein concentrations were estimated by Bio-Rad Protein Quantification Assay (Bio-Rad). 5x Laemmli buffer was added to a final concentration of 1x and samples boiled for 5 min at 95°C before separation by SDS-PAGE on a Bolt 4%–12% Bis-Tris gradient gel. Subsequently, proteins were plotted onto a PVDF membrane (Millipore). Antibodies for immunodetection were used at the following concentrations: total H2B (Active Motif, 39238, 1:5′000), H2BK119ubiquitin (Cell Signaling #5546, 1:3′000), H3K4me3 (Abcam, ab8580, 1:2′000), total H3 (Abcam, ab1791, 1:3′000), tubulin (Woods et al., 1989) (1:4'000), HRP-conjugate goat anti-rabbit or goat anti-mouse IgG (Jackson ImmunoResearch, 1:10000). Antibody detection was performed using Millipore Immobilon HRP substrate using the Azure Biosystem c400 Imaging System or the ImageQuant LAS-3000 (GE Healthcare). Equal expression levels of Mst2-FLAG in wt and pdp3Δ cells were validated by quantification using ImageJ. For the F109 point mutant of FLAG-tagged Pdp3, we noticed a two-fold decrease (see original blots in Mendeley Data, http://dx.doi.org/10.17632/98ywc24xv7.1).

For FLAG-tagged proteins, total proteins of exponentially growing cells were extracted by NaOH lysis and TCA precipitation as described (Knop et al., 1999). Samples were resuspended in HU Buffer to a final concentration of 0.1 OD/μl. Samples were

boiled for at least 10 min at 65°C prior loading and 0.5 OD per sample was separated by NU-PAGE on a 10% or 12% Bis-Tris gel. Subsequently, proteins were blotted onto an Immobilon-P PVDF membrane (Millipore). Antibodies for immunodetection were used at the following concentrations: anti-FLAG (Sigma, F3165, 1:1'000) and goat anti-mouse IgG (H + L)-HRP conjugate (Bio-Rad, #1706516, 1:10'000). Antibody detection was performed using Millipore Immobilon HRP substrate on a Fusion FX Vilber Lourmat CCD camera. Quantification was done using ImageJ.

QUANTIFICATION AND STATISTICAL ANALYSIS

P values were generated using the two-tailed, two-sample with equal/unequal variance Student's t test. Error bars are annotated in Figure legends if they show the standard deviation (SD) or standard error of the mean (SEM) and how many replicates were performed. For western blotting, a F-test was performed to assess if the variance between samples is equal or unequal before applying the corresponding Student's t test (two-tailed, two-sample equal/unequal variance).

DATA AND SOFTWARE AVAILABILITY

The accession number for the sRNA and DamID data reported in this paper is GEO: GSE93434. The accession number for the mass spectrometry raw data is ProteomeXchange: PXD005714. Original Western Blots were deposited in Mendeley Data and are available at http://dx.doi.org/10.17632/98ywc24xv7.1.

Molecular Cell, Volume *67*

Supplemental Information

The Histone Acetyltransferase Mst2 Protects Active Chromatin from Epigenetic Silencing by Acetylating the Ubiquitin Ligase Brl1

Valentin Flury, Paula Raluca Georgescu, Vytautas Iesmantavicius, Yukiko Shimada, Tahsin Kuzdere, Sigurd Braun, and Marc Bühler

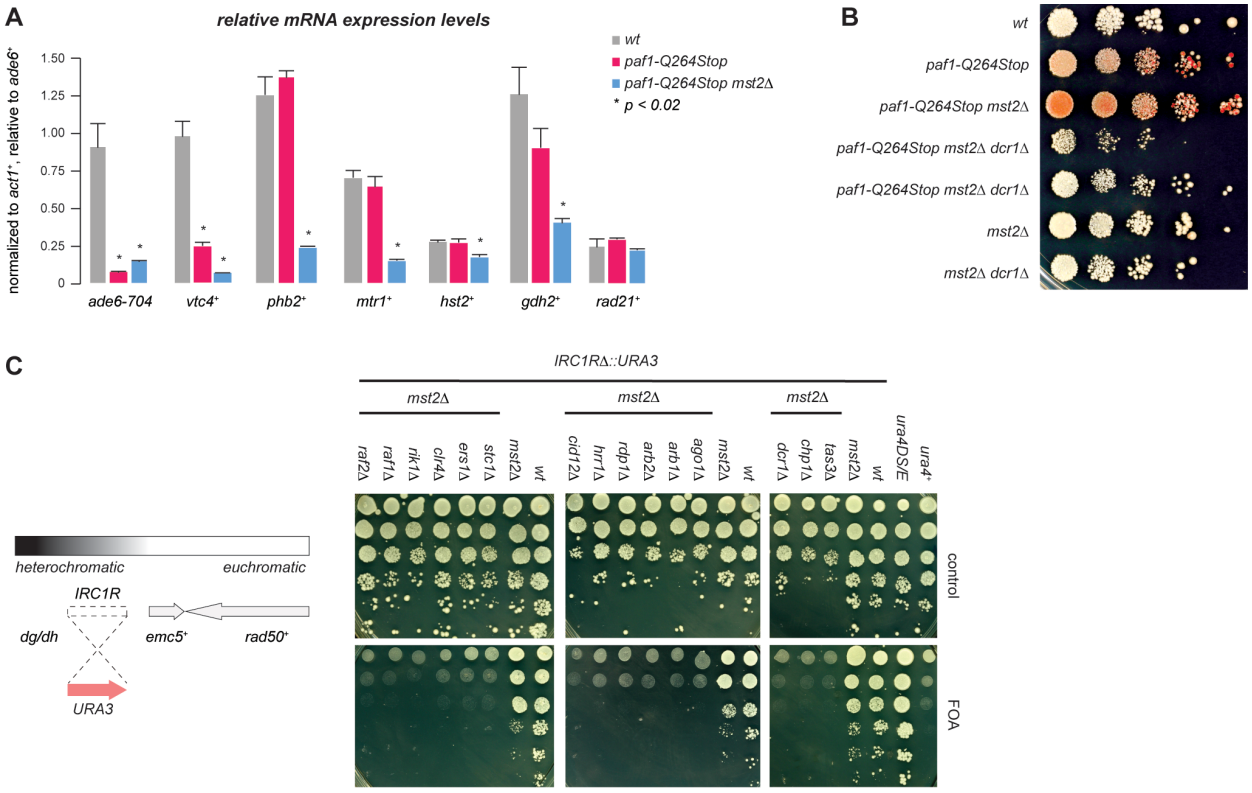

Figure S1 (related to Figure 2)

(A) Relative mRNA expression levels determined by RT-qPCR analysis in indicated mutants. Shown are transcript levels relative to *ade6-704* in *wt* (grey) after normalization to *act1*$^{+}$. *paf1-Q264Stop* and *paf1-Q264Stop mst2Δ* are shown in red and blue. Error bars indicate SD. n=3 independent biological replicates.

(B) Silencing assay with *ade6*$^{+}$ reporter in indicated strains to monitor siRNA-directed de novo heterochromatin assembly (see text for details). Cells were plated in a 10-fold dilution series onto YE-Nat (100 ug/mL nourseothricin).

(C) Silencing assay with *IRC1RΔ::URA3* in indicated strains to monitor siRNA-dependent heterochromatin spreading (see text for details). Cells were plated in a 10-fold dilution series on PMGc plates (control) or PMGc plates with 2g/L FOA.

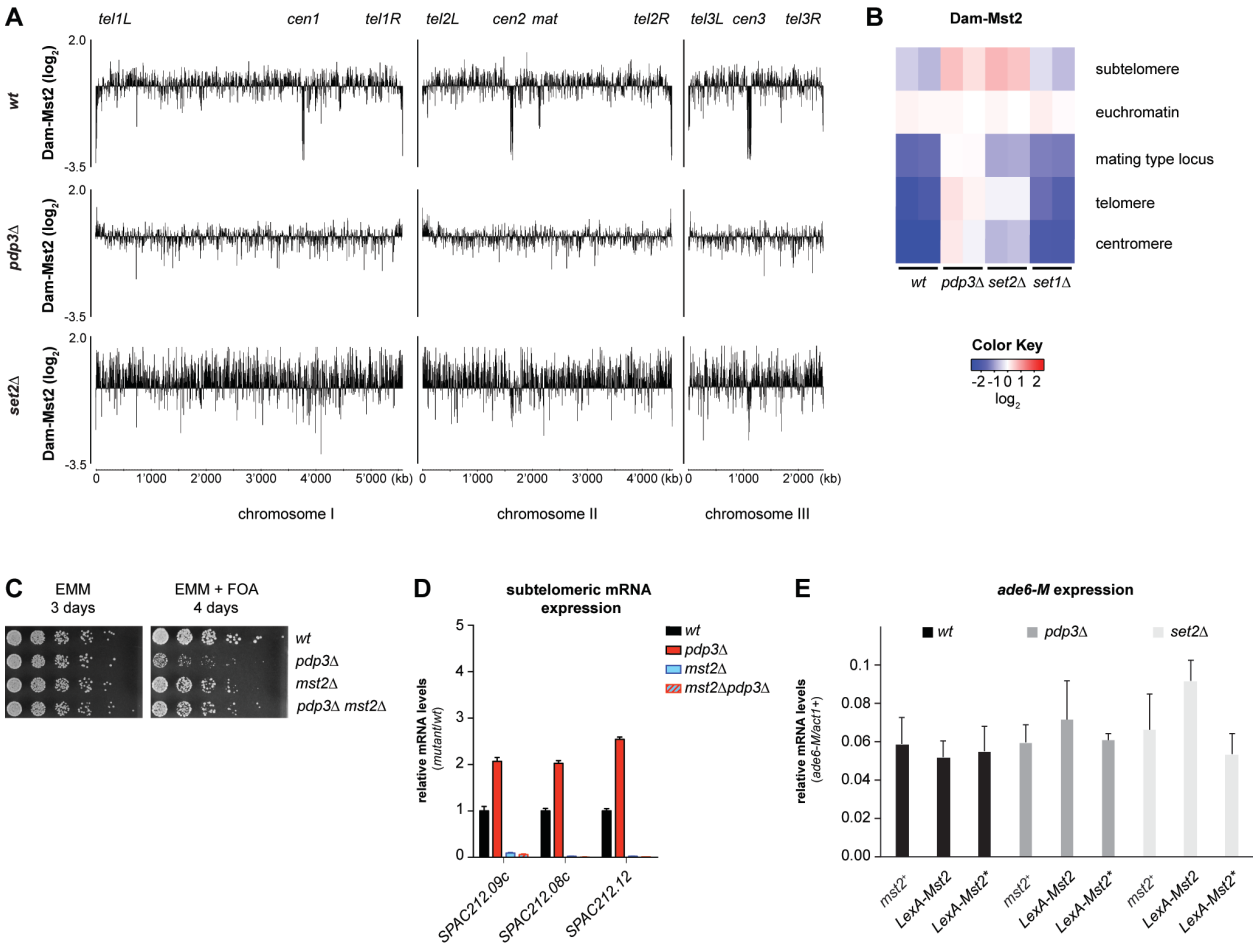

Figure S2 (related to Figure 5)

(A) Mst2 DamID maps of all three chromosomes in *wt*, *pdp3*Δ, and *set2*Δ cells. The signal of DamMst2 (normalized to Dam-only) was averaged over 500 probes and is shown in $\log_2$ scale. X-axis shows position on chromosomes.

(B) Enrichment of Dam-Mst2 at different genomic regions in *wt*, *pdp3*Δ, *set1*Δ, and *set2*Δ cells. Two independent replicates are shown (scale in $\log_2$).

(C) Silencing assay with *imr1L::ura4*$^+$ reporter in indicated strains to monitor heterochromatin maintenance (see text for details). Cells were plated in five-fold serial dilutions on EMM plates (control) or EMM plates containing 1g/L FOA and incubated for the indicated time.

(D) Relative RNA expression levels of subtelomeric genes at telomere 1 in *mst2*Δ, *mst2*Δ*pdp3*Δ, and *pdp3*Δ relative to WT. Transcript levels relative to wild type after normalization to *act1*$^+$ are shown. Data are represented as mean ± SEM from 4 independent biological experiments.

(E) Relative RNA expression levels at the endogenous *ade6-M210* locus in wild type (black), *pdp3*Δ (dark grey), and *set*Δ (light grey) cells with Mst2-tethering variants. Error bars indicate SD. n≥3 independent biological replicates.

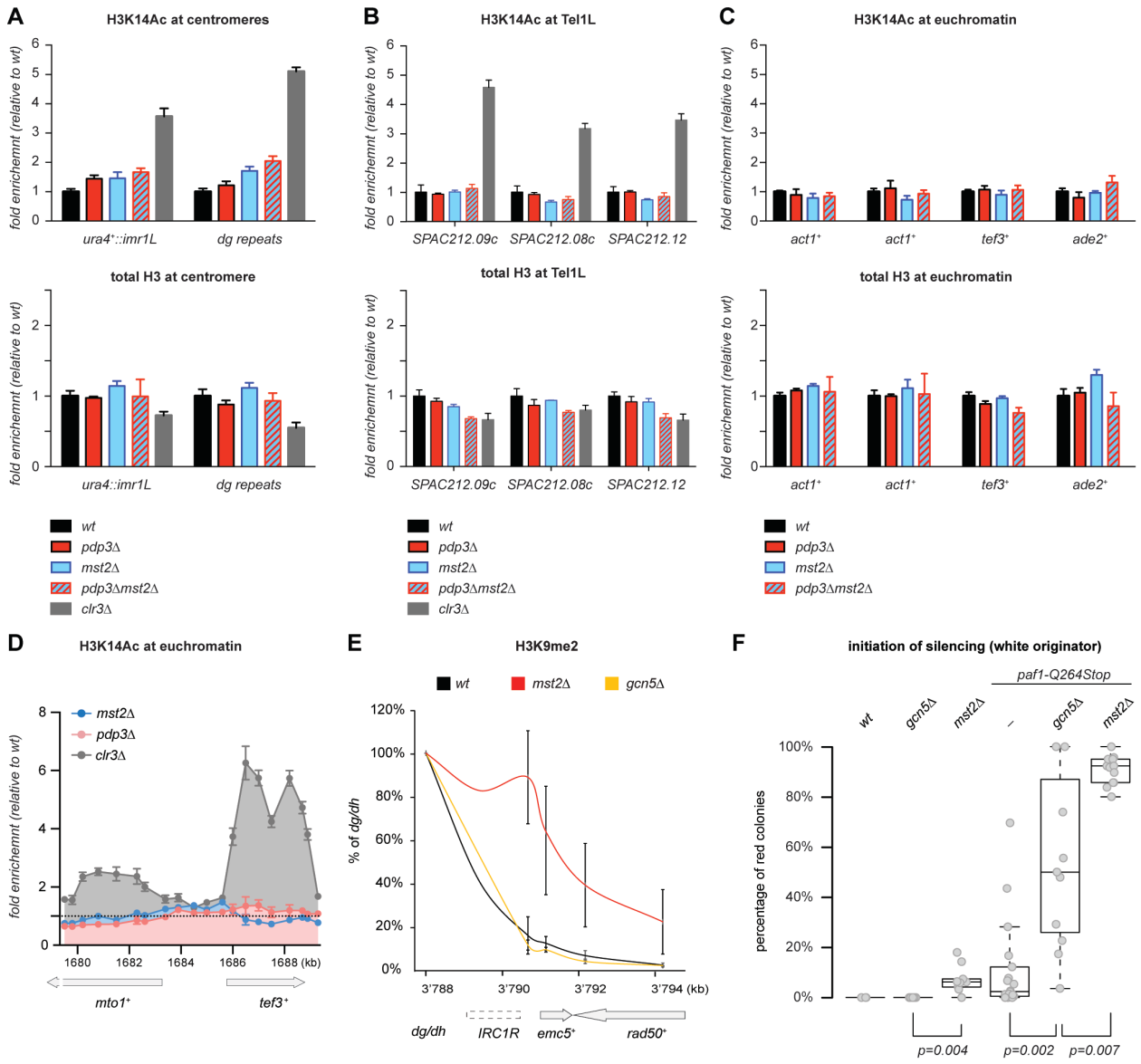

Figure S3 (related to Figure 6)

(A-C) ChIP enrichment of H3K14ac and H3 at centromere 1 (A), telomere 1L (B), and euchromatic loci (C) in indicated strains. Cells lacking the H3K14ac HDAC Clr3 served as a positive control. ChIP data at the indicated loci have been normalized to mitochondrial DNA and to input, and are shown relative to wild type. n=3 ± SEM from independent biological experiments.

(D) ChIP enrichment of H3K14ac at the *mto1*$^{+}$*/tef3*$^{+}$ locus. ChIP data have been normalized to mitochondrial DNA and to input, and are shown relative to wild type for each target, respectively. n=3 ± SEM from independent biological experiments.

(E) ChIP enrichment of H3K9me2 at the boundary of IRC1R in *wt*, *mst2*Δ, and *gcn5*Δ cells. Error bars indicate SD. n≥2 independent biological replicates.

(F) Initiation frequencies of siRNA-directed de novo heterochromatin assembly in different strains. Frequency was calculated as in Figure 1D. P-value was calculated using the two-sided, two sample Student t-test. n≥3 different white colonies. Exact numbers are listed in the STAR methods.

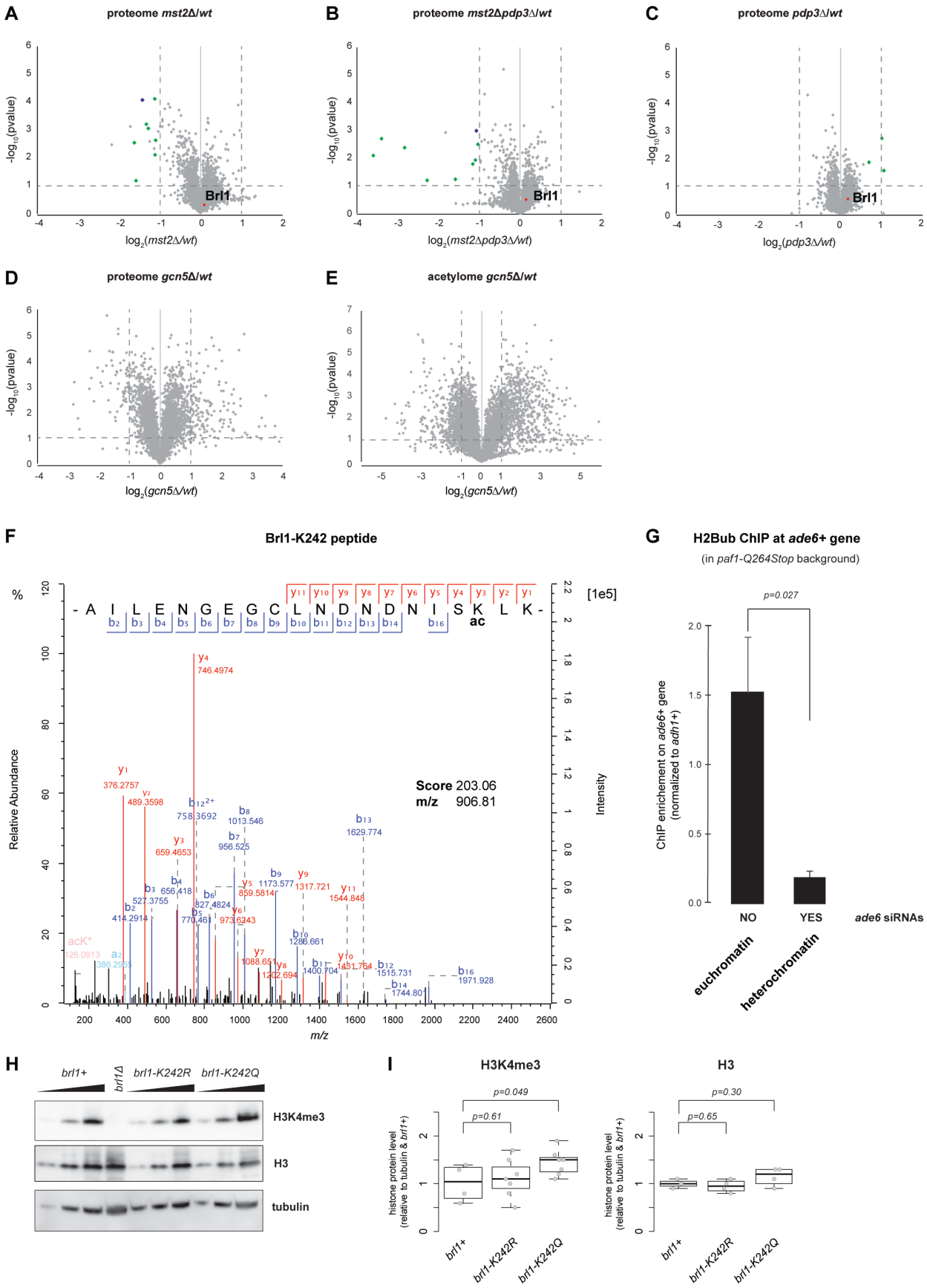
A
proteome mst2Δ/wt
-log10(pvalue)
log2(mst2Δ/wt)
Brl1
B
proteome mst2Δpdp3Δ/wt
-log10(pvalue)
log2(mst2Δpdp3Δ/wt)
Brl1
C
proteome pdp3Δ/wt
-log10(pvalue)
log2(pdp3Δ/wt)
Brl1
D
proteome gcn5Δ/wt
-log10(pvalue)
log2(gcn5Δ/wt)
E
acetylome gcn5Δ/wt
-log10(pvalue)
log2(gcn5Δ/wt)
F
Brl1-K242 peptide
- A I L E N G E G C L N D N D N I S K L K -
ac
Score 203.06
m/z 906.81
Relative Abundance
Intensity
[1e5]
m/z
G
H2Bub ChIP at ade6+ gene
(in paf1-Q264Stop background)
p=0.027
ChIP enrichement on ade6+ gene
(normalized to adh1+)
NO
YES
ade6 siRNAs
euchromatin
heterochromatin
H
brl1+
brl1Δ
brl1-K242R
brl1-K242Q
H3K4me3
H3
tubulin
I
H3K4me3
p=0.049
p=0.61
histone protein level
(relative to tubulin & brl1+)
brl1+
brl1-K242R
brl1-K242Q
H3
p=0.30
p=0.65
histone protein level
(relative to tubulin & brl1+)
brl1+
brl1-K242R
brl1-K242Q

Figure S4 (related to Figure 6)

(A-E) Volcano plots showing the relative changes in different strains. X-axis is in log_2 scale, y-axis depicts the inverted p-value. All experiments were performed in three independent biological replicates. A-C, relative proteome changes in *mst2*Δ (A), *mst2*Δ *pdp3*Δ (B), and *pdp3*Δ cells (C) compared to wild type. Proteins encoded by subtelomeric genes are highlighted in green, whereas Per1 (encoded by a locus adjacent to the cen1L boundary) is shown in blue. Brl1 is highlighted in red. (D) proteome changes in *gcn5*Δ cells compared to wild type. E, changes in the acetylome in *gcn5*Δ compared to *wt* cells.

(F) Annotated high resolution MS/MS spectrum of acetylated peptide fragmented with higher-energy collisional dissociation (HCD). The triply charged precursor ion located at m/z of 906.801 was isolated using quadrupole filter, fragmented with HCD and analyzed in the orbitrap detector. The acetylated peptide AILENGEGcamCLNDNDNISacKLK was identified and annotated by the Andromeda search engine assigning b- and y-ions with an Andromeda score of 203.

(G) ChIP enrichment of H2BK119ub at the *ade6+* locus relative to *adh1+*. n=3 ± SD from independent biological experiments. P-value was calculated using the two-sided, two sample Student t-test.

(H) Immunodetection of H3K4me3 and total H3 in different strains. Dilution series of 1/9, 1/3 and 1/1 of the respective protein extracts. Tubulin served as a loading control. A representative experiment is shown.

(I) Quantification of H3K4me3 (top) and H3 (bottom panel) levels normalized to tubulin and relative to *brl1+*. Multiple independent biological replicates for H3K4me3 (WT: n=4; brl1-KR/KQ: n=7) and H3 (WT: n=3; brl1-KR/KQ: n=4). P-value was calculated using the two-sided, two-sample Student *t*-test with equal/unequal variance according to prior evaluation with the F-test.